

Copyright Undertaking

This thesis is protected by copyright, with all rights reserved.

By reading and using the thesis, the reader understands and agrees to the following terms:

1. The reader will abide by the rules and legal ordinances governing copyright regarding the use of the thesis.
2. The reader will use the thesis for the purpose of research or private study only and not for distribution or further reproduction or any other purpose.
3. The reader agrees to indemnify and hold the University harmless from and against any loss, damage, cost, liability or expenses arising from copyright infringement or unauthorized usage.

IMPORTANT

If you have reasons to believe that any materials in this thesis are deemed not suitable to be distributed in this form, or a copyright owner having difficulty with the material being included in our database, please contact lbsys@polyu.edu.hk providing details. The Library will look into your claim and consider taking remedial action upon receipt of the written requests.

**MULTIDISCIPLINARY FORENSIC
INVESTIGATION OF BUILDINGS IN FIRE: THE
CASE OF THE PLASCO TOWER**

DOMADA VEERA VENKATA RAMAKANTH

PhD

The Hong Kong Polytechnic University

2025

The Hong Kong Polytechnic University
Department of Building Environment and Energy Engineering

Multidisciplinary Forensic Investigation of Buildings in Fire: The Case of the Plasco
Tower

Domada Veera Venkata Ramakanth

A thesis submitted in partial fulfilment of the requirements for the degree of
Doctor of Philosophy
Aug 2024

CERTIFICATE OF ORIGINALITY

I hereby declare that this thesis is my own work and that, to the best of my knowledge and belief, it reproduces no material previously published or written, nor material that has been accepted for the award of any other degree or diploma, except where due acknowledgement has been made in the text.

_____ (Signed)

D.V.V. RAMAKANTH (Name of student)

Abstract

The Plasco Tower, a 17-story building constructed in 1962, was the tallest building in Iran until its collapse in 2017. This high-rise building in Tehran collapsed due to a fire accident that started on the 10th floor and travelled both vertically and horizontally within the building. One of the biggest challenges faced by the researchers in carrying out the forensic study is the lack of structural and architectural information on the tower. Most of the information about the tower was obtained by studying the debris found after the collapse. Several researchers tried to analyse the tower to understand the reasons for the collapse, but faced limitations in terms of fire and structural modelling. One of the major difficulties in analysing tall structures against fires like the Plasco tower is the complexity involved in sequentially coupling multiple software.

This thesis aims to reconstruct the fire history and develop plausible theories explaining the collapse mechanism behind the partial collapse in the initial stages and the final global collapse. The thesis uses two approaches to integrating CFD (using software FDS) with the heat transfer and thermo-mechanical analysis modules of the OpenSees software framework. The first approach for software integration uses a Python-based interface called OpenFire, which is entirely open-source. In contrast, the second approach uses the GiD+OpenSees interface to achieve integration, which is faster, more flexible and allows for more complex and comprehensive simulation models to be developed. The OpenFire software package was used for sequential CFD, heat transfer, and thermo-mechanical analysis of a single floor. However, for conducting the full-scale forensic study of the Plasco tower collapse, the GiD+OpenSees interface was used. A detailed assessment of the strengths and design flaws of the Plasco tower against fire conditions was conducted. The thesis explores the reasons for the global collapse of the tower based on the detailed, sequentially coupled analyses carried out.

Publications arising from this thesis

Ramakanth Domada*, Asif Usmani (2024). A model-scale experimental study of tall building collapse in fire. **(Investigation in progress)**

Based on Chapter 3 of the thesis

DOMADA R*, Khan A. A., Khan M. A Robustness analysis of Plasco tower under fire conditions. **(Draft)**

Based on Chapter 5 of the thesis

DOMADA R*, Khan A. A., Khan M.A., Analysis of large-scale structures in fire using the OpenFire framework: The case of the Plasco tower. **(Draft)**

Based on Chapter 6 of the thesis

DOMADA R*, Khan A. A., Khan M. A OpenSees Simulation of the Collapse of Plasco tower in fire using an integrated simulation approach. (Invited: **Fire Safety Journal**, special issue for SiF 2024, Coimbra)

Based on Chapter 7 of the thesis

DOMADA R*, Khan A. A., Khan M. A OpenSees Simulation of the Collapse of Plasco tower in the fire. **(Draft)**

Other publications

Domada, R*, Khan, A. A., Orabi, A., & Usmani, A. (2024). OpenSEES simulation of the Plasco tower collapse using an integrated simulation approach. *Proceedings of the 13th International Conference on Structures in Fire (SiF 2024)*, 1265–1277.

Domada R*, Asif Usmani (2024). “A model-scale experimental study of tall building collapse in fire”. *CONFAB 2024, 4th International Conference on Structural Safety under Fire and Blast Loading, Proceedings. London*.

Khan, A. A., **Domada, R. V. V***, Huang, X., Khan, M. A., & Usmani, A. (2022, April). Modelling the collapse of the Plasco Building. Part I: Reconstruction of fire. In *Building Simulation* (Vol. 15, No. 4, pp. 583-596). Beijing: Tsinghua University Press.

Khan, A. A., Khan, M. A., **Domada, R. V. V^{*}**, Huang, X., Usmani, A., Bakhtiyari, S., ... & Aghakouchak, A. A. (2023). Fire modelling framework for investigating tall building fire: A case study of the Plasco Building. *Case Studies in Thermal Engineering*, 45, 103018.

Domada, R^{*}, Yarlagadda, T., Jiang, L., & Usmani, A. (2023, August). Preliminary Stage OpenSEES Simulation of the Collapse of Plasco Tower in Fire Check for updates. In *Proceedings of the Indian Structural Steel Conference 2020 (Vol. 1): ISSC 2020* (Vol. 318, p. 143). Springer Nature.

Ramakanth Domada^{*}, Tejeswar Yarlagadda, Liming Jiang, Asif Usmani (2019). “Preliminary analysis of the collapse of Plasco tower under fire using OpenSEES”. *CONFAB 2019, 3rd International Conference on Structural Safety under Fire and Blast Loading, Proceedings. London*.

Dedication

I dedicate this thesis to the memory of my late grandmother and mother, as well as all the women—sisters and teachers—in my life who have supported and nurtured me. Without them, I would not have achieved this milestone.

I also dedicate this thesis to all the Hong Kong taxpayers, whose contributions have enabled me to pursue my education and research.

Acknowledgements

I am deeply grateful to Prof. Usmani, my supervisor, for his invaluable guidance, unwavering support, and funding throughout my PhD journey. Over the past few years, he has been an invaluable mentor, guiding my studies with great wisdom.

My sincere appreciation goes to Dr. Liming, my co-supervisor, for his invaluable assistance with the OpenSees software. His guidance has been crucial in navigating its intricacies, which has significantly helped my research.

I am sincerely thankful to Dr Aatif Khan for his exceptional collaboration on this project. His dedication and cooperative approach have greatly enriched this research. I thank Dr. Yarlagadda for his guidance in modelling structures in OpenSees and his support in utilising the GiD+OpenSees interface. I sincerely thank Dr Anwar Orabi for providing his GiD version and facilitating the automation between the FDS and OpenSees models. Your support has been invaluable in streamlining our work processes. I express my gratitude to my friends Dr Melagoda, Dr Mustesin Khan and Ms Nandini Ravi for their assistance in reviewing and providing feedback on the thesis chapters. I thank you for your time in helping me improve the quality of my thesis. I thank my examiners Prof. Kazunori HARADA (Kyoto University) and Prof. Weiyong WANG (Chongqing University) for taking the time to read my thesis and for their valuable suggestions, which have contributed significantly to its improvement.

I am grateful to Prof. Pradeep Bhargav for his mentorship and financial support during my time at IIT Roorkee. His kindness and nurturing were instrumental in my journey to Hong Kong. I also extend my gratitude to Prof. Ashok Pandey for sharing his wisdom and encouraging me to pursue higher education. Furthermore, I would like to thank my teachers at IIT Roorkee, Prof. Manish Shrikhande and Prof. Yogendhra Singh, for their unwavering support throughout my journey to Hong Kong.

I am also indebted to Prof. C.N.V. Satyanarayana Reddy for his assistance and guidance during my time at Andhra University. Lastly, I express my most profound appreciation to my high school mentors and teachers, especially T. Subbarao (late), for igniting my scientific curiosity and passion.

Contents

Chapter 1: Introduction	1
1.1. Background	1
1.1.1. Fire incident	2
1.1.2. Architectural details	2
1.2. Field investigation	6
1.2.1. Reconstructed layout	9
1.2.2. Material testing	12
1.2.3. Occupancy of the tower	13
1.3. Safety assessment of the building (Shakib et al. (2018))	14
1.4. Need for analysing tall buildings against fires	14
1.5. Experimental simulation of tall building collapse	15
1.5.1. Construction of composite beam	16
1.5.2. Construction of the frame	21
1.6. Conclusions	26
1.7. Objectives of the thesis	26
1.8. Outline of thesis chapters	27
Chapter 2: Literature Review	31
2.1. Introduction	31
2.2. Tall building response against fires	32
2.3. Review of the Plasco tower investigations	37
2.3.1. Investigation by Behrouz Behnam	39
2.3.2. Investigation by Shakib et al.	42
2.3.3. Investigation by Aghakouchak et al.	48
2.3.4. Investigation by S. Epackachi et al.	52
2.4. Understanding the fire accident	56
2.4.1. Investigation by Khan et al.	56
2.4.2. Investigation by Ahmadi et al.	59
2.4.3. Investigation by Khan et al.	63
2.5. Using OpenSees for fire investigations	71
2.5.1. Introduction to OpenSees	71
2.5.2. Developing the OpenSees for fire	72
2.5.3. OpenSees analysis of structures against fires	73

Chapter 3: Robustness Analysis of Plasco Tower under Fire Conditions.....	77
3.1. Motivation for the study.....	78
3.2. Structural integrity of the Plasco tower	79
3.2.1. Classification of the collapse	80
3.2.2. Review of the structural arrangement	85
3.3. Finite element modelling	92
3.3.1. OpenSees for fire	92
3.3.2. Model description.	92
3.4. Gravity load transfer mechanism	95
3.5. Robustness analysis of the Plasco tower.....	100
3.5.1. Core columns	100
3.5.2. Primary beams	103
3.5.3. Secondary main columns	108
3.6. Conclusions.....	115
Chapter 4: Investigation of the Plasco Tower Fire	118
4.1. Introduction.....	118
4.2. The case of the WTC investigation.....	118
4.3. Fire investigation	119
4.3.1. Investigation aids	120
4.4. Fire in the Plasco tower.....	121
4.5. Reconstruction of the fire spread	127
4.6. Fuel distribution	129
4.7. Calibration of the fire.....	129
4.7.1. Vertical fire spread.....	130
4.7.2. Horizontal fire spread	132
4.7.3. CFD model calibration.....	133
4.8. Conclusions.....	134
Chapter 5: Analysis of the Plasco Tower Using the OpenFIRE approach.....	136
5.1. Introduction.....	136
5.2. A review of the attempts to couple CFD and FE software	138
5.3. Introduction to OpenFIRE	140
5.3.1. On extracting compatible FDS output	140
5.3.2. Coupling in OpenFIRE (Khan et al. (2023))	140
5.3.3. Modules of the middleware	142

5.4.	OpenSEES Modelling	148
5.4.1.	General modelling philosophy and aims and scope of the simulation.....	148
5.4.2.	Structural details of the building.....	149
5.4.3.	Preliminary analysis with Standard fire.....	150
5.5.	Modelling the fire	155
5.6.	Plasco tower analysis using OpenFIRE framework.....	156
5.6.1.	FDS Analysis	156
5.6.2.	Heat Transfer Analysis	159
5.6.3.	OpenFIRE coupling	160
5.6.4.	Thermo-mechanical analysis	162
5.6.5.	Structural response.....	163
5.7.	Conclusions.....	177
Chapter 6: Analysis of the Plasco Tower Using an Integrated Simulation Approach		179
6.1.	Introduction.....	179
6.2.	Aims and objectives.....	180
6.3.	Software integration approach	181
6.4.	Modelling the fire	183
6.4.1.	Timeline of the accident	183
6.4.2.	CFD modelling and analysis.....	184
6.4.3.	Resolution of the thermal load applied	188
6.5.	OpenSees Modelling.....	190
6.6.	Heat Transfer Analysis	192
6.7.	Structural response.....	194
6.7.1.	Response against ISO 834 fire.....	194
6.7.2.	Effect of composite floor action	202
6.7.3.	Response against CFD-based thermal load.....	206
6.7.4.	Comparison of the response against ISO 834.....	208
6.8.	Conclusions.....	210
Chapter 7: Collapse Simulation of the Plasco Tower		212
7.1.	Introduction.....	212
7.2.	Objectives of the chapter	213
7.3.	CFD-FE coupling scheme.....	213
7.3.1.	FE model.....	213

7.3.2.	CFD model.....	213
7.3.3.	Coupling	213
7.4.	Analysis parameters	217
7.4.1.	Heat transfer analysis.....	217
7.4.2.	Thermo-mechanical analysis	217
7.5.	Preliminary evaluation of thermal response	217
7.5.1.	16 minutes after fire initiation	219
7.5.2.	33 minutes after fire initiation	220
7.5.3.	50 minutes after fire initiation	221
7.5.4.	1 hour and 40 minutes after fire initiation	222
7.5.5.	2 hour and 50 minutes after fire initiation	223
7.5.6.	Moments before global collapse (i.e., 3 hours and 20 min after fire initiation).....	224
7.6.	Comprehensive analysis of thermal response	225
7.6.1.	Partial collapse of NW corner floors	225
7.6.2.	Interim developments	237
7.6.3.	Moments before the final collapse.....	240
7.6.4.	Global collapse	247
7.7.	Discussion.....	255
7.7.1.	Framing.....	255
7.7.2.	Structural segmentation	257
7.7.3.	Structural continuity	258
7.7.4.	Segmentation vs continuity.....	258
7.7.5.	Firefighting	258
7.8.	Conclusions.....	260
Chapter 8: Conclusions and future work		263
8.1.	Evolution of the research	263
8.2.	Insights from the research.....	264
8.2.1.	Plasco tower collapse pattern.....	264
8.2.2.	Weaknesses of Plasco tower against fires.....	265
8.2.3.	Predicted reasons for the collapse.....	265
8.2.4.	What if connections did not fail?.....	265
8.3.	Future work.....	266
8.3.1.	Fire-induced structural collapses	266
8.3.2.	Optimising firefighting efforts.....	266

8.3.3. Resolution of CFD-FD data mapping	266
References	267

List of Abbreviations

N	:	North
E	:	East
W	:	West
S	:	South
NW	:	Northwest
NE	:	Northeast
SW	:	Southwest
SE	:	Southeast
H	:	Length of the column between floors
FE	:	Finite Element
CFD	:	Computational Fluid Dynamics
FDS	:	Fire Dynamics Simulator
HT	:	Heat Transfer
F	:	Floor
(like in 11F)		
HVAC	:	Heating Ventilation and Air Conditioning
HRR	:	Heat Release Rate
DCA	:	Demand to Capacity Ratio
TDA	:	Temperature Domain Analysis
UNP	:	European Norm Channel
ISE	:	Integrated Simulation Environment

Chapter 1: Introduction

1.1. Background

Habib Elghanian, a renowned entrepreneur, built the Plasco building in 1962 (Figure 1.1) during a period of swift expansion in Iran. The building derived its name from his plastics enterprise. Upon completion, it stood as the tallest building in Iran, symbolising progress and modernisation during the reign of Shah Mohammad Reza Pahlavi and becoming a notable feature in Tehran's skyline.

The government seized the building after the 1979 Iranian revolution and transferred ownership to the state-controlled Islamic Revolution Mostazafan Foundation. The Mostazafan Foundation managed the building until its collapse. At the time of the fire, the Plasco building was used as a residential and commercial building, with a major shopping centre on its ground floor, a restaurant on its upper floor, and several clothing workshops.



Figure 1.1 View of the tower in the 1960s (Source: Wikimedia Commons (1961))

The Plasco tower is a 20-story high-rise (5 floors below and 15 floors above ground) landmark building in Tehran, the capital city of Iran. It was the tallest building in Iran and was considered an iconic part of the Tehran skyline.

1.1.1. Fire incident

The building caught on fire and collapsed on 19 January 2017. The collapse of the tower (Figure 1.2) resulted in the loss of lives of over 20 firefighters. Approximately 200 firefighters worked tirelessly to combat the fire in the tower, which tragically collapsed in a brief period. Additionally, around 70 individuals sustained injuries, with 23 of them in critical condition after the rescue.



Figure 1.2 Post-collapse view of the tower (BBC (Middle East), 2017)

The investigation of the Plasco tower fire incident differs from other incidents like WTC, as basic information about the structural system is unavailable. Details like the spacing of columns, floor heights, the thickness of slabs, and the strength of the concrete are determined after the collapse. This chapter deals with the background of the Plasco tower fire incident and how investigators depended on the post-collapse survey for gathering structural and architectural information. The reconstructed drawings helped investigators conduct a preliminary tower analysis (Govt. of Iran (2017)).

1.1.2. Architectural details

Plasco building combines two truss floor-based structures (see Figure 1.3) – a passage structure of 5 floors and a 16-storey tower which caught fire and collapsed. The tower part of the

building was constructed on a floor plan of 1000 square meters, whereas the 5-floor storey structure is on a land area of 3200 square meters. The building had a floor area of more than 33000 square meters. Both these structures are architecturally connected but structurally isolated; this can be seen in the photos taken during the construction stage of the building, see Figure 1.4.



Figure 1.3 Full view of Plasco building showing both the 16-storey tower and 5-floor passage structure (Source: Architizer)

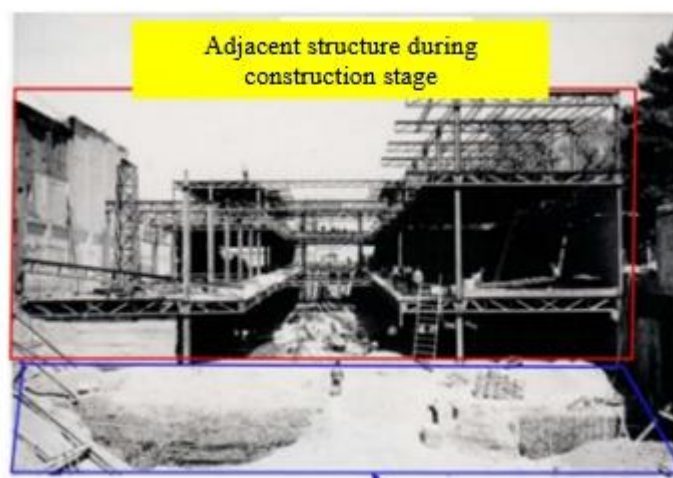


Figure 1.4 Photo of the 5-floor adjacent structure during the construction phase (Govt. of Iran (2017))

The five-floor passage structure had a specific purpose and usage. It had a large opening (atrium space) from the ground floor to the fourth floor and was absent on the fifth floor, as seen in Figure 1.5. The size of the opening reduced as we moved from the ground floor to the upper floors.



Figure 1.5 Atrium opening in the 5-floor passage structure (Govt. of Iran (2017)).

The passage structure did not collapse during the fire and was helpful for engineers and investigators in gathering crucial information about structural members. As no drawings existed, investigators measured the floor distances and the centre distance of columns from this 5-storey surviving structure. Photographs of the building gathered from the building users were also used to prepare architectural drawings in several stages by matching with multiple versions and correcting in each stage; as an example, the prepared layout of the 14th floor of the tower is shown in Figure 1.6. More details about the field survey are presented in the next section.

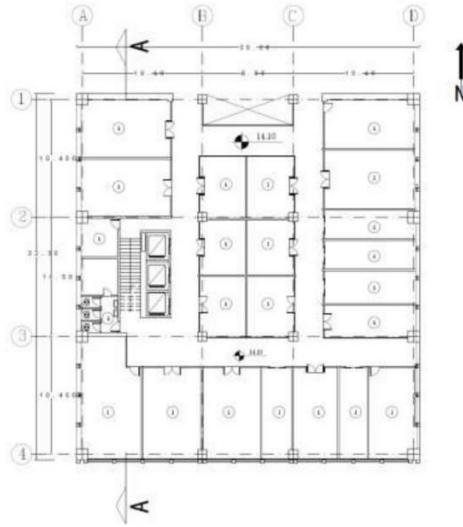


Figure 1.6 The layout of the 14th floor of the tower (Govt. of Iran (2017)).

The Plasco tower has been one of the most important places of business significance since its inception. The tower housed nearly 570 commercial units (fabric businesses) and was one of the first high-rise buildings in the city of Tehran and the country of Iran (Govt. of Iran (2017)). It was regarded as a symbol of modernity in the city for its bold architecture. The photograph of the façade on the south side shows the tubular (made using channel sections) sections and the bracing and non-load-bearing walls on the south side, as seen in Figure 1.7.



Figure 1.7 View of the building in later stages (Govt. of Iran (2017)).

1.2. Field investigation

The lack of both structural and architectural drawings posed a significant challenge to investigators and researchers trying to carry out a preliminary collapse analysis of the Plasco tower (Shakib et al. (2020) & Behnam (2019)). The only critical information investigators could obtain was from studying the surviving parts of the building and the fallen debris on the ground.

To identify and determine the types of steel members used for the main truss beam, secondary truss beam, Vierendeel truss beams and edge trusses, an extensive field survey was conducted. Also, existing photos and videos were gathered. Photos taken during the field survey are presented in Figure 1.8, Figure 1.9 and Figure 1.10.



(a) Survey of the location and dimensions of surrounding walls.



(b) Measurement of the distance between the columns on the west side.



(c) Measurement of the U-shaped wall in the middle of the building.



(d) Measurement of column distances using laser meter.

Figure 1.8 Photos taken during the post-collapse field survey for establishing the location of columns and spacing (Govt. of Iran (2017)).



(b) Secondary column



(a) Secondary main column



(c) Vierendeel beam

Figure 1.9 Photographs taken during the post-collapse field survey (Govt. of Iran (2017)).



(a) Corner column



(b) Core column



(c) Core column



(d) Secondary main columns



(e) Measurement of thickness of truss members



Figure 1.10 Photographs of column members found in debris (Govt. of Iran (2017)).

By conducting numerous field visits and studying available photo evidence, investigators like Behnam recreated structural and architectural drawings showing the location of columns and section dimensions of all structural members used for the tower.

1.2.1. Reconstructed layout

The Plasco tower had four central main columns, eight secondary main columns, four cruciform-shaped corner columns, and 32 box-shaped minor secondary columns (see Figure 1.13 and Figure 1.14). The arrangement of the columns is shown in Figure 1.11.

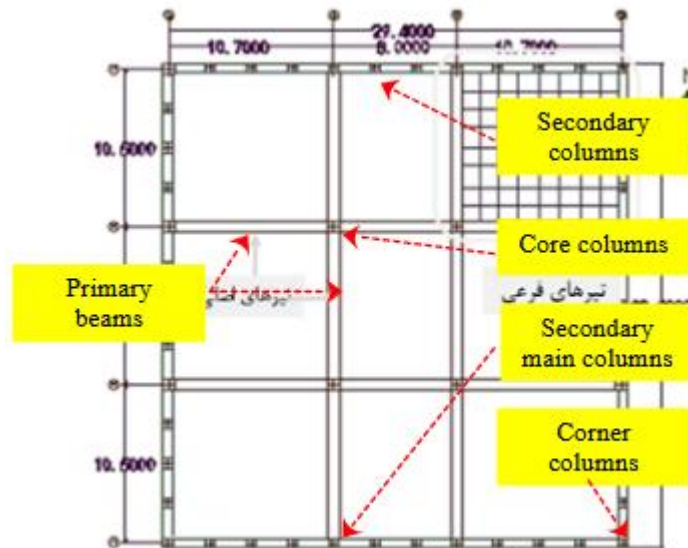


Figure 1.11 Reconstructed layout of the tower showing the location and spacing of columns (Govt. of Iran (2017)).

The plan of the tower is near square with a North-South (NS) length span of 32.8m and an East-West (EW) span of 29.4m. At the centre lie 4 core columns placed 10.5m apart in the NS direction and 8.0m in the EW direction. Along the periphery, it is observed that in North and South faces, there is an additional column when compared to East and West faces.

The floor system is made up of 3 structural components. They are...

- Primary truss beams
- Secondary truss beams
- Vierendeel truss beams
- Edge beams

There are two sets of primary truss beams which connect core columns with the main secondary columns; see Figure 1.12(a). This setup forms the basic skeleton, which transfers the majority of gravity loads to the foundation. Along the NS direction, secondary truss beams are

present, while in the EW direction, Vierendeel beams are present, and along the perimeter edge, truss beams are present connecting all columns along the boundary, including the cruciform-shaped corner columns, see Figure 1.13(c) and (d). Evidence of prestressing is found in Vierendeel beams as parabolic tubes are found in the debris; see Figure 1.12(b), (c) & (d).



(a) Photo of the floor truss system taken during the construction stage.



(b) Parts of distorted Vierendeel beam parts found in the debris.



(c) Bolted connection in the debris

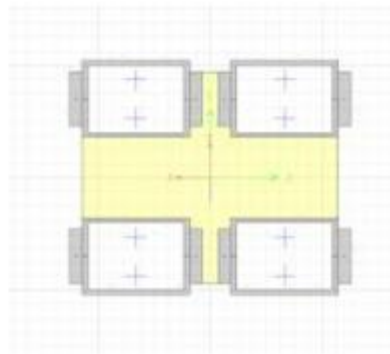


(d) Prestressing steel tubes in the debris.

Figure 1.12 Floor truss system of the Plasco tower (Govt. of Iran (2017)).



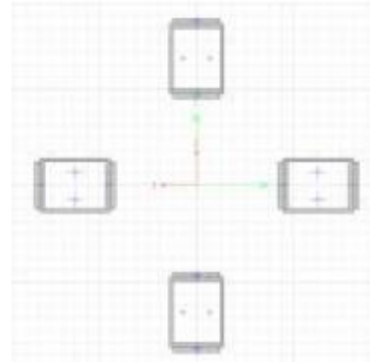
(a) Photo of collapsed core column



(b) Reconstructed detail of core column: 8 x Channel UNP 200



(c) Photo of collapsed corner column

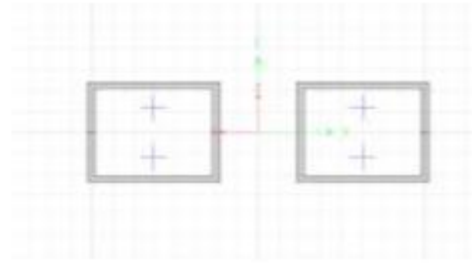


(d) Reconstructed detail of corner column: 8 x Channel UNP 160

Figure 1.13 Details of the core and corner columns (Govt. of Iran (2017)).



(a) Photo of collapsed main secondary column



(b) Reconstructed detail of Main secondary column: 2 x Channel UNP 200



(c) Photo of collapsed minor secondary column



(d) Reconstructed detail of minor secondary column: Channel UNP 200

Figure 1.14 Details of the secondary main and secondary columns (Govt. of Iran (2017)).

1.2.2. Material testing

The strength of the steel, concrete, and reinforcement bars used for the tower should be known to carry out structural analysis. The steel used in the construction is not locally made and was imported; hence, there is not much information about the strength of materials available in Iran's code books or standards. After identifying multiple sampling locations based on different member types (Figure 1.15) strength tests were conducted.

Material strength tests determined the yield strength of the steel used in the core column at approximately $320\text{--}325\text{ N/mm}^2$ and the ultimate strength at approximately $485\text{--}515\text{ N/mm}^2$. However, strength tests on perimeter columns showed yield and ultimate stress at lower values, $240\text{--}270\text{ N/mm}^2$ and $315\text{--}435\text{ N/mm}^2$, respectively. Concrete was sampled at different locations of the surviving parts of the tower, such as columns, beams, walls, and slabs. The values of compressive strength vary from 23.1 to 32 N/mm^2 . In the case of reinforcement bars, 18 tests were conducted for all sizes of rebars, which estimated the yield stress value range to be $315\text{--}360\text{ N/mm}^2$.



(a) A marked location for extracting steel sample



(b) A marked location for extracting concrete sample

Figure 1.15 Sample locations for carrying out material testing (Govt. of Iran (2017)).

1.2.3. Occupancy of the tower

In the beginning days, the usage of the tower was quite diverse, with the presence of film producers, filmmakers, and several other companies. However, gradually, as time went by, the building was occupied by textile businesses, clothing manufacturers and retailers (Ahmadi et al. (2020)& Khan (2022a)). The fuel information available in the literature or local fire department reports predominantly relies on accounts provided by witnesses or fire department staff. As a result, the existing literature does not provide a thorough and organised fire investigation.

1.3. Safety assessment of the building (Shakib et al. (2018))

- (a) **Electrical installations:** The assessment of the electrical installations revealed several issues such as uncertified wiring, lack of emergency power supply, and non-compliance with safety standards. Problems with transformers, wiring, and lack of fire safety equipment aggravated the fire incident.
- (b) **Mechanical equipment:** The mechanical equipment in the building, including power boilers and HVAC systems, played a role in the fire spread. Lack of fire dampers, fire safety systems, and inadequate HVAC systems contributed to the rapid-fire spread and the collapse.
- (c) **Building maintenance:** Lack of proper care and maintenance, non-compliance with regulations, and absence of regular inspections were significant factors leading to the disaster.
- (d) **Fire incident spread:** Fire spread within the building can be attributed to the abundance of combustible materials, lack of fire protection systems, and inadequate firefighting equipment. The absence of fire safety measures and ineffective evacuation procedures worsened the situation.
- (e) **Crisis Management:** Evaluation of the crisis management process revealed shortcomings in evacuation protocols, coordination among response teams, and a lack of emergency preparedness.

1.4. Need for analysing tall buildings against fires

The collapse of the WTC towers 1, 2 and 7 due to fire marked significant events prompting detailed investigations into tall building collapses post-9/11. Research at the University of Edinburgh, in collaboration with Arup, focused on modelling collapse mechanisms for structures like the WTC towers (A. S. Usmani et al. (2003) & A. S. Usmani (2005)).

Based on the research carried out by Lange et al. (2012a) two possible failure mechanisms in multiple floor fires caused by external column failures are discovered – weak and strong floor mechanisms.

- a. The weak floor failure mechanism initiates on a non-fire floor and spreads to adjacent floors above and below. It begins with significant compressive forces on the floor below the fire-affected level, potentially leading to buckling or flexural failure.
- b. Conversely, the strong floor failure mechanism may occur if floors withstand the initial stresses, leading to significant column deflection due to large moments caused by inward deformation near the fire floors.

Therefore, investigating tall building collapses could reveal novel collapse mechanisms, shedding light on previously unrecognised vulnerabilities and failure patterns. The fortunate absence of more catastrophic collapses in tall buildings is partly attributed to significant over-design in horizontal elements, as demonstrated by the Cardington tests (Kirby (2000), Gillie et al. (2002) & Rose et al. (n.d.))

Cardington tests confirmed that the thermomechanical behaviour of structural members when acting as components of a whole structure is significantly different from their behaviour as isolated members in furnace tests. Therefore, a thorough understanding of the global behaviour of structures against fires remains a topic of strong research interest, given the increasing preference for tall multi-storey buildings in modern urban environments worldwide and the unimaginable consequences of such collapses.

1.5. Experimental simulation of tall building collapse

Investigation of the WTC collapse by A. S. Usmani et al. (2003) showed that tall steel buildings could potentially collapse as a result of geometric changes caused by fires, even at relatively low temperatures, unless explicitly designed to prevent collapse. This study aims to investigate the collapse mechanisms of tall buildings subjected to multiple floor fires by experimentally reproducing a strong floor collapse mechanism. An 8-storey 2D composite frame, 2m tall and 1m wide, is constructed using aluminium and steel members and is subjected to a 3-floor fire with maximum member temperatures under 350°C.

1.5.1. Construction of composite beam

Composite steel-concrete floors are structural systems that combine the benefits of steel and concrete materials to create efficient floors in building structures. In a composite floor, composite action between the steel beams and the concrete slab enhances the overall strength and stiffness. During fires, the composite floors experience significant variations in temperature across the slab depth and steel members. Also, due to the influence of varying thermal conductivity and expansion coefficients, composite floors undergo large deformations induced by thermal bowing.

When it comes to building a small-scale 2D model, concrete is not a practical option due to its non-reusability and casting issues. In this context, the composite beam used in this study was constructed using steel and aluminium, as shown in Figure 1.16(c), offers a practical and effective alternative. The idea of employing two different metals is inspired by the working principle of bimetallic strips commonly used in thermostats. A bimetallic strip is a component formed by joining two different metal strips together. This strip is designed to bend when exposed to heat due to the differing expansion rates of the metals. Common combinations include brass and steel, brass and iron, or copper and steel. These metals are chosen for their varying thermal expansion properties, which cause the strip to bend upon heating.

For the current study, steel and aluminium materials are chosen for two reasons.

- a. An aluminium bar expands nearly 2.1 times more than a steel bar under the same temperature and physical dimensions (coefficients of linear thermal expansion for aluminium and steel are $23 \times 10^{-6}/\text{K}$ and $11 \times 10^{-6}/\text{K}$, respectively).
- b. They are widely used in the market and, hence, more accessible to procure.

Spacers are placed to maintain both metals at different temperatures and induce higher thermal gradients. Spacers of 10mm deep are bolted between the steel and aluminium bars at regular intervals; see Figure 1.16(a) and (b). The space between the bars is filled with rock wool as an insulating material. The idea is to expose aluminium to direct fire and insulate steel from the heat as much as possible. However, the steel bar cannot be insulated fully due to the metal spacers used and air convection. The design aims to produce thermal bowing upon heating, representing typical concrete-steel composite system behaviour in fires.

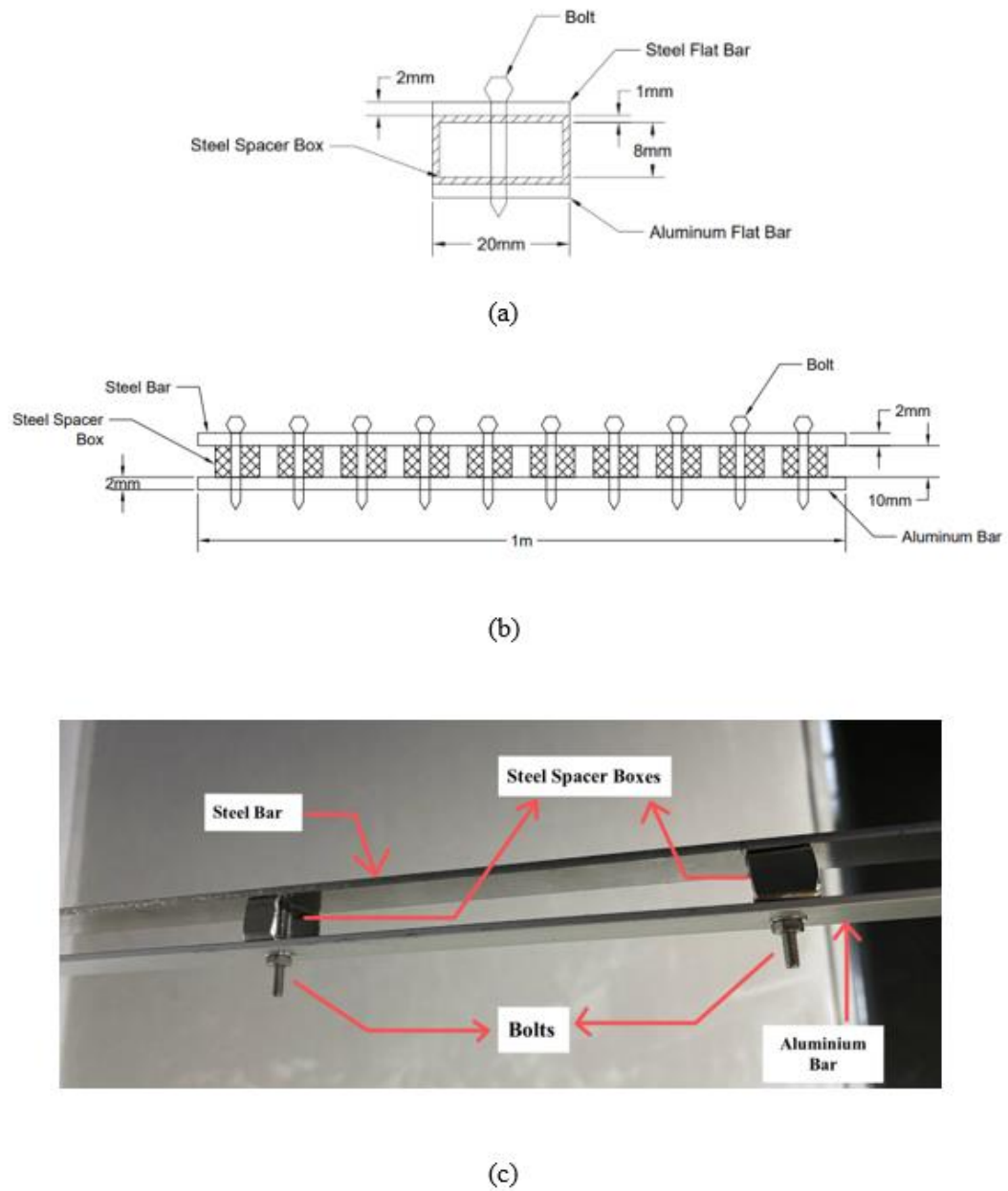


Figure 1.16 (a) Cross section and (b) side view details of the (c) composite steel aluminium beam.

Aluminium material

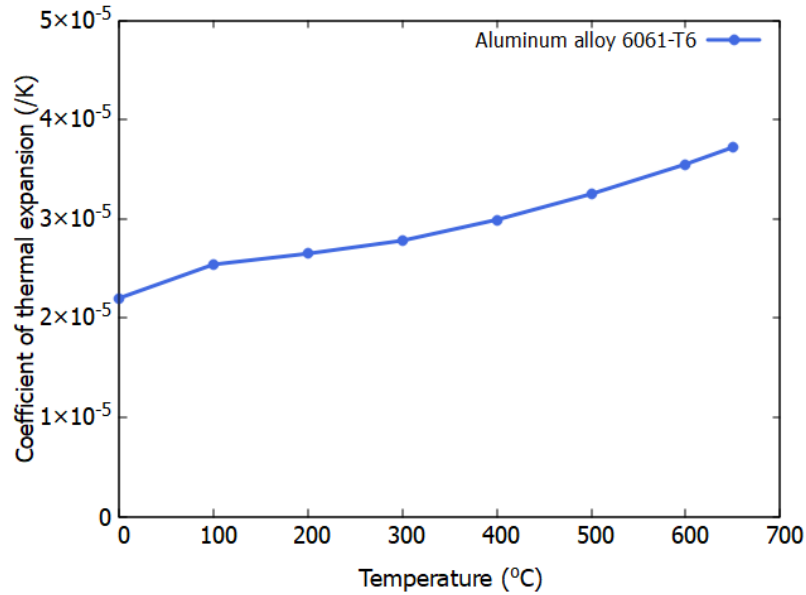


Figure 1.17 Variation of thermal expansion coefficient of aluminium alloy 6061-T6

In OpenSEES, the steel material class `Steel01Thermal` is available to model material behaviour at elevated temperatures, as defined in Eurocode. To model the behaviour of aluminium at elevated temperatures, a new material class with properties based on aluminium alloy 6061-T6 is added to the OpenSEES, see Figure 1.17.

Preliminary test: Thermal bowing simulation

Initially, a single beam is fabricated for experimental evaluation under fire conditions to induce thermal bowing and investigate the effectiveness of rock wool in protecting the steel bar. Subsequently, the observed displacements are compared with results from closed-loop solutions and finite element models developed using OpenSEES to validate the model.

Before the test, rock wool is placed in the space between the steel and aluminium to insulate the steel bar. Solid alcohol is used as fuel to heat the bottom aluminium bar. In the experimental setup, six blocks of solid alcohol fuel are placed under the beam and ignited, as seen in Figure 1.18. The left end of the beam is pinned to the stiff aluminium member, while the other end is placed on a roller support. Thermocouples are placed above the aluminium and steel surfaces to measure temperatures. Significant thermal bowing deformation was observed during the test, which lasted 10 minutes (see Figure 1.18). The slope at the end of the beam was measured to

calculate the downward displacement. For this purpose, a vertical metal bar is bolted near the right end of the beam, see Figure 1.18. The slope is calculated by measuring the rotation of the bar with respect to its initial position, which is roughly estimated to be 11 degrees. Since the beam is not loaded, the deflection profile due to the thermal bowing is assumed to be an arc of a circle. The displacement at the centre of the beam is calculated as 48 mm. The calculations based on the closed-form solution (arc of the circle) estimated deflection at the midpoint to be 56.4mm.

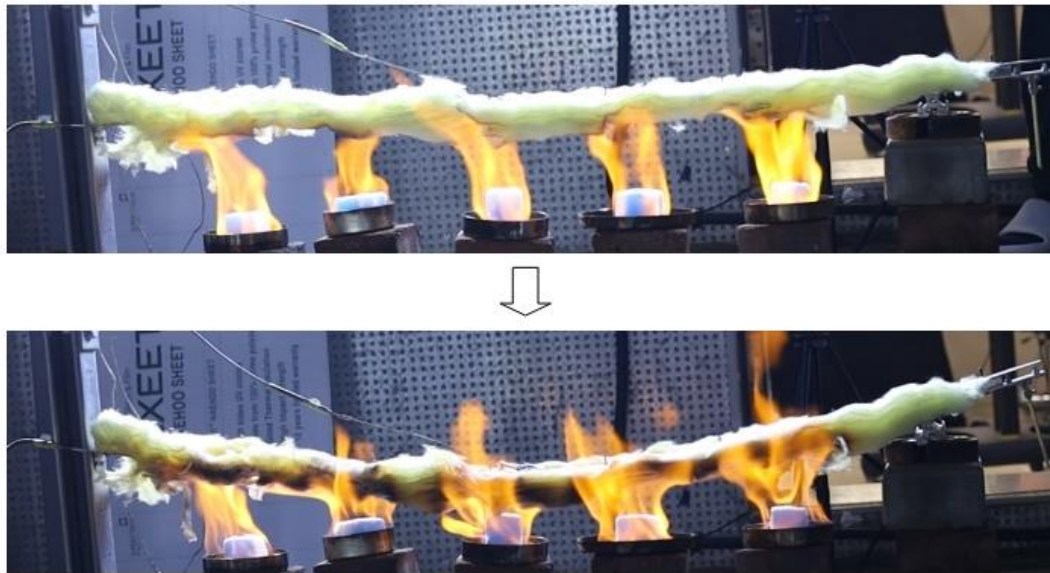


Figure 1.18 Thermal bowing deformation of the beam

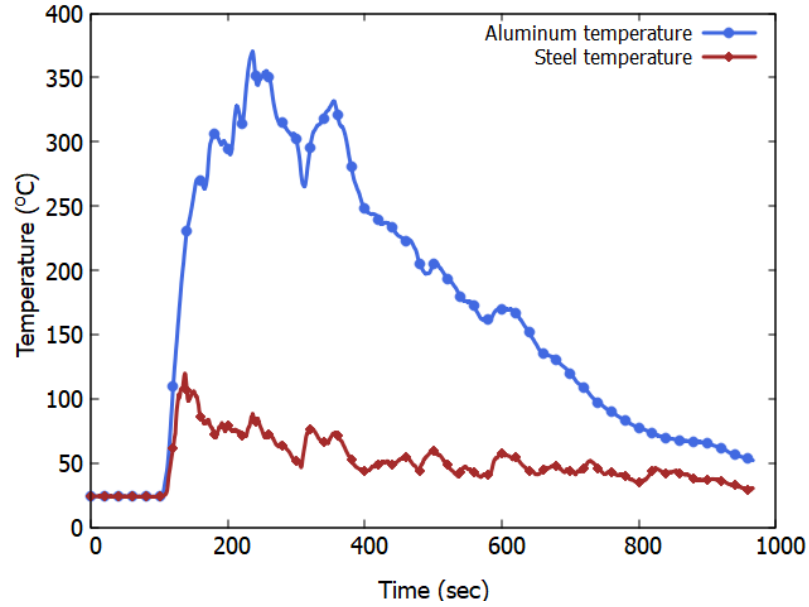


Figure 1.19 Thermocouple output at the steel and aluminium bars

Based on the test, at 30 seconds after the ignition, the temperature difference in steel and aluminium bars is 148 °C, and at 150 seconds it reached 300 °C, see Figure 1.19.

OpenSEES simulation

An OpenSEES model is created by using *dispBeamColumnThermal* class to model the beam. The section is modelled as two rectangular patches – the top patch was modelled as steel, and the bottom patch was modelled as aluminium. The self-weight of the bar is applied as a uniformly distributed load. The insulated steel section is subjected to a uniform thermal load of 150 °C while the aluminium is subjected to a 350 °C. Meshing details are shown in Figure 1.20. The displacements result at every node were extracted, and the profile is plotted in Figure 1.20. The mid-point displacement of the beam is estimated at 54mm. The value predicted by the FE model agrees well with the closed-form solution value, which is 56.4 mm. The discrepancy with the experimental value of 48mm can be attributed to the resistance offered by the supports, which are not ideal roller or pin supports. Therefore, the FE model and the added aluminium material class are validated.

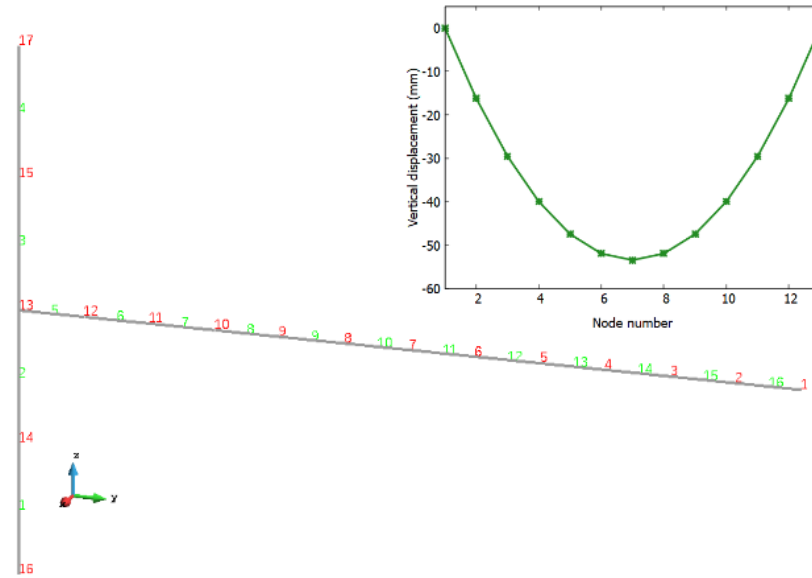


Figure 1.20 OpenSEES model of the beam and deflected profile

1.5.2. Construction of the frame

The frame was constructed by assembling eight (see Figure 1.21) composite steel aluminium beams and using the components listed below.

- (a) **Beam Assembly:** Eight composite beams of 1000 mm long are fabricated. Hinges are bolted to the bottom aluminium bars on either end (Figure 1.22(d)). Only three of eight floors are subjected to fire. Therefore, rock wool is placed on the three floors (Figure 1.22(a)).
- (b) **Column Installation:** The frame model is aimed at representing the 2D model of a tall tubular structure like the WTC towers. Therefore, one end of the beam is attached to a stiff aluminium column representing a rigid core. The other end of the beam is attached to a thinner steel column representing the external columns of tubular structures (Figure 1.21). Both connections to the columns are pinned. The spacing between beams is 250mm.
- (c) **Horizontal Support:** The top of the external column is connected (rotation allowed) to another column using a bar of 1000 mm long to stabilise the 2D frame against the movement in the third direction (Figure 1.22(f)).

- (d) **Fuel support cables:** A pair of steel cables is placed 100 mm below the bottom surface of beams, which are planned to be subject to fire load. Each cable supports six blocks of solid alcohol secured in an aluminium cup (Figure 1.22(b)).
- (e) **Loading:** All beams are loaded using 2 x 1 kg weights, and the top of the column was loaded with a 10 kg load (Figure 1.22(a)).
- (f) **Thermocouple location:** Thermocouples are attached above the aluminium surface, the steel surface of the composite beam and on the external column (Figure 1.22(a)).

The entire assembly was placed on a 5 mm-thick base plate of 500x1200 mm footprint. (Figure 1.22(c)).

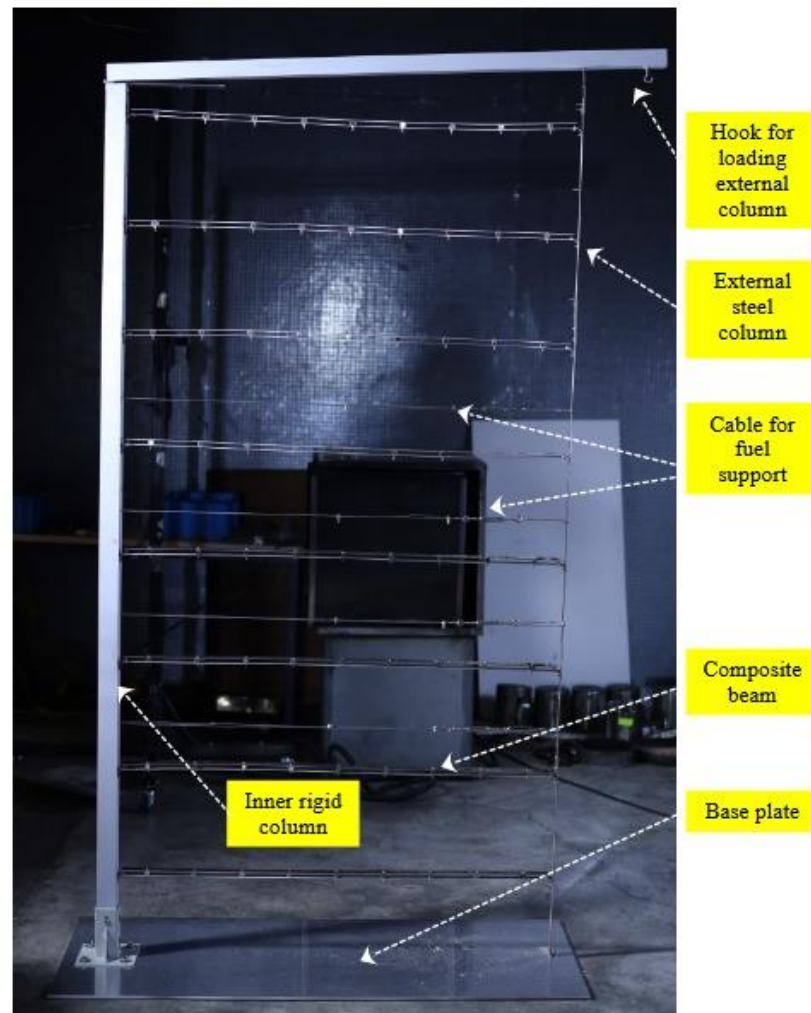


Figure 1.21 Naked frame showing the components



(a)



(b)



(c)



(d)



(e)



(f)

Figure 1.22 (a) Experimental frame set-up showing details - (b) cable support for fuel, (c) base plate, (d) hinge connections, (e) spacer detail and (f) horizontal support

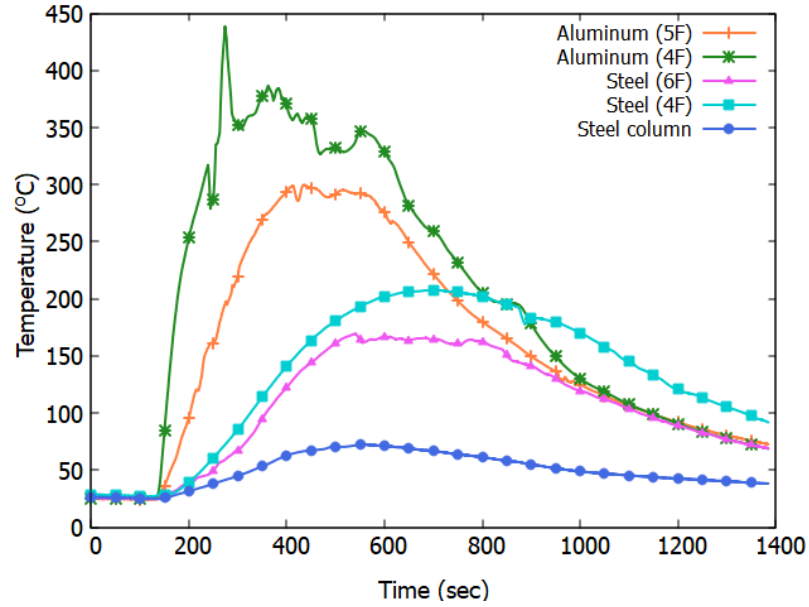


Figure 1.23 Thermocouple output from the main frame test

OpenSEES model

An OpenSEES model representing the 2D composite frame has been created. The beams are modelled using the fibre section approach. Steel and aluminium bars are assigned appropriate material properties. The members were given pinned support conditions where a rigid column was present. The other end of the beam was connected to the external column using equal degree of freedom (*EqualDOF*) constraints. On the left side, the extreme node on the beam is considered a master node, and the corresponding node on the column is considered a slave node.

The top node of the column is subjected to a 10 kg force, while the beam members are subjected to a 2 x 1kg force placed at 1/3rd length points.

Due to the thinness of the members, temperature distribution across the section profile can be assumed uniform. Based on the thermocouple data (Figure 1.23), floors 4,5 and 6 are subjected to 350 °C on the bottom aluminium member and 150 °C on the top steel member. The steel column is subjected to a uniform temperature of 75 °C. Dead load analysis was performed in 10 steps and thermo-mechanical analysis was performed in 100 steps.

Frame response vs simulation

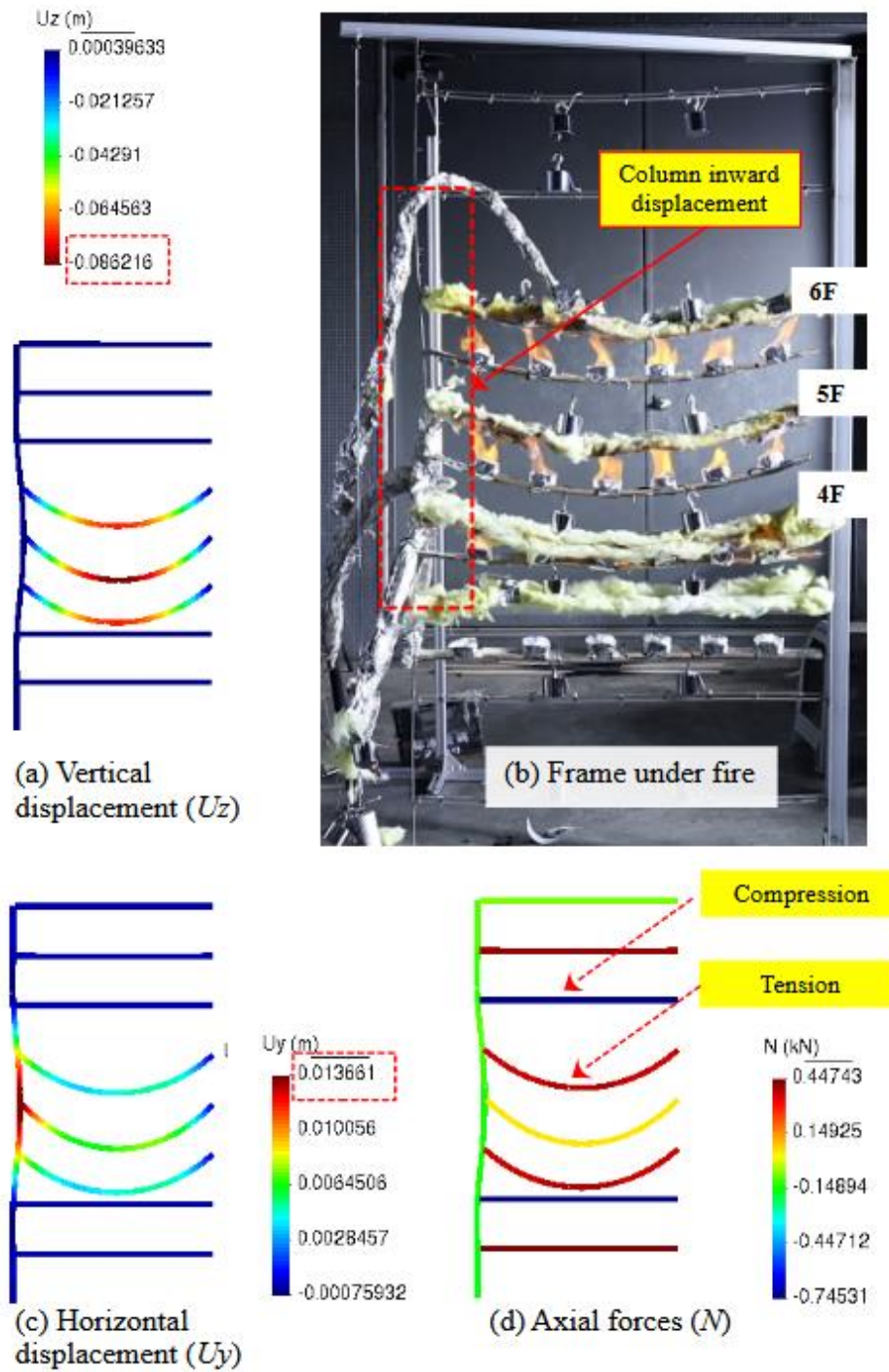


Figure 1.24 Comparison of the deformed frame under fire with simulated response

Deformations in the composite beam (representing the building floors) of the order of $L/100$ (mainly due to thermal bowing) and lateral column displacements of $L/300$ were observed. The simulation predicted a maximum deflection of 86.2 mm on the 4th floor, see Figure 1.24(a).

Maximum inward column displacement of 13.6 mm was observed, see Figure 1.24(d). The three heated beams (or floors) – 4F to 6F are seen under tension, while the beams above and below the heated floors are seen under compression, see Figure 1.24(d). The experiment displayed a deformation pattern tending towards a collapse mode like the one predicted in the numerical analysis of the collapse of the WTC towers.

1.6. Conclusions

The fire experiment with the 2D frame representing tall steel buildings underscores the hazards of fire-induced geometry changes to overall structural stability. OpenSEES software demonstrated its capability to accurately simulate and predict these critical responses, shedding light on the potential dangers of such fires in tall structures. Moreover, this exercise demonstrates a way to build scaled-down physical models for studying collapse mechanisms caused by fires. A scaled-down model of this kind could be of academic (education and research) interest due to its reusability and repeatability and the low cost and convenience of investigating complex thermomechanical behaviours in a controlled laboratory environment.

1.7. Objectives of the thesis

The objectives of the thesis "OpenSees Simulation of the Collapse of Plasco Tower in Fire" are as follows:

1. Analyse the robustness of the Plasco Tower against different fire load scenarios.
2. Integrate Computational Fluid Dynamics (CFD) with the heat transfer and thermo-mechanical analysis modules of the OpenSees software framework.
3. Compare and evaluate two approaches to software integration: one using OpenFire and the other using the GiD+OpenSees interface.
4. Conduct a full-scale forensic study of the collapse of the Plasco tower using the GiD+OpenSees interface. Compare the simulation results with the available visual evidence to validate the accuracy of the models.

These objectives aim to provide a comprehensive understanding of the factors leading to the collapse of the Plasco tower and to contribute to the field of structural fire engineering.

1.8. Outline of thesis chapters

Chapter 1: Introduction

This chapter introduces the Plasco tower fire accident in Tehran (Iran) in 2017. After the fire incident, the local municipality and the investigators appointed by the government released documents (in Persian) after carrying out multiple field studies. As no structural drawings existed, these documents were translated into English with the help of Iranian collaborators and used to develop models for forensic investigation. This chapter provides detailed descriptions of the Tower, the fire accident, and the firefighting efforts carried out until the moment of collapse. This chapter further discusses tall building collapse mechanisms discovered numerically and observed in past accidents like the WTC (2001). A laboratory-scale experiment was also conducted on a composite frame to explain how geometric changes can trigger global collapse, like what was observed in the case of the WTC towers.

Chapter 2: Literature Review

This research project requires reconstruction of the entire fire history – origin, vertical and horizontal travel of the fire, to carry out thermo-mechanical analysis simulating the collapse. This study demands sequential CFD, heat transfer and thermo-mechanical analyses. However, most researchers focused primarily on one aspect only, i.e., either CFD or thermo-mechanical analysis, and relied on simplified methods for the remaining analyses. This chapter presents the earlier research and the hypotheses proposed by the researchers. It discusses the pros and cons of the approaches employed in studying the Plasco tower and/or similar structures.

Chapter 3: Robustness of the Plasco Tower Under Fire Conditions

The 17-storey Plasco tower consisted of four large core columns to safely transfer the gravity loads and 44 peripheral columns to resist the lateral loads. The floor system consisted of primary trusses, secondary trusses, and Vierendeel beams spanning in both directions to support a thin concrete slab. The goal of this chapter is to study the behaviour and robustness of the tower under different fire load scenarios. Owing to the age of the tower, the degree of composite action mobilised between the slab and the truss system cannot be assessed accurately, which makes it difficult to find the structural behaviour and load redistribution mechanisms. This chapter aims to

study the load redistribution occurring under different cases of local fires and is the continuation of the preliminary study conducted.

Chapter 4: Investigation And Reconstruction of the Plasco Tower Fire Incident

This chapter explains the investigation carried out to reconstruct the probable fire scenario that led to the rapid spread of fire in the Plasco Building. To establish a timeline for critical events, data from photos and videos from all four elevations of the tower – East, West, North and South – is gathered. Evidence of fire signatures, such as smoke and fire, is used to decide whether the fire has travelled past a particular zone. The collected data is then organised to establish a coherent timeline of the fire spread. Ten events are identified on the timeline, where *Event 1* indicates the fire initiation and *Event 10* indicates the global collapse. The vertical and horizontal fire spread in the Plasco Tower is reconstructed using CFD fire modelling and calibrated with the evidence library generated. The thermal data obtained from the calibrated fire simulation is transferred to the OpenSees using the OpenFIRE framework.

Chapter 5: Analysing Structures Using the Openfire Framework.

The OpenFire is an integrated computational framework to carry out CFD, heat transfer and thermo-mechanical analysis sequentially developed by the fire team at The Hong Kong Polytechnic University. In this chapter, thermo-mechanical analysis of the severely affected floor of the tower i.e., the 13th floor, is carried out using the OpenFIRE framework with high accuracy in thermal load. This study shows the successful coupling of CFD, heat transfer and thermo-mechanical analyses achieved using the OpenFIRE framework.

Chapter 6: Analysing Structures Using an Integrated Simulation Approach.

This chapter details the approach followed for thermomechanical analyses involving multiple floor fire loading. The integrated platform, based on the GiD+OpenSees interface, combines various software functionalities to carry out thermo-mechanical analysis of tall buildings. The workflow begins with creating a BIM model for creating the basic geometry of a structure, which serves as a starting point for creating both the CFD and finite element models (in

OpenSees). The geometry is imported into the GiD+OpenSees interface and PyroSim for further model building and sequential analyses. The structural response of the multi-story model is simulated by subjecting it to the standard ISO 834 fire in the NW corner of the tower. The study shows the integration approach and offers insight into the behaviour of the corner area with and without the composite action.

Chapter 7: Collapse Simulation of the Plasco Tower

10 events mark the entire 219-minute time span of the fire incident, each indicating a key aspect related to the fire or the structural damage. The timeline starts with *Event 1*, which marks the time of fire initiation and ends with *Event 10*, which indicates the total collapse of the tower. *Events 1* to *7* indicate various stages of fire spread and firefighting efforts, whereas *Events 8, 9* and *10* highlight various levels of structural damage.

- **Partial collapse of the NW corner floors**

This section discusses the structural response against the fire load, representing the fire from *Event 1* to *Event 8*, when the first partial collapse of the NW corner of the tower occurred. The tower survived *Event 8* and was stable for 30 minutes until *Event 10*.

- **Interim developments and local collapses**

This section explains the structural response of the structure against the fire until *Event 9*. It aims to find the possible reasons behind the collapse of multiple floors near the Southeast corner. This marks a critical stage during which the structure was still stable, but for a short duration of 4-5 minutes.

- **Global collapse**

This section focuses on the structural response to the fire between *Event 9* and *Event 10*, which led to the complete collapse of the structure. The intention of this analysis is to simulate the structural response up to the point of instability; hence, the dynamic effects caused by rapidly moving floor systems are not considered. The simulated global response is compared with the available visual evidence at all stages.

Chapter 8: Conclusions

The concluding chapter discusses the probable mechanisms responsible for the collapse of the Plasco tower in a fire. Using the experience gained from the two approaches to software integration, the future direction for improving both approaches is presented.

1.9. Originality of the thesis:

1. Extension of the OpenFIRE framework facilitates the coupling of FDS with large structures. This is the first work that demonstrates a complete forensic investigation for a whole structure where thermal data was obtained from the history of fire on each fire floor. The most extensive work so far carried out by NIST for WTC 1,2, and 7, did the fire spread only on a few floors and did not take the thermal data from the calibrated CFD model. Furthermore, it demonstrates the capability of the open-source tool on a full building scale.
2. Forensic study of tall building collapses using open-source software is demonstrated
3. Analysis of Plasco tower under fire by employing nonlinear material models, evidence-based fire load, heat transfer analysis at a high thermal load resolution and geometric nonlinearity is carried out.
4. Load redistribution mechanisms, moments before the final collapse, were studied.
5. Demonstration of use and management of thermal data for a high-resolution thermo-mechanical analysis.

Chapter 2: Literature Review

2.1. Introduction

Since the collapse of the Plasco tower, multiple researchers have tried to find out how the fire spread occurred and the reasons for the collapse. Unlike the cases of fire incidents like the Triangle Shirtwaist Factory in Manhattan (USA, 1911), Winecoff Hotel (1946) in Georgia, the Windsor Tower in the financial centre of Madrid (2005), and the World Trade Centre Towers (WTC) 1, 2, and 7 in New York (2001), where information of architectural and structural details was available, no information regarding the tower survived the fire and collapse. The lack of information was one of the hurdles the forensic fire investigation faced. Gathering information of the material and structural details is crucial in building accurate computer models. Investigating fire-induced building collapses, unlike earthquake-caused collapses, is not a thoroughly explored area in the field of structural engineering. The study of collapses after the WTC incident raised particular interest among the scientific community. For example, Usmani et al. (2003) developed accurate 2D models of the tower and subjected them to a fire modelled as a generalised exponential time temperature. Their study revealed the inherent vulnerabilities of tall tubular steel buildings against fires. The accuracy of structural fire investigations depends on the information regarding the fire and structure. The detailed NIST reports produced by Gross & Mcallister (n.d.) and Zarghamee et al. (n.d.) after the collapse of WTC were one such example among the others. The NIST's study of the WTC collapse was akin to aeroplane crash investigations carried out by the National Transportation Safety Board (NTSB). A few years before the WTC collapsed, during the mid-1990s, researchers from the University of Edinburgh, Sheffield University, and Imperial College London conducted a series of large-scale fire tests on real structures (wood, steel-concrete composite, and concrete) at the BRE Cardington facility near Cardington, Bedfordshire, England. The tests, famously called the Cardington fire tests, after extensive computational and analytical studies, provided substantial insights into the thermal behaviour of tall buildings (Kirby (2000)). Cardington tests (A. Usmani et al. (2000)) confirmed that the thermomechanical behaviour of structural members when acting as components of a whole structure is significantly different from their behaviour as isolated members in furnace tests. Investigation of WTC collapse by A. S. Usmani et al. (2003) showed that tall steel buildings could collapse because of geometric changes

caused by fires, even at relatively low temperatures, unless explicitly designed to prevent collapse. Therefore, a thorough understanding of the global behaviour of structures against fires remains a topic of strong research interest, given the increasing preference for tall multi-storey buildings in modern urban environments worldwide and the unimaginable consequences of such collapses. After the collapse of the WTC towers, scientific interest in the global behaviour of tall buildings grew immensely.

2.2. Tall building response against fires

The collapse of buildings under fire cannot be ascertained due to material failure. It should be noted that buildings are very likely to fail through a collapse-triggering mechanism even before any significant material softening takes place.

During the design phase, engineers ascertain the section stiffness and lengths among the other parameters. Buildings greatly differ in size, shape, material used, and the floor area they occupy, owing to the purpose for which they are designed. In the study conducted by Lange et al. (2012b), how design parameters affect how a building responds to thermal load was studied. The authors proposed a methodology to assess the vulnerabilities of tall buildings under multiple-floor fires. It was reported that buildings might collapse in case of multiple-floor fires through two different mechanisms. They are called weak floor mechanisms and strong floor mechanisms, see Figure 2.1.

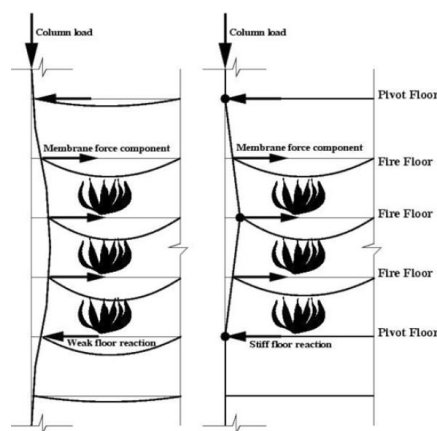


Figure 2.1 Collapse mechanisms in tall buildings under fire

A mechanism can be classified as a strong or weak floor collapse mechanism based on the stiffness ratio between the floor beam and external columns. In a weak floor mechanism, the

structural failure starts in the floors below the fire-affected floors first. From then on, the failure spread to the floors above and below the fire-affected floors. The analytical study showed that the floor immediately below the fire floor experiences huge compression forces in the axial direction, leading to P-delta moments. In addition, development of P-delta moments might cause buckling or bending failure of floor beams. Whereas, if the floor is strong enough, i.e., in the case of a strong floor collapse mechanism, the additional P-delta moments are caused in the columns. This will lead to an inward deflection of the columns near the floor on fire, which will reduce the load-carrying capacity of the columns, which might trigger the collapse of the structure.

Using these two types of categorisations, authors have arrived at a design criterion for calculating the column section capacity, which can help engineers at the design stage in reducing the structural vulnerabilities under fire thermal loads. These studies were carried out using simpler single-beam and frame models. With the help of the understanding gained from these studies and by extrapolating the knowledge, Lange et al. (2012b) attempted to provide a starting point for fire engineers to achieve a safer design of tall buildings against fires. The study demonstrated that the collapse of tall buildings in multiple-floor fires is a distinct possibility due to fire-induced geometric changes in the structure. One of the objectives of this thesis is to figure out the failure mechanism(s) that caused the collapse of the Plasco tower by subjecting the tower to a realistic fire load.

Gillie et al. (2002) carried out structural analysis of the Cardington corner test, and from the results of the study, it was understood that, in the initial stages of fire application, thermal expansion of structural members plays a major role in structural behaviour than any other parameter, like gravity load or degradation of steel material under elevated temperatures. Only in the later stages of fire do gravitational forces become essential because of material degradation and membrane action. The tensile forces in floor beams are due to the catenary action exerting horizontal forces on the external columns.

The conclusions from the Cardington tests showed how thermal restraint affects the floor response. It was observed that restraint arises from the heated areas of the floor as well as from the surrounding unheated areas. In the heated areas, there is thermal restraint against the steel members from the concrete slab. In composite action with steel, the concrete slab restricted steel members from expansion. The concrete has high thermal diffusivity and stays at relatively lower

temperatures. Because of this, high axial compression forces are exerted on the steel members. Under significantly high temperatures, the axial compression forces might cause axial yielding or buckling failure of steel members.

The other form of restraint comes from the relatively cooler areas of the floor surrounding the heated areas. In the case of the Plasco tower, it was known that the fire originated in the Northwest corner of the building (Shakib et al. (2018)). In the preliminary thermo-mechanical study conducted by Domada et al. (2020), thermal expansion of the floor was predominantly noticed outward towards the outer edges of the corner as the relatively cooler inner structure offered restraint to the free expansion. The thermal response phenomena observed in the Cardington corner test were comparable to what was noticed during the initial stages of the thermal response of the Plasco tower.

If restraints were from the floors above and below the heated floor, it would result in high thermal deformations and buckling of steel members, eventually resulting in membrane action. Though not as much restraint is possible in a corner fire as in interior fires, the results have shown that the membrane action will come into action due to high in-plane shear deformation.

The study shows that at elevated temperatures, the floor deformations are not only induced by axial compressions but also due to the thermal gradients in the floor slab (bowing deflection). Under the condition of bowing deformation, the positive thermal strains in reinforcement bars reduce the negative thermal strains induced by building service loads. This effect reduces the chances of rupture in the floor slab, and hence, it is beneficial to the safety of buildings to have slabs that can cope with high strains. However, due to the age of the structure or construction practice involved, the bonding between the concrete and steel members may not be fully mobilised. Hence, in the case of a building like Plasco tower, the thermal response of the floor might be different from the corner test response of the Cardington test building, which is a topic that is worth exploring in future studies.

In concluding remarks of the study, researchers recommended that increasing ductility of the floor system through reinforcement in the slab could delay or even prevent catastrophic events in the case of fire. One of the interesting suggestions made by the authors was to consider using mild steel bars to increase the capacity of slabs to accommodate high strains.

Flint et al. (2007) reported on their investigation of the effects of fire on long-span truss floor systems in a tall building environment. The authors carried out an investigation on a two-dimensional model of a multistorey office building representing World Trade Center Towers 1 and 2. In their study, the effects of fire spread over multiple floors of a building were studied to understand how progressive collapses of tall buildings occur. The local and global response of the model against the three-floor fire load with a peak compartment temperature of 800 °C was simulated. The results showed that large floor displacements may occur without failure in long-span structural floor systems. However, the deforming floors exert forces over the exterior columns that can lead to structural collapse. The study's authors provide a solution that adding structural components like hat trusses can help redistribute the loads away from the exterior columns to the core columns.

Lu et al. (2017) conducted a study on a tall RC building by subjecting it to an extreme fire event that lasted 7 hours before the collapse took place. The study revealed that the outward thermal expansion of the upper floors and the inward contraction of the lower floors induced significant bending deformations in the peripheral columns. The authors observed that when multiple stories were subjected to fire, the axial forces in the columns increased by approximately 100% through horizontal and vertical force redistribution by the Vierendeel truss mechanism, resulting in the collapse of the structure.

A study to assess the robustness of the Shanghai Tower against multiple-floor fires was conducted by J. Jiang et al. (2015). Shanghai Tower is a super high-rise building with mega frame-core-outrigger lateral resisting systems. During the design phase, engineers gave great attention to its structural safety. The authors of the study considered two fire models- standard fire and parametric fire curves. The real fire resistance periods of key components like the concrete core, mega columns, composite floor, outrigger trusses and belt trusses proved far beyond the design fire resistance.

The peripheral steel columns and web members of belt trusses with weak fire resistance were removed to study the resistance of the residual structure against progressive collapse. In this case, the results showed that Shanghai Tower has a minimum of 3 hours of fire resistance. The authors concluded that adding extra fire protection to the outrigger truss guarantees the connection

between the core and mega columns in case of fire. This study highlighted the importance of load redistribution to withstand extreme event fires in tall steel buildings.

J. Jiang & Li (2017) numerically investigated the progressive collapse resistance of a three-dimensional composite concrete steel structure (based on the eight-storey building in Cardington tests) exposed to localised fires using the explicit dynamic analysis capabilities of LS-DYNA. The authors chose a series of fire scenarios and heated individual columns on the ground floor, and the collapse modes and load redistribution scheme of the frame subjected to different load ratios were investigated. The numerical results of the 3D frame showed that in the case of single-column heating (based on the design fire load), the frame collapse took place only when column load ratios reached values of at least 0.5. In the cases of simultaneous four-column heating, the frame collapses occurred when the fire load was applied near the corner or the edge, but it withstood the collapse when the fire load was applied over the internal and edges with shorter spans. The authors, J. Jiang & Li (2017) It concluded that the collapse of tall buildings occurs under uneven or a lack of alternate load redistribution paths. The study showed that the critical temperature for the global collapse was about 50–100 °C higher than that of individual structural components.

Based on the investigations reviewed so far, one can conclude that structures possess reserve capacity against fire loads more than the conventional estimations based on the fire rating of individual structural components. Structures endure fire loads longer than their component parts (as in the furnace test) as alternate load distribution mechanisms come into action. Lamont, Lane, Flint, et al. (2006) argued that the presence of reserves of strength in steel frames resulted in cost savings on projects, as prescriptive fire resistance ratings based on furnace tests ignore load redistribution in real buildings. However, tubular structures with long spans, like the WTC tower, should be approached from a different perspective. Flint et al. (2006) observed that buildings with long-span composite floors can be more insensitive to fires than buildings with conventional shorter spans if not specially designed to resist fire-induced forces.

2.3. Review of the Plasco tower investigations

From the beginning, a lack of information was one of the most prominent challenges researchers faced in the Plasco tower investigation. After the collapse, the authorities in Tehran released two investigation documents in the Persian language. The document titled ‘National Report of Plasco Building Investigation’ was released by the Govt. of Iran (2017) helped extract the basic geometry of the building and the type of sections used in the structure. The report also provided information like post-collapse images of debris, a timeline of the collapse sequence, and other related information that could have been otherwise impossible to gather. Shakib H et al., 2017 published a report on the collapse of the Plasco tower, commissioned by Tehran’s City Council, in which a preliminary structural investigation was conducted using a 3D model developed using the SAP2000 software. In addition, the report provided information on how the firefighting efforts were undertaken from inside and outside the Plasco tower.

Shakib et al. (2018) published a non-technical document assessing the technical and administrative deficiencies of the tower at the time of the incident. The document discussed critical problems in the electrical and mechanical installations that led to the fire break and structural deficiencies. In a follow-up, Shakib et al. (2020) published a paper evaluating the collapse of the tower using simplistic thermal loading. Similarly, the preliminary investigation carried out by Yarlagaadda et al. (2018) too faced challenges due to the lack of information on the fire.

Behnam (2019) conducted a study in which CFD simulation of fire was involved, but it was limited to one compartment only. For this thesis, crucial information needed for modelling the structure was obtained from the works of researchers like Yarlagaadda et al. (2018), Behnam (2019) and Shakib et al. (2020) They are the first few researchers to have published their work in English.

Later, Aghakouchak et al. (2021) & Epackachi et al. (2022) worked on 2D and 3D models with simplistic fire models. Their studies focused on the role of connections in triggering the multi-stage collapse of the Plasco tower.

The first study of the fire investigation in Plasco tower was conducted by Ahmadi et al. (2020) based on the available video and photographic evidence. Khan et al. (2022) conducted a detailed study using the available evidence – photographic, videos, testimonies from firefighters, survivors, and the newly available articles. This study was the most comprehensive so far. He also

conducted numerical simulations to understand how the fire originated and progressed vertically and horizontally. The nature of the studies conducted so far is summarised in the table below. The objectives, assumptions, methodologies, and conclusions derived from the research on the Plasco tower will be discussed in detail in the coming sections.

Study	Study type
Shakib et al. (2020)	Preliminary study.
Ahmadi et al. (2020)	A study on fire spread using available evidence.
Aghakouchak et al. (2021)	A detailed study limited to one part of the tower. A study based on 2D and 3D models with simplistic fire modelling
Epackachi et al. (2022)	A detailed study was limited to one part of the tower.
Khan, Khan, et al. (2022)	Study the effect of different fuel distributions.
Khan (2022a)	Study on the timeline of the fire and CFD analysis.
Yarlagadda et al. (2018)	A preliminary study with simplistic fire loading.
Behnam (2019)	A study based on a composite 2D model with a multifloored thermal load.

2.3.1. Investigation by Behrouz Behnam

Behnam (2019) was there among the team of researchers who conducted site inspections after the Plasco tower collapse. He was one of the first investigators to publish accurate section details of the Plasco building. In his paper, a preliminary investigation of the Plasco tower accident was carried out using a realistic fire load representing the then conditions of the tower. In this investigation, two different structural analyses were performed. The structure was analysed first against gravity, and live loads represented the service state at the time of the accident. For this study, SAFIR, a commercial thermo-mechanical software, was used, which has the ability to carry out the coupled thermal and structural (mechanical) analysis. The study assumed no slip between the concrete slab and the steel truss floor; hence, the shell and beam elements were linked using multiple-point constraints. It should be noted that the loading and the load combinations used for the analysis reflected the changed structure usage from the illegal storage of fabrics and related machinery. The gravity load analysis revealed that the ceiling truss members reached a stress ratio of more than 0.9. Hence, the safety margin was reduced to dangerous levels before the fire accident. In the case of columns, the stress ratio was more than 1.0 for the stories between 1 and 3 and less than 0.5 for the upper stories. On the 10th floor, where the fire accident took place, the stress ratio in the internal columns was 0.74, whereas, for the external columns, it was 0.57, leaving a margin of safety such that these columns could accommodate additional load from the load redistribution caused through the load shedding from the failing columns.

Columns	Stories 1–3	Stories 4–6	Stories 7–9	Stories 10–12	Stories 13–15	Storey 16
Internal	1.27– 1.05	1.02– 0.91	0.86– 0.79	0.74– 0.66	0.59– 0.51	0.45
External	1.08– 0.91	0.87– 0.73	0.69– 0.61	0.57– 0.51	0.47– 0.38	0.33

Table 1 The stress ratios of the columns under gravity load (reported by Behnam (2019)).

Fire modelling and analysis

The authors conducted a CFD analysis using the Fire Dynamics Software (FDS) for this study. The analysis showed that the HRR (Heat Release Rate) rose sharply during the first 50

seconds and then stabilised for the remaining duration of the analysis. Results showed that temperatures increased until 500 seconds of the analysis time, reached a maximum of 1000 °C, and remained almost constant until the end of the analysis. It was assumed that the temperature distribution in the compartment was uniform.

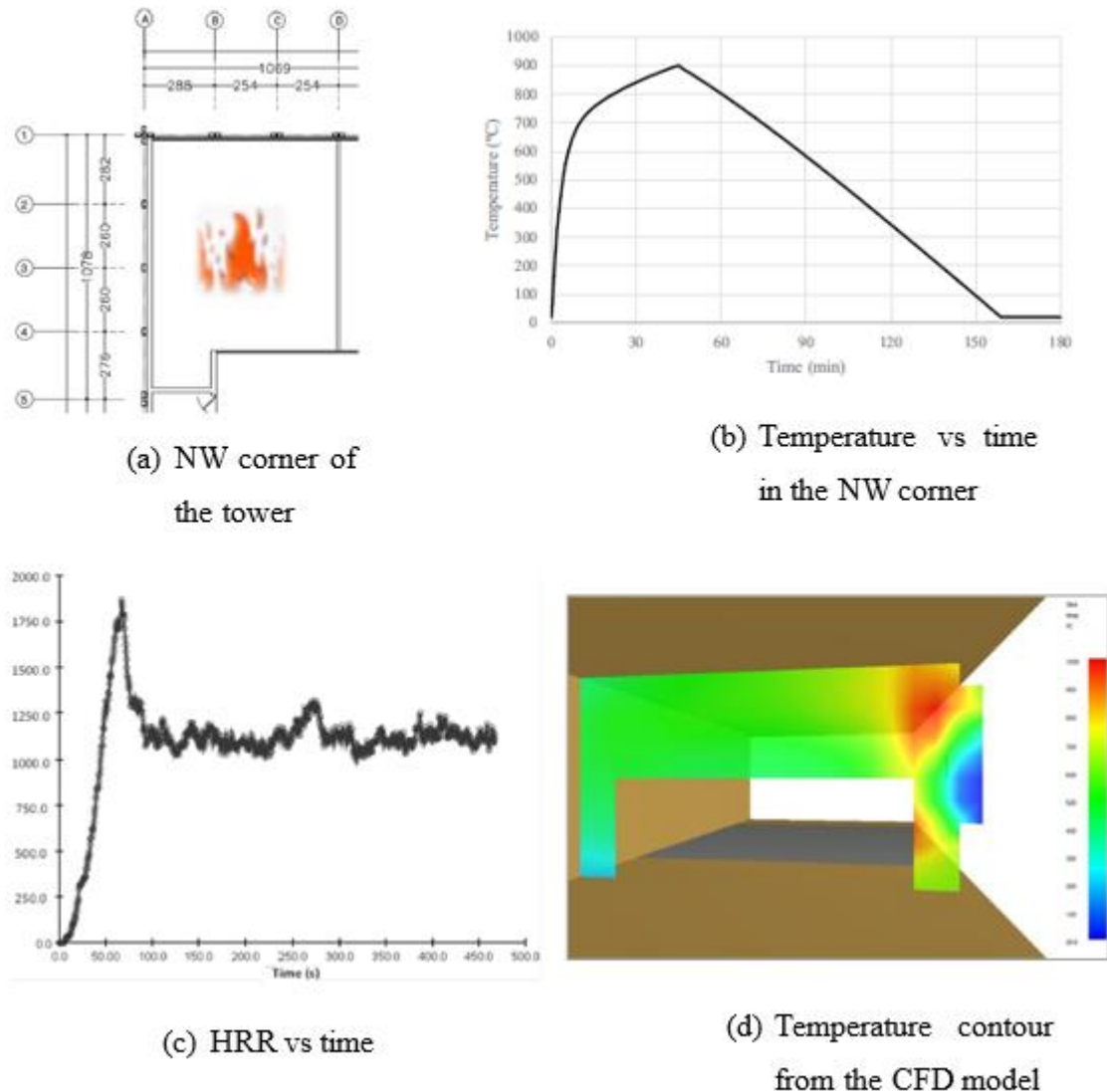


Figure 2.2 Output from the FDS analysis conducted by (Behnam, 2019)

The characteristic fire load for a light commercial building, according to Eurocode 1, is 511 MJ/m². The authors reported that when the structure was simulated against the fire load of

511 MJ/m², no global instability/collapse was discovered. The National Report of the Plasco Building released by the Govt. of Iran revealed that the building owners had stored additional clothing material in the ceiling areas. Hence, for this study, a fire load of 1900 MJ/m², nearly four times higher than the code-recommended value, was considered. Based on the field studies, the increased fire load represented the condition of the building before the accident.

Heat transfer analysis

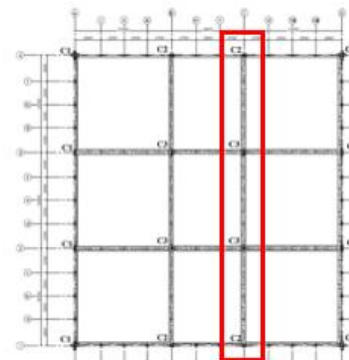
The study assumed that, except for the top of the top chord truss beams, all other members of the truss beams were directly exposed to the fire. The results from the analysis showed that the bottom chord members of trusses reached 650 °C in 15 minutes while the top chord members reached 600 °C. Both bottom and top chord members reached their peak temperature of 900 °C at 45 min fire duration. The maximum and minimum temperatures observed in the concrete slab were 250 °C at the bottom and 150 °C at the top surface.

Thermo-mechanical analysis

Thermo-mechanical analysis was conducted on a 16-storey model with fire load applied in three stages. The visual evidence from the Figure 2.3(a) showed that the collapse was initiated in the frame located on the third axis (Figure 2.3(b)), Hence, it was chosen to carry out this study. In stage one, fire load was applied only on the 10th floor, representing the fire initiation, and in the next stage, fire load was applied over the 11th floor with a 29-minute delay. In the final stage, floors 12-14 were subjected to concurrent fire load, implying minimal time lag (<10min) in fire reaching these floors.



(a)



(b)

Figure 2.3 (a) South tower elevation with external column collapsing inwards; (b) location of the frame chosen for the study.

The failure criteria considered for this study were based on the performance-based design norms advocated by Eurocode 1. According to the standard, the displacements higher than $L/20$ and velocities higher than $L^2/9000d$ mm/min are considered failed, where L is the span length in mm and d is the effective depth of the beam. The displacements and velocities of the heated structural members were monitored during the analysis. In the case of columns, lateral displacement higher than $3H/1000$ was considered a failure, where H is the height of the column. The results showed the frame was stable if the fire was within the 10th and 11th stories. When the fire reached the above three floors, i.e., the 12th, 13th and 14th floors, the nodal velocities higher than the failure limits were noticed. Under the condition of a five-floor fire spread, the results showed that the lateral displacement of the columns gradually increased but never crossed the failure limits. Hence, the columns were not considered as failed. The study concludes that the global collapse of the structure was initiated by the sequential collapse of the floors, leading to a situation with columns without lateral bracing support, which buckled and failed.

In this study, a CFD analysis of fire was performed using natural fire. The temperatures inside the compartment were assumed to be constant. Heat transfer analyses were carried out only on the ceiling trusses. Heat transfer analysis was not carried out on columns, assuming they were fully protected because of partition walls at all stages of the fire. Therefore, this study presumed that the columns had no significant thermal deformation. The maximum temperatures in the columns were taken as 300 °C. This investigation led to the conclusion that the failure of the building had taken place due to the loss of lateral support of the perimeter columns. In this study, a 2D frame was chosen, thereby ignoring the forces and resistance coming from the third dimension.

2.3.2. Investigation by Shakib et al.

In 2020, Shakib et al. (2020) conducted a study to understand the mechanisms involved in the progressive collapse of the Plasco tower. Like Behnam (2019), this study relied on the structural information obtained after field investigations. Information needed to estimate the

service state loads on the day of the incident was gathered by studying the adjacent 5-floor shopping complex that survived the collapse of the tower.

A 3D finite element model was built using SAP2000 software. Abaqus was used for modelling and deriving beam-column interaction, which was then applied as connection behaviour in the SAP2000 model. The secant stiffness obtained from the Abaqus model, categorised as a semi-rigid connection, was used to model the beam-column connection. The authors conducted gravity and live load analysis first and concluded that the strength of the Plasco building structure was adequate to resist the service loading. It was observed that the stress ratio of all the beams and columns was less than one, except for a few columns located on the ground floor. The study revealed that the structure could withstand extra imposed loads. Even though the building had an additional capacity, some elements, like ground floor columns, reached a higher stress ratio due to the change in the occupancy type.

The progressive collapse of the structure was simulated by subjecting the 3D SAP2000 model to various failure scenarios. The authors produced a three-stage collapse sequence based on the scenarios that matched the available photographic/video evidence.

Stage 1: Partial collapse of the NW corner of the tower (10th and 11th floor)

Stage 2: Partial collapse of all the floors from the 11th to the ground floor

Stage 3: Total collapse of the building (31 minutes after stage 2)

The fire, which initiated on the 9th floor (10th as per other researchers like Behnam (2019) and Ahmadi et al. (2020)) spread to the floor above and heated ceiling of the 10th and 11 floors. Due to abundant free air in the corner zone, the fire reached its fullest potential, resulting in very high temperatures. The study showed that only the secondary trusses were damaged, and the primary trusses and columns were not critically affected in the first stage. By the end of this stage, the ceilings of both the 10th and 11th collapsed on the 9th ceiling.

In the second stage, the collapse of all floors in the NW corner of the tower took place. Due to the overloading caused by the fallen 10th and 11th ceilings on the 9th, the connections failed. This led to a sequence of sandwich-style failures of one floor over the other. This left the perimeter columns in the corner freely standing, supported only by the edge beams; this was

supported by the visual evidence, where a few floors were seen missing from the view, see Figure 2.4. Even though considerable damage occurred in the structure, the building was stable for a 31-minute period.

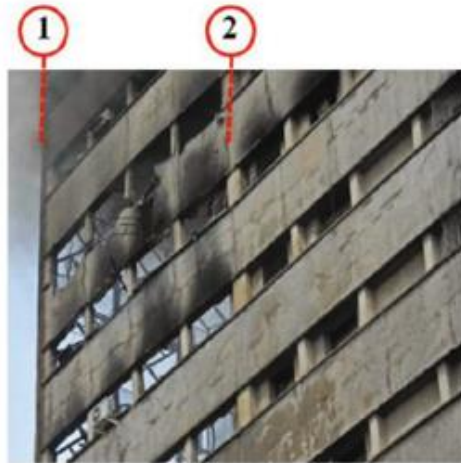


Figure 2.4 The west side view of the corner shows the multiple collapsed ceilings.

Analysing the final stage was challenging; it required the review of many videos and photographs for hours. It was discovered that the failure was initiated near the Southeast corner of the 11th ceiling. The authors reasoned that the fire in this location was severe due to the abundant availability of free air, as in the NW corner in Stage 1. It was believed that global collapse occurred due to the failure of a critical structural component in the zone encompassed by the axes C-D-3-4, as seen in Figure 2.5(a). Three different failure initiation scenarios were identified. They were...

1. Failure of one of the columns
2. Failure of one of the main trusses
3. Failure of secondary trusses

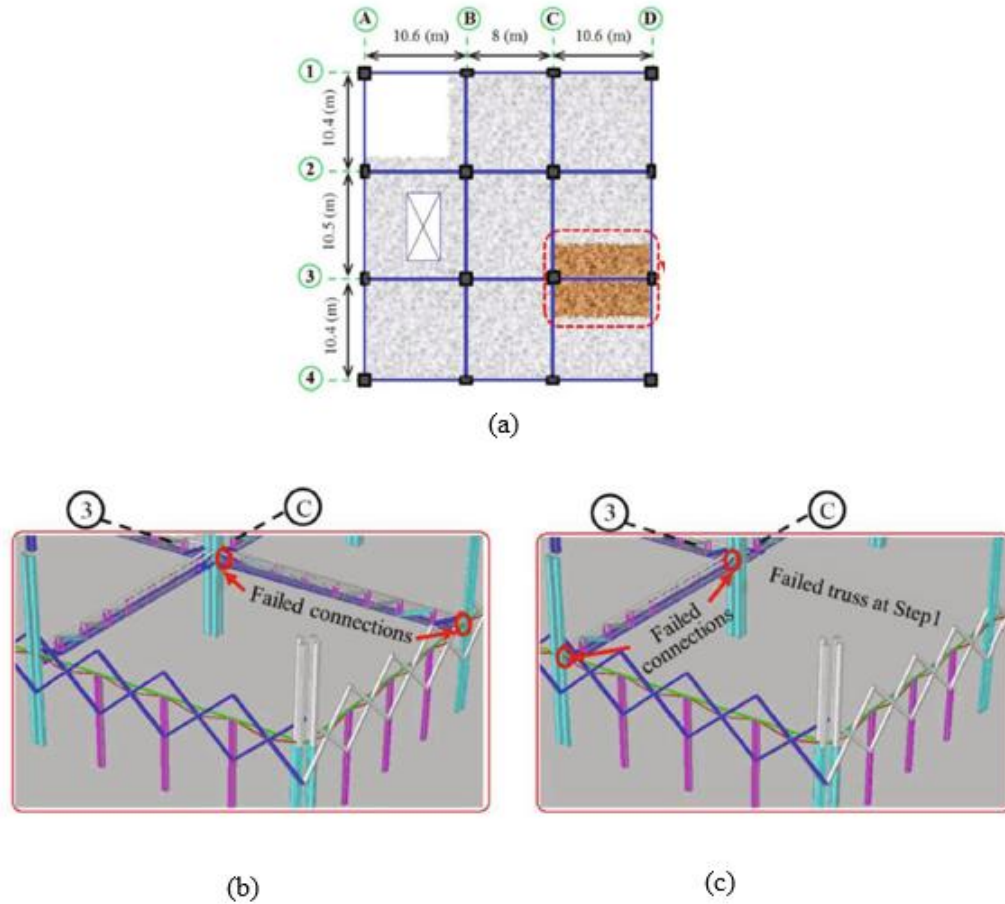


Figure 2.5 (a) Location of Stage 3 collapse initiation; (b) and (c) show the failed connections and trusses in the Southeastern corner of the 9th and 10th ceiling, respectively.
Source: Shakib et al. (2020).

The authors believed that the probability of failure initiation mechanism due to the failure of main trusses (i.e., the second scenario) is higher than the other two scenarios. Failure scenario one was ruled out as no roof deformation was observed in videos or images. Still, it could also be likely that loads were successfully redistributed due to the overcapacity of perimeter columns. The probability of scenario 3 was also lower because it would have resulted in a partial collapse like the NW corner. In the available video evidence, the inward slope of the perimeter column was visible; see Figure 2.5(a). Hence, it is possible that failure was initiated due to the failure of one of the main trusses in the Southeast corner. Since the main trusses had a higher stress ratio, it was highly likely that the main trusses in the corner were more vulnerable to fire. The study estimated that a temperature of 530 °C is high enough to cause the failure.

The authors have created the load combinations necessary for this study based on the standard ‘*Design of the Buildings to Prevent Progressive Collapse*’ by the Department of Defence (2016). When calculating the loading, dynamic loads caused by the failed ceilings were considered by applying the load-increasing factors. As there were numerous local fires during the 3.5-hour fire and due to a lack of information about the fuel, the thermal load was applied in a simplistic way, i.e., uniform temperatures across the depth and along the length of the members.

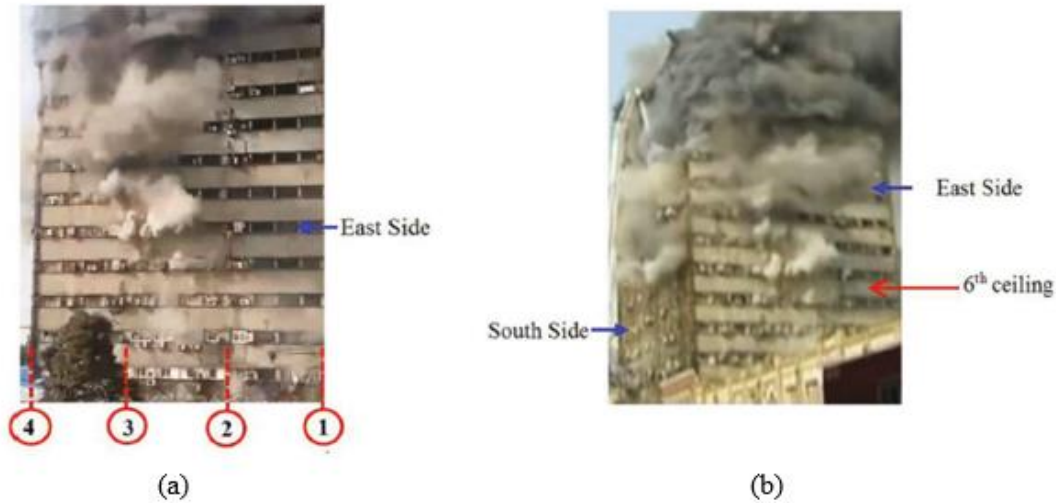


Figure 2.6 (a) Photo showing the inward slope of the South side perimeter columns; (b) dust clouds emerging from the South and East faces of the tower.

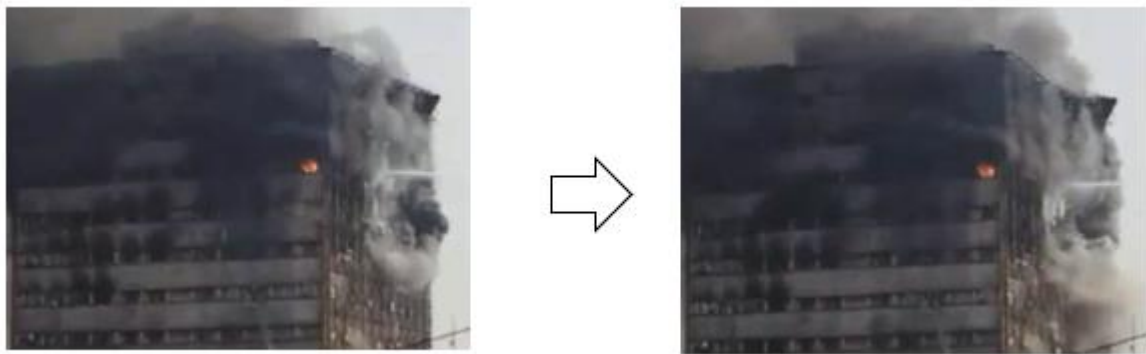


Figure 2.7 Before and after photos showing the downward displacement of the roof near the South face.

In this study, the maximum temperatures of external columns were chosen to be at 450 °C. Structural elements from the 10th to 15th floors were subjected to 550 °C when the fire was nearby and 450 °C for distant fire conditions. The analysis was of a linear static type with consideration

for P-delta effects and geometric nonlinearity. Since the failure was modelled through non-linear beam-column connection interaction, the failure of connections in all three stages of the collapse was studied. The study identifies that connections of the main trusses in the Southeast corner were the most vulnerable of all the connections since DCRs (Demand to Capacity Ratio) were the highest in the corner. By comparing the DCRs of connections and structural members, the authors claimed that the connections were the weakest components of the structure. Hence, the response of connections to elevated temperatures was given importance. The study predicted the failure of connections of the main truss in axes 3-C-D. The collapse was triggered by the loss of the connection between the main truss and the external column at the axes 4-C, which can be validated using the photographic evidence available. Figure 2.7 shows the downward displacement of the roof above the column at the axes 4-C. At this stage, with the loss of connections of the main trusses, identified by the axes 3-C-D and 3-4-C, the floor slabs of the 10th ceiling of the Southeast corner fell on the floor below, causing a sequential failure of all the floors below them. The loss of multiple floors near the southeast zones leads to the condition of external columns without any lateral support. This can be verified by the video evidence, which shows the global inward inclination of the tower at the upper floors; see Figure 2.6(a). Photographic evidence shows the dust clouds emerging from the Southern and Eastern faces of the tower simultaneously, see Figure 2.6(b). Even at this instant in time, the roof near the North and West sides of the tower was seen flat with a slight inclination towards the Southeastern corner. In the final moments, all external columns on the South and Southeastern faces buckled; this caused the floors to pull the perimeter columns on the North and West faces inwards, leading to the global collapse of the structure. The study concludes that the collapse could have been prevented if the connections were designed to be stronger than trusses. In summary, the analyses indicated that global stability was not compromised despite the partial collapse of the floor system in the Northwest corner of the building. The failure of connections between the main trusses and columns led to the global collapse of the Plasco building.

Despite most of the structural elements being designed to overcapacity, the structure failed as there was a lack of additional load redistribution paths. The fire on the top floors (11-16) was detrimental in causing severe dynamic loads due to the sandwich failure of multiple floors. The authors of the study highlight the inadequate design of connection joints and the lack of ductility and continuity in the overall structure. The non-existence of any fire protection strategies and

deficiencies of structural provisions in the design of the building and Iran during the Plasco tower construction were believed to have contributed to the severity of the accident. The drawback of the study lies in unrealistic temperatures applied to the structural members. The study was carried out using linear models with nonlinearity modelled through plastic hinges.

2.3.3. Investigation by Aghakouchak et al.

Aghakouchak et al. (2021) conducted a series of studies to evaluate the local and global response of the Plasco tower through 2D and 3D structural models. Since the fire originated and grew intensely in the NW corner of the tower, a 3D model of the quarter area was developed. The goal was to study the floor and truss behaviour, including the behaviour of connections, the response of joist chords and the concrete floor. Two full-scale 2D and 3D models were developed in the OpenSees and ETABS software to evaluate the global response, respectively.

The quarter model in the Abaqus software was developed with detailed modelling of main truss girders, secondary truss beams, tie beams, and reinforced concrete slabs to simulate the NW corner response in fire, as shown in Figure 2.8. In the Abaqus model, welds joining the steel beams to columns were modelled using surface-to-surface interaction models. The connection between the concrete slab and the top chords of the truss was assumed to be fully composite. The slab was assumed to be fully elastic, and the temperature effects on the concrete were neglected. This study used a simplified fire load by adopting the thermal load in the temperature domain (TDA). Therefore, the temperature applied to the elements was uniform along the length as well as across the depth. Temperatures estimated using the standard fire curve were used to carry out thermal analysis over steel cross sections. This exercise did not predict any collapse other than visible buckling deformation in the top and bottom cords of the truss members at the connections.

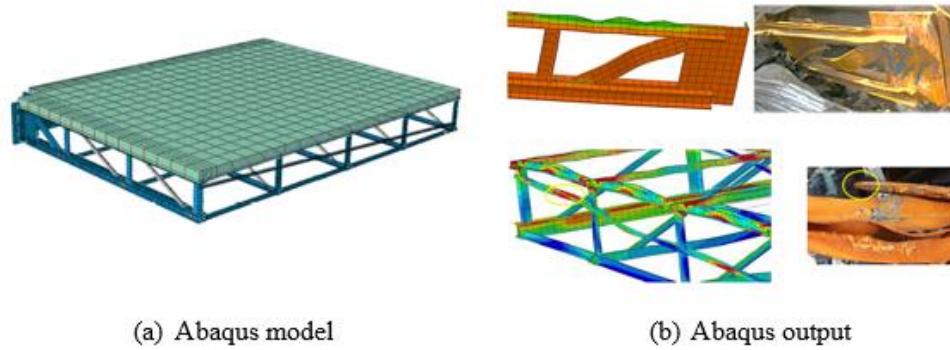
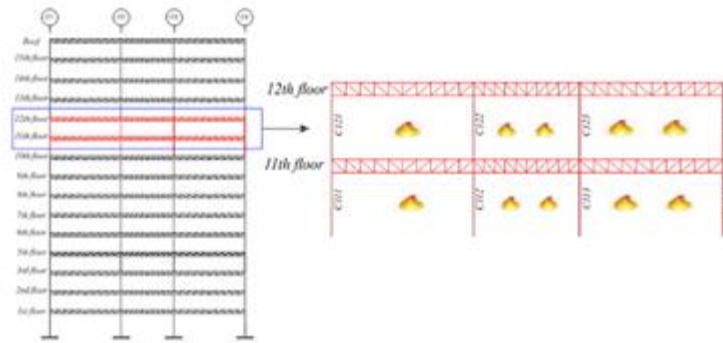


Figure 2.8 A quarter model of the NW corner of the tower (Aghakouchak et al. (2021)).

Figure 2.8(b) shows the plastic deformation and buckling of the top and bottom chords of the truss, which match closely with the deformed truss members found in the debris. The study concludes that the floor failure was caused by the connection failure of the main trusses, caused by the out-of-plane deformation of gusset plates.

To study the global behaviour of the building, an internal 2D frame was modelled in the OpenSEES software. Two different models are developed based on the location of the thermal load applied – Heating model 1 and Heating model 2. In the first model, thermal loading was applied on the 11th floor only, and in the second model, thermal loading was applied on the 11th and 12th floors and the external columns. The results from Heated Model 1 showed the formation of catenary deformation, causing the reduction of adjacent column capacity. Heated model 2, as seen in the Figure 2.9(b) showed the large catenary deformation along with the global failure of the external column due to the increased unbraced length of the column. This failure aligned with the collapse video, which illustrates the structural collapse of an external column located near the South face of the tower.



(a) 2D OpenSees model



(b) OpenSees output

Figure 2.9 OpenSees simulation of Heated model 2.

To study the load redistribution and global failure of the tower, four 3D models were developed, each representing a distinct damaged state. For this study, the authors employed ETABS software to build the models by selectively removing sections of the structure that were deemed to have failed during the fire event. The first model included all members of the structure intact; it represented the undamaged state of the structure. This model was utilised to perform gravity load analysis and calculate the section utilisation in the steel members. The remaining three models – Damaged Model Stage 1, Stage 2 and Stage 3 represent different levels of damage, as seen in Figure 2.10 (a), (b) and (c). Nonlinearity in the model was introduced by modelling lumped plastic hinges at the ends of frame members. The temperature imposed on the structural members remained below 700 °C.

The Damaged Model Stage 1 findings did not indicate the development of plastic hinges in any member located next to the damaged (removed) sections. Results from the Damaged Model

Stage 2 showed the formation of plastic hinges in the columns adjacent to the removed parts. However, the still global collapse was not predicted because of the safe redistribution of loads. Damaged Model Stage 3, the final model with large areas of structure removed, showed the formation of plastic hinges in the perimeter columns on the south and east sides of the structure (Figure 2.10(e)), indicating a collapse pattern similar to what was predicted previously in the 2D OpenSees model.

In conclusion, the authors argue that the connection failure was the reason for the floor collapse in the NW corner and other areas of the building. Due to the loss of floors through partial collapses, the perimeter columns on the NW and SE corners lost lateral bracing support. Since the extent of the flood damage in the NW corner was less than in the SE corner, the columns near the NW did not buckle while the columns on the SE corner buckled, eventually leading to the global failure of the tower. The study, however, relied on unrealistic linearly rising thermal loading.

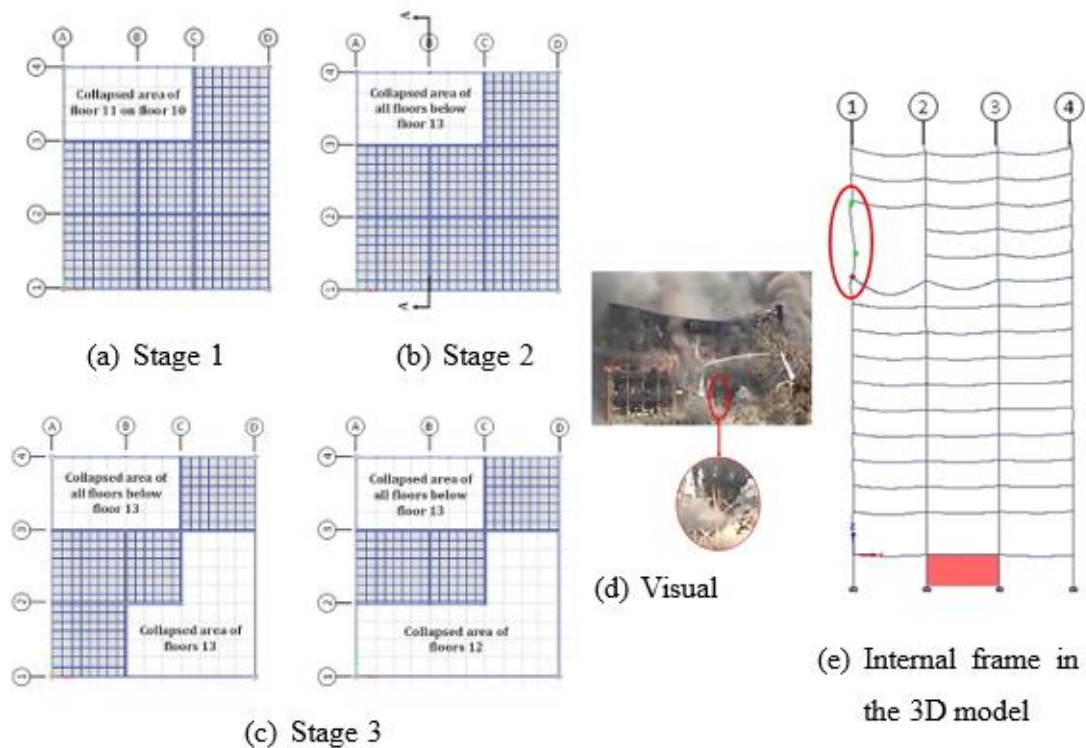
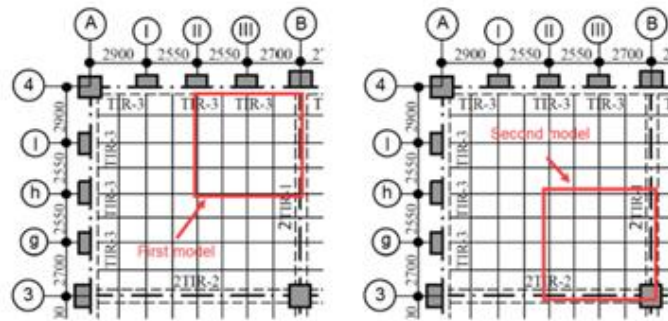


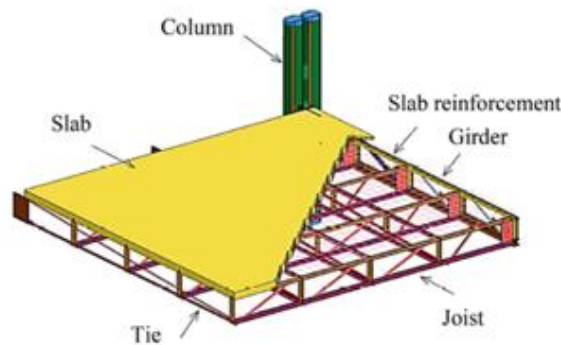
Figure 2.10 Damages states considered in the ETABS model & response of the external column before the global collapse.

2.3.4. Investigation by S. Epackachi et al.

Epackachi et al. (2022) in their study modelled, in detail, a quarter part of the 11th floor of the Plasco tower and analysed the response in the software LS DYNA.



(a) Modelled zones in NW corner



(b) LS-DYNA Corner model

Figure 2.11 Quarter locations were chosen for the study.

The primary emphasis of this investigation was placed on modelling the response of the connection between the structural components. The conclusions derived by the authors in this study state that the global collapse of the tower was triggered by the failure of gusset plates connecting the main girders and external columns near the South face of the tower. A thorough numerical examination was conducted on the structural elements of the Plasco tower, including girders, joists, slabs, columns, and connections. This analysis encompassed both dead loads and thermal loads. The effect of temperature on steel material properties was considered by modelling Young's modulus and yield stress as a function of temperature. Still, the effect on the concrete and steel rebar material was ignored. The research employed the data acquired from field tests to create

models for the strength of both steel and concrete materials. The gusset plates and welded joint connections between the girders (Primary truss beams) and columns were modelled in detail. Due to a lack of experimental data, the properties of the welds were assumed to be equal to those of the E60 electrode.

The analysis findings demonstrated a similarity between the damage observed during post-collapse field visits and the damage observed in the simulated response. The local failure of each member-to-member type connection was also studied. Local yielding and rotation of joists, buckling of vertical members and complete cracking of RC slab were observed in the simulation.

Table 2. As the temperature loading applied to the columns was insignificant, the column response remained in the elastic zone by the end of the analysis.

Member type	Status at the end of the analysis
RC Slab	Complete cracking of the bottom surface.
Tie beam (Vierendeel beam)	Complete fracture
Edge beam	Rotation due to slab failure
Joist (Secondary truss beam)	Buckling of vertical members
Girder beam	Fracture of the top and bottom chords and the vertical member to the bottom chord connection
Column	Elastic behaviour
Connection	Complete fracture

Table 2 Failure modes were observed in the analysis.

The study highlighted, as expected, the severe lack of fire-resistant design in the building design. The authors have also pointed out the deficiency of a fundamental structural requirement: the continuity of structural elements that disrupt the load path travel. For example, all the columns in the building were fabricated by assembling the built-up tubular sections, which were built using UNP 200 and UNP 160 channel sections; the joints along the seam were welded together using

plate sections. It cannot be estimated how efficiently the plate sections enable built-up tubular sections to act as one single entity. The study did not provide specific details regarding the type and intensity of the thermal load imposed on the structure. However, it was clarified that the columns experienced temperatures 200 °C lower than those truss beams were subjected to due to the presence of concrete walls and other floor materials.

The development of axial restraint at the ends of girders because of the elevated temperatures created conditions that caused catenary action. This mode of resisting load, i.e., tension along the axial direction, exerted a pull force on the connections along with a vertical force component coming from the main girders. The connections that were not designed for this additional load have failed, thus triggering the global collapse.

In their conclusion, the authors recommended the design of connections to account for the extra loading resulting from catenary action. The lack of continuity of load paths in the connections and columns for safe load redistribution was considered a severe design flaw from a fire safety point of view that caused the collapse of the Plasco tower. The study primarily focused on examining the response of the floor and connections, as evident from the model used for the study. As the thermal loading on the columns was within 500 °C, their response was mainly within the elastic zone. Hence, this study could not evaluate the role of unsupported external columns in causing the collapse progression.

2.3.5. Findings and drawbacks of earlier research

Previous researchers Behnam (2019), Shakib et al. (2020) and Ahmadi et al. (2020) predicted that the failure was caused by the loss of lateral support in the external columns using linear analysis and 2D models. However, their models are limited, so the sequential developments in the final stages, like load redistribution and the order of external main and secondary columns in the SE area, cannot be estimated.

Ahmadi et al. (2020) and Epackachi et al. (2022) used researched 3D models to understand the detailed local behaviour of beam and column connections. The study using ABAQUS by Ahmadi et al. predicted the local buckling of truss chord members. The key finding of the study was that the beam-column connection failure was due to the out-of-plane movement of gusset plates. The 3D ETABS models predicted that the failure of the external main column was only due

to the increased unbraced length, but the role of the other perimeter columns and the tie beam action of edge beams was not studied. The study by Epackachi et al. (2022) of quarter structure using Abaqus software concluded that connections in the tower failed due to the axial forces resulting from catenary action. Detailed information each forensic study based on the Plasco tower is provided in Table 3 and Table 4 in Section 2.4.

Full-scale model studies by the above researchers found that the global collapse was triggered by the failure of the external main column near the SE area, reflecting what was noticed in the video evidence. These studies used 'damaged state models', i.e., multiple floors were removed, which increased the unsupported column length. Therefore, the conclusions of the above studies could not show load redistribution in the external columns before the global collapse.

2.4. Understanding the fire accident

According to Behnam (2019) who conducted field investigations, the Plasco building, originally designed as a light commercial structure, changed its occupancy over time. It became one of the largest commercial centres for clothing production and distribution.

The building was never designed to resist fire loads and did not have any fire safety features, including sprinklers. There was no fire alarm system, no reliable evacuation plan, and no safe refuge area. The mechanical and electrical systems in the building were old and worn out. The importance of maintenance was not given due attention, and the building owners disregarded warnings and notices issued by the Tehran Fire Safety Department (TFSD).

Because of the change in occupancy type, the fire load of the building increased significantly. According to reports, during the fire incident, the basement, ground, and top floors of the building housed cloth production and storage shops. This information indicates that the top floors contained a significant fire load in the form of fabrics. The author estimated that the fire load was at least four times higher than the allowable limits. It should be observed that an increase in static load accompanies an increase in fire load.

In the studies conducted by Behnam (2019), Shakib et al. (2020), Aghakouchak et al. (2021) and Epackachi et al. (2022), the distribution and package characteristics of the fire load were not given attention. They can be important factors that significantly influence the magnitude and distribution of fire load. Information regarding any fire parameters did not exist in any official reports or the literature.

2.4.1. Investigation by Khan et al.

To handle this lack of information on the fire load characteristics and distribution, Khan (2022a), developed two scenarios to determine the potential definition of the fire load. In the first scenario, fabrics were assumed to be stored in the form of stacks, while in the second scenario, it was assumed that fabrics were stored in larger carton boxes, as seen Figure 2.12.

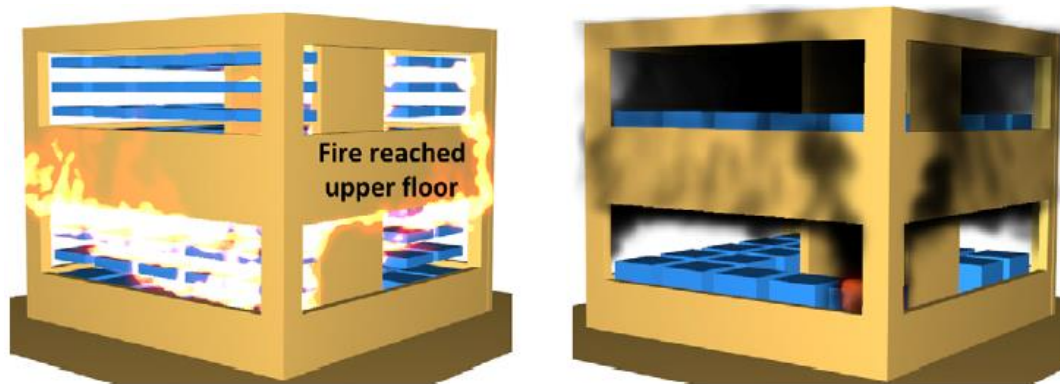


Figure 2.12 CFD models representing varying fuel packing cases.

The computational fluid dynamics (CFD) models of the two scenarios predicted temperatures with substantial variations in magnitude. The first case estimated the maximum temperature at around 980 °C, while the second at 1270 °C. It should be noted that though the first case has a higher surface area than the second one, the maximum temperature is lower. Khan explained the reasoning behind these counterintuitive results using fire dynamics principles and burning rate differences.

Using the temperature data from both cases, heat transfer analyses conducted on the concrete and steel sections revealed that the disparity in maximum steel temperatures between the two scenarios amounted to 400 °C. The significant difference in the temperatures highlights that storing fabric in large carton boxes would be quite dangerous for structural stability, as in the second case.

However, this does not imply that the risks associated with storing fabric in stacks are less. Due to the extensive surface area of fuel, the first case exhibited a higher burning rate, leading to higher steel temperatures during the early stages of the fire. The temperatures in later stages were not high because hot gases were replaced with inflowing cooler air.

The study established how both cases could prove detrimental to the structure. However, the ventilation factor becomes a crucial consideration in simulating the actual conditions of the Plasco tower. The study investigated vertical and horizontal fire propagation from the fire origin by considering two key factors: fire load distribution and ventilation.

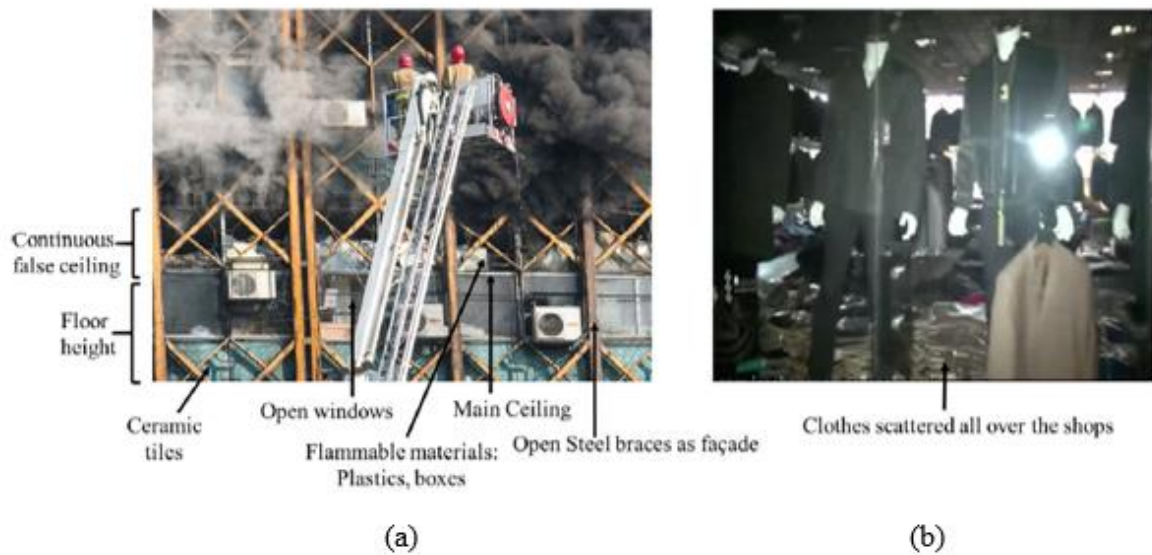


Figure 2.13 Photo showing (a) the ventilation conditions of the tower and (b) the interior of a shopping unit filled with fabrics.

Two CFD models were generated to understand the vertical and horizontal fire travel scenarios.

Vertical fire spread

For vertical travel fire simulation, the CFD model representing a section of the two-floor tower with ventilation conditions modelled in the form of windows and a staircase was created. The staircase provided vertical ventilation, and the windows provided horizontal ventilation.

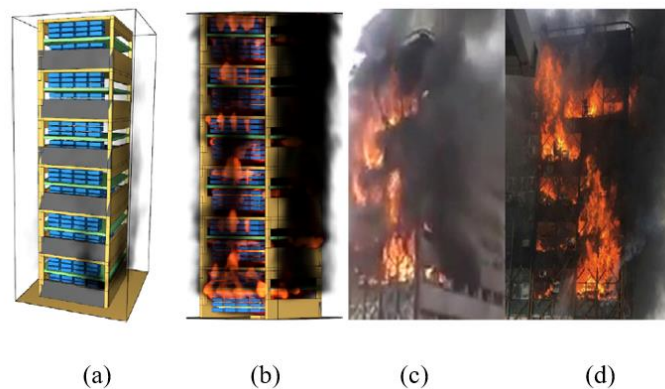


Figure 2.14 (a) CFD model, (b) simulation of the corner fire observed in the initial stages of the incident, (c) & (d) visual evidence from the North and South faces.

In the analysis of Case 1, the vertical fire travel simulation indicated that it took 25-30 minutes for the fire to grow and spread to the other floor vertically; this fire spread simulation fits well with the available video evidence, accident and personal testimonies of onlookers and firefighters. In the simulation of horizontal fire travel, it was assumed that the partitions at the ceiling level failed, thereby facilitating the rapid spread of fire across the floors. To simulate the accurate initial stage fire, the authors have created another 7-floor model representing the Northwest corner of the building. The temperature data from this analysis is used for the structural analysis of the building in the later chapter of the thesis.

Horizontal fire spread

In the Plasco tower, the window covering burnt out or fell off during the fire, and the false ceiling was open to the atmosphere. It was reasonable to assume that the fire entered the false ceiling during the early phases of the fire accident and that fuel distribution played a major role in the fire spread. Figure 2.13(b) indicates the high density at which fabric was stored in the shopping units of the building. Khan developed an FDS model and simulated the fire spread on each floor based on the available evidence. The fire was initiated in the Northwestern corner of the building, which can be verified with the help of visual evidence and security personnel who responded first and tried to extinguish the fire. During the simulation, the fire could not reach the adjacent compartment when a false ceiling was present. Hence, the false ceiling was removed using obstruction removal techniques (after the 900s), as seen in Figure 2.12. When flames reached the adjacent compartment, the fire travelled westwards on both the 10th and 11th floors, where firefighting efforts successfully contained the further spread. The fire on the 12th floor and above spread unhindered, extending across the entire floor.

2.4.2. Investigation by Ahmadi et al.

While this study does not explicitly focus on fire modelling, Ahmadi et al. (2020) have presented a comprehensive account of the architectural aspects and specific details related to the fire incident in their report. The information collected for this investigation encompassed structural details obtained from the debris and interviews conducted with firefighters. Fire accident details

were obtained through frame-by-frame analysis of multiple video sources. Using all the information collected, the authors have attempted to explain the sequence of events and the causes from an engineering point of view.

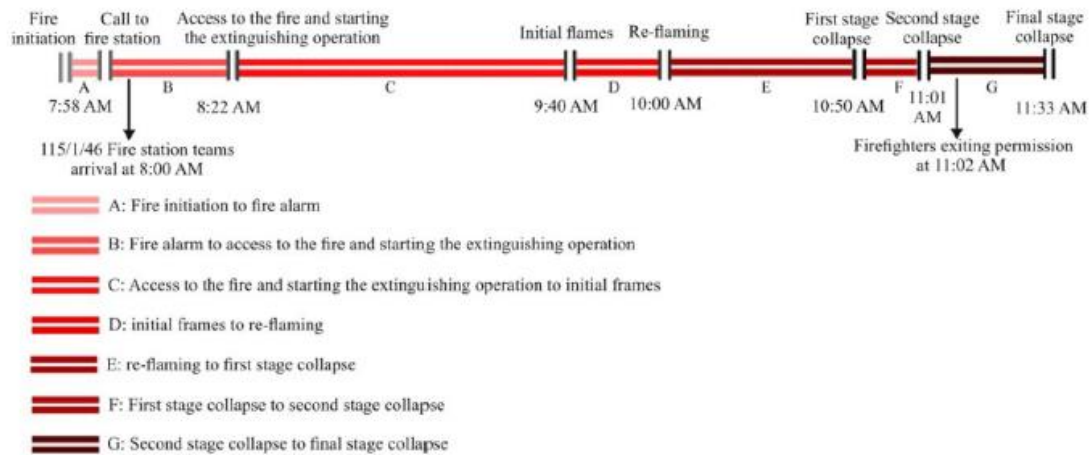


Figure 2.15 Timeline of the incident.

This paper classifies and interprets the collapse incident into three stages, excluding the final stage, which is challenging to analyse due to the limited duration captured in the video evidence. Fire was present in the NW corner for about 3 hours (i.e., 10:50 am) before the local collapse of the 11th floor onto the 10th floor. Firefighters reported that in the northwest corner of the building, the bottom and top cord trusses that supported them had visible deformations. It was hypothesised that the collapse was due to the failure of the connections of the main girder to the perimeter columns. Approximately ten minutes after the initial collapse, the 12th and 13th floors collapsed onto the 10th floor, resulting in a partial collapse that left columns standing without any lateral support. But still, the vertical void of such size extending multiple floors did not cause any global instability; the structure was still stable. This stage lasted for about 30 minutes, after which the complete collapse of the building took place.

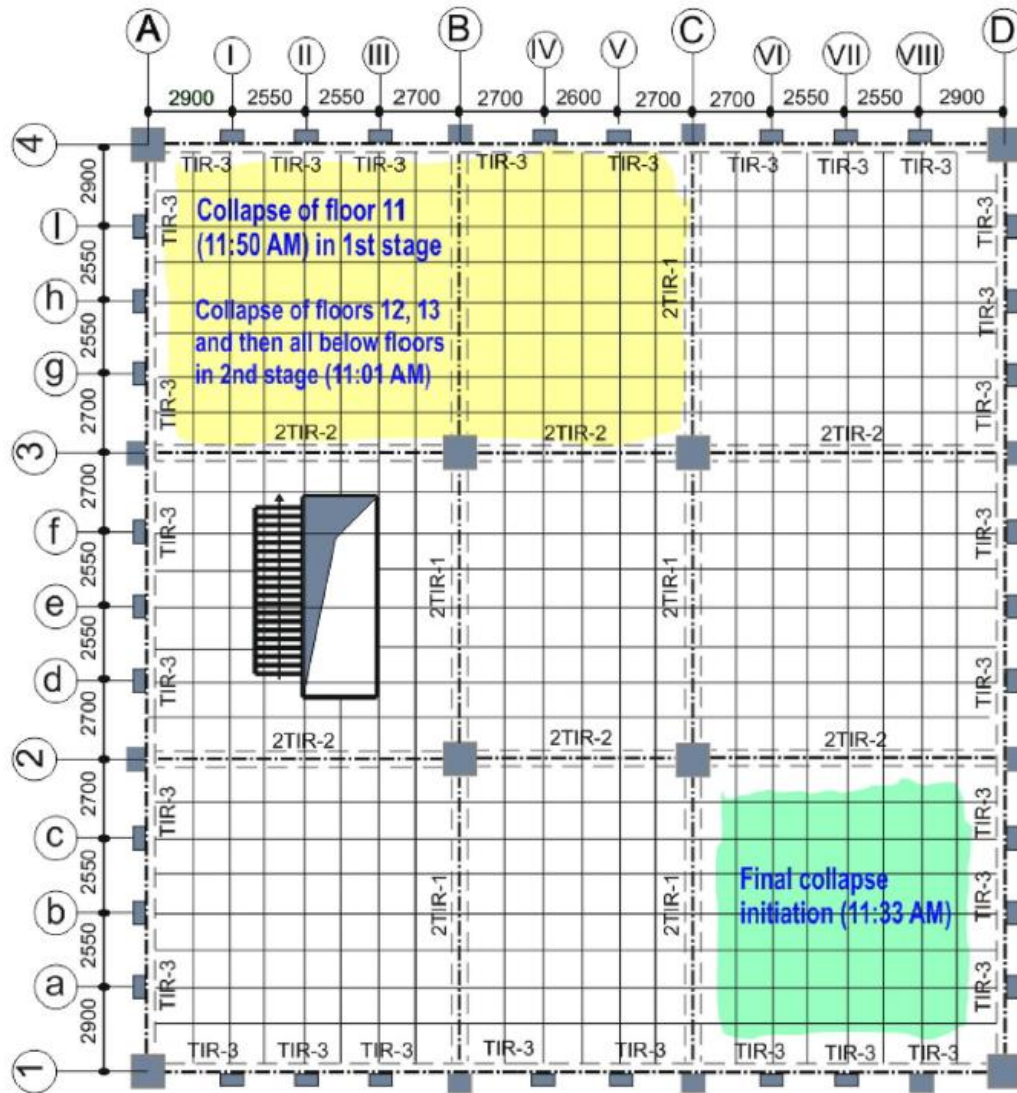


Figure 2.16 The floor plan of the tower indicates the stages of damage on different floors.

Meticulous analysis of the video evidence uncovered that two distinct floor collapses occurred in the Southeast corner of the building within a timeframe of 3 seconds; see Figure 2.16 and Figure 2.18. It was understood that those two collapses occurred on the 12th floor of the 11th floor first, followed by the 13th floor on the 11th. The structure collapsed after this incident.

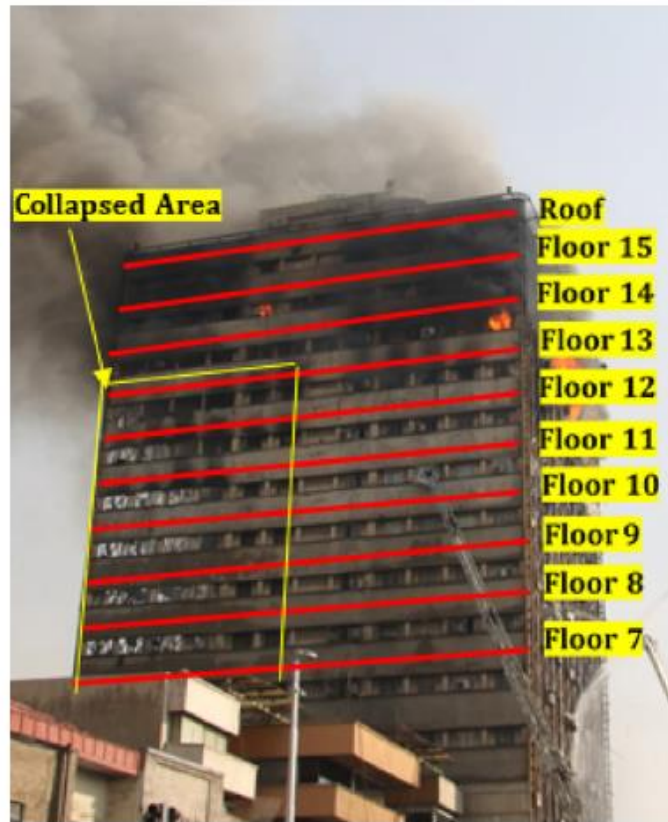


Figure 2.17 The west view of the building shows the partial collapse (Second stage).

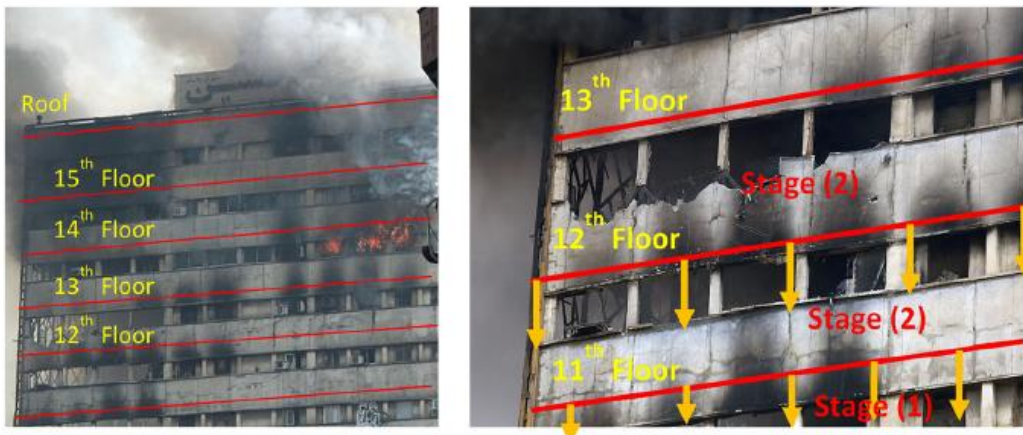


Figure 2.18 Closer view of the West elevation of the building showing the two stages of the partial collapse in the Northwestern corner.

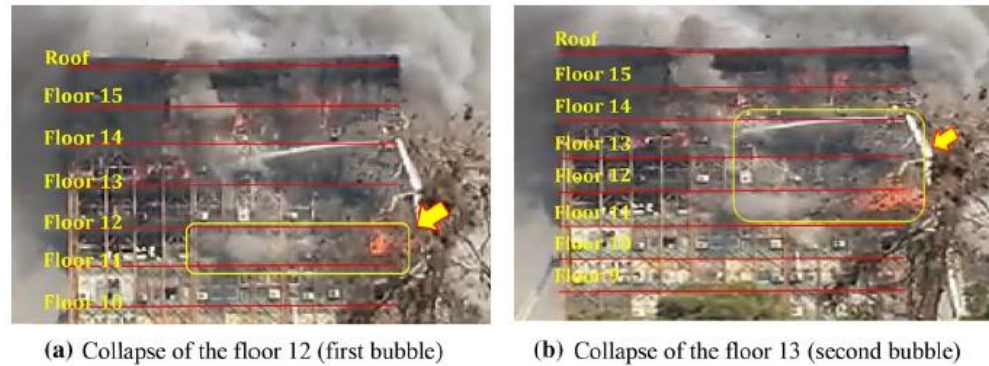


Figure 2.19 Southern elevation of the building moments before the final collapse.

2.4.3. Investigation by Khan et al.

A study conducted by Khan, Khan, et al. (2022) aimed to assess the impact of various fuel distributions on fire behaviour. The study explored two distinct fuel distributions, maintaining consistent fuel load and ventilation, to investigate the horizontal and vertical propagation of fire. The Plasco tower was a busy commercial building with numerous business units separated by partition walls. Horizontal fire is an expected fire travel phenomenon when it comes to large open-floor offices. Hence, in the case of the Plasco tower, partition walls were expected to limit the spread of fire. However, testimonies from firefighters indicate the opposite, suggesting that the partition walls did not effectively restrict fire spread. The reason for the easier fire spread could be ascertained by the presence of continuous space at the ceiling level. It was later learned that the ceiling spaces at every level were illegally used by the businesses to store fabrics, as reported by Ahmadi et al. (2020).

To analyse the fire in the Plasco tower incident, a CFD model was developed and validated using the available information, such as the building plans, visual evidence, and possible fuel load. Two cases of fuel distribution– Case 1 and Case 2 were considered, where Case 1 represents fuel load distributed in the form of small stacks with 0.1m of gap between the stacks, and Case 2 represents fuel load densely packed in large carton boxes, see Figure 2.20.

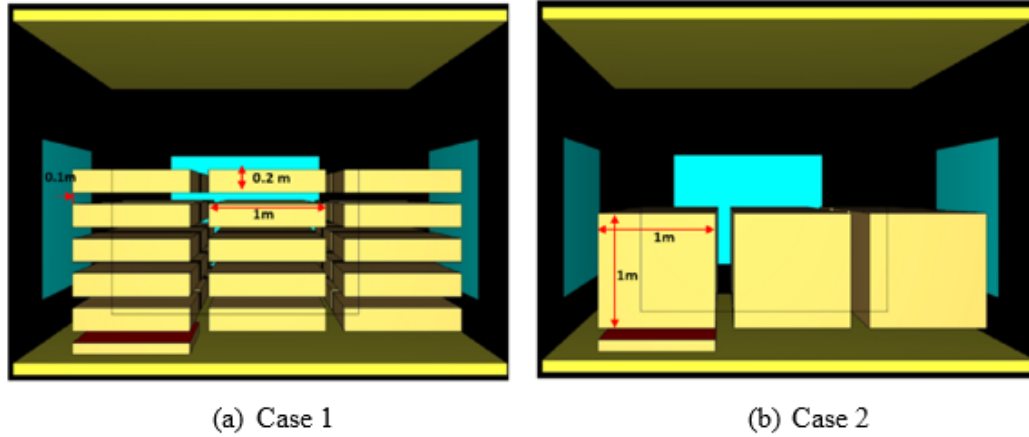


Figure 2.20 The two fuel distribution cases of the study (Khan, Khan, et al. (2022)).

In both cases, the fuel load was kept at 1910 MJ/m (based on the estimation by Behnam (2019)) for the 60-minute CFD simulation. The compartment was modelled to represent the conditions of the NW corner of the 10th floor of the tower.

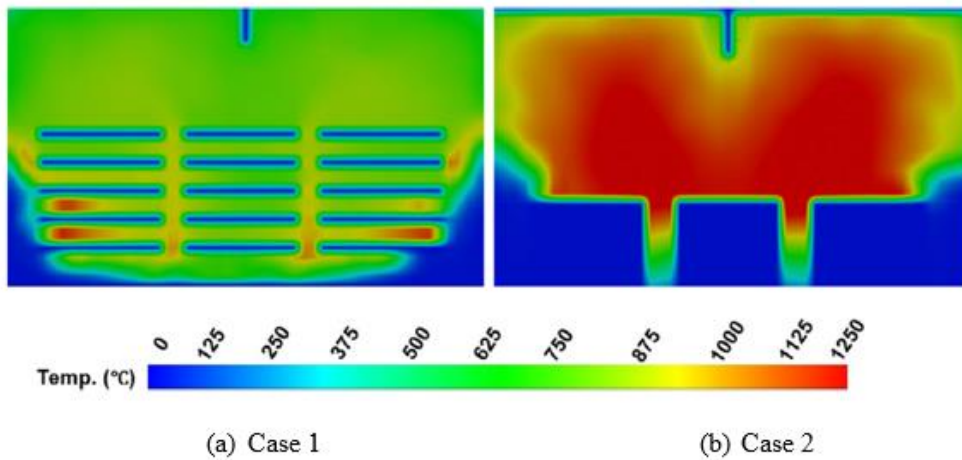


Figure 2.21 Temperature contours in degrees Celsius at 45 minutes.

The later section of the study discusses the vertical and horizontal fire spread simulations carried out using multi-floor CFD models. The observation was that the fuel distribution in Case 2 did not result in vertical or horizontal fire spread, whereas in Case 1, such fire propagation was observed. The authors explained that one of the reasons for Case 1 causing the fire spread was the physical height of the fuel, which is a key factor that increased the flame height. The study

concludes that factors like breakage of the false ceiling, open ventilation on the sides of the tower, fuel height and distribution pattern contributed to the rapid fire spread in both vertical and horizontal directions.

Study	Scale	Fire Modelling	Heat transfer	Thermo-mechanical analysis	Limitations
Hamzeh Shakeb et al (2020)	Global 3D	Linear rising temperature	Uniform temperature profile	Linear static analysis with P-delta and geometric nonlinearity	Simplistic thermal loading and linear FE analysis.
M. T. Ahmadi et al (2019)	Global	-	-	-	-
Ali Akbar Aghakouchak et al (2020)	Local 3D	Linear rising temperature	Members near the slab are subjected to heat transfer analysis in Abaqus	Nonlinear static analysis	Simplistic thermal loading
	Global 2D	Linear rising temperature	Uniform temperature profile	Nonlinear static analysis	Simplistic thermal loading
	Global 3D	Linear rising temperature	Uniform temperature profile	Linear static analysis with modelled plastic hinges and element removal approach	Simplistic thermal loading and linear FE analysis
S Epackachi et al (2022)	Local 3D	Linear rising temperature	Uniform temperature profile	Nonlinear static analysis	Column modelling absent

Mustesin Ali Khan et al (2021)	Local 3D	CFD analysis using two different fuel distributions	Heat transfer analysis of slab and truss sections using the OpenSees	-	Structural response is not the focus of the study.
Aatif Ali Khan et al (2021 & 2023)	Global 3D	CFD analysis simulating both vertical and horizontal fire spread	Heat transfer analysis of slab and truss sections using the OpenSees	-	Structural response is not the focus of the study.
Tejeswar Y et al (2018)	Global 3D	Linear rising temperature	-	Nonlinear static analysis	Simplistic thermal loading
Behrouz Behnam (2018)	Global 2D	CDF analysis representing the fire in the NW corner was simulated	Heat transfer analysis of all critical sectional members was done.	Nonlinear dynamic analysis	3D response not considered.

Table 3 A summary of the analysis was carried out in the reviewed literature.

Study	Analysis type	Software	Remarks	Collapse trigger
Hamzeh Shakeb et al (2020)	Finite element	SAP2000 for structural analysis, Abaqus was used for obtaining connection behaviour	A preliminary study simulating the collapse with an appropriate connection model	Failure of the main truss near the SE corner
M. T. Ahmadi et al (2019)	Visual analysis based on videos and photos	-	This study gives the timeline of how the fire spread took place & gives extensive details of the damage.	Pull-in failure of the external column near the South due to catenary forces from main trusses
Ali Akbar Aghakouchak et al (2020)	Finite element	Abaqus for modelling a quarter of the floor panel.	This study used a detailed 3D solid model representing 1/4th of the area of the North side floor.	This detailed exercise predicted large floor deformations and failure of web girders and weld connections.

		OpenSees	This study is based on a 16-storey 2D model with two models. The first model is subjected to elevated temperatures on one floor, whereas the second is considered a 3-floor fire.	This study predicted significant load redistribution towards the perimeter column thereby increasing their load ratio, resulting in failure.
		ETABS	This study is based on a 16-storey 3D model with one intact model and three damaged models.	Failure of perimeter columns
S Epackachi et al (2022)	Finite element	LS-DYNA	Based on a quarter model of the NW corner floor model	Local failure of each member element was simulated. The fracture of the connection between the gusset and column causes the collapse of the whole structure.

Mustesin Ali Khan et al (2021)	Finite element	FDS for CFD analysis and OpenSees for heat transfer analysis	In this study, the effect of different fuel distribution on fire travel and steel temperatures is studied	-
Aatif Ali Khan et al (2021 & 2023)	Finite element and Visual	FDS for CFD analysis and OpenSees for heat transfer analysis	This study establishes a conclusive timeline of fire accidents. CFD analysis of both vertical and horizontal fire spread are calibrated.	-
Tejeswar Y et al (2018)	Finite element	OpenSees	A preliminary study simulating the response of the structure	Results did not point to a specific collapse, but similarity with WTC behaviour was hypothesised
Behrouz Behnam (2018)	Finite element	SAFIR	A study based on the 16-storey composite 2D model with multifloor thermal load.	The results of the study confirm that the Plasco building collapsed. due to the failure of the ceiling trusses.

Table 4 Summary of remarks and conclusions in the reviewed literature.

2.5. Using OpenSees for fire investigations

2.5.1. Introduction to OpenSees

OpenSees (Open System for Earthquake Engineering Simulation) is an open-source object-oriented software framework developed by F. T. McKenna (1997), at UC Berkeley. OpenSees allows users to create finite element models to simulate the response of structures (or geotechnical systems) against earthquake loads. This framework was developed by Frank McKenna and Gregory L. Fenves with significant contributions from Michael H. Scott, Terje Haukaas, Armen Der Kiureghian, Remo M. de Souza, Filip C. Filippou, Silvia Mazzoni, and Boris Jeremic.

The open-source nature of the code allows developers to add new materials, elements, solvers, integrators, etc.; this has led to the widespread adoption by developers and users of making changes to the source code and using it for their research work. Over time, OpenSees' capabilities increased to handle complex problems like soil-structure interaction and large structures that require parallel computing, etc.

OpenSees was developed to calculate finite element solutions for earthquake loads on structures. Mainstream structural engineering usually focuses on loads like snow, wind, impact, and earthquake origin. Fire load falls into a niche category among different types of loading, as there are relatively few engineers trained to conduct nonlinear thermal analysis specifically for fire-related scenarios. Additionally, fire load is often not emphasised significantly in university teaching. Also, the popular structural analysis software does not take fire load analysis seriously, except for a select few, which are expensive. The absence of comprehensive analysis software can be attributed to the disparity in the temporal and spatial resolution required for conducting CFD, heat transfer, and thermo-mechanical analyses. Consequently, no single software is capable of effectively handling investigations involving fire load. Hence, OpenSees was chosen to extend its capabilities in handling thermal loads; it was the first step in analysing large-scale structures against fires as conveniently as earthquake loads.

2.5.2. Developing the OpenSees for fire

The fire research team at the University of Edinburgh led by A. Usmani et al. (2012a) developed the OpenSees to handle problems with thermal load. The addition of the fire module enables users to carry out fire modelling by providing boundary conditions for heat transfer analysis on structural components. Temperature effects on structural materials like steel and concrete were implemented in the OpenSees framework. Effects like temperature-dependent transient strain or LITS (Load-induced thermal strain) were also implemented in the *OpenSees for fire*. Beam and shell elements were modified to take thermal loads.

Fire modelling in *OpenSees for fire* allows the users to model post flashover compartment fires. Fires evolving according to the time-temperature curves established in the codes and standards like ISO 834 and ASTM E119 and various parametric time temperature curves recommended in the research literature and codes can be modelled. In addition to the above, zone models and localized fires have also been implemented to model fires realistically. Y. Jiang et al. (2013) implemented the travelling fire model in the OpenSees framework, thus expanding the fire modelling capabilities of the *OpenSees for fire*.

After modelling the fire, users can carry out heat transfer analysis on the cross sections of structural components to compute temperatures within the structure. The heat transfer module of OpenSees takes advantage of the “fibre section” elements, which are already meshed in the plane of the cross-section for calculating internal forces. The heat transfer analysis calculates temperature values on each fibre and generates time-temperature data for the subsequent thermomechanical analysis.

The coupling of heat transfer to thermo-mechanical analysis is one-way, meaning there is no feedback from the deformed structure to the heat transfer module. As a result, the impact of structural deformation on heat transfer is not considered. This is a reasonable trade-off for achieving faster computation in analysing large structures against fires.

OpenSees library contains many material models of concrete and steel, but few of them (uniaxial models of concrete and steel) were modified to include temperature-dependent stress and strain, including effects such as LITS. The properties of the uniaxial materials were based on the Eurocode standard. The class and sequence diagrams presented by Jian et al. (2015) provide a

logical overview of the hierarchy and relationship between the newly created and modified classes in OpenSees. OpenSees non-linear beam column elements were modified considering the temperature-dependent material properties. The thermal loading is calculated by integrating the thermal expansion of each fibre across the depth of the fibre sections. The tangent stiffness matrix terms of the beam elements were modified based on the temperature-dependent properties of the fibre. Y. Jiang et al. (2013) extended the OpenSees software framework for modelling the composite steel-concrete structures subject to thermal loads. The shell element, *MITC4ShellThermal*, was formed by a combination of membrane elements and Mindlin plate bending elements using a general total Lagrangian formulation. The OpenSees material, *DruckerPrager*, was modified to model the concrete in the composite slab at elevated temperature with temperature-dependent material properties. L. Jiang et al. (2021a) implemented a thermo-mechanical nonlinear shell element, *ShellNLDKGQThermal*, to simulate the significant deformations of slabs under fire conditions. This multi-layered shell section considers the temperature-dependent characteristics of materials, such as plasticity and thermal expansion. While the previously developed element *MIT4ShellThermal* lacked the nonlinearity needed for simulating large deformations under thermal load, *ShellNLDKGQThermal* can undergo large deformations. A plane-stress formulation of the concrete damage-plasticity material to simulate concrete behaviour at elevated temperatures was introduced to model the slab response and damage in fire effectively.

2.5.3. OpenSees analysis of structures against fires

J. Jiang et al. (2014a) published the paper which detailed the application of ‘OpenSees for fire’ after the successful implementation of thermal classes into the OpenSees framework. In their study, though intended to demonstrate the capability of OpenSees in simulating thermos-mechanical response of structures, the topic of possible collapse scenarios for 2D multi-storey structural frames was explored.

The implicit dynamic analysis method (Newmark method) was used to study the influences of the load ratios, beam sizes and fire scenarios on the collapse behaviour of frames. Single-compartment fire scenarios in the central bay and edge bay were considered. The authors discovered a total of four collapse mechanisms of steel frames by varying the influencing factors

of the structural model. It was found that collapses in steel frames are likely triggered by the buckling of the heated columns.

It was recognised that the typical failure mechanisms of frames entail the initial failure of heated columns, followed by the failure of adjacent columns on the same floor due to the additional load resulting from load redistribution. While studying the influence of load variation on failure mechanism, it was found that at lower load ratios, the failure of structures begins with the expansion of the floor system first, then catenary action and then collapse, confined to one storey. However, at higher load ratios, the buckling failure occurred in columns at low temperatures of 250 °C. It was reported that fires in edge bays are of serious concern and easily create a progressive collapse compared to the fires in the central bays. In edge fires, the failure occurred at lower loads, whereas in central bay fires, failure occurred at higher loads. The results have shown that increasing the beam section strength transformed the failure mechanism from a weak beam mechanism to a column collapse mechanism. The study proved that OpenSees could simulate known failure-causing thermal responses in structures under fire, that is, expansion of floors at lower temperatures and catenary action at higher temperatures.

As the development of OpenSees through the addition and modification of the classes was going on, L. Jiang & Usmani (2018) built OpenSees-SIFBuilder, a new integrated tool using the existing thermal classes, that can carry out coupled heat transfer and thermo-mechanical analysis within framework of the OpenSees software. The tool is a script-based solution specifically developed to perform a comprehensive analysis, beginning with realistic fire modelling. It then proceeds to conduct heat transfer analysis with automated boundary conditions to generate thermal load, ultimately concluding with the thermo-mechanical analysis stage. SIFBuilder provides an environment where users can quantify the structural behaviour under various design fire scenarios.

All the added elements, materials and fire modelling classes were extensively verified and validated against benchmark solutions by the developers, mainly by Y. Jiang et al. and L. Jiang et al. The research advancement towards using OpenSees for fire in analysing larger structures like frames was done by J. Jiang et al. (2014a). They validated the extended OpenSees software framework by simulating the shallow two-bar toggle frame test proposed by Williams (1964) and plane steel frame tests at elevated temperatures performed in Germany by Rubert and Schaumann (1986). J. Jiang et al. studied the progressive collapse mechanisms of steel frames under different

fire locations, loads and beam stiffnesses. This demonstrated the effectiveness of extension work, excluding shells, in using OpenSees for fire for thermo-mechanical analysis.

Yarlagadda et al. (2018) built an 8-storey model of the Plasco tower using the original version of the GiD+OpenSees interface. As the information on fuel load, structural, & architectural details were not available, an FE model based on rough estimations was analysed against simplistic uniform temperatures. Their study applied temperatures up to 800 °c to simulate the thermal response of one, two and three-floor fire conditions. Though the study could not provide a conclusive theory behind the collapse of the Plasco tower, the robustness of OpenSees for fire in analysing tall buildings against extensive thermal loading was proven. R. Domada et al. (2020) extended the above work by remodelling the structure using the latest structural details information. In their study, an 8-storey steel and concrete structure was built to study the reasons for the partial collapse of the NW corner of the tower. The compartment fire-based fire curve ISO 834 was used to apply thermal load on the three floors of the structure. In another study of R. V. Domada et al. (2020), the OpenFIRE framework (developed by Khan, Khan, et al. (2021)) was used to couple CFD, heat transfer, and the thermo-mechanical response of the structure. It was established by Khan (2022a), Ahmadi et al. (2020) and Behnam (2019) The fire originated in the NW corner of the 10th storey and quickly spread to the same corner on the 11th and 12th storeys. The fire on the 10th and 11th storeys did not spread and was limited to the corner area, whereas the fire grew and spread over the entire floor area of the 12th floor. Therefore, in their study, the response of the ceiling of the 13th floor (as the fire on the 12th floor heats the 13th floor) was simulated.

Orabi, et al. (2022) modified the code of the commercial GiD+OpenSees interface to achieve heat transfer and thermo-mechanical analysis coupling. Even though very efficient and user-friendly CFD and FE software exist, there is no single software or tool that can enable sequential coupling of CFD and FE analyses. This was due to the fact that the temporal and spatial resolution demanded by CFD models is considerably higher than what is demanded by an FE model.

In the case of commercial software like Abaqus, sequential analysis is possible if the modelling of structures is done using 3D brick elements. Small-scale, detailed modelling or component modelling would benefit from the 3D approach, whereas in the case of large-scale

models like tall building structures, the computational costs increase significantly. Researchers like Zhang et al. (2016), Silva et al. (2016a) and Prasad & Baum (2005a) made attempts to couple CFD and FE models, but mostly, they are targeted towards commercial software (ANSYS) whose code is not open source. Khan, et al. (2021) built an open-source tool, Openfire, to couple the software, but it was limited in its ability to generate complex geometry without a preprocessor or 3D rendering.

Complex structures can be modelled using the ISE (Integrated Simulation Environment) of the GiD+OpenSees interface, unlike SiFBuilder, which lacks capabilities in handling composite structures. Even though the degree of coupling achieved in SiFBuilder is superior, GiD+OpenSees provides better preprocessing.

The heat transfer script of the interface was validated against one of the protected composite beams tested by Ramesh et al. (2019) and studied by Li et al. (2021). The workflow and accuracy of the interface were demonstrated by simulating the Cardington large compartment test. Later, the interface was used in analysing potential collapse mechanisms behind the collapse of WTC 7 (M. A. Orabi, Jiang, et al. (2022)). In his PhD thesis, M. A. Orabi (2022), built two WTC7 models of different scales and purposes using the ISE to examine the hypothesis that a mechanical room fire might have resulted in the collapse of the tower. The first model of three floors was aimed at studying whether a failure could occur because of the burning of hydrocarbon fuel within the mechanical room of the tower. The second model, bigger than seven floors, was built to study the overall structural behaviour and potential collapse propagation found in the first model. The study demonstrated seamless integration achieved between the heat transfer and thermo-mechanical modules of the OpenSees software framework.

Chapter 3: Robustness Analysis of Plasco Tower

under Fire Conditions

This chapter aims to examine the susceptibility of the structure of the Plasco tower towards progressive/disproportionate collapse when subjected to thermal loads of varying intensities and locations. During the fire incident in the Plasco tower, multiple local fires occurred, causing significant local damage to the structure (Govt. of Iran (2017)). In this chapter, the response of the Plasco tower to localised fire affecting critical load-bearing elements is studied. The fire load scenarios employed in this study are not intended to accurately represent the thermal load of actual fire event(s). It is envisaged that the analysis is carried out by applying thermal loads to the floor surface areas and/or critical structural elements that could have triggered the collapse. Since the fire affected the stories between the 11th and 17th floors, a six-storey composite structure is modelled using the OpenSees finite element software. For modelling the steel beam and slab, *displacementBeamColumnThermal* and *ShellNLDBGQThermal* element classes (for beam and shell elements) of the OpenSees fire module are used (A. Usmani et al. (2012)). Steel thermal degradation properties recommended by Eurocode 1 were used for the study. Concrete material was modelled as layered plane stress concrete with Concrete Damage Plasticity (CDP) material model, and on the other hand, rebar material was modelled as a biaxial plane-stress steel layer using the J2 plasticity material model (L. Jiang et al. (2021a)).

This chapter evaluates the ratios of column loads under ambient conditions and aims to review the structural design from a fire safety perspective. In the first case, a fire load was applied on one of the core columns of the tower, and the impact caused by the load shedding is discussed. Likewise, the study examines the mechanisms of load redistribution in other critical components, such as primary beams and secondary main columns. Through the analysis of the Plasco tower under diverse fire load scenarios, this study investigates the possible collapse mechanisms. It identifies the inherent strengths and weaknesses of the structural design. The heat transfer analysis is performed to obtain the temperature history, assuming the temperature-

time variation per the ISO 834 fire curve. However, it should be noted that the application of thermal load in the time domain is solely for practical convenience.

3.1. Motivation and objective of the study

Accidents offer structural engineers an opportunity to learn and improve. The Broadgate Phase 8 fire, which occurred in 1999 in a modern steel fast-track building, which incorporated steel deck/concrete floor construction (Newman (1991)). There was no collapse, but the examination of damage provided an opportunity to consider the validity of design codes developed from small-scale fire test data. This eventually led BRE and erstwhile British Steel to carry out six full-scale fire tests on an 8-storey steel frame composite structure at the BRE Large Building Test Facility at Cardington, Bedfordshire, UK (Kirby (2000)). The collapse of the WTC Buildings in 2001 following a terrorist attack also offered valuable lessons with regard to adequate preparedness for fire safety and structural stability in fires. Initial attempts to analyse the WTC collapse indicated that although there had been considerable progress, there were too many counterintuitive and subtle phenomena in the thermo-mechanical response of large frame structures to fires, which were not well understood, even by experts in the profession. Therefore, multiple explanations for the WTC collapse surfaced. A. S. Usmani et al. (2003) & Lange et al. (2012a) at the University of Edinburgh found that the WTC towers had an unusual vulnerability to large fires. The team was able to produce a credible scenario of collapse, which did not depend upon any gross assumptions about the fire or failure of connections or even structural damage. A clean stability failure mechanism was evident from a simple computational analysis. Not only this, but the analysis was also entirely consistent with the fundamental principles developed previously during the simulation of Cardington Tests led by the PI. Greater understanding and knowledge of structural frame performance in fire can only be gained by rigorous analysis, just as it is customary to determine the response of structures to earthquake or wind loading.

The objective of this study is to examine the susceptibility of the structure of the Plasco tower towards progressive/disproportionate collapse when subjected to thermal loads of varying intensities and locations. During the fire incident in the Plasco tower, multiple local fires occurred causing significant local damage to the structure (Govt. of Iran (2017)). In this study,

the response of the Plasco tower to localized fire affecting critical load-bearing elements is studied. The fire load scenarios employed in this study are not intended to accurately represent the thermal load of actual fire event(s). It is envisaged that the analysis is carried out by applying thermal loads to the floor surface areas and/or critical structural elements that could have triggered the collapse.

3.2. Structural integrity of the Plasco tower

In the case of the WTC collapse, it was observed that during the initial phase of the fire, long floor beams expanded and pushed the external columns outwards. After the floor beams weakened, resulting in catenary action, the external columns were pulled inwards, leading to the progressive collapse (A. S. Usmani et al. (2003) & Lange et al. (2012b)). The collapse took place progressively, with one failing component leading to the failure of other key members. Once the external columns buckled inward, the failure was uncontrollable due to the instability induced in the load transfer mechanism.

In the case of the Plasco tower incident, the structure withstood the initial structural damage caused by the fire for at least 30 minutes (Behnam (2019) & Ahmadi et al. (2020)). The researcher observed that the connection failure of the floor system in the Northwest corner of the tower caused the failure of the 11th and 12th floors of the tower, in terms of falling freely onto the lower floors. The impact caused by the falling floors caused further damage to the lower floors locally. Nevertheless, the damage did not impact the vertical load-carrying members of the structure, see Figure 3.1. The failure of connections was the main reason for the spread of damage in the structure horizontally. In the Plasco tower, core columns, secondary main columns and primary beams form the major load transfer system of the tower. The four core columns form the vertical spine of the building by carrying nearly half of the total gravity load. The truss, Vierendeel, and edge beams form the secondary load transfer system. The stability and resilience of the structure, even after the multiple floor failures in the NW corner, proves that key structural components of the building were unaffected by the accidental consequence of the NW compartment fire.



Figure 3.1 Photo showing the partially collapsed floors in the NW corner of the tower (West elevation)

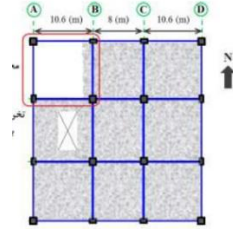
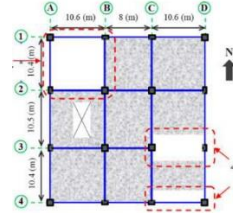
In the later stages of the fire, the collapse of the floors near the Southeastern (SW) corner was initiated due to the failure of at least one primary beam. Primary beams in the Plasco tower are the key components of the primary load-carrying system. The Plasco tower investigation report was published by Shakib et al. (2020) explains that the failure of primary beams in the SW area caused a large portion of floor failure. The dynamic effects generated by the falling floors caused the collapse of a few lower floors, thereby pushing the structure into relatively unstable conditions. The failure of any single structural member did not trigger the collapse of the Plasco tower. Instead, the collapse incident should be seen as a combination of local pancake-style collapses that lead to a condition favourable towards a disproportionate style collapse.


3.2.1. Classification of the collapse

WTC tower collapses are a good example of pancake-type collapses (NIST (2005)). The loss of vertical load-bearing capacity (limited to a few stories) induced the pancake-style collapse. The upper damaged part of the structure moved downwards and accumulated kinetic energy. The subsequent collision with the lower part of the structure caused large dynamic forces beyond the capacity—this chain of events led to the ultimate collapse of the WTC towers. The classification of progressive collapses is explained by Starossek (2007). The key

characteristics of pancake-type collapse are the separation of structural components, the release of potential energy and the occurrence of impact forces.

Table 5 gives a brief view of collapses as classified by Starossek, which are observed in tall buildings and may have occurred in the collapse of the Plasco tower.

Collapse	Characteristics	Remark
Pancake type (WTC collapse)	<ul style="list-style-type: none"> a. Initial failure of vertical load-bearing elements b. Separation and fall c. Transformation of potential energy into kinetic energy d. Impact loading e. Vertical collapse propagation 	 <p>Initial collapse of floors in the NW corner of the 11th and 12th floors (Shakib et al. (2020)).</p>
Zipper type (Tacoma Narrows Bridge)	<ul style="list-style-type: none"> a. Initial failure of one or two key elements b. Redistribution of forces c. Impulsive loading due to the suddenness d. Collapse progression in a direction transverse to the principal forces in failing elements 	<p>It is not relevant as this type of failure occurs in thin structural members under tensile forces.</p>
Domino type	<ul style="list-style-type: none"> a. Initial failure of one element b. Overturning effect and rigid body motion c. Like the pancake-type collapse, but the impacts occur at an angle 	 <p>There is a good chance of such failure occurring in the tower. For example,</p>

		connections on one side of the Primary beam (in the SW corner) fail, and the other side doesn't or gradually fails (Shakib et al. (2020)).
Section type	<ul style="list-style-type: none"> a. Initial failure of a part of the section b. Failure occurs as the redistributed forces cross the allowed limits that members can bear. c. It can be identified through the rupture of section members. 	 <p>The secondary main column, built using 4xUNP200 sections, was seen rupturing into two pairs of boxed columns moments before the collapse. This may have played a significant role in the collapse but reduced the buckling strength of the column (Ahmadi et al. (2020)).</p>

<p>Instability type</p>	<ul style="list-style-type: none"> a. Initiated by imperfections and transverse loading. b. Failure of bracing elements can trigger an instability-type collapse. c. Usually occurs in elements under compression. d. Transformation of potential energy into strain energy. 	<div data-bbox="1423 196 1822 516" data-label="Image"> </div> <p>The decoupled external column section and loss of bracing support due to the failure of the floors lead to the inward buckling deformation. This caused the final collapse of the structure (Ahmadi et al. (2020)).</p>
-------------------------	--	--

Table 5 Collapse types observed in the Plasco tower collapse.

The characterisation of structural failures depends on the nomenclature and definitions adopted for describing progressive and disproportionate collapses. Kiakojoury et al. (2021) identified and discussed the absence of a clear distinction between the nomenclature currently used for describing the structural collapses. He analysed the works of many researchers and the definitions of progressive/disproportionate collapse made by them. Kiakojoury et al. summarizes the list of definitions provided by the authors and building codes for progressive collapse and identifies three key terms – initial damage, collapse propagation and final collapse. According to the Kiakojoury et al., “Three characteristics must be available to consider a structural failure as a progressive collapse: first, the initial failure must be *local*; second, the failure must spread to other members; and third, the final collapse state has to be *disproportionate* to the initial failure”. In the case of the Plasco tower, the local failure of the floor slabs in the NW corner propagated the damage to the other areas but did not result in a disproportionate collapse. In later stages, i.e., when a key component was affected due to a local failure, the damage propagated and resulted in a disproportionate final collapse.

This study aims to identify inherent weaknesses and vulnerabilities of the structural design adopted by the designers in the case of the Plasco tower. The robustness of the structure will be assessed by subjecting component(s) of the primary and secondary load transfer system of the Plasco tower to a simplistic thermal loading based on the ISO 834 curve. The extent of the damage is calculated, and the likelihood of propagating the damage and collapse is studied in the following sections.



3.2.2. Review of the structural arrangement

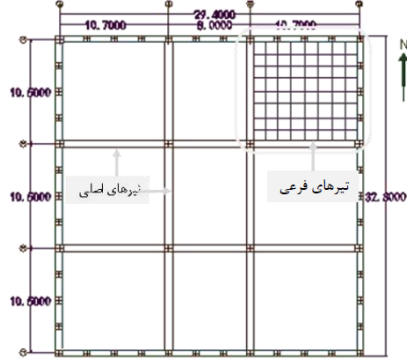

Robust structural design is crucial for the life safety of firefighters and building occupants, and protecting assets and property. Hence, ensuring structural robustness while designing structures and assessing the robustness of old structures should be given importance. The Plasco tower was an old building designed without considering fire safety and structural performance in case of fire. The structure had no passive fire protection, and at the time of the fire accident, the active fire protection system failed due to a lack of maintenance. Shakib et al.


(2018) published a fire safety report based on the then-current conditions of the Plasco tower before the fire incident. The report discussed a brief account of the state of electrical installations and unmaintained mechanical equipment. It was also observed that there was no proper care and maintenance during the 54-year operation of the building.

Reviews of Cao et al. (2023), Suwondo et al. (2021) and Porcari et al. (2015) give a detailed account of works by various researchers in evaluating the influence of different structural parameters on the building performance. Through analysing experiments like Broadgate Fire and the Cardington building tests (Newman (1991), Kirby (2000) and Gillie et al. (2002)), many insights are gained in understanding building behaviour and furthering fire-resilient structural design. In the past 15 years, both UK and European institutions have dedicated significant resources to structural fire engineering research. As a result, the scientific community acquired a comprehensive knowledge and understanding of how structures react when exposed to fire.

Table 6 provided a concise list of a strong and reliable structural steel arrangement designed explicitly for fire situations, which has emerged as a direct outcome of the research over the two decades in the UK and Europe (Lamont, Lane, Jowsey, et al. (2006)). This section details a structural arrangement review to analyse how robust the design of the Plasco tower was against fire.

Component of the structure	Reason for robustness	Plasco tower
Composite floor	Structural continuity	 <p data-bbox="1276 748 1801 781">Partial composite action can be expected.</p>
Shear studs on beams	Structural continuity	 <p data-bbox="1276 1159 1864 1300">The photo of the steel trusses taken during the construction stage does not show any details clearly.</p>
Dovetail deck	Increased concrete mass	<p data-bbox="1276 1325 1766 1357">The thickness of the slab was uniform.</p>

Anti-crack mesh	Tensile action	Only the nominal steel reinforcement was used.
Short spans	Less thermal action	 <p>The shortest span length was 7.6m, and the longest was 10.5m, at least 2-3 times the floor height.</p>
Universal beams over cellular beams	Better temperature distribution	

		 <p>The steel sections of the truss are thin, angular sections whose temperature distribution was almost uniform. The columns were built up using UNP channels, so all parts of the sections (webs and flanges) were exposed to the fire.</p>
Square bays	Stronger tensile membrane action	<p>The aspect ratio of corner floors was 1.01, while edge floors were 1.31, but the support for the edge and inner floors was better than the corner floors.</p>


Columns on gridlines	Resistance against twisting forces	 <p>All 42 columns of the tower were continuous.</p>
Intermediate columns	Alternative load paths	<p>There were no intermediate columns present. The structure had four core columns in the centre and 38 columns on the perimeter.</p>

Table 6 The structural arrangement of the Plasco tower

Examining each component individually with the help of the table above provides basic information about the potential vulnerabilities and strengths of the tower when exposed to fire. Due to the age of the building and limited available information, it is impossible to evaluate the composite action that occurs between the concrete slab and the top chords of the truss members. Therefore, the full composite action cannot be expected during the fire accident. In later parts of the thesis, two models were utilised to simulate the structural response: one considering full composite action and another assuming no composite action. In the reports published by Tehran's city council, authors Shakib H et al. (2017) and Behnam (2019) mentioned the presence of a nominal single layer of steel reinforcement.

Another factor of structural design that negatively affects the structural performance under fires is the length of unsupported spans. The Plasco tower had trusses of span length 10.6m present in the corner areas. Theoretical analyses by Flint et al. (2006) & Li et al. (2021) showed that long spans can be more sensitive to fire than conventional short spans. A steel beam can yield in axial compression at temperatures less than 200 °C if it is restrained at both ends from expanding (Lamont, Lane, Jowsey, et al. (2006)). This is not necessarily a vulnerability if composite action is available through the shear connection between beams and floors, which is doubtful in the case of the Plasco tower. The thin, unprotected floor beams can be added to the list of vulnerabilities of the Plasco tower against fires. The presence of a false ceiling unintentionally protected the floor trusses, but ironically, the false ceiling is believed to have facilitated the fire's propagation (Khan, Khan, et al. (2022) & Khan (2022a)). The floor plan of the tower can be seen as a group of 9 individual segments of floors with aspect ratios ranging from 1.01 to 1.38, which is good enough to produce double curvature displacement. Several studies reviewed by J. Jiang et al. (2022), showed that the tensile membrane action produced in a two-way slab is stronger than in a one-way slab of the same thickness and reinforcement.

In the following sections of this chapter, the load distribution pattern in the tower will be studied by subjecting key components to elevated temperatures. To carry out this exercise, an FE model representing the top six stories of the tower was generated in OpenSees.

3.3. Finite element modelling

3.3.1. OpenSees for fire

Realistic fire modelling was not done in this investigation. Chapters 4 and 5 provide a thorough examination and discussion based on the CFD-based fire spread analysis by Khan (2022a). The heat transfer analysis conducted on the steel and concrete sections involved applying temperature-time profiles derived from the standard fire curve. The GiD+OpenSees interface was employed as a post-processing tool to develop the FE model and visualize the outcomes of the thermomechanical analysis.

3.3.2. Model description.

GiD+OpenSees interface

GiD is a flexible pre- and postprocessor (Melendo et al. (2018)) with the ability to be extended for various purposes, like automation. It provides functionalities for creating and modifying geometries, generating meshes, and performing post-processing tasks. However, it does not include a preconfigured numerical solver as part of its built-in features. To carry out numerical analyses, including a solution engine, is necessary, such as the *OpenSees for fire* module. This is achieved by integrating the readily available GiD interface libraries already incorporated within the software onto the existing interface. The supplementary functionality is implemented as a "problem type" that permits the user to specify one of three generic objects: general problem data, materials, and conditions. The GiD+OpenSees problem type, developed by researchers at Aristotle University of Thessaloniki (Papanikolaou et al. (2017)), enables the simulation of earthquake behaviour in structures using the combined capabilities of GiD and OpenSees.

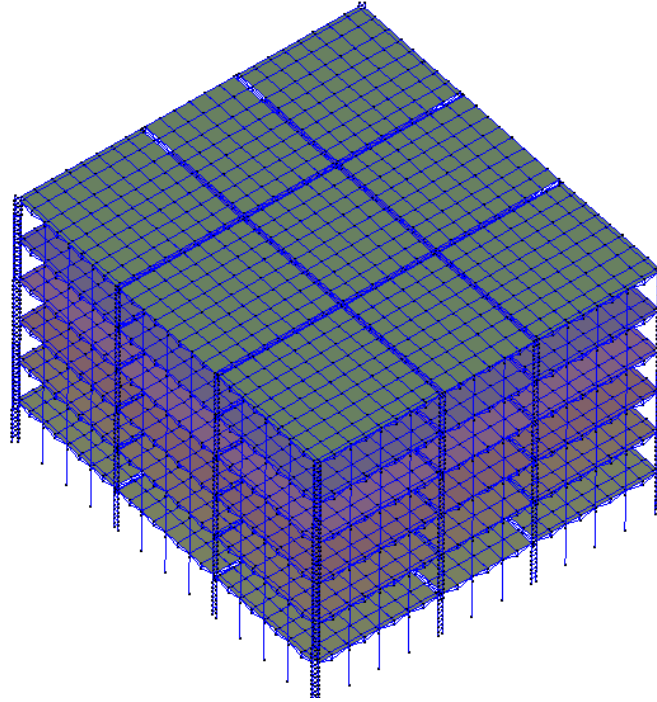


Figure 3.2 GiD+OpenSees visualisation of the multistorey model of the Plasco tower in OpenSees.

Details of the model

The GiD pre-processor was used to model the Plasco tower. To reduce the size of the problem, only the top 6 floors of a total of 17 floors have been considered in the FE model. As mentioned, the Plasco tower floor plan can be seen as nine individual segments separated by two primary beams running in both directions. The ceiling trusses spanning in both NS and EW directions ensured structural continuity among segments. Trusses were installed in the NS (North-South) direction, while Vierendeel beams were used in the EW (East-West) direction. The overall layout of the structure in the plan view appears nearly square, except that the distance in the NS (north-south) direction is slightly greater than that in the EW (east-west) direction.

The fibre section approach has been followed in the modelling of sections. Each Fiber Section object is composed of fibres with thermal properties, with each fibre containing a uniaxial thermal material, an area and a location (y, z). The original *fiberSecThermal* object class enables the user to apply thermal load at 2,5 or 9 points across the depth of the section. Using

the latest additions to the *fiberSecThermal* object class, thermal loading over the shell and beam elements was applied through the temperature history, which was defined over 15 points spread over the web and flanges of a fibre-based beam-column element. Figure 3.3 shows the location of the 15 temperature points, from T1 to T15, corresponding to the web and flanges of an I-section, a modification over the convention originally defined by Jian et al. (2015). Similarly, an additional thermal load definition with 25 temperature points was added to apply thermal load over stiffened I sections (M. A. Orabi (2022)).

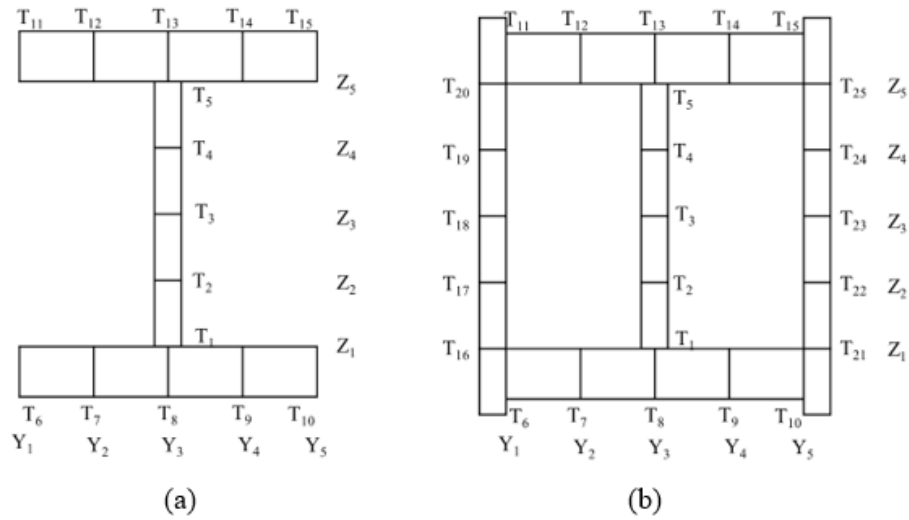


Figure 3.3 Temperature points within the OpenSees fibre-based beam-column element (a) I-section, and (b) stiffened column section (M. A. Orabi (2022))

The estimated dead load of the typical stories, which encompasses the weight of the concrete slab and the joinery, amounts to 6.2 kPa. Due to the partitioning of the stories with brick walls, an additional equivalent partition load of 1.3 kPa is included in the dead load. This results in a total dead load of 7.5 kPa. Following the Iranian Building Regulations 6 (IBR6), the prescribed live load for the typical stories is 5.0 kPa. However, for the Plasco building, an estimation suggests that the minimum live load on the typical stories was 6.0 kPa (Behnam (2019)).

Analysis parameters

The following analysis parameters were used in the OpenSEES analysis. The dead load has been applied in 10 load increments, whereas the temperature load (3600 seconds of fire duration) is in 100 steps.

Analysis commands	Dead load	Thermomechanical
System solver	UmfPack	UmfPack Davis (2004)
Numbered	Plain	Plain
Constraints	Plain	Plain
Integrator	LoadControl	Newmark (Newmark (1959))
Convergence test	NormDispIncr	NormDispIncr
Algorithm	ModifiedNewton	KrylovNewton (Scott & Fenves (2010))
Analysis	Static	Transient

Table 7 Analysis parameters used in the study (Command Manual - OpenSeesWiki (n.d.)).

An element size varying from 100-300 mm is used for meshing the truss members, 300-400 mm for columns at 750mm and shells are discretised at 300-500 mm. The fully meshed model was composed of 71000 nodes and 105000 finite elements.

3.4. Gravity load transfer mechanism

The floors of the Plasco tower can be seen as a group of 9 individual structural segments, as seen in Figure 3.4, with each segment having at least one core column near a corner. The interior part has four core columns near the four corners, and the edge segments have two core columns on one side. The corner columns were designed to resist the global twisting and

swaying loads. There were 42 columns in total, all made using the UNP 200 and UNP 160 steel sections, see Figure 3.6. Among the total of 42 columns, only 12 columns play a substantial role in transmitting the gravity loads to the foundation. At the same time, the remaining 30 were designed to resist the lateral forces acting on the structure. The dead load transfer of the corner area is skewed as the load distribution towards the corner columns is low.

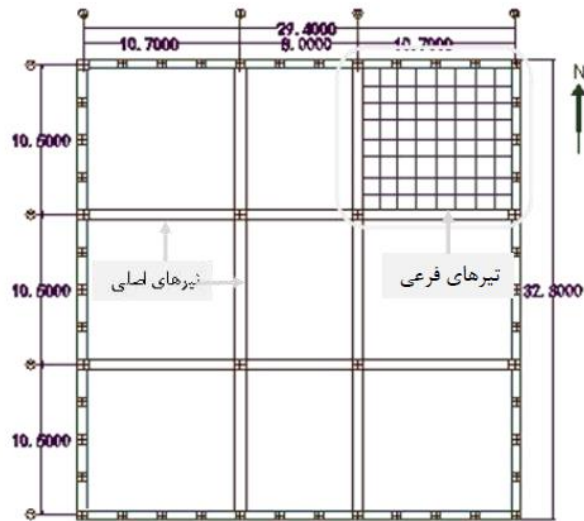


Figure 3.4 Plan view of the tower showing the location of core and perimeter columns.

The dead load analyses revealed that the central core columns in the Plasco tower transfer 45% of the weight of the tower to the ground, i.e., each core column carries nearly 11% of the total dead weight of the structures. Figure 3.5 shows the bubble chart with the radius of circles proportionated to indicate the magnitude of vertical reaction forces. The safety of core columns is critical to the global integrity of the tower. The columns on the periphery, which are supporting primary beams, are carrying nearly 20% of the total gravity load. The remaining 36 secondary periphery columns are resisting 35% of dead weight.

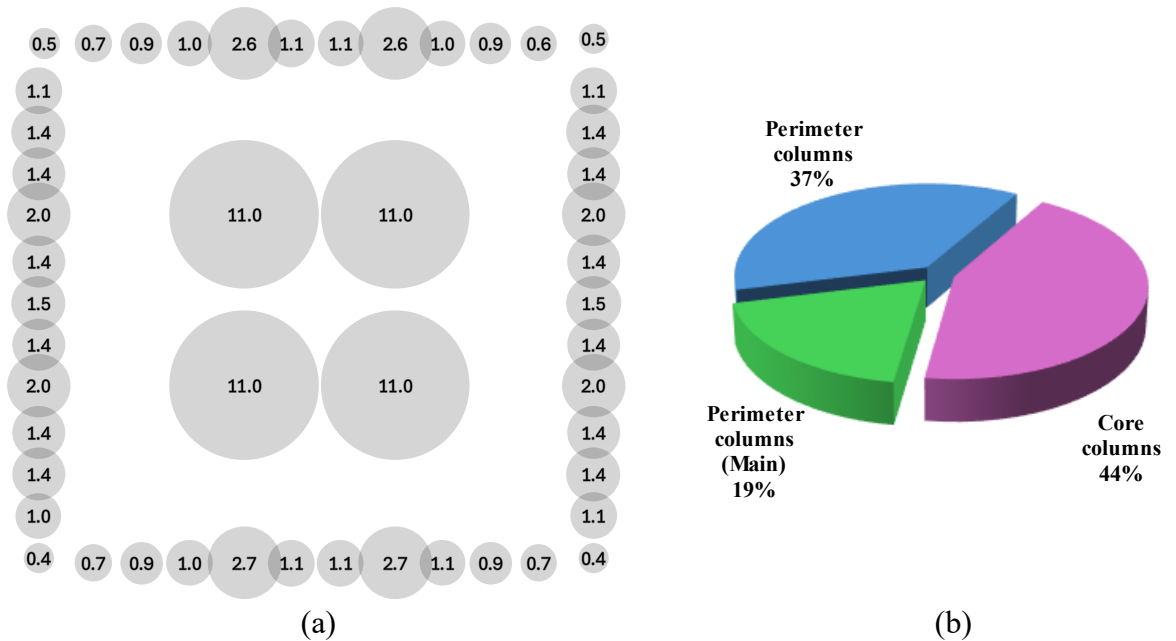


Figure 3.5 (a) Bubble chart indicating the ground reaction forces (in percentage) of all the columns; (b) percentage of load sharing among the core and other perimeter (secondary) columns.

Ambient load ratios

Calculations based on the EC1 showed that the load ratios of all the columns are less than 1, with the highest values in the core columns on the ground floor, where the load ratios reached up to 0.84. Shakib et al. (2020), in their preliminary analyses, pointed to the higher utilisation ratio of core column sections on the ground floor.

Yang & Yang (2015) studied the response of restrained welded box steel columns under fire conditions. It was observed in their study that the fire resistance of steel columns depends mainly on the load ratios the columns were under before subjecting them to fire loading. In the ten columns they tested, under constant load ratios, the critical parameters that affected the fire resistance were penetration of weld and the width-to-thickness ratio of sections used.

The columns in their study were not fire-protected and were heated over their entire length on all sides. In partially penetrated welded columns, the mode of failure under fire occurred through cracking of welds. The authors hypothesised that a partial weld penetration

could leave a crack-like gap between the connected plates. This thin line of gap was the likely cause for failure at lower thermal loads and temperatures of 500 °C. In addition, in local floor collapses, i.e., in the case of the initial partial collapse of the NW corner, the effective length of the column increases due to the loss of lateral support. In such cases, the load ratio on the column increases significantly because of reduced buckling strength. As steel columns would be under a service load state before being subjected to thermal loads, the magnitude of the service load is a crucial factor affecting the fire performance of steel columns. Therefore, this study calculated the loading on the columns based on the state the Plasco tower was in before the accident. The likelihood of reduced performance of column sections due to aged, welded connections (see Figure 3.6) in the case of the Plasco tower is an important factor, but it is not considered in this study. By not modelling the connections, it is possible to study whether the structure could sustain the applied thermal load irrespective of connection failures.



(a) Core column



(b) Corner column



(c) Secondary column



(d) Secondary main
column

Figure 3.6 Photos of built-up column sections taken after the collapse.

Various researchers like J. Jiang & Li (2017), Sun et al. (2012) and Shepherd & Burgess (2011), studied the effect of load ratios on the failure time of steel columns. It was understood from the existing literature that ambient state load ratios were a key factor in assessing its behaviour during fire loads. In a building fire, the affected columns expand axially, push the floors upward, buckle and then freely hang between the floors. The buckling behaviour of columns during heating is highly unstable and dynamic in nature. Hence, the load shedding caused by the failing column can cause dynamic loads on the surrounding columns. In such cases, safe load transfer can be expected if the surrounding columns have a lower load ratio. If load ratios are higher, the failing column can initiate the buckling of surrounding columns. In the case of the Plasco tower, core columns at a load ratio of 0.34 (conservative estimation) are loaded to an extent that their reserve capacity cannot be relied on in case of extreme fire events, even if the fire spread is not large and is limited to local zones.

The values of load ratios of the secondary main, secondary, and corner columns at ground level are 0.51, 0.43 and 0.1. Hence, the columns of the Plasco tower, with DL+1.5LL load combination, were well within safe load ratios in the service state condition. The load ratios in the columns at higher levels are lower due to the reduced dead weight; the load ratios of the 11th floor are given in Table 8.

Column	Load ratio. (Level: Ground floor)	Load ratio. (Level: 10th floor)
Core column	0.84	0.34
Secondary main column	0.53	0.19
Secondary	0.43	0.21
Corner	0.1	<0.5

Table 8 Maximum load ratios of different columns of the Plasco tower at the ground and 11th-floor level.

While calculating the load ratios, it was assumed that the effective cross-section of the is equal to the full cross-section area. The actual load ratios in the column might be higher than

the calculated values if the effect of welds in the built-up column section is considered. It should be noted that the core column comprised eight sections of UNP 160 type steel members; see Figure 3.6(a). In a real fire scenario, the performance of welding cannot be taken for granted. Due to the lack of data on the welding and age of the structure, the welded sections of the columns are likely to fail at reasonably lower temperatures than properly welded sections/single cold-formed sections of the same strength.

3.5. Robustness analysis of the Plasco tower

3.5.1. Core columns

In the first study, the core column on the SE (Southeast) corner of the tower was chosen for the investigation. Figure 3.7 shows the location of all core and perimeter columns of a single floor; for clarity the secondary truss beams, Vierendeel beams, and slab members are hidden. The SE core column was subjected to heating until it reached a point of failure in order to investigate the impact of the failed column on the surrounding columns caused by load shedding.

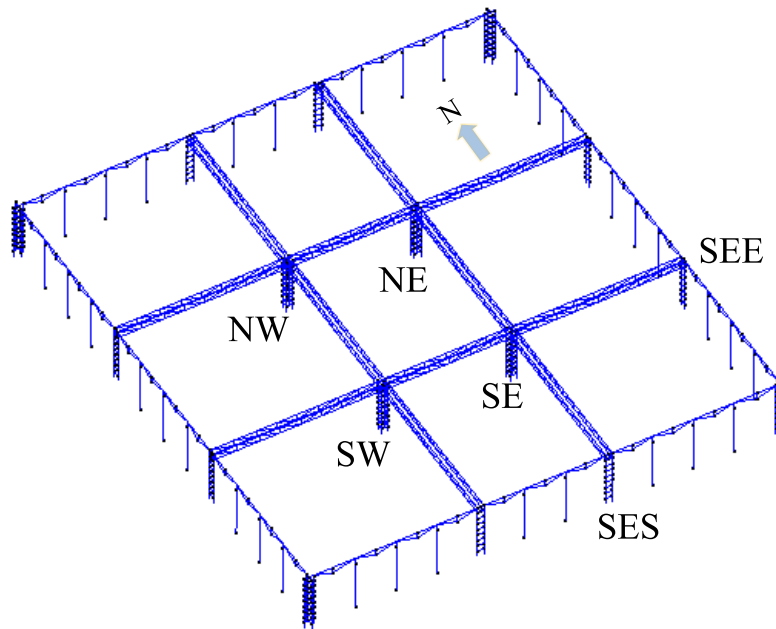


Figure 3.7 Isometric view showing the location of columns.

As a result of the failed SE core column, the load on the adjacent columns increased by varying proportions. The adjacent SW core column received a higher redistributed load than the NE core column. It can be seen in Figure 3.9(c) that the SW core column received 35% of the additional load while the NE core column received only 4-5% of the additional load with respect to the loads they were under during the service state. The aspect ratio of the floor segment in the core area can explain this disproportionate distribution of load transfer. In the case of the Plasco tower, the distance between the SE and NE core columns was 10.5m, while the distance between the SE and SW columns was 8m. When a column supporting a square-shaped floor fails, an even redistribution of loads to the neighbouring columns is expected. Similar failures due to uneven load redistribution were observed in the progressive collapse analysis studies of composite steel frames by J. Jiang & Li (2017). The graph depicted in

Figure 3.9(c) shows that the reaction forces in the SE column rise during the initial phase of fire due to restricted thermal expansion. Consequently, the ground reaction in the SW core column decreases by 10% compared to its initial value. However, the reaction forces in the other adjacent columns mostly remain unchanged during this period. At a later stage, once the gas temperatures exceed 550 °C, the ground reaction in the SE core column begins to decrease. The findings indicate that the secondary columns located around the edges did not undergo a noteworthy rise in the ground reaction forces. Hence, in a fire affecting a core column, the outward redistribution of load is nearly even over the columns along the edges, see

Figure 3.9(b). The plot shows that the main secondary columns – SES and SEE received additional redistributed loads of 5-10% of their initial magnitudes.

Realistically, between the core columns, there was masonry present till the false ceiling level. This results in a potential exposure of only 400mm length of steel columns to extremely high temperatures. Some evidence shows that only a tiny portion of the wall comprised of masonry was present; the rest of the height was provided with thin partition boards, as seen in the Figure 3.8. If masonry protected a significant portion of columns, then high section temperatures are not likely. However, a considerable length of core columns can be exposed to severe temperatures when masonry walls are destroyed due to collapse debris.



Figure 3.8 Interior view of the surviving 5-storey building beside the Plasco tower.

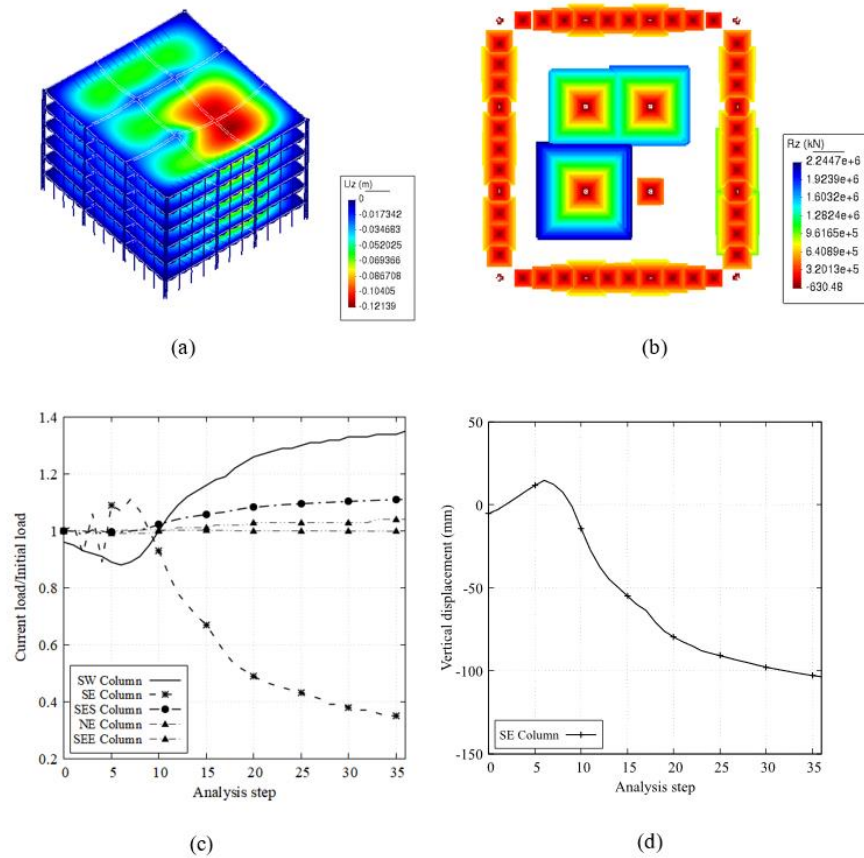


Figure 3.9 (a) Global response of the structure under localised fire load on the Southeastern core column; (b) contour plot showing the ground reaction forces of columns; (c) evolution of ground reaction forces; and (d) vertical displacement of the SE column.

If a fire occurs involving the SE core column, a significant area around it will also be directly exposed to the fire. Therefore, such a situation will affect the primary beams, which are crucial for redistributing loads in the horizontal direction. In beams or truss beams, horizontal load redistribution occurs through the beam action initially and gradually shifts to catenary action if exposed to fire. If the connections of the primary beams with columns are sufficiently strong, the catenary action may exert an inward force on the external columns, resulting in a potential global failure. However, if the connections fail, a local failure can be expected. The following sections of this chapter analyse how the failure of primary beams affects the overall structural robustness.

3.5.2. Primary beams

Primary beams serve as the essential horizontal structural elements of the Plasco tower. The structure of the tower comprised a total of four primary beams, which spanned in both the North-South and East-West directions. Figure 3.10 shows that the primary truss beams connect core columns with the secondary main column near the perimeter. Each primary beam consisted of two trusses positioned at a separation of 400mm from each other; see Figure 3.11. The combination of core columns, secondary main columns, and primary beams forms the major load transfer system of the Plasco tower. This system is responsible for transferring 63% (as shown in Figure 3.5(b)) of the total gravity and service state loads to the foundation.

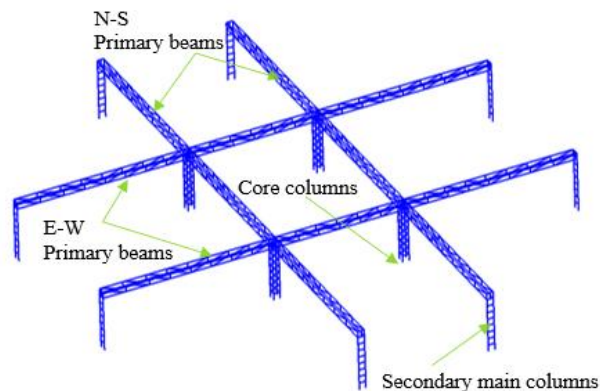


Figure 3.10 The primary load transfer system of the Plasco tower structure.

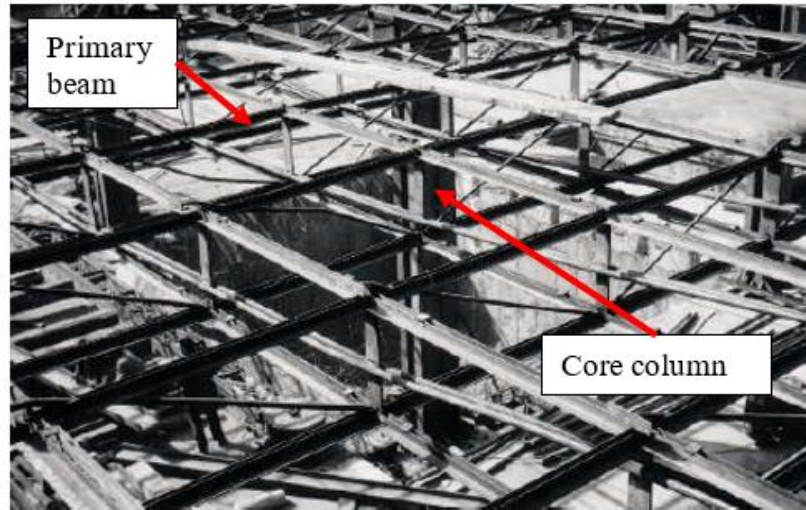


Figure 3.11 Construction stage photo showing the view of the truss floor system

In the first study, thermal load was applied the SE core column till failure. A significant load increase on the SW core column was observed and remaining load was redistributed to all the columns in the Southeastern perimeter of the tower. The primary beams, secondary trusses, and composite floor played a crucial role in facilitating this horizontal load redistribution.

In the second study, the performance of the tower is studied when the primary beam joining the SE core column and the SES secondary main column fails under thermal load. Thus, for this particular study, a region measuring 3 x 10m (see Figure 3.13(a)), which encompasses the primary beam mentioned earlier, along with the composite floor and secondary truss elements, is chosen. Within this zone, all the steel members and concrete slab are exposed to temperatures determined by the ISO 834 curve to conduct heat transfer analysis and subsequent thermo-mechanical analysis. Since the steel cross sections are thin, the temperature variation at the end of the heat transfer analysis is not significant. The temperature profile across the concrete slab can be seen in Figure 3.12(d) which shows that the temperature attained at the bottom surface of the slab is 900 °C, and the top surface is around 85 °C.

The results from the simulated structural response showed large floor deformations near the Southeastern portion of the floor slab. The importance of the primary beam can be understood from the fact that an intense localised fire near any primary beam can cause displacement closer to 150-200mm in large portions of the floor (Figure 3.12(c)). In the current study, nearly 200 m² of the floor was affected by the localised fire case scenario. Figure 3.12(a)

shows simulation results, which show that displacements in a large portion of the slab are higher than 100mm.

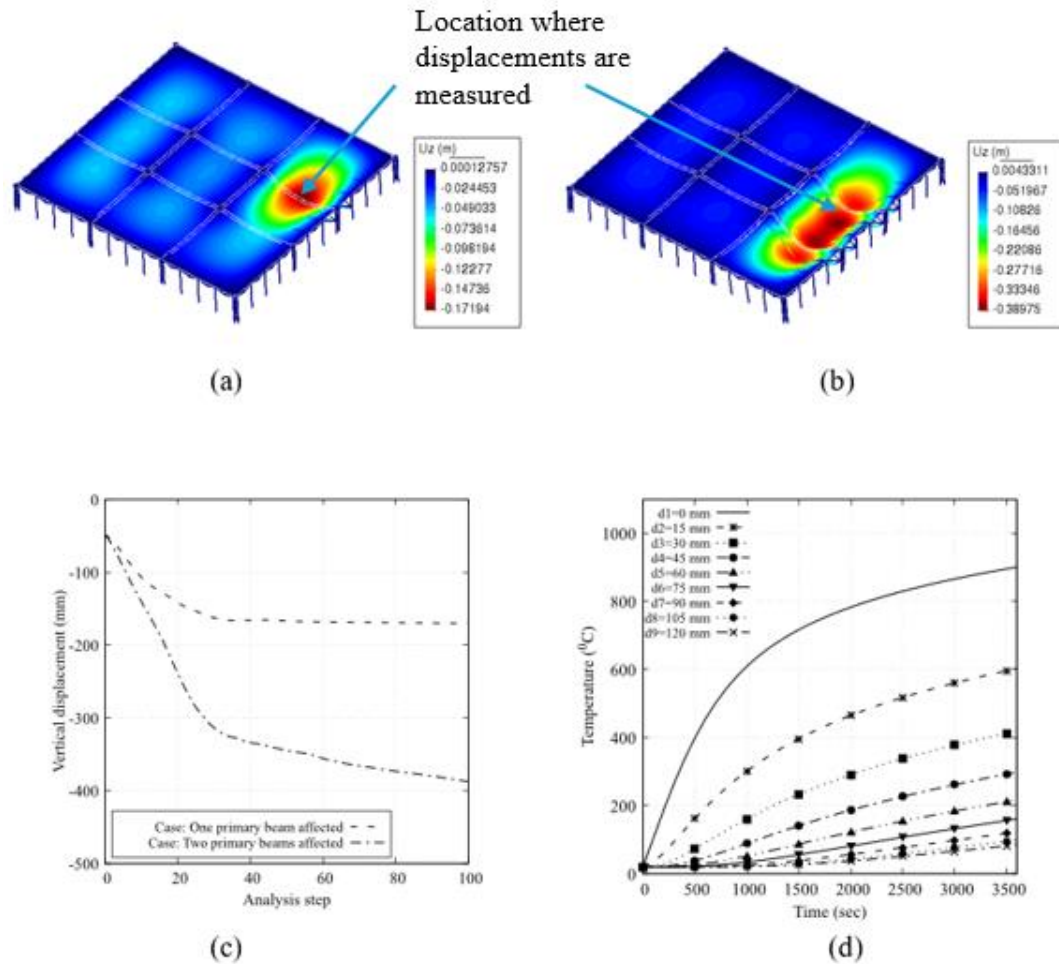


Figure 3.12 Response of the floor when (a) only one primary beam is heated, (b) two primary beams are heated, (c) comparison & (d) slab temperature profile.

In a normal ambient temperature condition, the two-floor segments adjacent to the primary beam will undergo deformation with a double curvature. Under fire conditions, if the primary beam is protected, the two-floor segments would still experience double curvature because of the two-way bending action. A floor slab deforming in a double curvature (two-way bending) experiences stronger tensile membrane action (TMA) than a slab deforming in a single curvature (one-way bending). The tensile forces within the slab caused by single-curvature catenary action are significantly lower than those generated by double-curvature tensile

membrane action. As a result, the slab may experience much greater deflections before the reinforcement reaches a fracture point. When the slab deflections are high, it will result in larger lateral displacement of the connected columns, which can potentially exceed safe limits and may even induce high forces in connections or buckling failure of external columns.

Tensile membrane action can considerably increase the capacity of two-way slabs with aspect ratios below 2, whereas one-way slabs with aspect ratios greater than 2.5 can resist loads through catenary action (Moss et al. (2008) & J. Jiang et al. (2022)). In the case of Plasco, due to the boundary support provided by the primary beams, the aspect ratios of the slabs are within the value of 2. The slabs in the corner are nearly square with an aspect ratio of 1.01, while the interior slab has an aspect ratio of 1.31. However, the load-bearing mechanism at large displacements is not well-defined for slabs with aspect ratios ranging from 2 to 3. These slabs appear to be more influenced by boundary conditions and reinforcement arrangement, as their behaviour can transition between tensile membrane action and catenary action.

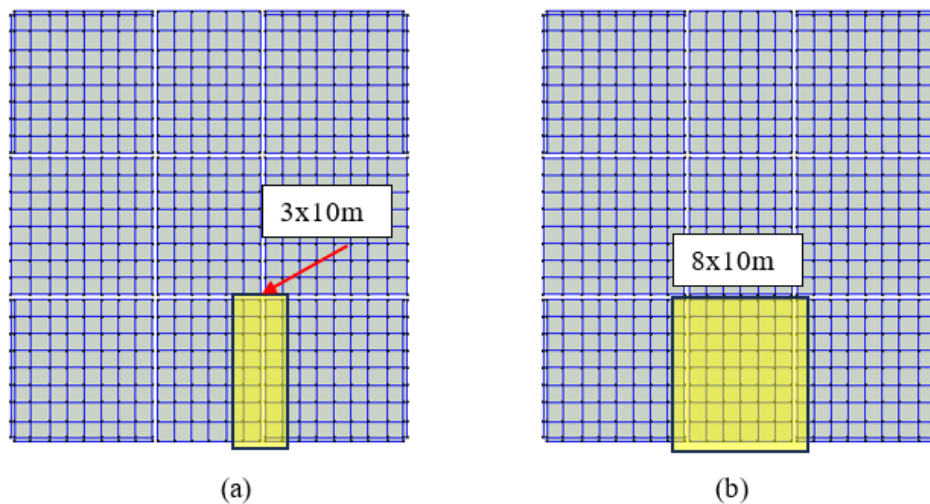


Figure 3.13 Zones in the edge compartment considered for applying the fire load.

If fire affects a portion of the floor such that it involves at least one primary beam, then the adjacent floor segment loses support over the edge along the primary beam. In the study case of fire spread over an area of 8 x 10m zone (Figure 3.13(b)) engulfing two primary beams on the same floor, which was a probable scenario during the Plasco tower fire incident, see Figure 3.14. Then, the floor segments might behave like slabs whose aspect ratio is equivalent to 3. To simulate the response of the floor when two primary beams are affected, both primary

beams near the south side are subjected to thermal load. The results showed large vertical floor displacements in three-floor segments near the south face. The magnitude of displacements when two primary beams are heated (Figure 3.13(b)) is nearly 3 times higher than the case where only a single primary beam (Figure 3.13(a)) was heated. Figure 3.12(c) compares the maximum vertical displacement obtained in both cases. It can be seen in the contour map of Figure 3.12(b) that in the event of two primary beams under severe fire, a one-way single curvature floor deformation is unavoidable.

In such cases, the catenary action of the floor might pull the external columns inwards, leading to a collapse scenario. If the floors collapse due to failure of connections, like in the Northwestern corner of the tower, then a partial collapse can be expected.



Figure 3.14 Photo of the tower showing fire possibly heating two primary beams simultaneously.

Based on the available fire travel history provided by Khan (2022a), there is a high possibility that the extent of fire spread is large enough to affect two primary beams simultaneously. In the initial and later stages of the fire, partial collapses of floors occurred in the NW and SE corners. It is likely that a large fire in the edge compartment affects two primary beams. Since primary truss beams provide edge support for all the floor slab segments, a corner fire might undermine support from two adjacent sides, whereas a fire near the edge undermines support from two opposite sides, as seen in Figure 3.12(b). The case of two adjacent primary beams under fire near the south face of the tower is realistic. Ahmadi et al. (2020), in their

study, provided evidence of unobstructed fire progression engulfing the entire South face of the 13th and 15th floors of the tower. The study claims that the trigger for the final collapse was the buckling of the secondary main column (SES) near the Southeast corner of the tower. In the next section, the robustness of the tower is studied by subjecting a secondary main column to elevated temperatures.

3.5.3. Secondary main columns

In the case of the floor collapse that took place in the NW corner, it was reported by researchers like Shakib et al. (2020), Ahmadi et al. (2020) and Khan (2022a) The collapse of the 11th and 12th floors near the NW corner caused a sandwich collapse of multiple floors below them. Even though no buckling of columns was observed in the NW corner, the failure was mainly caused by the failure of connections. The collapse propagation occurred vertically while not affecting the column and bracing supports in the zone.

After the core columns and primary beams, secondary columns play an important role in the global stability of the structure. In the final study, a secondary main column of two storeys in height and the connecting primary beams are subject to elevated temperatures. Initially, the study was limited to single-storey, and it was realised that the load shed by the heated columns was successfully redistributed to the adjacent columns. Therefore, the thermal load is extended to two storeys, as seen in the Figure 3.15(a) to study the response of the structure.

The simulation results showed large floor displacements in the region with a maximum value of 340mm, which is nearly thrice the value (Figure 3.12(a)) observed in the previous case, where only a single primary beam (near SE zone) was heated in the same region.

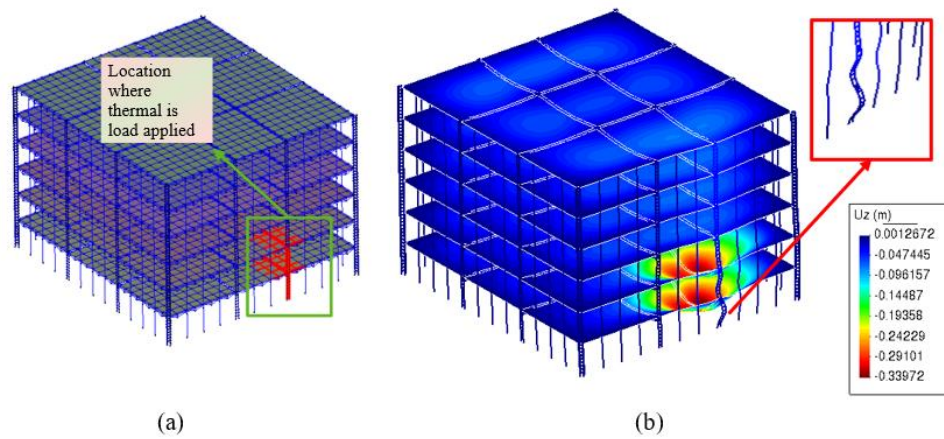


Figure 3.15 Simulation of the tower with primary beams and secondary main columns subjected to fire.

The secondary main column buckled at analysis step 23 corresponding to column temperature of 500 °C. At this point, the global stability of the structure was not affected unless connections failed. If connections fail, then progressive collapse of floors can be expected due to the action of dynamic loads. However, if connections sustain temperature-induced forces, then redistribution of loads towards the adjacent columns can be expected.

The columns of the Plasco tower are well within the safe load ratios during the ambient state, see Table 8. The load ratio of the secondary main and secondary columns in the perimeter of the 10th floor was around 0.21 and 0.19, respectively. In the event of secondary main column failure, the adjacent secondary columns may have sufficient reserve capacity to withstand additional loads. It depends on the number of floors on which the fire spread occurred. If the number of floors affected is more than 2, it may result in reduced buckling strength of the columns. In the case of fires affecting more than two levels of floors, the load ratio in the adjacent secondary columns was higher than 0.5 due to increased effective length. Hence, the combination of higher load ratios and reduced buckling strength can be detrimental to the stability of the structure. In a best-case scenario, if the horizontal spread of damage is curtailed, a localised floor collapse encompassing 20-25% on each fire floor can be expected. If the damage spreads horizontally due to the successive failure of overloaded members from load

redistribution, then a potential global collapse is imminent. J. Jiang et al. (2014b) in their study on the progressive collapse of steel frames exposed to fires, highlighted the risks of edge bay fires. When fire loads are applied near the edge bays, the global deformation of the structures observed is usually asymmetric, and columns experience P-delta effects. The study concluded that edge bay fires are more prone to progressive collapse than central bay fires due to less availability of load redistribution paths. The research also found that when the load ratios increase, the critical temperature for columns decreases significantly, reaching as low as 250 °C.

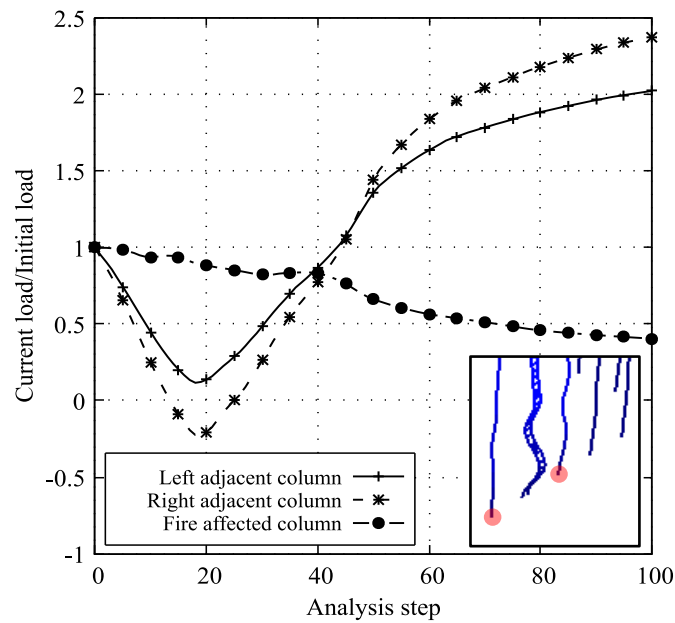


Figure 3.16 Plot showing the increased load due to the load shedding of the fire-affected column.

The plot in Figure 3.16 shows the pattern of load redistribution in the adjacent columns. The x-axis shows the analysis step values, and the y-axis shows the non-dimensional load in the form of $P_{current}/P_{initial}$. The load shedding caused by the heated columns induced an additional load of more than 100% in the adjacent secondary columns. The plot shows that the column reactions in the left and right adjacent columns increased by a factor of 2.0 and 2.37, respectively.

Under such increased load ratios, the risk of adjacent columns buckling depends on the

degree of lateral support present. If heating is applied to multiple floors, the possibility of collapse propagation along the perimeter through buckling of remaining columns becomes plausible.

Column effective length factor	0.50	1.00	1.25	1.5	2.00
Slenderness ratio (Eurocode)	0.48	0.65	0.86	1.04	1.38
Load ratio	0.40	0.46	0.60	0.66	1.00

Table 9 Increased load ratios in the adjacent secondary columns.

Table 9 shows the increased load ratios in the adjacent secondary columns based on the Eurocode formulae. If the influential length factor of the column increased from 0.5 to 2, representing a range of available lateral support. The value 0.5 means the column boundary conditions represent fully fixed supports on both sides. In contrast, the value 2.0 represents a condition where lateral support from one floor is lost, and end supports are of pin type. In the first case, using the conservative assumption of 0.5 effective length, the load ratio is quite at 0.4. At effective length ratios of 1, 1.25, 1.5, the load ratios increase further to 0.46, 0.60 and 0.66, respectively.

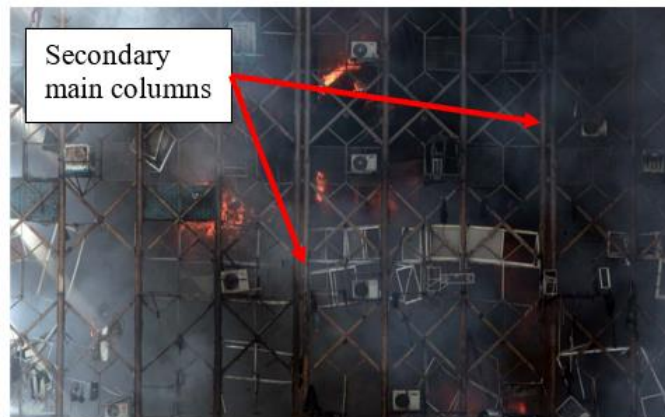


Figure 3.17 Photo showing the Northern elevation of the tower under a fully grown fire over multiple floor levels.

In a different scenario representing the fire condition, as shown in Figure 3.17, the fire load was applied across multiple floors, impacting the compartments at the edges. Temperature load was not applied to the edge beams as masonry was present along the periphery. As anticipated, the simulation outcome from this analysis showed significant displacement in the slabs of all three-floor segments. Figure 3.18(a) shows the buckled secondary main columns and the secondary columns across multiple floors. These failed columns account for not more than 10% of the total gravity load of the structure. The deformation observed is of a magnitude of 520mm in the centre of the edge bay floor slab segment; see Figure 3.18. In reality, catenary deformations exert substantial forces on the connections, increasing the likelihood of partial floor collapse. It should be noted that connections were not modelled as the focus of the study was to look for the load redistribution patterns and collapse mechanisms that can lead to global or partial floor collapses. The load shed by the buckled columns was transferred to the other secondary columns on the same plane as the edge frame. It can be seen in Figure 3.18(b) that the contour plot shows the thickness of line elements proportioned to the axial forces the columns are experiencing. The ground reactions of the secondary columns adjacent to the buckled secondary main columns are 2.72 times their initial value. Therefore, there is a possibility of a progressive collapse of the columns in the periphery where load shedding and load redistribution happen along the edge, leading to an inward collapse of the structure. Or suppose lateral propagation of failure of buckling did not take place. In that case, the structure will achieve a temporary stable condition where edge beams and corner columns resist the inward pull forces caused by the catenary action of trusses, as depicted in Figure 3.19. The overloaded adjacent columns did not show buckling as lateral support was present from colder parts of the structure. In a real scenario, under partial collapse, a lack of lateral support for the columns can be detrimental to the stability of the structure.

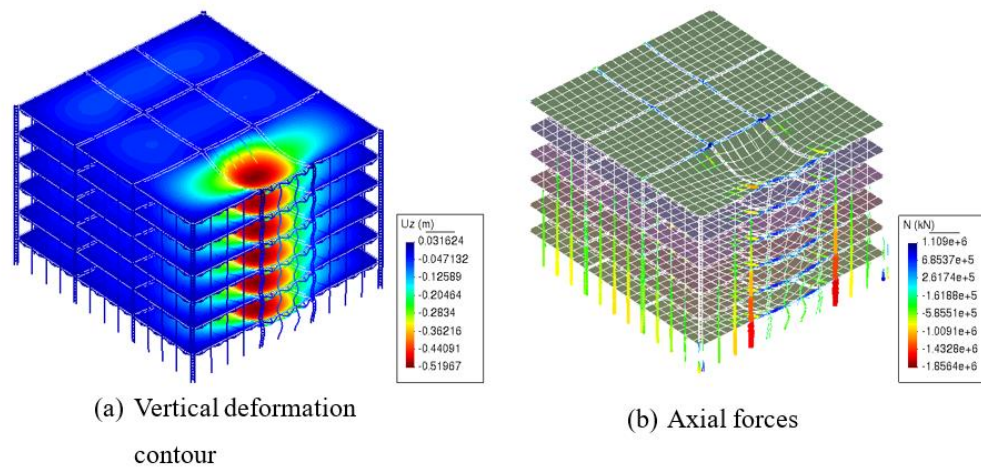


Figure 3.18 Structural response against edge compartment fire over multiple floors.

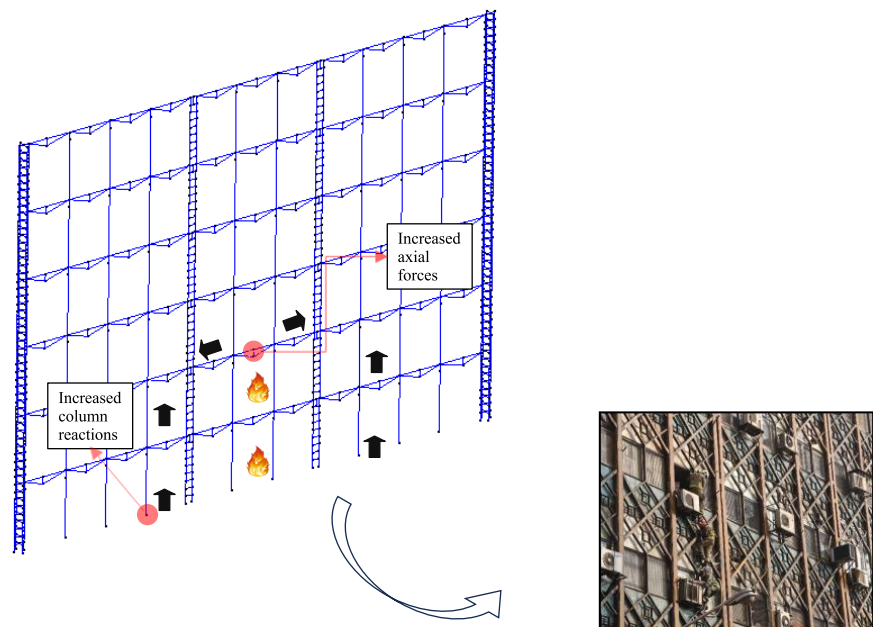


Figure 3.19 Load redistribution in the edge frame due to the fire in multiple edge compartments.

In this chapter, a robustness analysis of the components of load transfer systems is carried out, and various possible global progressive collapse mechanisms for the Plasco tower are discussed. While the buckling failure of the core column triggers global collapse, the failure of primary beams and/or secondary main columns likely causes local failure of the structure,

potentially creating conditions for disproportionate collapse at later stages. Hence, a safer structural design against fires warrants member-level fire protection for primary load transfer components such as core columns, whereas components such as primary beams should be approached from a global safety point of view. The two design approaches -preventing local collapse through structural continuity or implementing structural isolation by segmenting to prevent disproportionate global collapse need further enquiry in the case of fire safety design. Table 10 highlights the key insights derived from the robustness study conducted in this chapter. The study highlights the importance of using a performance-based design to increase the robustness of the structure. Based on the current study, it can be said that prescriptive design can help prevent progressive collapse resulting from core column failure only. The other inherent collapse-inducing mechanisms depend highly on the member-to-member interaction under elevated temperature conditions. During a fire, factors like load ratios, mode of load carrying mechanism (shifting from bending to catenary tension), lateral support, etc., drastically change over short durations, as observed in the case of the Plasco tower. However, considerable research remains to be done, and structural engineers must also be made aware of the risks associated with neglecting global-level fire safety in structural design.

Components under multiple floor fire	Global collapse	Partial collapse	Need specific local resistance	Presence of alternative load paths in the event of component failure
Core column	Highly likely	-	Yes	No
Primary beam	It is likely under multiple-floor fire spread.	Likely due to connection failures	No	Yes
Secondary main columns	Unlikely	It is less likely if adjacent columns withstand the load redistribution	No	Yes

Table 10 Critical observations derived from the robustness study.

3.6. Conclusions

This chapter focused on understanding the behaviour of the Plasco tower structure when key components or areas are subjected to different fire loads. The collapse of the tower was thoroughly examined to gain insights into the specific collapse mechanisms and to categorise the damage/collapses at various locations.

- (a) Four kinds of local collapse mechanisms are identified based on the analysis and available evidence - pancake, domino, section and instability-type collapse mechanisms. The global collapse of the tower began with the pancake-style collapse mechanism in the NW corner of the tower, i.e., 11th and 12th floor ceilings. The dynamic effects of these two floors caused the failure of multiple floors below them. The damage sustained by the tower was not critical to global stability. As the fire continued to spread, the damage and subsequent collapses of the components near the South and SW corner involved sectional failure, instability, and possibly domino-type collapses.
- (b) A review of the structural configuration of the Plasco tower was carried out. Design aspects beneficial to the tower in resisting collapse, such as structural continuity and tensile membrane action, were discussed. The near-square shape of the floor slabs in the Plasco Tower likely enhanced their capacity for tensile membrane action. Because tensile membrane action is more efficient when the slabs undergo double curvature rather than a single curvature deformation. Given the limited information available about the shear studs and the age of the composite floor slabs, it is not possible to confidently assume the full composite action during the fire. While the floor slabs maintain structural continuity, uncertainties surrounding the shear studs prevent a definitive conclusion about their effectiveness under fire conditions.
- (c) The secondary main column near the SE corner underwent splitting failure before the collapse. Visual observations indicated that the welds used in the steel sections failed, resulting in noticeable separation. This introduces uncertainty when modelling and evaluating the structural integrity of the buildings, particularly due to the use of built-up sections and the inclusion of baton members in constructing steel elements. These factors contribute to the complexity of accurately modelling the structures and assessing their resilience against fire loads.

- (d) The Plasco tower's structure was designed with columns only along the perimeter and core, lacking any intermediate columns that would have provided alternative load paths. The long-span truss beams of 10.7m in length tend to cause higher restraint forces on the perimeter columns than shorter-span truss beams. Long-span beams are sensitive to fire and experience compressive failures at relatively lower temperatures of 200 °C. The buckling of bottom truss chords was also confirmed by inspecting the debris from the Plasco tower.
- (e) The gravity analysis showed that the four core columns resist 44% of the weight of the tower, while the eight secondary main columns resist 19% of the total weight. The remaining 30 secondary columns resist 37% of the total weight. The primary means of transferring gravity loads to the perimeter columns is through the primary beams. The research findings highlight that the key elements of the structural system of the tower are core columns, secondary main columns, and primary beams. Consequently, the overall stability of the structure is heavily reliant on these three components.
- (f) The robustness analysis involving the thermal load application on core columns revealed that load redistribution from any failed core column to the adjacent core columns is not uniform. The core column (SW in the study) on the shorter end of the primary beam received a higher proportion of the redistributed load. The results showed that the ground reaction force in the SW core column increased by 35% of its initial value. In the case of sudden buckling failure, the load increase due to dynamic effects can be higher than the value predicted. Though there was a presence of masonry near and around the core columns, evidence showed that the masonry did not protect the full length of the columns. Although the core columns are less prone to experiencing high temperatures, it is important to highlight that the design relying on a smaller number of core columns requires careful consideration from a fire safety perspective.
- (g) The responsibility for transferring 63% of the total weight to the peripheral columns lies with the composite floor system, primarily supported by the primary beams. The robustness studies involving the primary beams showed that failure of one single primary beam (away from the core) can cause failure of 20-25% of the floor area (2 slab segments). If two primary beams on one face are affected, the failure of 33% of the floor area (3 slab segments) can be expected. The failure of floor segments may not cause

global failure of the tower, which can be corroborated based on the partial failure in the NW corner of the tower. The dynamic effects of falling floors might cause the failure of multiple floors below. The possibility of fire affecting the interior primary beams is highly unlikely. However, it can have a significant impact on the global stability of the structure as the interior primary beams play a crucial role in connecting and supporting all the core columns.

- (h) The secondary columns form the critical load-carrying components of the tower after the core columns and primary beams. The robustness analysis involved applying thermal load to the edge compartments over multiple floors. The analysis results did not predict collapse-causing conditions when the fire load was limited to a single floor. However, when the thermal load was applied to multiple floors, the results indicated the potential buckling of secondary main columns due to loss of lateral support. In multiple-floor fires affecting the edge compartments, the load shed caused by the secondary main columns may result in a temporary stable condition if adjacent columns and edge beams remain stable under additional compressive forces.

Chapter 4: Investigation of the Plasco Tower Fire

4.1. Introduction

When performing a forensic examination of a building affected by a fire, it is crucial to establish a clear timeline, starting from the fire ignition and ending with the structural impairments. The forensic analysis of the building should involve determining the cause, studying the fire propagation patterns, analysing the behaviour of the fire from its initiation to its decline, assessing compartmentalisation, evaluating the efficiency of fire protection systems, and scrutinising firefighting tactics. Leveraging available photographic and video documentation, this chapter aims to reconstruct the fire incident for the forensic assessment of tall structures.

4.2. The case of the WTC investigation

Following the tragic events of 2001, when WTC Towers 1, 2, and 7 collapsed due to the impact of two aeroplanes on towers 1 and 2 of the WTC, NIST (National Institute of Standards and Technology, USA) undertook an extensive investigation into the collapses. Several independent researchers also conducted detailed examinations, given the enormous significance of those collapses. WTC Tower 7 was the first steel-framed tall structure to completely collapse solely due to uncontrolled fires that originated from the debris of the collapsed WTC Tower 1 adjacent to it. (Gross & Mcallister (n.d.), NIST (2005) & A. S. Usmani et al. (2003))

To simulate the response to such complex structural failure of Towers 1 and 2 of the WTC, A. S. Usmani et al. (2003) conducted a parametric study to simulate potential conditions and model structural behaviour under fire. To establish temperature distributions for structural analysis, the authors utilised a range of fire scenarios outlined by Torero (2011). However, the study aimed to understand the structural response; hence, the fire spread within the building was not explicitly described to reconstruct the fire for estimating the thermal load.

In the past twenty years, the predominant method for reconstructing the structural

response to fire has been to simulate all three aspects of the fire event: characterising the fire, transferring heat to the structural elements, and analysing the structural reaction. Though using empirical or analytical idealised models in which a great deal of information can be generated to understand the structural response to fire, reconstructing actual fire events could not be replicated, especially for large fire scenarios such as the collapse of the WTC towers (New York, 2001) (NIST (2005), A. S. Usmani et al. (2003) & Eurocode (2002)). The distinctive structural system of a building, coupled with particular fire scenarios, can result in unique forms of structural failure, thus demanding a thorough examination of the actual fire propagation. Multiple studies carried out on the fire spread history within the WTC towers have revealed specific fire scenarios, notably where the fire propagated along the open-floor plates, called "travelling fires." (Stern-Gottfried & Rein (2012) & Dai et al. (2016))

This chapter focuses on examining the case of the fire accident at the Plasco tower to analyse the progression and extent of fire spread in both vertical and horizontal directions, culminating in the total collapse of the structure. To achieve this, all accessible evidence, such as images, testimonies, videos, reports, and additional sources of information, are compiled.

4.3. Fire investigation

The first step in any fire investigation involves gathering evidence to reconstruct the fire incident. Typically, fire investigations focus on determining the cause and origin of the fire rather than conducting an extensive analysis of the fire spread within the building. (DeHaan et al. (2011)). For any complex incidents like the fire-induced collapses of the WTC towers, Torero recommends that investigators set objectives for their study before performing the investigation (Torero (2011)).

The primary aim of a forensic investigation into structural failures in fires is to understand how structures react to different fire scenarios. Understanding key parameters is crucial to realistic fire modelling after establishing a coherent fire timeline based on critical fire events. This process helps accurately simulate the structural response during fires. These essential factors are the ignition source and fire origin, characteristics of combustibles and fire load distribution, architectural layout, partition structures, and ventilation status, among other relevant elements that influence fire behaviour within a building. Understanding these

parameters is crucial for accurately modelling and simulating the fire.

In the past twenty years, CFD has established itself as a practical method for simulating fire dynamics in forensic investigations and design scenarios. For instance, NIST utilised CFD models to examine the collapse of the WTC towers, correlating fire spread with visual evidence from photographs and videos. Nevertheless, inherent uncertainties are present in numerical fire modelling, primarily due to the variability in fire-related parameters. In an attempt to address this ambiguity, Khan (2022a), initially structured the gathered data into a logical timeline. Subsequently, they employed this timeline as a benchmark for calibrating CFD models. The calibration procedure aimed to achieve accurate predictions of temperatures and heat release rates, aligning with the observed progression and timing of the fire.

4.3.1. Investigation aids

As a fire initiates, it causes various changes in the surroundings, including the generation of heat, smoke, char, and other indicators known as fire signatures. As the fire progresses, it leaves behind discernible clues helpful in the investigation, such as charred or unburnt materials, smoke residue, and structural deformations caused by heat exposure. Khan (2022a) proposed a framework (Figure 4.1) called ‘Fire Investigation of Tall Buildings’ (FITB) facilitates the systematic reconstruction of any fire incident. It is employed in modelling realistic fires and carrying out thermo-mechanical analysis.

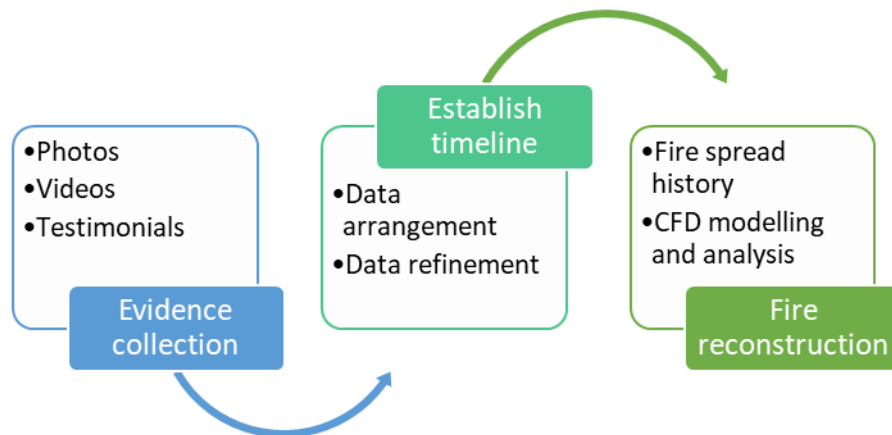


Figure 4.1 Working of FITB: a fire investigation framework used in the study.

4.4. Fire in the Plasco tower

Chapter 1 of the thesis discusses the geometry and structural specifics of the Plasco building. Therefore, this section focuses only on aspects like the fuel load, distribution of fuel, and fire safety breaches that were evident in the building before its collapse.

The Plasco Building had two separate structural blocks (see Figure 4.2). They are...

- a. 5-storey shopping mall
- b. 16-storey commercial tower

The building exterior had concrete walls on the eastern and western sides, while steel braces supported facade elements on the northern and southern sides, with wall panels constructed from ceramic materials. (Ahmadi et al. (2020))



Figure 4.2 Plan view of the Plasco building (Shakib et al. (2018))

Initially intended for commercial purposes, the 16-story building transformed into a major garment distribution and production centre over time. This change led to the accumulation of substantial static and fire loads due to the presence of garments within the building.

According to Behnam (2019), one of the post-collapse field investigators, at the time of the fire, the fuel load was almost four times higher than the designed fuel load of the building. Based on visual indications and witness accounts, the situation appeared more extensive, with fabric materials strewn across various floors. During the fire incident, the Plasco Building comprised a ground-floor shopping centre, along with restaurants, workshops, and storage for

clothing materials on the higher levels, as detailed in the investigation findings. Consequently, the primary fuel source on the floors affected by the fire was the accumulation of fabric materials within the building.

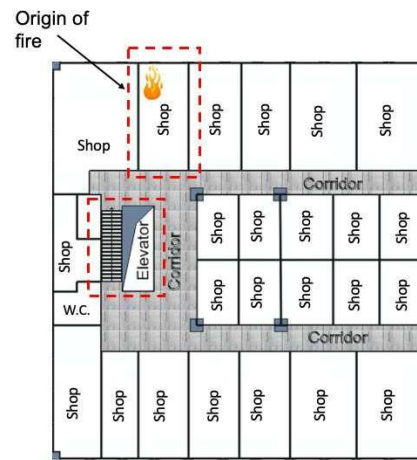


Figure 4.3 Typical floor plan of upper floors in the Plasco Building (Govt. of Iran (2017))

Fire safety requirements	Violations in the Plasco building
Sprinkler system	Absent
Standpipe system	Not working
Fire alarm system	Absent
Egress	Only one exists, while two are recommended by the Life Safety Code (NFPA 101 (2012))
Smokeproof exit enclosure	Absent
Occupancy	Transitioning from standard business occupancy to a mixed occupancy setup

Table 11 Some of the violations of the Plasco Building with the current codes of practice (Khan (2022b))

On January 19, 2017, the 16-story Plasco Building collapsed during a fire incident. The

accidental fire originated from an electrical short circuit on the 10th floor of the northwestern side of the building; see Figure 4.3. The electrical wiring was outdated, according to the firefighters, and the building had no automatic sprinkler system installed. (Govt. of Iran (2017)). The fire travelled rapidly in the vertical direction and in the early stages it reached the upper floors.

While the Plasco Building met the design codes applicable during its construction, later investigations revealed significant deviations from building codes and regulations, indicating non-compliance with several essential standards, as shown in Table 11. In their study, Ahmadi et al. (2020) outlined a crucial sequence of events that resulted in the collapse of the Plasco Building. However, they did not provide any information regarding the fuel load, fuel distribution, fire spread, and fire trajectory. Understanding the impact of these factors is essential in conducting a comprehensive forensic investigation.

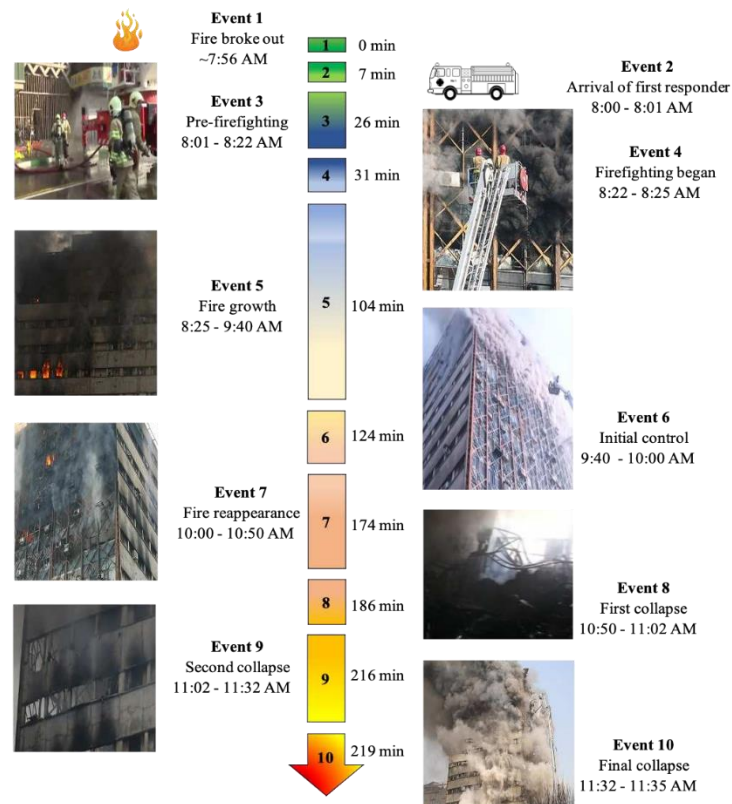






Figure 4.4 Timeline of the critical events (Khan (2022b))

The FITB framework proposed by Khan (2022b), investigated the fire spread and the collapse of the Plasco tower, and finally established a fire timeline (Figure 4.4) of the critical

events with the help of *FireEvolutionMap*, which is available online in high resolution at GitHub (Aatif) (n.d.). *FireEvolutionMap* includes a grid of photographic evidence with numerous images of the tower displayed from all four elevations—east, west, north, and south—captured throughout the entirety of the fire incident. The significance of the critical events identified is provided in Table 12.

Time	Event Number	Significance
7:56 AM	1	Fire initiation
After 2 minutes		The fire was reported to the FSD.
After 5 minutes	2	Emergency responders arrived
Till 8:22 AM	3	Pre-firefighting operation begins
By 8:22 AM		
At 8:25 AM	4	Firefighting begins

		<p>The fire was visible on the 10th and the floors above near the northwest side.</p> 
8:25 AM - 9:40 AM	5	<p>The fire was growing at the 10th, 11th, and upper floors. One hour elapsed with fire on 10th and 11th floors.</p>
9:40 AM – 10:00 AM	6	<p>Temporary fire suppression on the 10th and 11th floors in the northwestern corner.</p> 
10:00AM – 10:50 AM	7	<p>Re-ignition of fire in the areas where it was suppressed. Fire observed in the western and eastern side of the building on the 12th and above floors.</p>

		
Collapse events		
10:50 AM – 11:02 AM	8 (First partial collapse)	A notable section of the 11th floor collapsed onto the 10th floor on the northern side of the building. The fire extended up to the 15th floor and spread across multiple floors on the southern side of the tower.
11:02 AM – 11:32 AM	9 (Second partial collapse)	Nearly all the floors below the 13th on the northern side experienced collapse. The fire expanded in two directions, advancing towards the southwest and southeast, eventually meeting at the southeast corner.



		 <p>Multiple floors in the northwestern corner collapsed, as seen from the west elevation.</p>
11:33 AM – 10:35 AM	Event 10 (Global collapse)	<p>Intense heat was produced at the southeast corner of the building, where the onset of the global collapse originated.</p>  <p>Intense flames on the south side</p>

Table 12 Sequence of the events and significance.

4.5. Reconstruction of the fire spread

The horizontal and vertical progression of the fire from its point of origin, along with all significant events, is graphically depicted in the Figure 4.5. Each floor plan where the fire initiated and the floors above it is illustrated (not to scale) where the known fire locations, verified using the *FireEvolutionMap*, are denoted by 'yellow flame signs,' while extrapolated data to fill gaps is marked with 'black flame signs.' This detailed analysis, incorporating various

sources such as interviews, fire dynamics principles, experimental data, and previous fire incidents, aims to complete the fire spread representation for calibration with a CFD model.

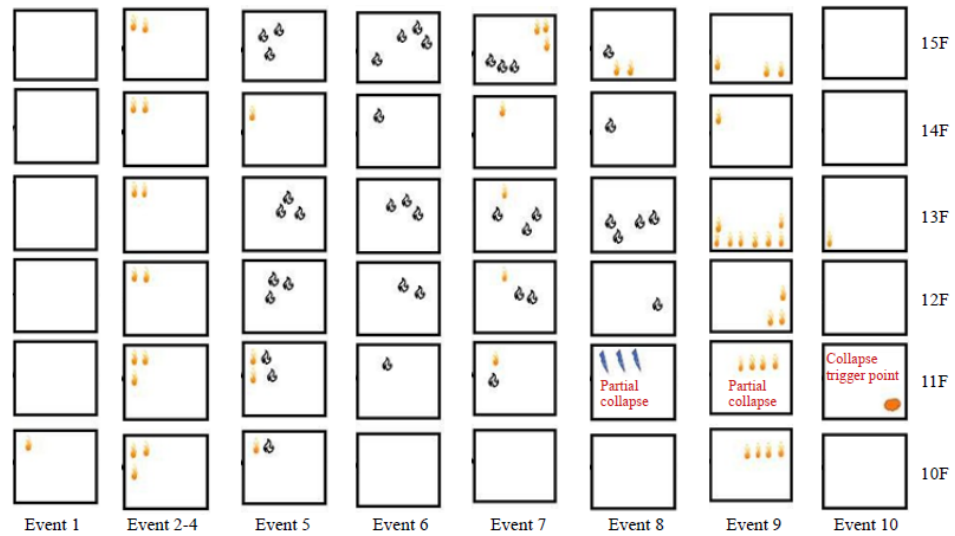


Figure 4.5 Multiple-floor fire spread sequence in the Plasco building (Khan (2022b))

Once the fire path and fuel load are estimated, specific local fire scenarios can be established to model fires in various locations within the building. By combining these local scenarios, an appropriate overarching global fire scenario can be derived. For example, certain areas in the Plasco building may exhibit characteristics of travelling fires, while others, like compartments in some parts of the 12th and 13th floors (especially near the south region), might align with analytical or zone models. Through simulations based on probable scenarios, a credible reconstruction of the structural failure of the Plasco tower can be accomplished.

The investigation of the Plasco tower revealed that the fire spread throughout the structure can be effectively represented/modelled through a combination of distinct local fire scenarios. Given the prevalence of travelling fire behaviour in a significant portion of the building, conducting CFD fire modelling becomes essential. This analysis requires reasonable model calibration using detailed input parameters from the evidence collected to ensure accurate temperature profiles and heat release rates. Using the thermal data from the CFD model, a realistic simulation of the fire dynamics within the Plasco Building can be achieved. Through the calibration of the CFD model, precise temporal and spatial temperature resolutions can be attained, thus facilitating a thorough analysis of structural failures.

4.6. Fuel distribution

Khan, Khan, et al. (2022) This study investigated the effects of different fuel load distributions on fire behaviour in the Plasco building. It considered two different fuel distribution scenarios while maintaining a stable fuel load and ventilation settings. The study examined fire behaviour to determine probable horizontal and vertical fire spread patterns. This study was discussed in brief in the section 2.4.3 of Chapter 2. Based on the study conducted, four key variables (as in Table 13) can significantly affect the fire behaviour in the Plasco building: the density of high and loosely stacked fuel, the bed height of the fuel, and the damaged ceiling.

Key variable	Effect on fire behaviour
Densely stacked fuel	In scenarios where densely packed fuel (e.g., in cartons) is stored within a compartment, fires are more severe due to higher temperatures and prolonged durations than loosely stacked fuel, which burns more slowly but may not incite further fire spread.
Loosely stacked fuel	Loosely stacked fuel reaching the ceiling height can lead to fire propagation to adjacent rooms, potentially crossing fire barriers if false ceilings are continuous.
Height of the stacks	Fuel height significantly influences fire propagation vertically and horizontally. In one fuel distribution with a greater fuel bed height, fire spread occurred in both directions. The vertical fire spread to upper floors is governed by heat release rate factors, such as flame height and oscillatory motion, alongside the height of the fuel load.
Damaged ceiling	Horizontal fire spread is notably impacted by false ceiling breakage, opening locations, and partition walls. Fuel storage in the Plasco Building likely comprised a combination of different storage methods.

Table 13 Key parameters affecting the fire behaviour in the Plasco building.

4.7. Calibration of the fire

The primary aim of this chapter is to provide context regarding the Computational Fluid Dynamics (CFD) simulations conducted by Khan (2022b) as part of his doctoral research, subsequent sections discuss how the reconstructed fire sequence in the Plasco Building is

integrated into CFD fire modelling and analysis. The results derived from the CFD simulations will serve as foundational boundary conditions for heat transfer analysis and structural evaluation of the Plasco building. Detailed structural analysis will be conducted in progressive stages involving variations in the structural modal and thermal load scale in the forthcoming thesis sections. The effects of staircases and window openings on the upper floors were incorporated into the CFD model to assess vertical fire spread and determine when the fire reached the upper floors. Additionally, window openings and open false ceilings were considered in the CFD modelling. The information for opening was obtained from visual evidence and witness testimonies. Description of estimated temperatures

4.7.1. Vertical fire spread

The Plasco Building featured windows around its perimeter, enabling a continuous air supply that sustained the ongoing combustion. These conducive circumstances led to the collapse of the Plasco building within three hours. In contrast, in the case of WTC 7, the collapse occurred seven hours after the ignition of the fire (Majid Haghdoust (2017)).

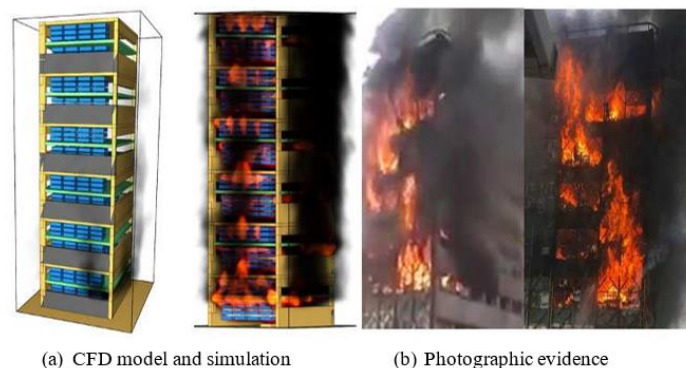


Figure 4.6 CFD model simulating vertical fire travel in the northwestern corner of the tower.

A CFD simulation was conducted to confirm the fire propagation through openings to the upper levels. Specifically, the simulation focused on the northwest corner of the Plasco Building from the 10th to the 15th floors, a scenario that aligns with photographic evidence of the fire accident in the building (refer to Figure 4.6). This simulation was designed to simulate

the vertical spread of fire and to calibrate the entry of the fire into the upper stories through external windows. Given that fabrics were typically stacked in tall piles towards the rear of each shop, the fuel was modelled up to the height of the false ceilings and also within the space of false ceiling itself.

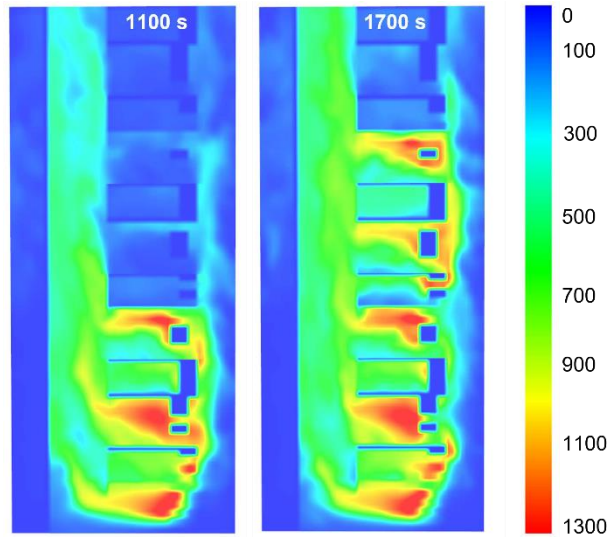


Figure 4.7 Temperature contours observed in the vertical fire travel simulation (Khan (2022a)).

As shown in the Figure 4.6, following the ignition on the 10th floor, the fire reached the upper levels during the initial phases. The false ceiling allowed for open airflow, and the window coverings consisted only of basic wire mesh on the north and south sides of the building. The availability of ample air supply facilitated a rapid escalation of the fire, leading to the substantial release of heat and high temperatures (see Figure 4.7), thereby aiding its progression to the upper stories.

This simulation indicates that the fire had reached the upper levels in the initial phases and began spreading horizontally from a similar area (the northwestern corner of the structure), aligning with visual observations and eyewitness testimonies. The combination of visual evidence and the fire simulation provides two crucial insights.

- a. The fire had ascended to the upper stories early on in the fire outbreak, preceding any firefighting intervention, and

- b. The fire originated from a similar location on each floor. This rationale justifies the focus on simulating the fire for several floors to calibrate the model effectively and derive realistic thermal data for all levels.

Due to firefighting efforts, the fire on the 10th, 11th, and 14th floors was notably shorter than on the other levels. Consequently, the CFD simulations for these three floors are similar, only with varied fire initiation times. The fire simulation for the upper floors, specifically the 13th and 15th levels, will be conducted independently.

4.7.2. Horizontal fire spread

Within the Plasco building, windows either burned out or were dislodged during the fire, thereby maintaining the fire within a fuel-controlled state. Additionally, the false ceiling remained exposed to the external environment, allowing the fire to infiltrate in the initial phases of the fire outbreak. Typically, fire can spread to neighbouring compartments through windows and false ceilings or due to decompartmentalisation (the failure of partition walls). The fire could extend through gaps in the false ceiling or due to the complete collapse induced by intense heat. The pattern of fuel distribution and the significant amount of fuel in the Plasco building facilitated the rapid growth and spread of the fire.

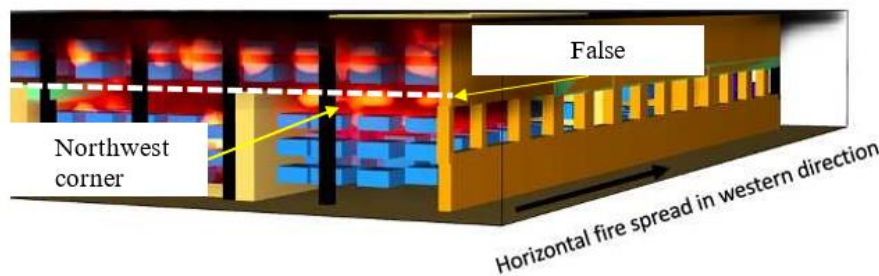


Figure 4.8 CFD simulation showing the horizontal fire spread (Khan (2022a)).

Subsequently, the fire breached into the adjacent compartment located at the north-western corner once the false ceiling was removed, hence failure of the false ceiling is pertinent to the horizontal fire spread, see Figure 4.8. Upon reaching the neighbouring compartment, the fire progressed along the western side of the structure, intensifying in size. Notably, firefighting

efforts within the building were concentrated solely on the 10th and 11th floors, given the absence of an active fire protection system (both sprinklers and standpipes were absent). External efforts to contain the fire using elevated monitors proved ineffective. Subsequently, the fire quickly encroached upon nearly all upper levels. The calibrated model accurately depicts a plausible horizontal fire propagation scenario within the Plasco Building.

4.7.3. CFD model calibration

Visual evidence and witness accounts indicate that the fire did not fully engulf the entire 10th and 11th floors due to the prompt actions of firefighters during the initial stages. Manual firefighting operations were focused on these two floors exclusively. Unfortunately, the first and second collapses restricted firefighters from accessing the 12th floor and above. On the 14th floor, following an initial rapid growth, minimal fire spread was noted, possibly attributed to firefighting efforts or the inability of fire to breach into adjacent areas.

Firefighting operations for the upper levels (floors beyond the 11th floor) relied solely on elevated monitors. The fire predominantly remained in the north-western section of the building on the 10th and 11th floors. Consequently, the CFD model was calibrated for the 10th floor to represent the fire dynamics on the 11th and 14th floors.

Similarly, the fire patterns observed on the 12th and 13th floors were comparable, except for a more intense fire in the southwestern region of the 13th floor. To model the fire accurately, data from the 13th floor is utilised, with some calibration for the 12th floor to establish realistic boundary conditions for structural assessments. The fire propagation rate on the 15th floor exceeded that of other levels, with early fire observations near the north-eastern and eastern corners whose simulation can be seen in the Figure 4.9. Consequently, simulations for the 15th floor are performed to refine the model.

On the 10th floor, the fire originated near the northern side of the building, predominantly affecting the northwestern area. Due to a substantial fuel supply, the fire persisted for approximately one and a half hours until containment efforts by firefighters. Hence, in the 90-minute fire simulation for this floor, all available fuel was allowed to burn without any suppression measures.

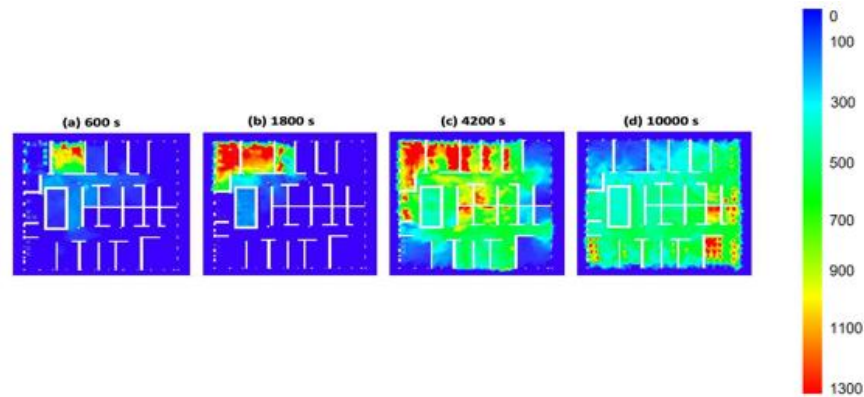


Figure 4.9 Temperature contours of the simulated 13th floor (Khan (2022a)).

During the calibration of the 13th-floor fire scenario, fuel was spread throughout the floor, except in the northeastern region, which showed no fire or smoke. The placement and quantity of fuel in the model were changed to reflect the observed fire spread closely. Images from the simulation and the actual fire incident show that the fire intensified dramatically when it reached the southeastern corner of the 13th floor. The significant heat created was caused by the convergence of fires from the building's eastern and southern sides.

Similarly, in calibrating the fire model for the 15th floor, controlled conditions allowed the fire to breach adjacent compartments through false ceiling failures. Given the intricate nature of a complex building fire, achieving an exact simulation of fire spread, even with a full-scale experimental study, is highly improbable, especially when precise data on factors influencing fire propagation, such as fuel distribution, compartmentation failures, changes in ventilation due to window failures, gaps, or openings facilitating fire spread, are lacking. Nonetheless, the calibration method described here, rooted in thorough forensic analysis, enables a meticulous reconstruction of the fire incident.

4.8. Conclusions

- a. Traditional fire investigation methods typically do not encompass structural collapses when reconstructing fire events. In this study, the fire history established by the Fire Investigation Framework (FITB) is utilised for subsequent heat transfer and structural

analyses in the following thesis chapters.

- b. Through simulating two distinct scenarios of fuel distribution while maintaining consistent fuel load and ventilation conditions, the study observed fire behaviour to identify key parameters crucial for modelling fuel behaviour within the Plasco building. The research highlighted the stacking density of fuel, height of the fuel bed, and ceiling partition as the key factors significantly influencing fire propagation in the structure.
- c. By employing CFD modelling, the fire spread history across various floors is calibrated as depicted in the visual evidence. The fire simulation closely aligns with the visual evidence. Subsequently, the information derived from the CFD simulation is converted into a compatible format for subsequent heat transfer and thermo-mechanical analyses.

Chapter 5: Analysis of the Plasco Tower

Using the OpenFIRE Approach

5.1. Introduction

In the previous chapter, a significant volume of evidence related to the Plasco Building fire was gathered to create a cohesive timeline for reconstructing the progression of the fire. By employing computational fluid dynamics (CFD) fire modelling and aligning it with the compiled evidence, the vertical and horizontal spread of the fire within the building was reconstructed. The fire modelling generated a spatial-temporal temperature history that accurately represents the fire scenarios, which was then used to simulate the structural response. These fire simulation outcomes were incorporated as boundary conditions in the finite element model used in this chapter.

This chapter will discuss the insights obtained from a preliminary stage analysis carried out based on a standard fire curve. The chapter will also introduce a new framework to link FDS to OpenSEES called OpenFIRE (Khan, Khan, et al. (2021)) in analysing large-scale structures. OpenFIRE software framework can simulate the entire sequence of construction of a fire situation, heat transfer to the structure, and the thermomechanical response of the structure using a sequential coupling of CFD tools and FE software. OpenFIRE incorporates accessible tools like FDS and OpenSEES to create a free, efficient, and open-source computational framework with customisable source codes.

Frequently, fires exhibit a tendency to propagate horizontally across floor levels within expansive structures, a phenomenon exemplified by notable incidents such as the WTC Towers in 2001, the Madrid Windsor Tower fire in 2005, and the Faculty of Architecture building fire at TU Delft in 2008. In the instances of the Grenfell Tower fire in London (2017) and the Plasco Building fire in Tehran (2017), the fire demonstrated a vertical progression towards the upper floors.

Many fire scenarios remain to be investigated in order to achieve a higher level of realism in fire simulations. Simulating the structural response to these complex fire scenarios using existing software tools would require significant time and effort, rendering it practically

unfeasible. Additionally, the inherent uncertainties associated with fire phenomena prevent their a priori modelling. Hence, the development of a practical methodology, such as OpenFIRE, becomes necessary for facilitating a comprehensive, performance-based approach to structural fire engineering.

Most widely used commercial software packages lack the necessary functionalities to support highly customised applications or incorporate new fire models. Additionally, researchers often face limitations in their ability to freely change the source code of these software packages to accommodate their specific needs or introduce new fire models.

OpenFIRE is created as a completely open-source framework (Figure 5.1) by combining open-source CFD and FE software. This framework will be accessible to professionals, researchers, and developers for utilisation and ongoing enhancements.

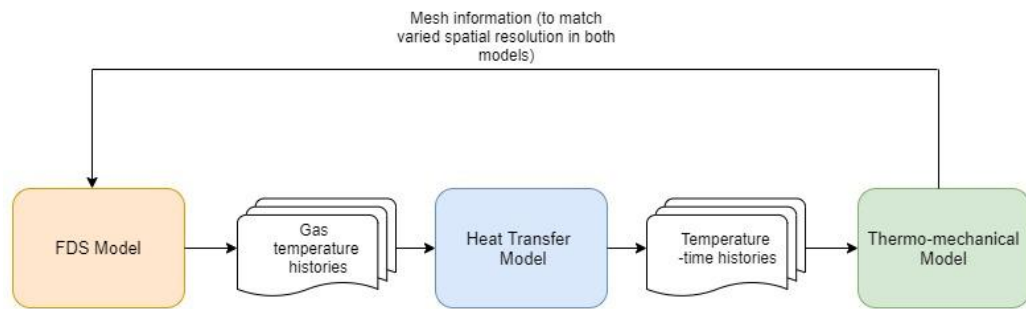


Figure 5.1 A broad view of data flow from FDS to FE models

OpenFIRE integrates two efficient and open-source computational tools, namely FDS (Fire Dynamics Simulator), developed by NIST (National Institute of Standards and Technology) McGrattan et al., and OpenSEES software provided by PEER (Pacific Earthquake Engineering Research Center) at the University of California, Berkeley (F. McKenna (1997)). This integration allows for a comprehensive analysis, using FDS to generate realistic fire scenarios and then employing OpenSEES for conducting heat transfer and structural analyses.

To couple the CFD and FEM tools, a middleware—Fire Structure Data Mapping (FDSM, Khan, Khan, et al. (2021))—A Python-based middleware serves as a data mapping

tool, bridging the gap between OpenSEES and FDS software. This middleware effectively maps data from the CFD simulation to the appropriate locations within the heat transfer and thermo-mechanical models of structural geometry by creating relevant script files for each of these models. By integrating this middleware, the structural analysis of tall buildings is streamlined and simplified.

5.2. A review of the attempts to couple CFD and FE software

CFD (Computational Fluid Dynamics) has emerged as the preferred and economical method in recent years for modelling realistic fire scenarios. In contrast to the simplified fire models commonly used (such as standard fire curves or parametric fires), the coupling of CFD with Finite Element (FE) analysis offers a highly detailed resolution. This detailed resolution enables carrying out realistic analysis while adhering to the principle of energy conservation throughout the analysis process.

After the WTC (World Trade Center) disaster in 2001, there was a notable increase in efforts to integrate realistic fire models with structural finite element models. This was done with the aim of gaining a deeper understanding of the structural response to fire. Since then, the structural engineering community has increasingly acknowledged the significance and potential of developing realistic fire scenarios for comprehensive analysis.

In order to replicate the structural behaviour in authentic fire scenarios, three models must be crafted: (a) a fire model, potentially a CFD model, (b) a thermal or heat transfer model, and (c) a thermo-mechanical model. Nevertheless, sequentially coupling all these models poses a challenging endeavour.

The main challenge in simulating the structural response against a fire load lies in the disparity Prasad & Baum (2005b) between the length and time scales used for fire and structural models. This discrepancy necessitates the adoption of different computational approaches, involving varying grid configurations and resolutions in both spatial and temporal domains. Consequently, the coupling of CFD and FE models becomes a challenging task. The characteristic time of a fire model is higher than a solid model and the meshing in CFD simulations may have larger dimensions than the thickness of structural elements. Furthermore, performing analysis using a fine mesh in CFD is not practical and computationally very expensive.

Several methodologies have been proposed to enable the sequential coupling of CFD models with FE models developed using commercial software. These techniques have their own advantages and limitations. proposed a method called Fire-Structure Interface (FSI) by employing a zone-model approach to investigate the effects of radiative heat transfer from combustion products on a structure and coupled results obtained from FDS with ANSYS. This interface was utilised to investigate the collapse of the WTC. Prasad. Similarly, Silva et al. (2016b) proposed a methodology (FTMI) in which ANSYS was coupled with FDS; however, this model is limited to ANSYS scripts only.

When CFD is employed to simulate the net heat fluxes at solid boundaries, it becomes possible to approximate the time-temperature profiles of structural elements through heat transfer analyses. Nevertheless, accurately predicting convective and radiative heat transfer coefficients at these boundaries is notably uncertain within the dynamic setting of a fire scenario.

Wickstrom Ulf et al. (2007a) introduced the concept of Adiabatic Surface Temperature (AST) to produce accurate boundary conditions for conducting a heat transfer analysis. In essence, the Apparent Surface Temperature (AST) concept represents the temperature of an ideally insulated surface when subjected to the same environmental conditions as a real surface. AST can be seen as an effective temperature in the fluid phase, which can be utilised to calculate both radiation and convection heat transfer. AST method is a robust, practical, and straightforward approach for determining boundary conditions in the thermal analysis of structures, but its applicability depends on the optical depth, which is an unlikely scenario to exist in the case of achieved in large compartment fires. Limitations and applicability of various fire models, including the AST method, are presented in the review paper of Khan, Usmani, et al. (2021).

Since the introduction of the AST concept, numerous researchers have employed it to investigate the structural response in fire scenarios. utilized the AST methodology to calculate gas temperatures derived from FDS for conducting heat transfer analyses on structural components. Additionally, they employed ANSYS software to model the three-dimensional behaviour of the structure during fire exposure. Similarly, Alos-Moya et al. (2014) performed a study to model the collapse of a composite bridge in a fire scenario by integrating Computational Fluid Dynamics (CFD) with Abaqus software.

The frameworks discussed earlier are limited in their capability to integrate exclusively with commercial Finite Element (FE) software such as Abaqus and ANSYS. This limitation stems from compatibility challenges with the scripts and elements utilised in thermal and structural analyses. Additionally, these tools are usually only available to a limited set of research teams and lack avenues for wider enhancement or refinement by engineers and the research community.

The overall aim of this chapter is to discuss the preliminary analysis and detailed analysis of a single floor of the Plasco Building and introduce a new CFD-FE framework, which is being developed to accurately model fire load and carry out heat transfer and thermomechanical analysis sequentially. FDS developed by NIST (FDS-SMV (n.d.)) is used to perform the CFD analysis in the fluid domain, and OpenSEES as the FEM tool for the thermal and structural domain.

The OpenFIRE approach begins with the creation of an FDS model of Plasco Tower, and the output is post-processed and made compatible with conducting heat transfer analysis in OpenSEES. The temperature history obtained from heat transfer analysis is applied to all structural elements in the OpenSEES Finite Element model. This is a three-step process which will be streamlined with the help of automation.

5.3. Introduction to OpenFIRE

5.3.1. On extracting compatible FDS output

The OpenFire is an integrated computational framework to carry out CFD, Heat Transfer and Thermo-mechanical analysis sequentially project being developed at The Hong Kong Polytechnic University fire team (Khan, Khan, et al. (2021) & Khan et al. (2023)). Specifically, the initial step of OpenFire begins with creating the geometry of the fire compartment through input code in FDS. To ensure accurate mapping of necessary data from FDS to the FE model at specified positions, it is essential that the global coordinates in the FDS model and the structural model align regardless of their geometric dimensions.

5.3.2. Coupling in OpenFIRE (Khan et al. (2023))

A middleware has been created to simplify the sequential coupling of FDS and

OpenSees. Figure 5.2 outlines the procedure of the proposed coupling and the creation of all scripts required to conduct the three types of analyses.

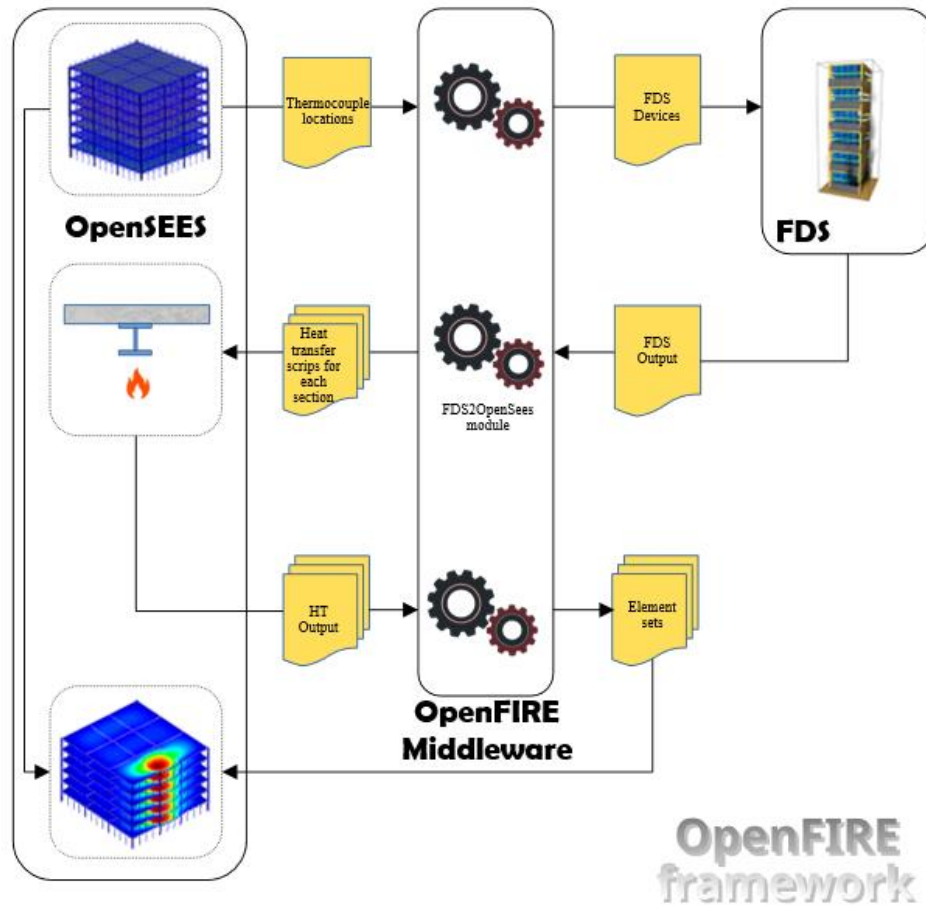


Figure 5.2 Data flow in the OpenFIRE framework.

FDS analysis

Input for FDS model: location of thermocouple devices, spatial information of nodes and elements.

The first step involves building the structural model in OpenSees and generating a script with nodes and elements of the structural model. Subsequently, the middleware uses this geometric data from the structural model to create data recording devices in the FDS model at designated positions (such as thermocouples, heat flux, AST devices, gas temperature devices, etc.). The FDS Device script is imported into the FDS model, initiating fire simulations that yield output files from these analyses.

Heat transfer analysis

Input: time-temperature history from the above step

When creating thermocouples or other data recording devices, the middleware generates scripts to analyse heat transfer and thermo-mechanics (HT Script and Element Sets). Another part of the middleware converts the FDS output into the format needed by OpenSees to carry out the heat transfer analysis.

Thermo-mechanical analysis

Input: Section temperature definition from the above step

The results of the heat transfer analysis are used as a boundary condition for the thermo-mechanical analysis in OpenSees. This analysis is conducted using the script (Element Sets) generated by the middleware. The entire process of conducting all three analyses using the suggested middleware is explained in the following section.

5.3.3. Modules of the middleware

This section details the middleware developed to integrate the FDS with OpenSees to perform all three analyses- fire modelling, heat transfer analysis, and thermo-mechanical analysis.

The middleware generates scripts for three analyses: FDS Devices script, HT script, and Element Sets script automatically. These scripts are essential in creating a smooth interface between the three models. The FSDM system consists of various modules written in Python programming language to facilitate this process.

The middleware consists of two main modules:

- a. The Devices and Elements module generates a portion of the script for all three analyses. This includes:
 1. Defining the locations of thermocouple devices in the FDS script.
 2. Creating the heat transfer script with elements assigned to each device, where the FDS output is utilised as a thermal boundary condition.

3. Establishing elements in the structural model script to receive thermal loads from the heat transfer output.

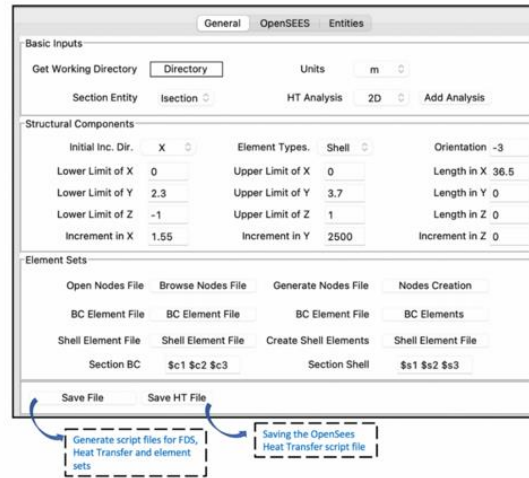
b. The FDS2OpenSees module converts the FDS output data into the necessary format for OpenSees.

Devices and Elements module

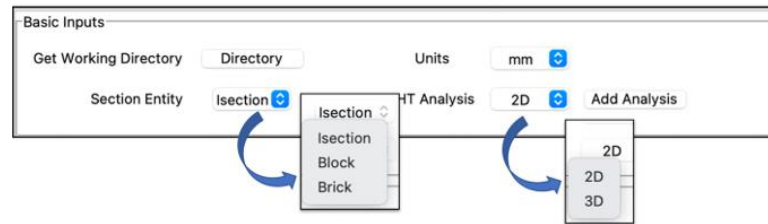
This module relies on user-provided input concerning the geometry of the structure, see Figure 5.3. This input is necessary for the module to accurately generate the required scripts and establish the necessary connections between the different components.

FDS devices and other essential inputs

Although it is not necessary to define the structural components within the FDS model, specifying the "quantity" of data recording devices at specific locations is crucial. This specification is required to capture the necessary data to be utilised as boundary conditions in the heat transfer and Finite Element (FE) models. The relevant data can be accurately recorded and employed in subsequent analyses by defining these devices. The FDS Devices script is coded in FORTRAN, while the input files for OpenSees are scripted in the *.tcl format. The middleware possesses the capability to convert these scripts into suitable formats for both FDS and OpenSees. Upon receiving all the input data from the user, the Devices and Elements module generates an FDS-compatible script containing device information in the designated directory.



(a)



(b)

Figure 5.3 Screenshot from of the module of “Devices and elements” module with (b) the basic inputs (Khan et al. (2023))

OpenSees heat transfer entities

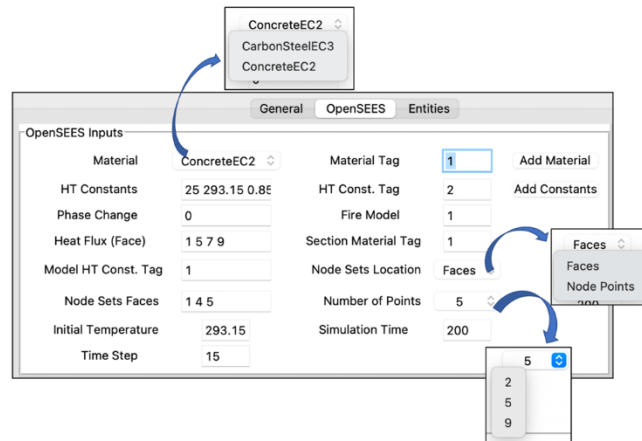


Figure 5.4 Input for heat transfer analysis (Khan et al. (2023))

After establishing initial specifics like material type, heat transfer constants, and surfaces delineating thermal boundary conditions for conducting the heat transfer analysis, the subsequent phase involves inputting parameters for the section type and dimensions to create the HT entities, as shown in Figure 5.4.

This module creates an entity in the heat transfer model for every data recording device in the FDS model. The thermal data (AST data) acquired from each device in the FDS model is subsequently applied as thermal boundary conditions for the corresponding entity in the heat transfer model. This method facilitates the computation of the time-temperature profile throughout the depth of the member sections; see Figure 5.5.

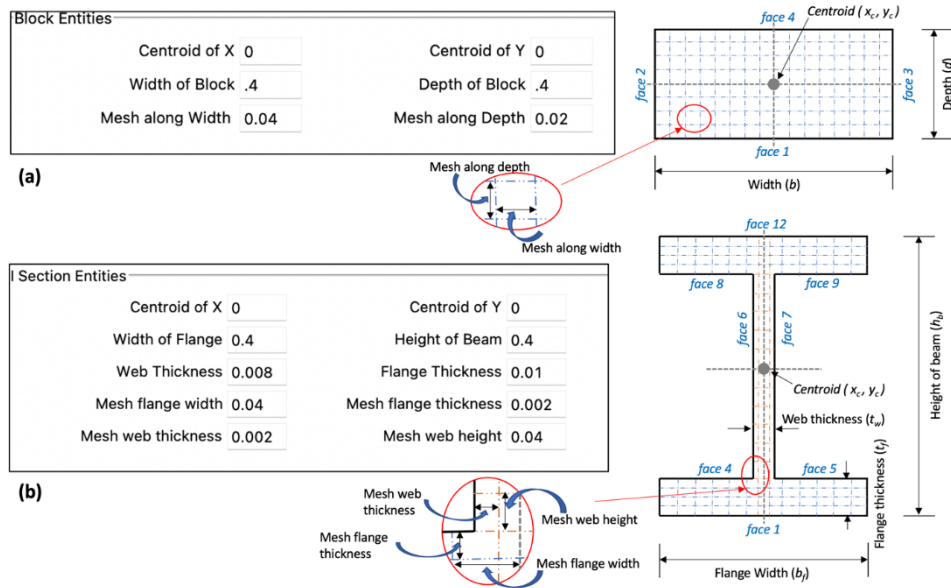


Figure 5.5 Screenshot of the module showing defining OpenSees heat transfer (HT) entities for (a) a block section and (b) and I section (Khan et al. (2023)).

Elements sets

Unlike commercial Finite Element (FE) packages like Abaqus and ANSYS, OpenSees does not have a built-in feature for direct mapping of data from the heat transfer analysis to the thermo-mechanical analysis. However, this middleware provides a solution for this by enabling a smooth mapping of data from the heat transfer (HT) analysis to the thermo-mechanical FE model. The output data obtained from the HT analysis is converted into thermal load scripts,

which are applied to the structural elements in the OpenSEES model.

The thermal data derived from the heat transfer (HT) analysis output is structured in each file based on the required number of section points ('nodesets') across the depth, as depicted in Figure 5.5. The output files consisting of the time-temperature profiles for each entity, comprising the 'nodesets' data, are applied to the structural components at the exact locations consistent with both the heat transfer and FDS models.

In large structures, identifying and mapping the correct entity output with the structural model is complex and could raise the likelihood of human errors. Hence, locating elements linked to specific geometric positions where the entity output can be designated as the thermal loads is vital.

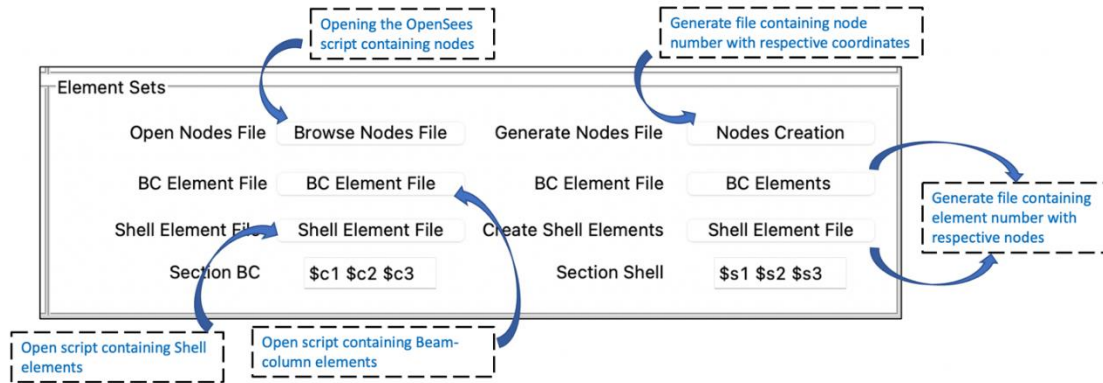


Figure 5.6 Screenshot of the module showing input needed for generating element sets (Khan et al. (2023)).

Since all three numerical models share the exact coordinates, the middleware can identify the elements in both the heat transfer and structural models at specific device locations. Consequently, during generating devices and OpenSees section entities, the middleware assigns distinct identification numbers to the heat transfer (HT) analysis output files. These identification numbers are based on the device location and elements in the structural Finite Element (FE) model. This approach ensures proper integration between the HT analysis output files and corresponding elements in the FE model, facilitating efficient data flow.

In the end, the module generates thermal load scripts (Figure 5.7) for the thermo-mechanical model, which includes the necessary information for the analysis.

```
eleLoad -ele 28 -type -beamThermal -source "temp1.dat" $y1 $y2
```

Figure 5.7 A typical line from the thermal load script generated by the module (Khan et al. (2023))

FDS2OpenSees module

This module transforms the FDS output data into the necessary format for OpenSees. FDS generates a "*.csv" file containing the data from all recording devices. On the other hand, for carrying out HT analysis in OpenSees, each HT entity (in "*.dat" format) needs a single file with all material constants defined. This module writes an input file for each entity. Figure 5.8 Shows the module that generates the files needed for the HT analysis.

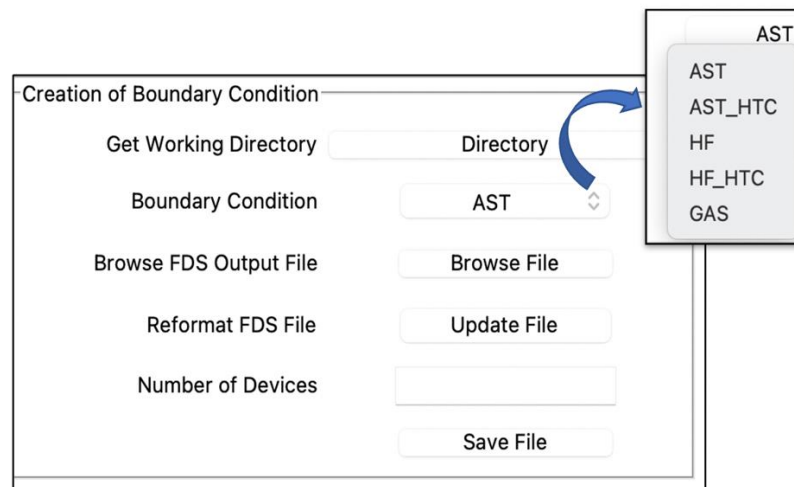


Figure 5.8 Screenshot of the module which converts FDS output into OpenSees format (Khan et al. (2023)).

5.3.4. Author's contribution to OpenFIRE framework

- 1 The authors' contribution is work carried out in scaling up the OpenFIRE software. Dr Khan developed OpenFire to couple CFD with structural models.
- 2 It was initially conceptualised and tested on FDS and Abaqus software. Later, the candidate worked with Aatif to build up OpenFire to produce OpenSees-compatible FDS output.
- 3 OpenFire framework was successfully applied to a full floor fire analysis. This required multiple code updates. Major work produced in Chapter 3 was during beta testing stage of OpenFIRE.

5.4. OpenSEES Modelling

5.4.1. General modelling philosophy and aims and scope of the simulation

This research aims to investigate the factors leading to the complete collapse of the Plasco tower. This will be achieved by subjecting a detailed 3D finite element model of a single floor within the building to the realistic fire conditions that led to its collapse. Chapters 6 and 7 present the study to understand the reasons behind the progressive collapse of the building with respect to the travelling fire phenomenon as observed during the fire disaster.

This chapter is dedicated to simulating the structural response of the tower under the most severe fire conditions it encountered during the fire incident. The fire started on the 11th floor (ceiling of the 10th floor) and was observed to have travelled along the floor horizontally and through the staircase and windows vertically. The fire spread to the 12th floor (ceiling of 11th floor), and severe burning occurred in the NW corner across two-floor levels. The progression of the fire towards the west direction was successfully contained on the 11th and 12th floors, while it continued to spread within the interior compartments on the 13th floor. The fire on the 13th floor proved challenging to suppress, mainly when firefighting efforts were initiated externally from the north and west sides. Based on the findings of Khan (Khan (2022a)), the fires on the 14th, 15th and 16th floors were relatively smaller in scale and intensity. Visual evidence shows that the failure of the secondary main column occurred near the southern face of the 13th floor. Therefore, for this study, the structural response against the

entire fire event was explicitly modelled on the 13th floor of the tower. By examining visual evidence captured from different vantage points around the building during the fire, diverse fire propagation trajectories were discerned. These identified trajectories will be used to carry out the OpenSEES analysis.

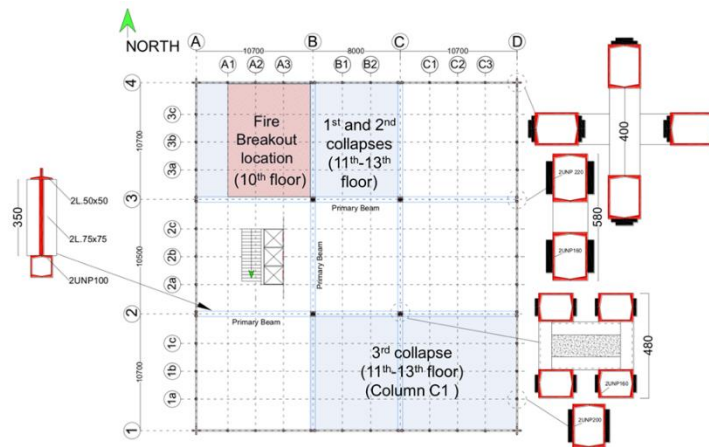


Figure 5.9 The layout of the Plasco tower and areas of collapse (Shakib et al. (2020))

5.4.2. Structural details of the building

The schematic of the Plasco tower is depicted in Figure 5.9. The structural system consisted of four columns in the core supporting the loads transmitted by the primary beams, supported by built-up box columns along the perimeter. All steel sections were fabricated using standard European channel or angle profiles without any applied fire protection. In the FE model, the beams were modelled using OpenSEES fibre-based sections and displacement-based beam-column elements, while concrete slabs were represented using shell elements. The material properties of the steel were derived from tests conducted on samples obtained from the collapsed structural components (Govt. of Iran (2017) and Shakib et al. (2020)).

Structural model of the floor system

In this investigation of the Plasco Building structural system, a definitive answer to whether the concrete floor slab was composite with the supporting grillage or rested on top of

it could not be found. Therefore, this preliminary study assumes a non-composite grillage floor system with supported primary trusses and continuous secondary floor beams spanning over the primary beams. The plan looks almost square, except the length along the North-South direction is slightly longer.

All the members in the structure were modelled using displacement-based beam-column elements available in the OpenSEES library (*dispBeamColumnThermal*). The fibre section approach is followed while modelling the sections, where each Fiber Section object comprises multiple fibres. A uniaxial thermal material is assigned to all the fibres. The *fiberSecThermal* object class allows users to impose thermal loads at 2, 5, or 9 points along the depth of the section. Given the slender sections utilised in the Plasco tower, the temperature rises almost uniformly across the depth of the section.

Loading applied

A gravity dead load of 5.3 kN/m^2 is assumed, including load from the composite floor and partition walls. For these floors, a storage live load of 6.0 kN/m^2 was taken. Generally, only a part of the live load is assumed to be present in the building during the event of the fire, but in this particular case, due to its usage as storage space, the whole live load is assumed to be active in the analysis.

5.4.3. Preliminary analysis with Standard fire

A composite slab model of the Plasco Building has been created, as shown in Figure 11 (a), by creating shells on the plane of the truss members and merging the nodes on the shells with the nodes of the top cord members of the truss. The shell elements are made of the MITC4Thermal class present in the OpenSEES for fire. Because of a preprocessing shortcoming, the shell elements and truss beams are created separately and merged into a single model.

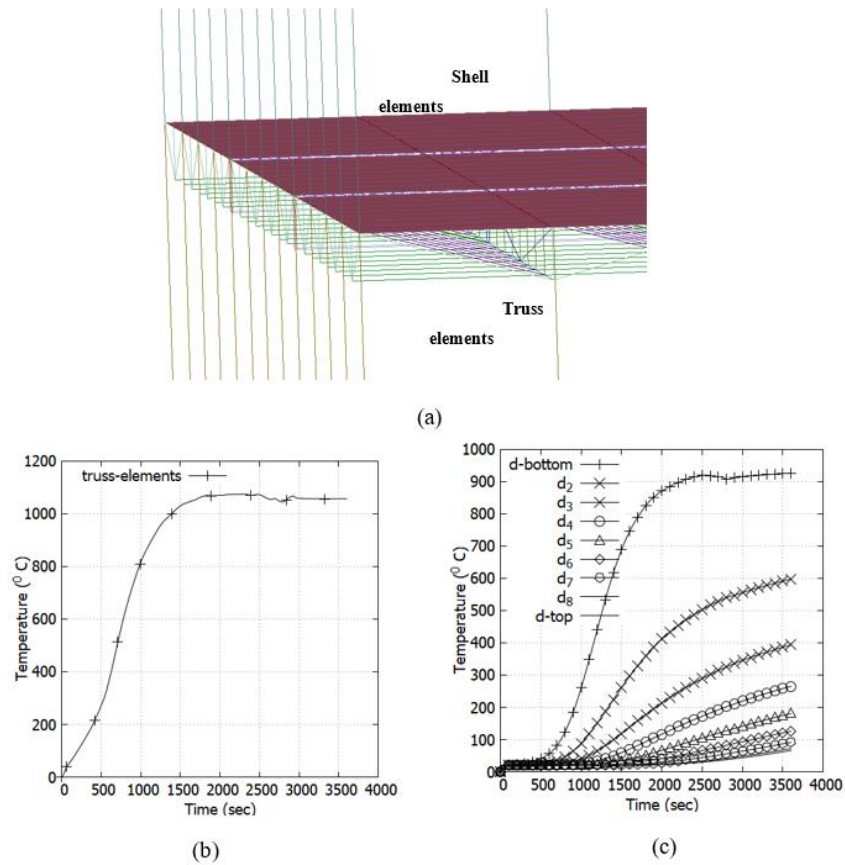


Figure 5.10 Picture (a) shows the building floor system comprised of truss beams and shell elements (visualised using GiD + OpenSEES interface); (b) and (c) show the temperature vs time histories of truss members and across the slab depth.

Subsequently, the model will receive suitable heat flux boundary parameters, such as the convection coefficient to or from the ambient environment and air temperature. Following the description of heat loss to the surroundings, specifications for fire exposure are outlined in the fire model, from uniform fire to localised fire exposure, and the analysis is initiated. The standard fire curve has been employed (see Figure 5.11) in this initial examination to generate temperature profiles. The ISO fire curve is used to improve the integration of HT and FE models by taking advantage of the simple fire model. These temperature histories will then be applied as a load in the thermo-mechanical analysis.

The entire floor has been modelled with nine structurally independent zones if slabs crossing over parallel trusses of primary beams are fully cracked because of their age and hogging bending action, as seen in Figure 5.11. In the model, only three floors subjected to

thermal load are modelled with composite floors to reduce the computational load. Thermal load was applied over the three levels of floor segments in the north face of the tower to understand the global response of the structure.

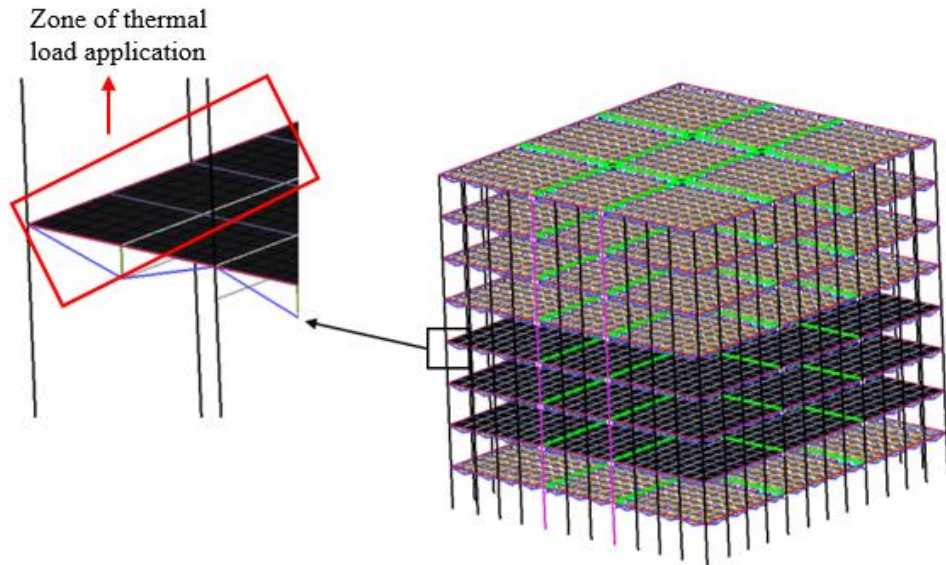


Figure 5.11 Visual representation of the OpenSEES model featuring a composite slab designed through the GiD+OpenSees interface.

Observations

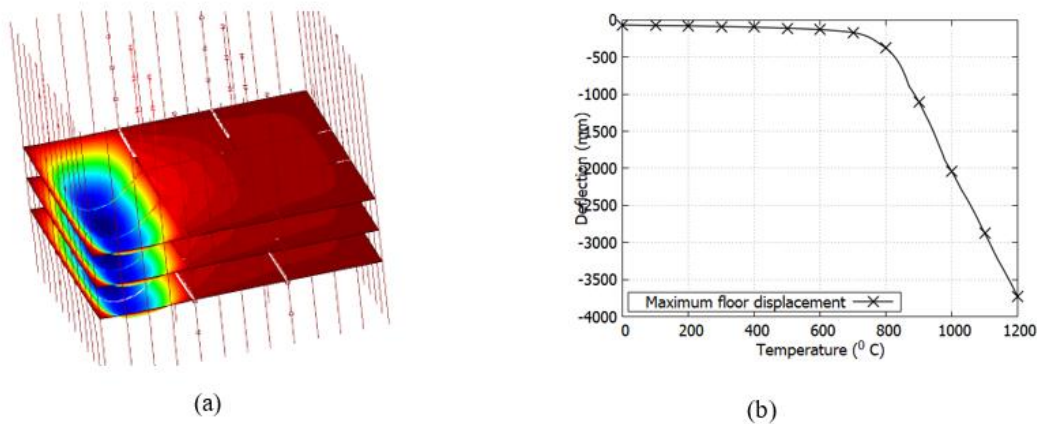


Figure 5.12 (a) Response of the three heated floors; (b) Plot showing maximum floor displacement against steel truss temperature.

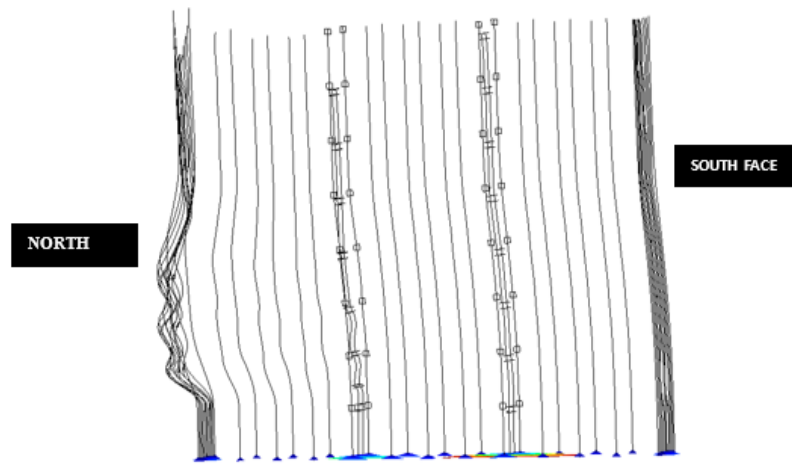


Figure 5.13 Global column response with the North face on the left side and the South face on the right (shown at exaggerated scale for clarity).

The preliminary analysis conducted showed that the corner floor slabs deformed in a partial 2-way bending moment, whereas the edge slab experienced one-way bending action, as seen in Figure 5.12–(a). Large floor displacements of order 350mm are observed; see Figure 5.12 –(b). The deformation rate started increasing after steel temperatures reached 500 °C, and a rapid rate of downward displacements was noticed after 660 °C. The temperatures shown in the plot represent steel truss temperatures. It was observed that the temperature at the bottom face of the concrete is 530 °C when steel truss members are around 660 °C.

The global response of the perimeter columns near the north face at the end of thermo-mechanical analysis can be seen in Figure 5.13, where the floor system is hidden for clarity. The top nodes of the central core columns can be seen at a lower position than the edge and corner columns. This differential vertical column displacement indicates redistribution of the load towards the edge columns. The load carried by the core columns, up to that point, is redistributed to edge columns present on the East and West sides of the tower. This caused a sideways displacement of the building globally.

The material model used for the steel members follows the Elastic modulus deterioration against temperature as specified by the Eurocode 1993. As per the Eurocode, the loss of elastic modulus majorly occurs between temperatures 300 °C and 400 °C. It has been

noticed in the analysis that the core columns are reaching their maximum load-carrying capacity at 300 – 400 °C under thermal load conditions. Beyond 400 °C, the column seems to be losing its load-carrying capacity by 50%, i.e. a drop from 9000kN to 4500kN.

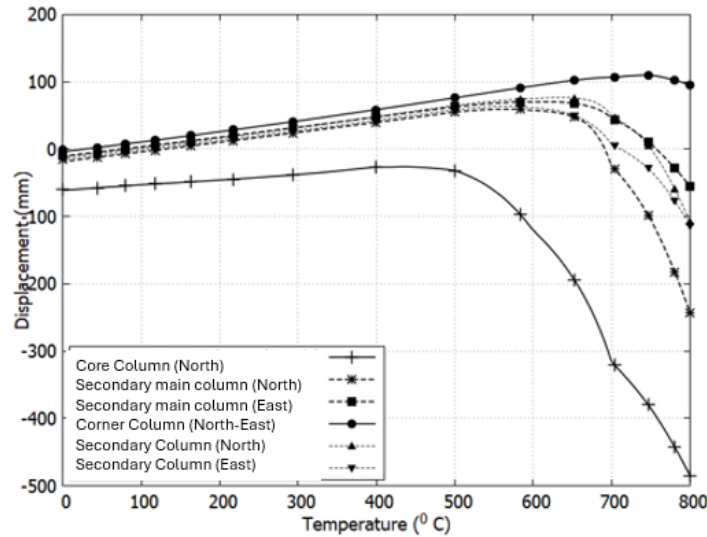


Figure 5.14 The plot shows the vertical displacements in all types of columns.

Figure 5.14 Highlights the vertical displacements of all columns on the northeast corner of the tower that are involved in the fire load. This explains how dependent the global stability of the tower is on the core columns. The likelihood of two core columns reaching critical temperatures cannot be ruled out entirely based on the fire travel pattern observed on the 13th floor. In the coming section, a single-floor model of the structure is subjected to the CFD-based temperature time loading to explore the other possible scenarios that could cause global collapse.

5.5. Modelling the fire

A whole floor ($30 \times 30 \text{ m}^2$) is simulated to obtain realistic temperatures from the CFD analysis; see Figure 5.15. Before advancing towards the full-scale model with complete vertical and horizontal travel fire cases, the authors have decided to analyse a simple single floor representing the fire event limited to the 13th floor of the tower, where fire spread all over the floor (except at the northeast corner). The CFD intends to present the travelling fire in the Plasco Building. In Chapter 7, the fire for all floors will be reconstructed, and realistic temperatures based on calibrated models will be used. The computational domain to simulate the fire on the 13th floor is presented in Figure 8. The cell size represents a reasonable fire spread at a lower computational cost in the current study. A finer mesh may be required for a more accurate fire spread in any fire accident. After carefully performing a few numerical tests in this study, a cell size of 0.2 m is used in all fire simulations. For more information on the CFD model, please refer to Chapter 6 of the PhD thesis of Dr. Khan (2022).

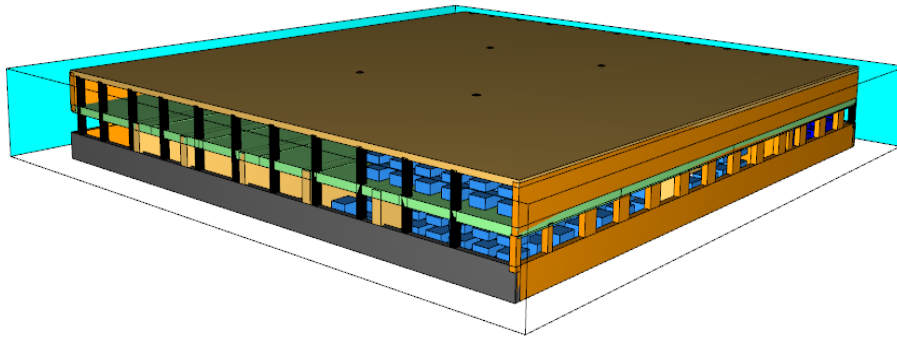


Figure 5.15 Shows the Computational domain for the 13th floor of the Plasco tower.

5.6. Plasco tower analysis using OpenFIRE framework

In this section, a thermo-mechanical analysis of the entire floor area of floor number 13 of the Plasco tower was carried out using the OpenFIRE framework. With the help of OpenFIRE, accuracy in thermal load can be achieved. Hence, an in-floor travelling fire scenario has been considered for this analysis. This means the thermal load has been applied on one zone at a time over the entire floor, simulating the travelling fire. Consequently, as the analysis progresses, large deformations occur in different zones at different times.

5.6.1. FDS Analysis

According to the investigations of local bodies, the nature of the usage changed at the time of the accident. The building users had stored large amounts of cloth/fabric material in the ceiling areas. As a result, the fire hazard increased substantially before the fire incident. As the primary combustible in the Plasco Building was clothes, nylon material is considered fuel in the simulation, and its properties are taken from the SFPE handbook (SFPE, 2016). The travelling nature of the fire has been realised based on the visual evidence available from multiple sources. Accordingly, fire movement on the floor is simulated for 3hr 20 min, i.e., 12000 sec. The fire was initiated near the northwest corner using a burner, as shown in Figure 5.16. According to the interviews of firefighters, the fire reached an adjacent compartment through false ceilings (Khan (2022a)). To present the fire spread in the adjacent compartment, false ceilings are removed progressively, as shown in Figure 5.16 and Figure 5.17. Several numerical tests have been carried out to calibrate the model and match the results with visual evidence. Ceiling failure is controlled by FDS obstruction removal techniques. The timing is approximated (calibrated) based on the visual data (Khan (2022a)). However, it is worth noting that due to uncertainties embedded with fire and fire modelling, it is impossible to re-create the exact fire, especially inside the building, which even firefighters did not witness (firefighters did not reach the 13th floor. However, such a calibrated model provides an approximate method to investigate structural failure to improve the fire safety design.

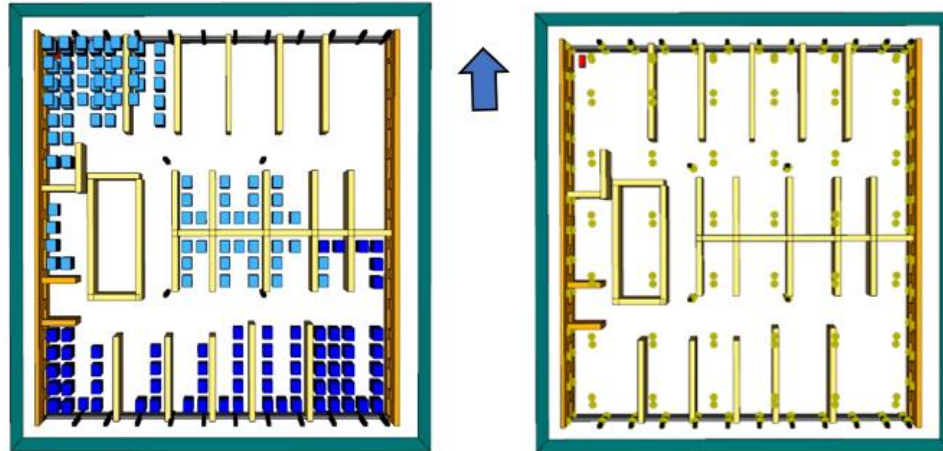


Figure 5.16 FDS models show (a) the distribution of fire load and (b) the placement of sensors at different locations and the location of fire initiation (yellow and red points).

Adiabatic surface temperatures have been obtained on the floor every five meters in both directions. Sensors have been put in every 5m x 5m zone area on the FDS models shown in Figure 5.16(b). This would give a good resolution for fire load and, at the same time, not cause many data handling issues. Nearly 50 thermocouple sensors have been placed for the OpenFIRE framework to extract gas. In Chapter 6, while carrying out the complete analysis of the building, more sensors (at a closer distance) are added to get more accurate data.

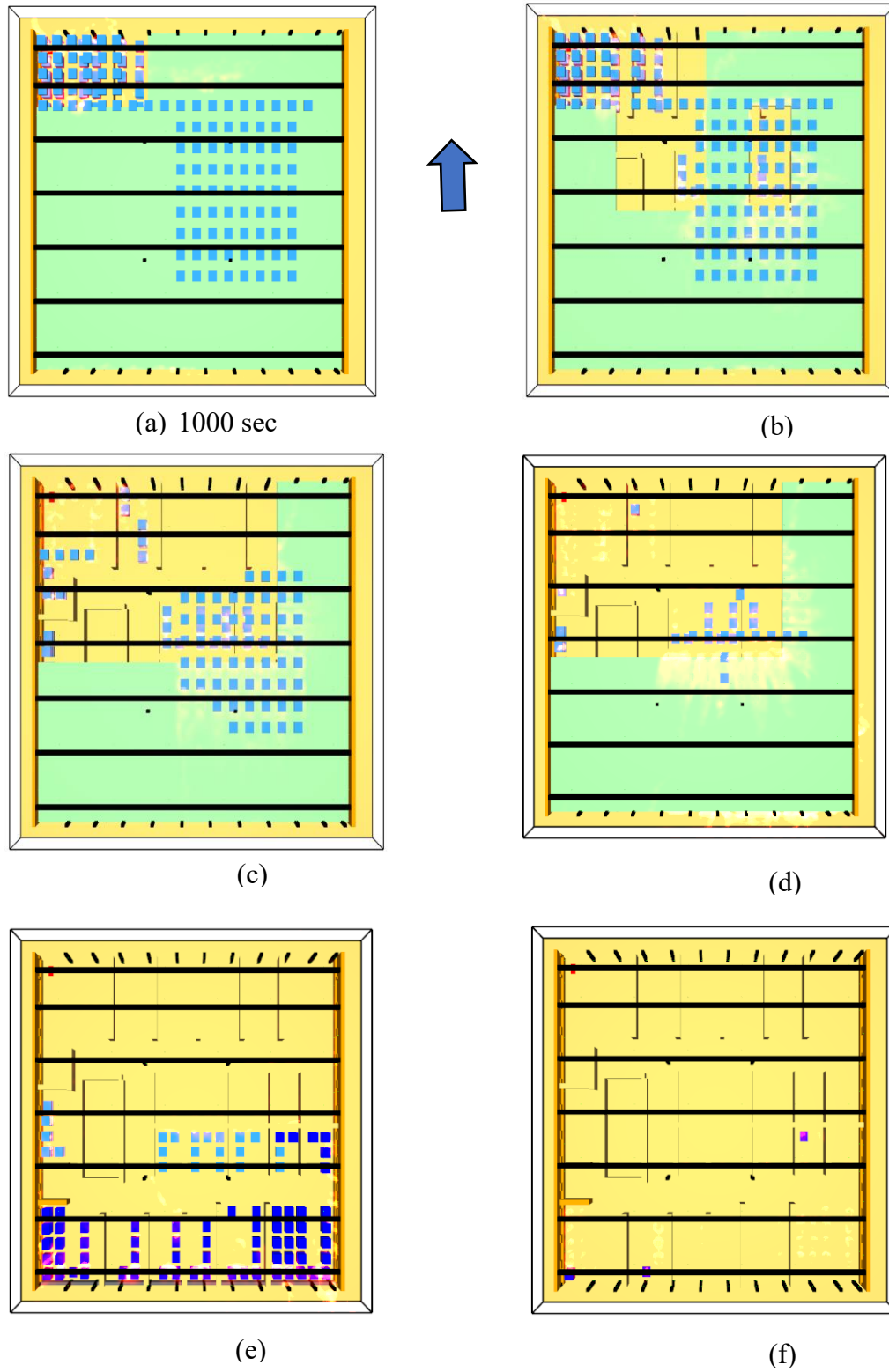


Figure 5.17 Fire travel and fuel consumption simulation in the FDS model at different times.

5.6.2. Heat Transfer Analysis

Using the OpenFIRE framework, the adiabatic surface temperatures (Wickstrom Ulf et al. (2007a)) obtained in the FDS analysis are transferred to the heat transfer model. Here, rectangular entities available in OpenSEES have been used for HT modelling for all structural members, considering the small thicknesses of truss members. For this reason, the thermal gradients on the steel sections are negligible. The thermal load files generated after conducting heat transfer analysis contain information on each and every element of the temperature history present in the thermomechanical model. The thermal load files can be used without modification for thermo-mechanical analysis.

The following plot, in Figure 5.18, shows the temperature vs. time history of FE elements at different zones on the floor. It can be observed that they have different rising and falling slopes and the time taken to reach peak temperature. The zone close to where the fire broke out (the corner area of the NW zone) was seen to have a quick rise in temperature and reached a peak faster. In the far field (6m away from the near zone, indicated by the green colour in the plot), the temperature rises gradually until the fire arrives.

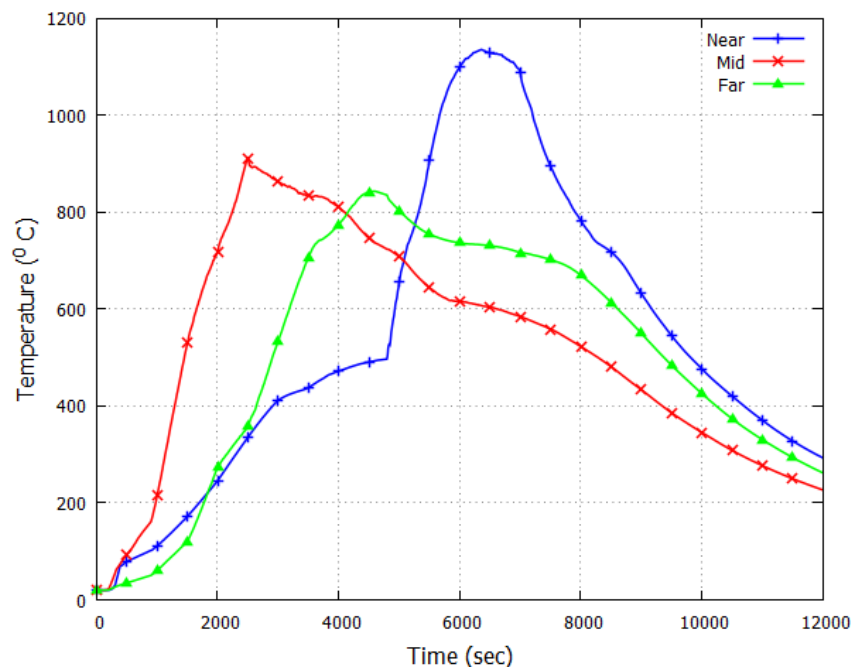


Figure 5.18 Plot of temperature vs time at three different distances representing near, midrange and far away zones.

5.6.3. OpenFIRE coupling

The transient temperature data generated by the FDS analysis is utilised for heat transfer analysis on the structural components. This study considers a concrete slab of 130 mm thick and 400 mm deep truss. The temperatures in the form of Adiabatic Surface temperatures (AST), a concept proposed by Wickström (Wickstrom Ulf et al., 2007b) , are used as the boundary condition for heat transfer analysis. Figure 5.19 – (a), (b) and (c) show the surface temperature obtained after heat transfer analysis for the steel truss and sectional temperatures for the concrete slab near the location where the fire broke out (northwest corner of the building). The study of heat transfer was conducted to determine the structural temperatures resulting from both convective and radiative heat transfer mechanisms. This analysis was carried out using the OpenSEES software.

Figure 5.19 shows sample data to depict the typical workflow among three different models used in the OpenFIRE framework. Figure 5.20 –(c) represents the temperature profile across a typical composite floor in Plasco Tower. The time-temperature behaviour for structural members, i.e., steel truss and concrete slab, can be generated. The overall surface temperatures reached in steel are higher than in concrete due to its smaller heat capacity.

In this analysis, the starting point for fire on the 13th floor is taken as 0, while in reality, the fire started on the 13th floor 900 seconds after fire initiation. The short time for column failure is due to the sharp temperature increase, as seen in Figure 5.19(b). Therefore, in future studies, core columns are not subjected to elevated temperatures to avoid early global failure of the tower. The results imply that, core columns were either exposed to temperatures at late periods or the global failure occurred due to failure of structural components other than the core column.

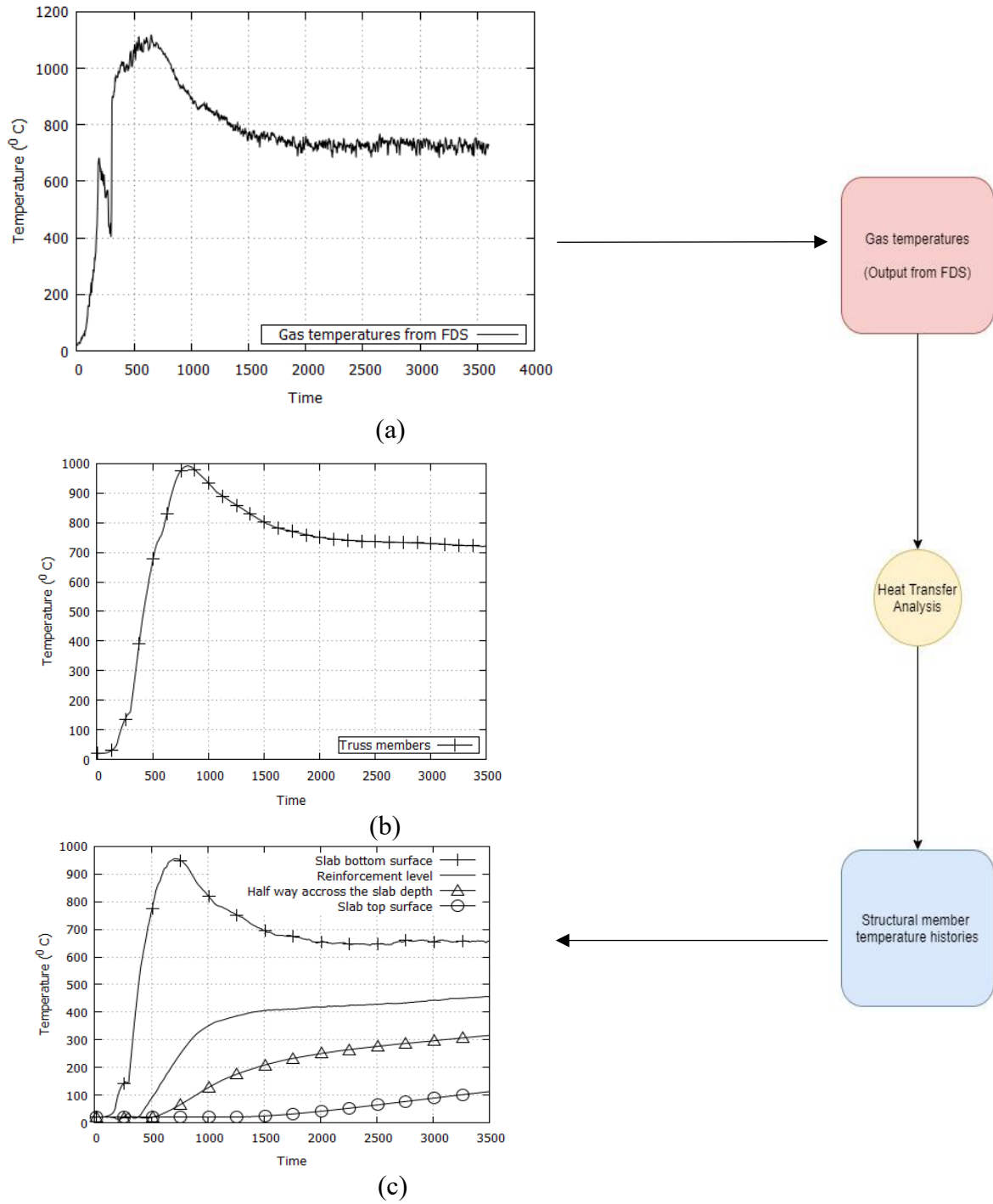


Figure 5.19 Shows typical (a) output from FDS analysis; (b) and (c) shows output from heat transfer analysis for truss elements and slab at different locations across the depth.

5.6.4. Thermo-mechanical analysis

As a final step in the OpenFIRE framework, the OpenSEES model has been created to be compatible with the OpenFIRE framework. The algorithm of this framework imposes restrictions on mesh size and demands the presence of nodes in specific, pre-defined locations. The model (Figure 5.20) considered in the study consists of 13000 nodes and 16000 displacement-based beam-column elements in total. All three models work in a cyclic process, which means any change in the FE mesh in OpenSEES will affect the sensor placement in the FDS model. Therefore, the selection of mesh has a significant effect on analysis time and effort.

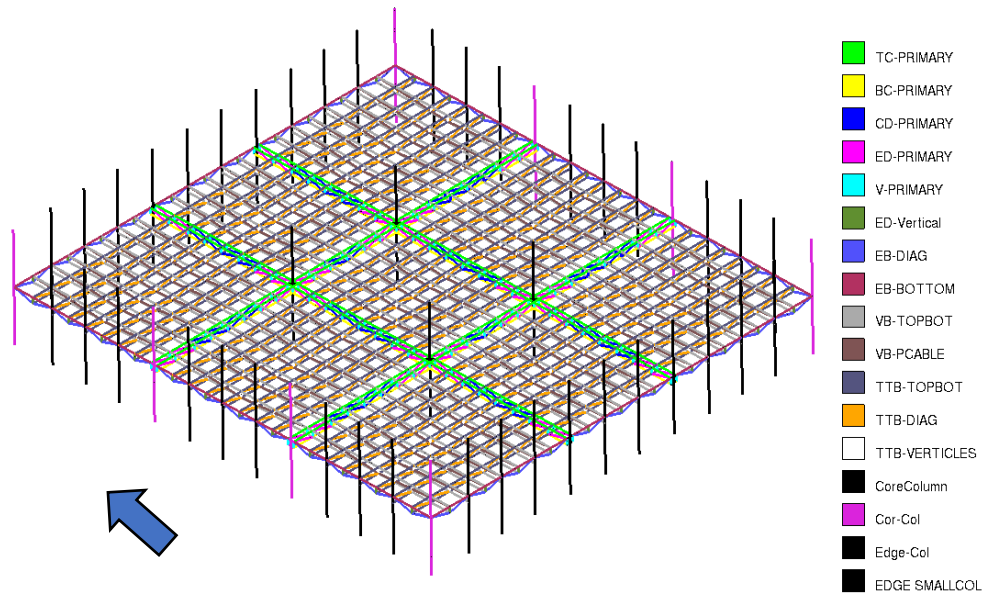


Figure 5.20 This figure shows the GiD visualisation of the OpenSEES model that was created.

The initial findings indicated significant deformations, leading to substantial difficulties in achieving convergence during the analysis. Therefore, in the testing stage of the OpenFIRE framework, a few assumptions have been made to simplify the structural analysis. The slab has been assumed to be non-composite, and its action on the truss floor has been considered through dead load action. The effect of the nature of the slab, i.e., composite vs non-composite, is explored in Chapter 6 of the thesis. Transient OpenSEES analysis with complete material non-linearity has been carried out using the GiD+OpenSees interface.

5.6.5. Structural response

The simulation results showed large deformations occurring in the northwest corner of the Plasco tower where the fire originated. Based on the magnitude of deformations predicted, it is reasonable to consider that this part of the model failed locally. Conclusively, this argument aligns with the available video evidence, which shows the failure of the NW floor that resulted in a condition of unsupported columns in the corner. After the corner fire, the fire progressed further, causing large deformations in the floors towards the East face of the tower, where the fire grew and later spread towards the interior parts.

The fire that broke out in the NW corner in the initial stage could not cause damage as the fire did not engulf any core column or component/s of the primary load transfer system, as described in the previous chapter. But in the later stages, the fire spread towards interior areas, potentially compromising the core column or the primary beams connected to it. Based on the video evidence, which shows the final moments of the collapse, the peripheral column on the south side was pulled inwards before it detached from the floor. The evidence indicates the severe presence of fuel and fire in the interior parts near the Southeastern (SE) corner of the tower. Accordingly, the fuel distribution and fire travel patterns were considered for this analysis.

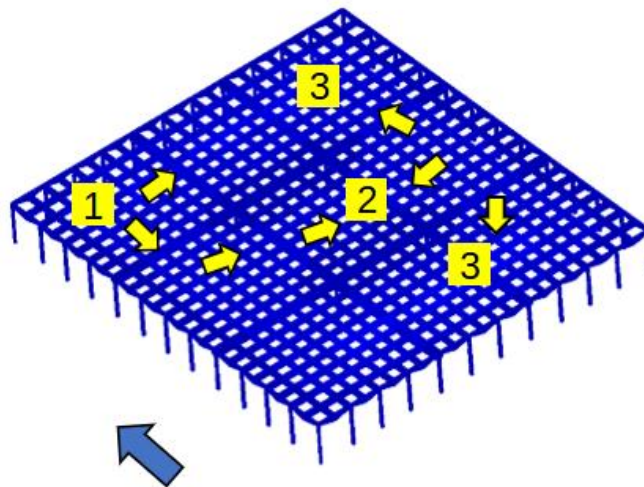


Figure 5.21 The fire travel scenario can be categorised into three significant developments.

The structural response is divided into three stages based on the extent of fire spread, see Figure 5.21. In Stage 1, the structural response in the NW corner of the building is discussed. In this stage, probable reasons for local floor failure are investigated. Stage 2 of the investigation examines the structural response and instability effects created by the fire spreading in the inner regions of the floor. Finally, in Stage 3, the possible reasons for building collapse are discussed using the floor model.

Stage-1: Local failure and fire travel to the building core

It is known that the fire broke out in the Northwest corner of the Plasco tower on the 10th floor (Ahmadi et al. (2020)). The fire was initially concentrated in the NW corner within the boundaries of two primary beams running in both directions. Still, it had spread rapidly to multiple floors in the vertical direction. By the time the tower collapsed, the fire had engulfed 6 tower floors in the NW corner. The analysis results based on the NW corner of the 13th floor predicted large deformations higher than 500mm over a large section. The following Figure 5.22 This shows the area of deformations greater than 500mm (the region outside the contour limits) at different time steps.

The steel temperatures in the centre of the NW corner remain within 200 °C up to 15 minutes, and after 10 minutes, temperatures rapidly increase to 800 °C, as shown in the Figure 5.23. It should be noted that setting up equipment for external firefighting took nearly 20 minutes after the arrival time. The rapid rise of steel temperatures caused a significant increase in floor deformations in a short time. Floor deformations increased to 360 mm from 50mm within a short duration, see Figure 5.23. Relatively, the temperatures near the Primary beam locations increased slowly. The NW corner is where the first local damage occurred, as firefighters reported. The temperatures in critical members like primary beams were around 150 °C, while temperatures in secondary trusses in the middle of the NW corner crossed 800 °C. This significant temperature difference would have exerted immense force on the floor–beam connections in the area.

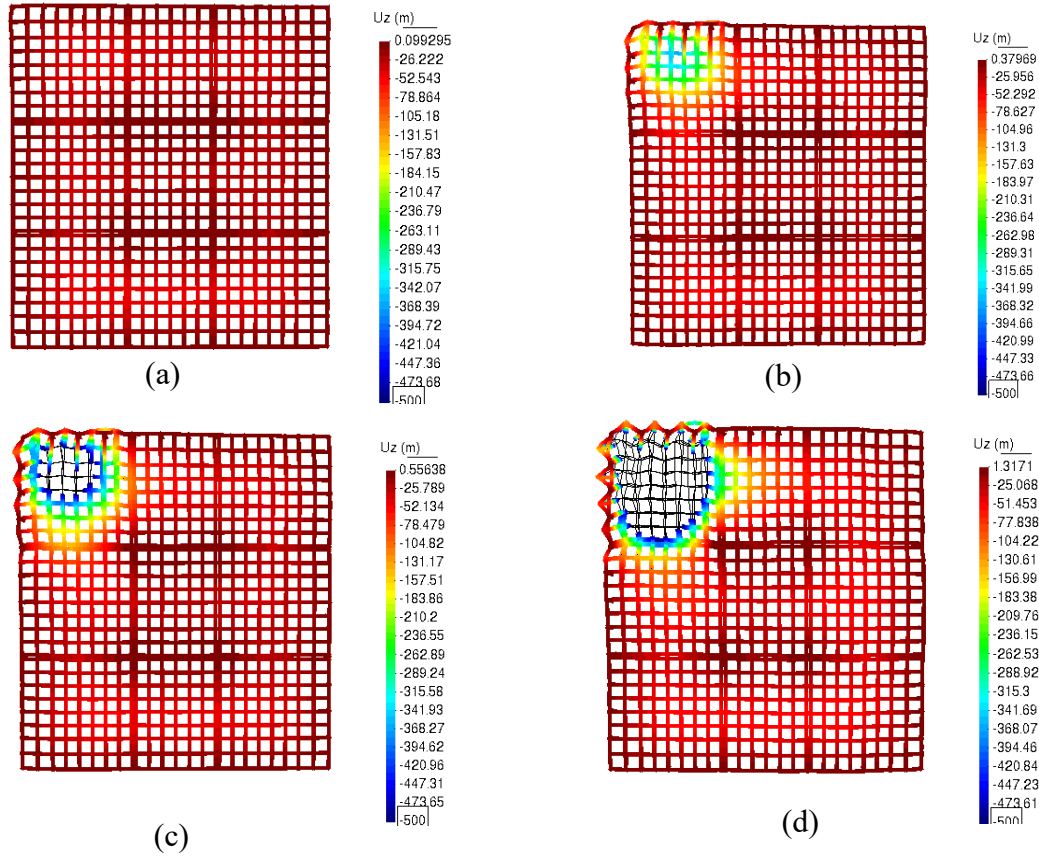


Figure 5.22 The plot shows the areas of large deformations beyond 500 mm at different stages of fire progression in the NW corner in Stage -1 (the areas outside the contour colour limits).

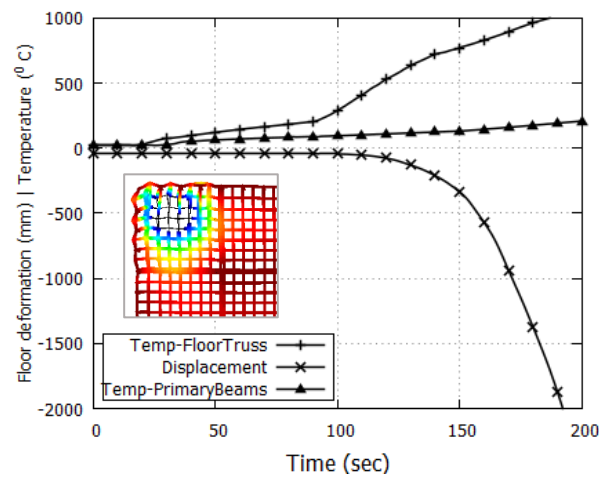


Figure 5.23 The plot shows the floor deformations at the centre of the corner and temperatures in an FE element in the floor area, and the midpoint of primary beams. The positive

scale on the graph represents temperature values, and the negative values represent displacements.

In order to discuss the local failure, the nature and load redistribution pattern under the ambient load state need to be understood. The robustness studies carried out in the previous chapter showed that core columns, primary beams and secondary main columns form the primary load transfer system of the tower. The Plasco tower had 50 columns, out of which twelve columns take a significant share of the gravity load, which is nearly 45% of the total weight. There are four core columns and eight perimeter columns, which are essential for the global structural integrity of the building. The remaining columns are used less for gravity load transfer and exist mainly to resist lateral loads. The corner area of the tower is structurally isolated, and damage that occurred in the corner did not propagate to other areas, which is usually expected in cases where catenary action is expected. In the case of the NW corner of the Plasco tower, there was no catenary action as connections could not withstand the axial forces arising from the expanding/sagging floor truss beams.

Thermo-mechanical analysis indicated that, under thermal expansion of the floor system, the thinner perimeter columns are pushed farther than the main perimeter columns. Each face of the tower has two main columns supporting the primary beams. Lateral displacement under a thermal expansion of the floor truss beams can be visualised (the deformation scale is increased for clarity), as seen in Figure 5.24.

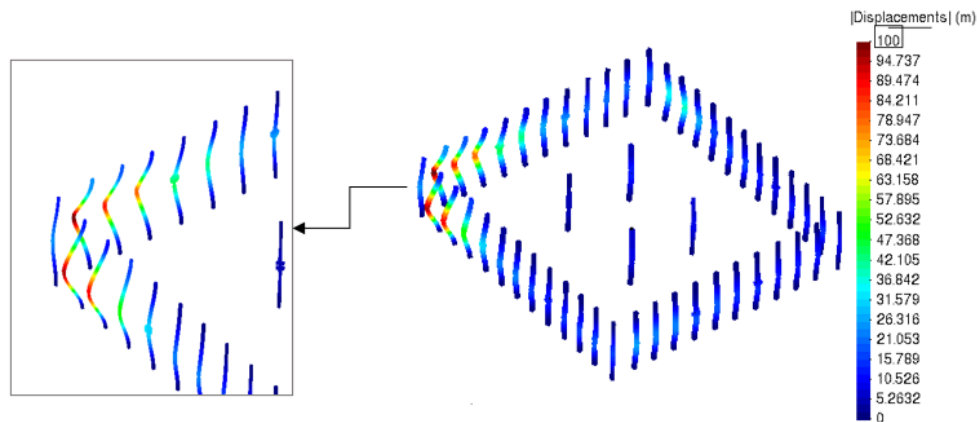


Figure 5.24 Lateral column displacement in NW corner (Floor system is hidden for clarity).

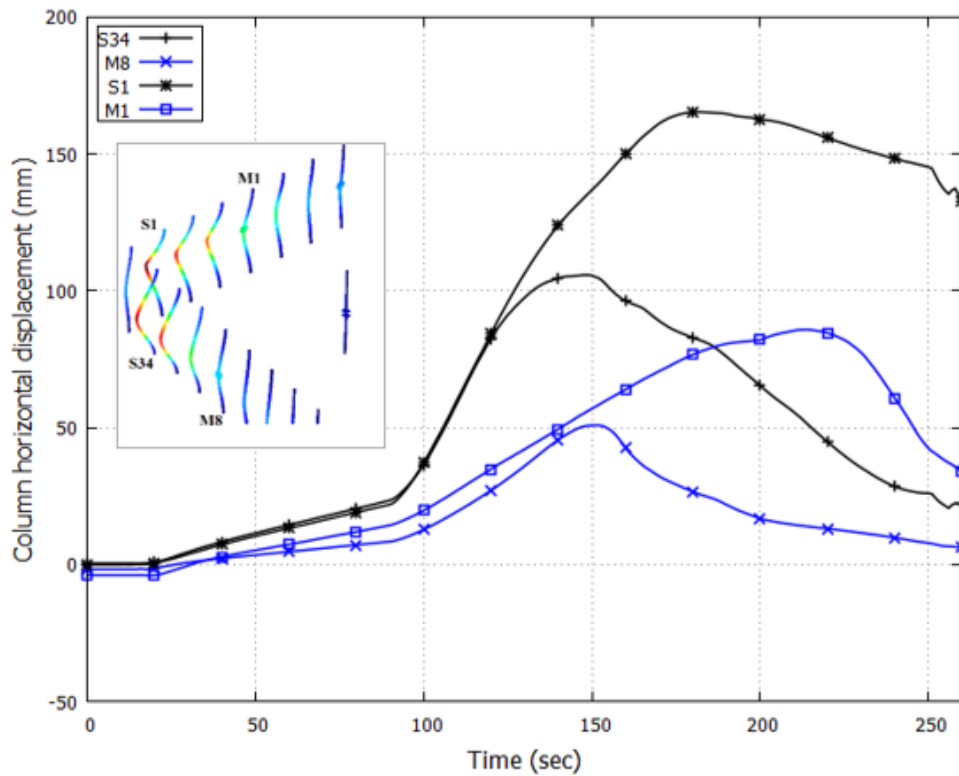


Figure 5.25 Lateral displacement of columns in the corner.

The main perimeter beams are denoted by M1 and M8, whereas secondary perimeter beams are denoted by S1 and S34. M1 and S1 exist on the West side of the corner, whereas M8 and S34 are on the North. The plot in Figure 5.25 shows that the maximum relative lateral displacement between the columns could go as large as 100mm. Other than strength and stiffness reasons, this variation in lateral displacement can be attributed to the variation in floor temperatures and the difference in inner and outer face temperatures of thick and thinner columns. These complex built-in section columns have been idealised using available block element classes in the HT module of the OpenSEES for fire. The temperature differences on both faces can be noticed in the plot of time-temperature histories of a selected FE element; see Figure 5.26. Elements at the top of the column have higher temperatures with higher gradients, whereas elements at lower levels have temperatures of 300-400 °C with lower gradients. As temperature variations along the length and across the depth at multiple levels are considered, it is not possible to show temperature plots at member levels. Hence, the plots below indicate a

selected element closer to the floor.

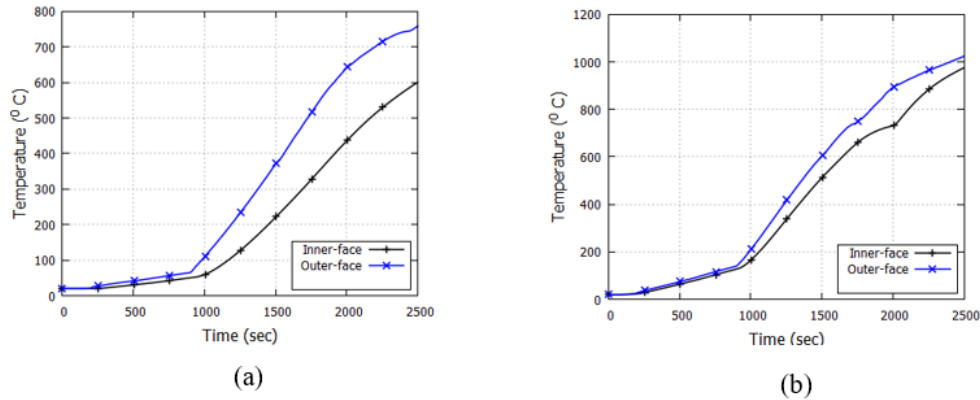


Figure 5.26 Temperature-time histories of an element selected on (a) thicker M8 and (b) thinner S34 column at a higher level close to the floor.

The thinner columns, which were displaced laterally because of the floor, experienced larger lateral deformation under gravity loads; see Figure 5.27. But since each secondary column (S1, S2, S3, S32, S33 and S34) bears around 0.5-1% of the total gravity load, they cannot cause global failure of the structural system even if those columns buckle.

It can be seen from the Figure 5.28 that the stiff corner and core columns underwent maximum vertical elongations of order 25-35mm; in contrast, secondary columns (denoted with the prefix S) underwent a maximum of 20mm axial expansion earlier than the stiffer columns. Still, they experienced a quick reversal as deformations started in the downward direction. Both horizontal displacement and vertical thermal elongations showed a significant variation in the behaviour of secondary perimeter columns with respect to other stiffer columns at four corners (C1, M1, M8 and CR1) of the structure. The loss of strength of secondary columns would eventually not significantly affect the stability of the structure, even locally. However, it is reasonable to believe that significant displacement variations in both horizontal and vertical directions would have weakened the steel connection in the NW corner, thus causing a local structural failure.

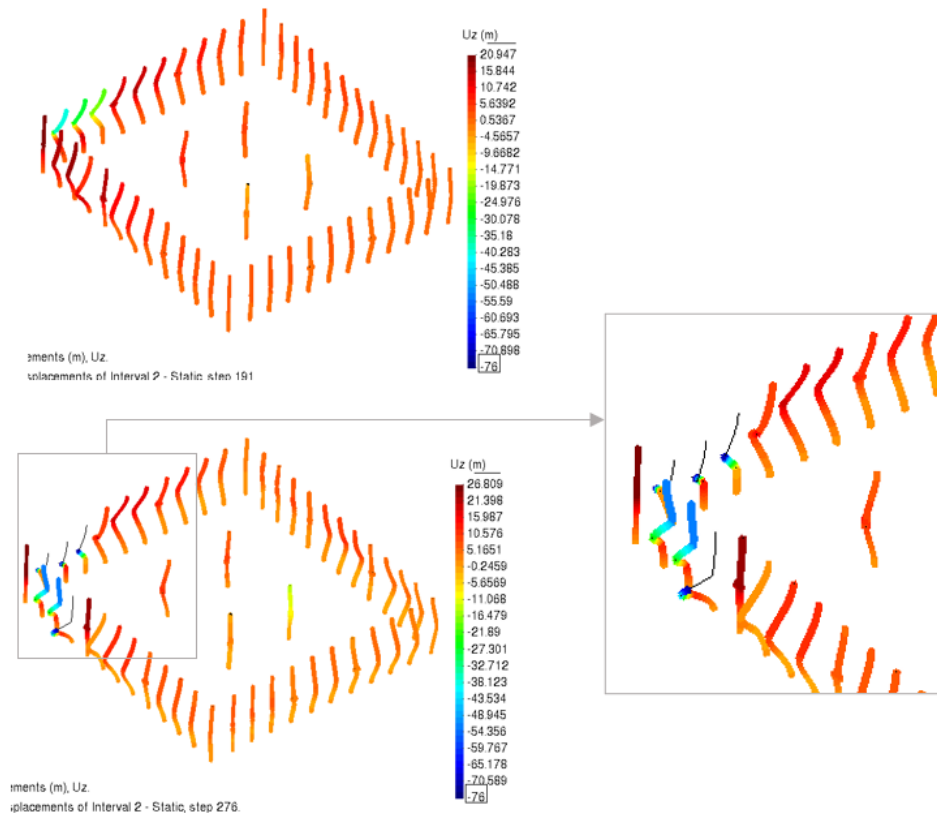


Figure 5.27 Vertical column displacements at different stages.

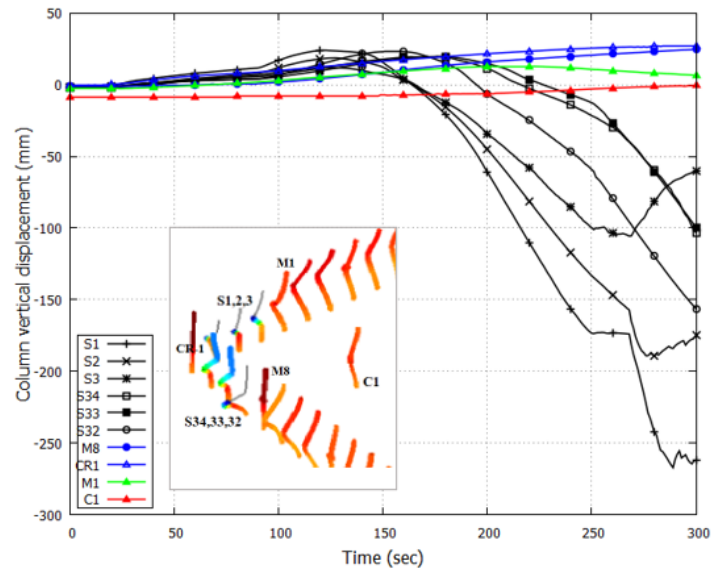


Figure 5.28 Vertical column displacements in the NW corner

Stage 2: The conditions for global failure are set

From the NW corner of the building, the fire travelled towards the core and the eastern edge of the floor, as shown in the Figure 5.29. The first leg of the fire travelled progressed towards the East (horizontal direction in the image) and towards the core. According to the floor plans, there was a staircase opening /floor entry point on the western side of the building, which would have allowed the second leg of fire to travel towards the core. They travelled fire subjected both the primary beams running in North-South directions in the core to deform greatly, marked in the Figure 5.29(a). It has been established already that the primary beams of the floor, being a part of the primary load transfer components, are major strength providers. The primary beams are also responsible for holding all load-carrying columns together. Hence, the progression of fire in the core of the building can be seen as a moment after which the global stability of the floor began to be compromised.

The fire intensified near one of the primary beams connecting the core columns towards the Eastern side, as indicated in Figure 5.29 –(b). The core columns and primary beams are critical components of the tower, and their failure ensures the failure of the structure, at least locally. The load redistribution mechanism in the case of critical member failure is not considered at the design stage. Therefore, a potential primary beam failure in the core or core column buckling could potentially lead to the progressive collapse of the structure.

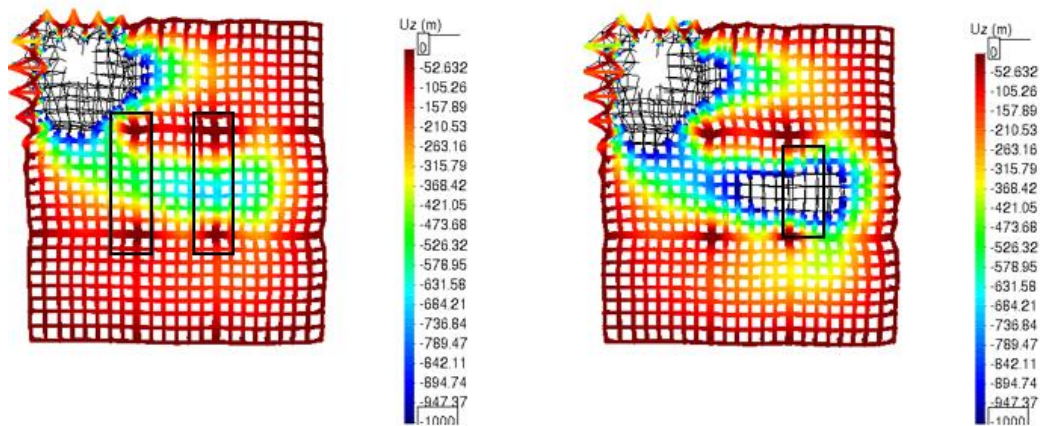


Figure 5.29 The contour plot shows the areas of large deformations beyond 1000 mm at different stages of fire progression in Stage 2.

As the fire progressed, the columns on the east face were pushed outwards, similarly to Stage 1. However, unlike the NW corner of the building, there is no visual evidence of floor collapse in this location at this stage of the fire.

The firefighters extinguished the fire in the NW corner and began re-positioning themselves to fight on the East and South faces. Despite their efforts, the fire inside the eastern part of the building's core started making its way towards the South face. The fire surrounded the regions where the South-East core column was situated. Simulation results showed that deformations up to 500mm in the eastern part of the core and primary beam, see Figure 5.30 – (a).

Even though there was masonry in the core, the height of the masonry walls at many locations was shorter than the height of the columns. At a few locations, photographic evidence showed the presence of thin boards in the place of walls, thus exposing the parts of unprotected core columns to potential fire loads. Hence, in this model, columns, too, were exposed to elevated temperatures as predicted by the CFD models. The results showed that the SE core column underwent a relative downward displacement of more than 2% of column length with respect to other core columns. This can be visualised in the column-only contour plot, as shown in Figure 5.30 –(b). In the absence of visual evidence to further the investigation and to check for possible global mechanisms, it is assumed that connection failures did not occur during Stage 2. The focus has been on looking into the inherent weakness in the form of collapse-triggering mechanisms.

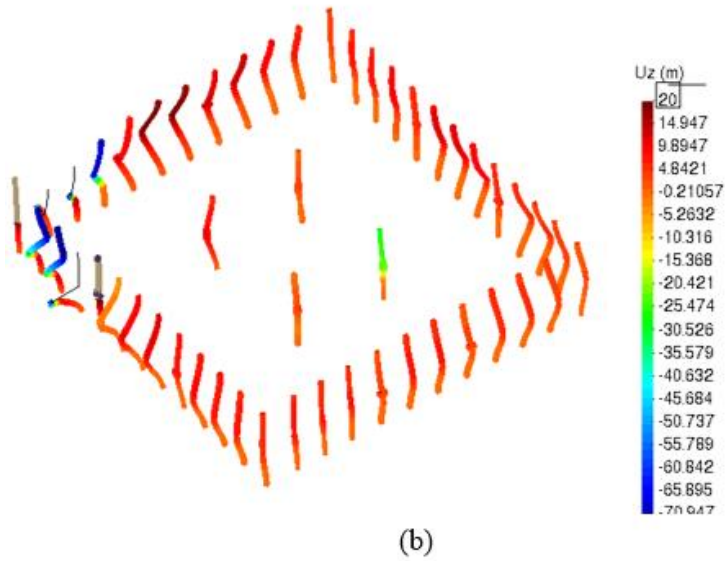
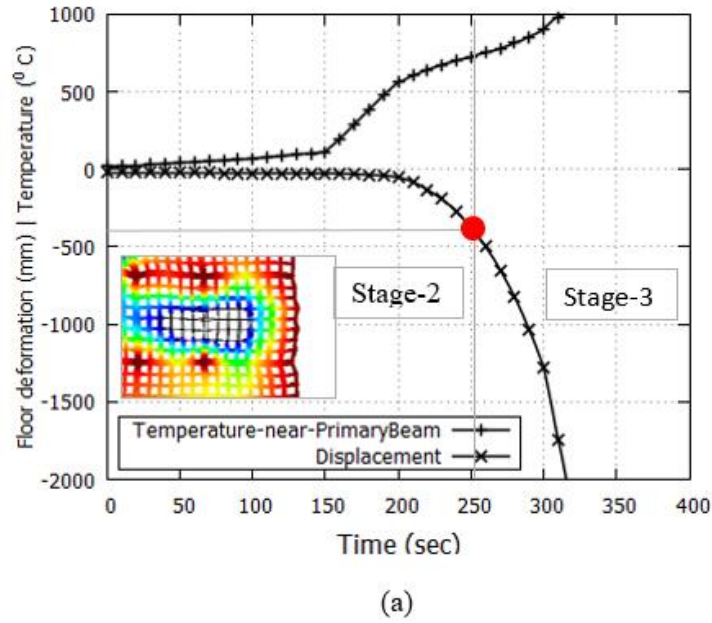


Figure 5.30 (a) Primary beam deformation vs temperature core area; (b) Vertical column displacement in Stage 2.

Stage-3: Collapse initiation

After affecting the core area and the adjoining eastern region, the fire progressed towards the southern part of the floor, as seen in the Figure 5.31. The simulation results showed zones of large deformations beyond 1000mm, as indicated by uncoloured areas. The extent of such high deformation is seen all over the floor model, particularly in the South and surrounding

areas where the Southeast core column was situated. In a real-world scenario, the extent of fire damage could be lesser due to the physical obstructions. It should be noted that the simulation results reflect the response of the tower with the complete failure of the obstruction provided by the false ceiling.

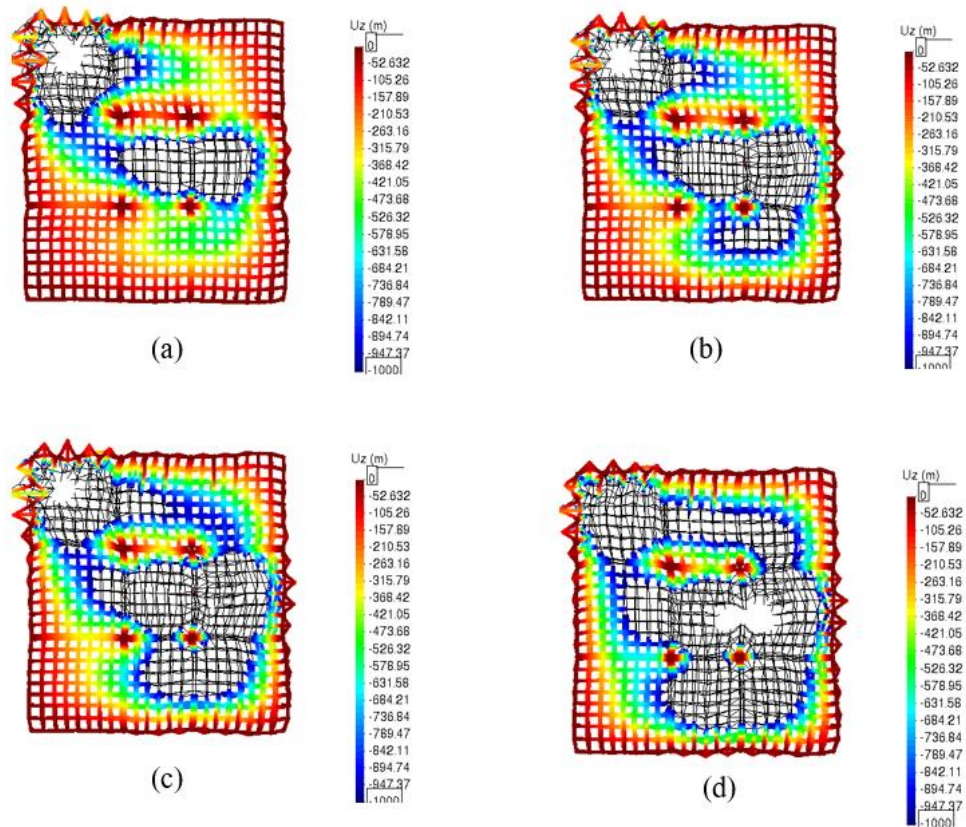


Figure 5.31 The plot shows the areas of large deformations beyond 1000 mm at different stages of fire progression in Stage 3.

The effect of fire on truss beams joining the core column might isolate the core column structurally. The isolated core column with lesser bracing support from primary beams increases the effective length of the column. At this stage, the failing SE core column causes load redistribution towards adjacent core columns in the SW and NE directions. The robustness study on the core column revealed that the load redistribution in the SW and NE core columns is not uniform /equal. The unequal load distribution can be attributed to the rectangular aspect ratio of the floor segment in the core area. However, the fire spread pattern shows that the SW

core column had the presence of a colder floor area on the western side, whereas the NE core had none. Hence, even a smaller load redistribution might be detrimental to the safety of the column. It can be seen in Figure 5.32 that the NE core column experienced 25mm downward displacement, while the SE core column experienced 66mm. The failing SE core column and primary beam near it created destabilising effects on the NE core column.

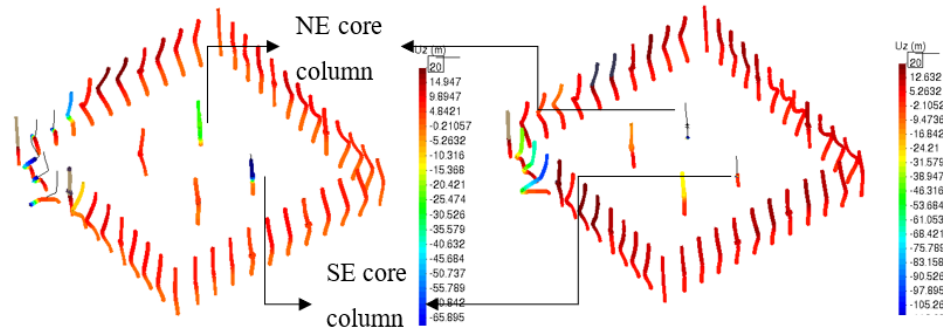


Figure 5.32 Response of SE and NE core columns on the 13th floor before and after SE core column failure.

The thermomechanical analysis progressed further, and the simulation showed an equally higher magnitude vertical column displacement in the NE core column, see Figure 5.32 and Figure 5.33. The contour shows that vertical deformations of the columns are more than $0.03H$, whereas $0.01H$ (H is the height of the column) is generally considered as failure compression displacement in the case of fire resistance tests on columns.

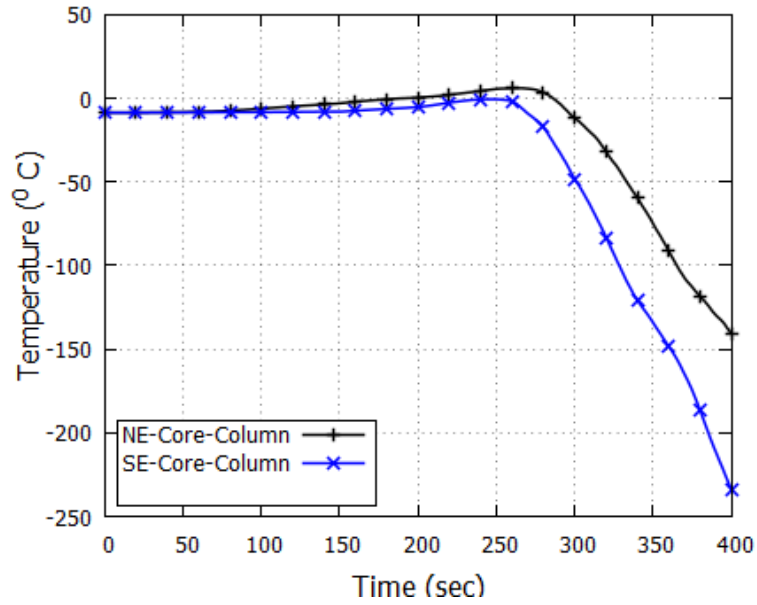


Figure 5.33 Vertical displacement of both the core columns

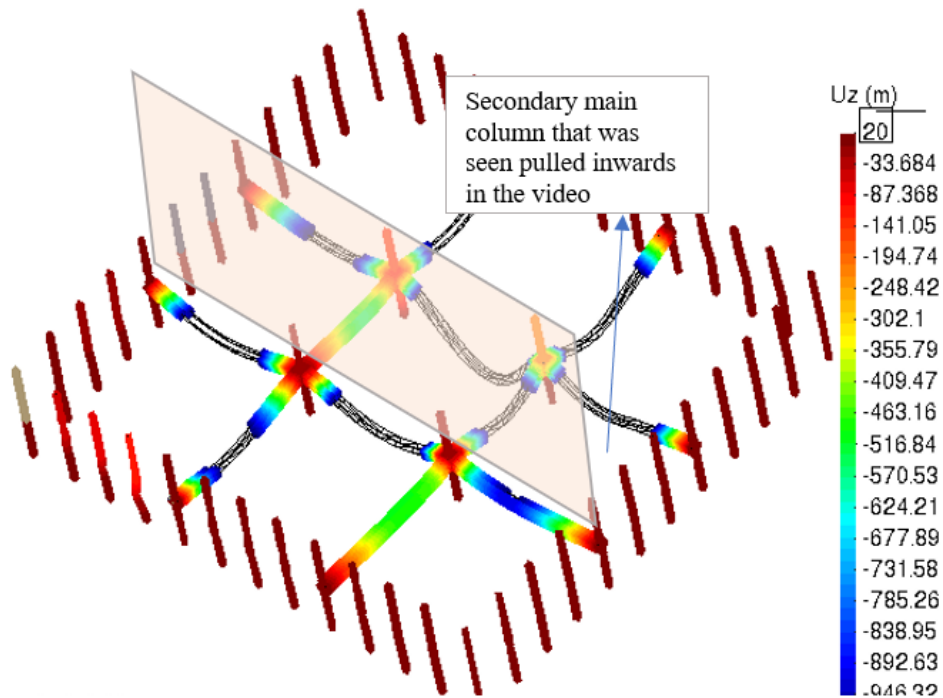


Figure 5.34 Frame of collapse initiation

The analysis concludes that the failure of the core column on the 13th floor could be a potential reason which triggered the collapse of the Plasco tower. Large downward displacements of the SE pulled the primary beam, which in turn exerted pull forces on the external secondary main column. The primary beam running in North-South directions

connecting the SE corner core column is seen undergoing catenary action, see Figure 5.34. This would exert a horizontal pull on the main perimeter column connecting to it, or even an impact force from the partially collapsing debris from the above floor will have a similar effect. Video evidence, as shown in Figure 5.35, captured the initiation of the collapse from this perimeter column, which aligns with the predicted response of the 13th floor of the tower.



Figure 5.35 Screenshots (a) and (b) from video evidence show the South side peripheral column being pulled inwards seconds before the tower collapses.

In this investigation, the analysis was limited to a single tower floor to identify the reasons behind its collapse. However, a comprehensive analysis of the entire building, considering multiple floors subjected to fire loads, could potentially reveal additional collapse triggers, such as buckled columns. Evidence indicates that the southern and southeastern regions of the tower were exposed to fire over multiple floors. Therefore, it is highly probable that several columns within the tower might have lost lateral support, suggesting that the structure could have encountered various destabilizing conditions before the final collapse. Although the OpenFIRE framework was capable of coupling CFD and FE analyses, the GiD+OpenSees interface is employed to manage multiple floor models. The subsequent chapter will demonstrate the approach involving GiD+OpenSees by subjecting the tower to multiple-floor fire loading.

5.7. Conclusions

1. The present work has been carried out to demonstrate the successful coupling of FDS, heat transfer and finite element models achieved using the OpenFIRE framework. The simulation of the critically affected 13th floor of the Plasco tower was successfully simulated against the 3 hr 20 min duration of the travelling fire. The study used mapped temperature data from the FDS model at every 5x5 m grid interval for heat transfer and thermo-mechanical analyses.
2. The key finding from the study is that large variations in axial floor truss displacements in the NW corner of the building could have led to severe damage to the steel connections, potentially causing a local failure. CFD and heat transfer analysis revealed that the steel temperatures are higher in the centre and lower near the edges, where primary beams and secondary main columns are located. The combination of thinner members at higher temperatures and stiffer members at relatively colder temperatures caused significant differences in the magnitude of their lateral displacement. Secondary columns were seen experiencing larger displacements than the secondary main columns. This uneven out-of-phase movement of columns and floor truss could have caused the failure of connections in the NW corner.
3. In the Plasco tower, partial floor failures on the 11th floor occurred due to the connection failure, but the remaining floors below them collapsed due to the impact loads caused by the dynamic actions of falling floors. Therefore, most floor failures in the Plasco tower occurred suddenly. The main reason for not incorporating the connection models in the structure is to understand the load redistribution mechanism in the tower. By not modelling the connections, it was possible to study whether the structure could sustain the applied thermal load irrespective of connection failures.
4. The stability of the core columns is a critical factor for the overall stability of the structure. In the case of the Plasco Tower, the core columns carry approximately 50% of the dead weight of the building. The spread of fire towards the core of the building would have compromised the structural integrity. Robustness studies revealed that the load redistribution in the event of a core column failure is uneven. Specifically, the failure of the southeast (SE) core column would transfer a higher load to the southwest (SW) column compared to the northeast (NE) column. However, the pattern of fire

progression affected the NE core column, leading the study to predict that the collapse of the tower was primarily triggered along the plane formed by the southeast and northeast core columns.

5. The simulation results suggest that the global collapse was initiated by the inward pull exerted by the failing southeast core column or potentially by the impact of falling debris. This prediction aligns well with the available video evidence, further validating the accuracy of the in-floor fire spread modelling employed in this study.

Chapter 6: Analysis of the Plasco Tower

Using an Integrated Simulation Approach

6.1. Introduction

In the previous chapter, a single floor of the tower was analysed using the OpenFIRE approach, which is fully open source. For the analysis, the fire load and pattern of the 13th floor of the tower were modelled and used as a thermal load for thermomechanical analysis. With the OpenFIRE framework, the coupling of CFD and FE models was seamless; it required user interference at different stages. While the workflow is clear and transparent, it requires thorough checks and attention, which might be time-consuming in the case of handling models of large-scale structures like the Plasco tower.

OpenFIRE requires data from the FE model, like meshing, nodal and elemental information, for placing thermocouple devices at chosen intervals. Hence, in the case of OpenFIRE, a higher degree of compatibility is required between the CFD and FE models. This chapter focuses on using the GiD+OpenSees interface, modified by M. A. Orabi, Khan, et al. (2022), to streamline the connection between the FDS and FE models. To achieve this, the GiD+OpenSees interface is leveraged, reducing the effort required from the user utilising its user-friendly features and graphical interface. The overall aim of using this approach is to enhance the efficiency of the sequential analysis by minimising user involvement in the data transfer.

In this chapter, the thermo-mechanical response of the tower against the fire in the NW corner of the tower is studied (Figure 6.1). In Chapter 4, it was discussed that the fire initially ignited in the northwest (NW) corner and spread in both vertical and horizontal directions. The vertical fire remained confined to the NW corner until the floors partially collapsed.



Figure 6.1 Photograph showing the NW corner of the Plasco tower engulfed in flames, spreading across multiple floors.

6.2. Aims and objectives

The objectives of this chapter are twofold, i.e.,

1. To develop plausible theories explaining the collapse mechanism of the partial collapse of the Northwest corner of the Plasco Tower, which occurred during the initial phase of the fire.
2. To demonstrate the open-source integrated approach used for the investigation, developed by the Structural Fire Engineering Group at PolyU, Hong Kong.

The integrated approach implemented in this work will demonstrate the capabilities of FDS and OpenSEES in performing a complete sequential analysis of fire, heat transfer and thermo-mechanical analysis at a desirable level of fire load resolution. The specific aim of this work is to understand the reasons for the partial collapse of corner floors in the Plasco tower by exposing a reasonably comprehensive 3D finite element model of the building to the type of

fire loading it experienced during the initial phase of a fire incident.

6.3. Software integration approach

This study uses an integrated platform for building OpenSees models without needing manual creation of *tcl/tkl* scripts. This integrated platform combines functionalities of multiple software programs to carry out thermo-mechanical analysis of tall buildings.

The workflow begins with the creation of a BIM model using line and node objects to create the basic geometry of a structure. The BIM model serves as a starting point for the subsequent creation of both CFD and finite element models, see Figure 6.2. The geometrical objects of the BIM model, i.e., line and node objects, are imported into the GiD+OpenSees interface and PyroSim for further model building in the respective software. As both software share the same input, it is easier to minimise conflicts that arise due to mismatching of inner and outer dimensions, location of columns and the orientation of structure, etc. Once both FE and CFD models are created, thermocouple devices are first generated in the GiD interface, and their data is shared with the CFD model; then, gas temperature histories recorded by the thermocouple devices in the CFD model are sent back to the FE model. The GiD+OpenSees interface then invokes the heat transfer module of OpenSees and carries out heat transfer analysis on every section assigned with a thermocouple device. The output from this step is then input as thermal load for the final step, i.e., thermo-mechanical analysis in OpenSees.

Technically, the way GiD+OpenSEES and OpenFIRE operate is quite similar. Both frameworks follow the same workflow, i.e.,

1. Convert FDS output into OpenSEES-compatible time-temperature data
2. Heat Transfer
3. OpenSEES-compatible thermal load

Among the three steps, using the OpenFIRE framework demanded user interference in heat transfer analysis. Though simple to use, the OpenFIRE framework increased the user effort needed due to the sheer size of the Plasco tower. So, to speed up the research work and minimise human error, the GiD+OpenSEES interface is employed to carry out the heat transfer analysis (step 3). The other steps, 1 and 2, remain unchanged in how they are implemented in both frameworks.

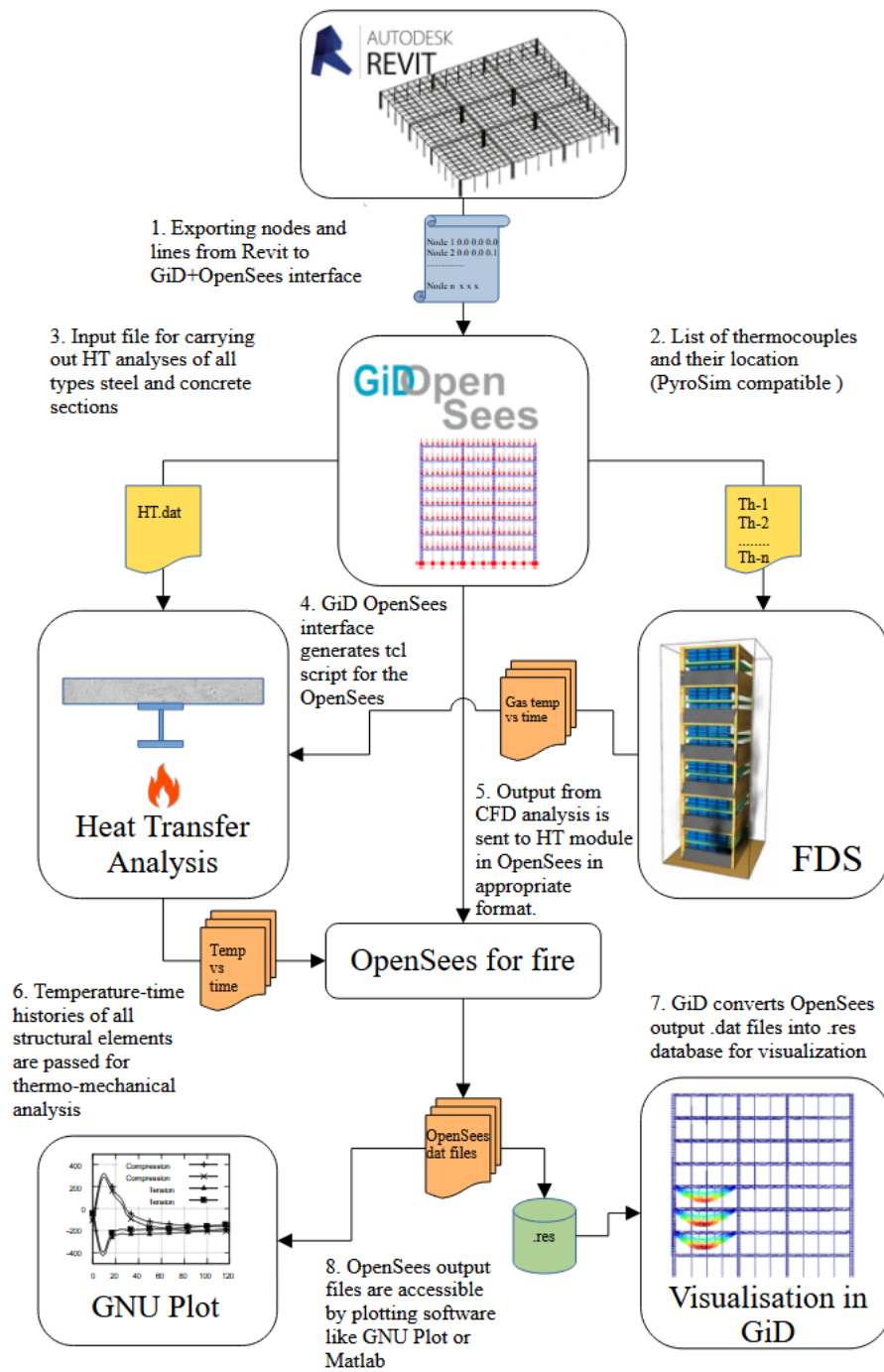


Figure 6.2 Workflow in the integrated simulation approach

6.4. Modelling the fire

6.4.1. Timeline of the accident

Khan (2022) conducted studies on how vertical fire spread in the Plasco building. The fire, which started in the NW corner, travelled in both vertical and horizontal directions. The vertical fire stayed in the NW corner until the partial collapse of the floors. The travelling fire was reconstructed based on visual evidence gathered from multiple sources.

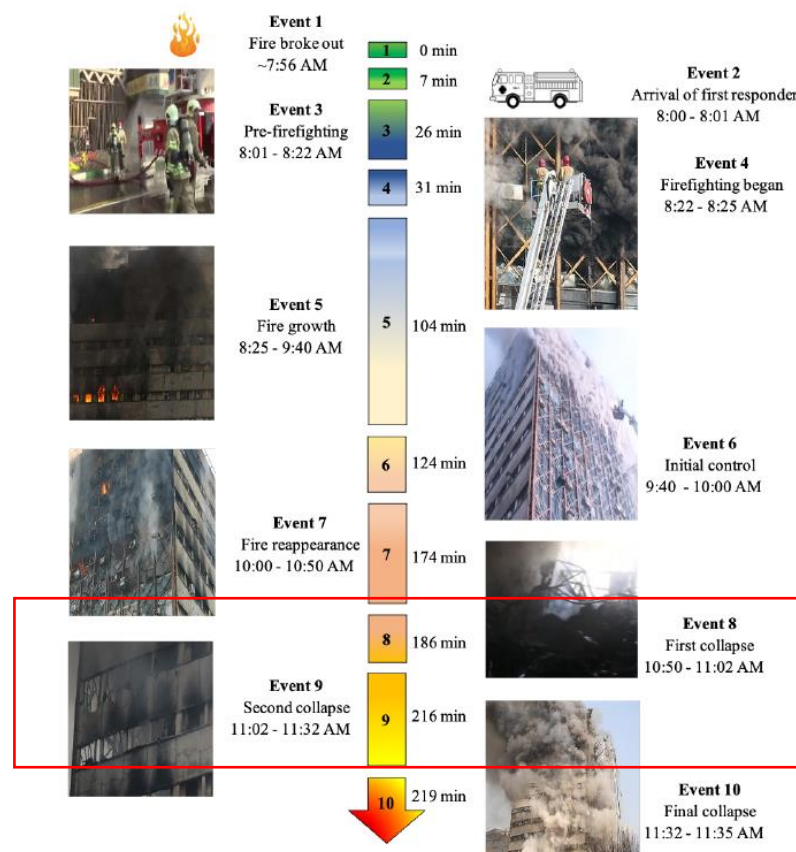


Figure 6.3 Timeline of the Plasco tower fire accident.

The entire 219-minute time span of the fire incident was divided into ten events (Figure 6.3), each marking a key aspect related to the fire or the structural damage that occurred. The timeline starts with Event 1, which marks the time of fire initiation and ends with Event 10, which indicates the total collapse of the tower. Events 1 to 7 indicate various stages of fire spread and firefighting efforts, whereas Events 8, 9 and 10 highlight different levels of structural

damage. The focus of the current study is to simulate the structural response against the fire that occurred from Event 1 to Event 9, where the first and second partial collapses of the NW corner of the tower took place.

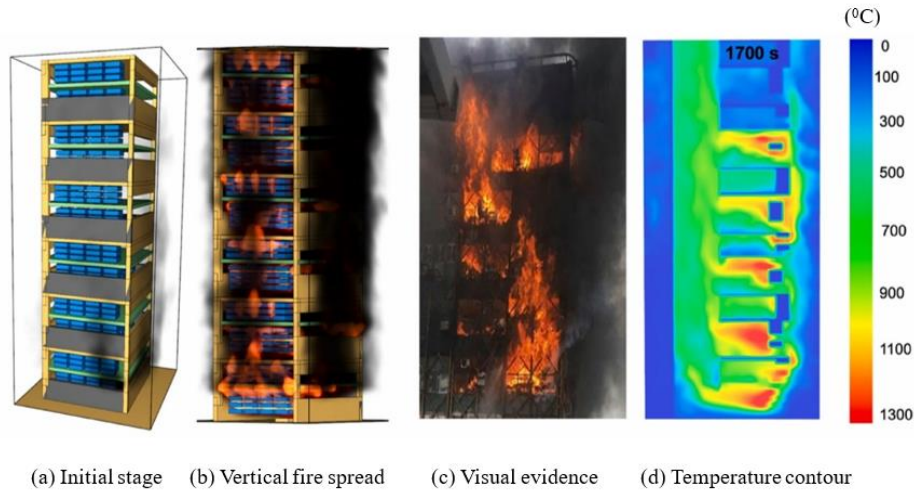


Figure 6.4 CFD model visualisation compared to the visual evidence (Khan et al., 2022).

6.4.2. CFD modelling and analysis

For vertical fire spread, the north-western corner of the Plasco Building from the 10th to 15th floors was simulated. The CFD model was calibrated to match the available evidence of the fire. The simulated vertical fire spread closely matched with the available visual evidence, as shown in Figure 6.5. This vertical fire spread, as confirmed by witness testimonies, occurred in the early stages of the fire, i.e., during the first two hours of the fire incident. The easy availability of fuel, ventilation, and sufficient quantity of air can ascertain the reason for the rapid-fire spread. The vertical spread fire modelling provided the time of fire reaching the upper floors. The FDS simulation (Figure 6.5) shows that the fire reached the upper floors within 30 minutes of the ignition, similar to what was observed during the fire accident.

Model calibration

In large open floor plans, fire tends to travel across the floor plates with localised burning; this process is often termed the travelling fire. In such spaces, fire spreads quickly until

all the fuel is consumed. When there are partitions, i.e., in a compartment, fire spread is usually slower.

In the case of Plasco Tower, the floor was partitioned due to the presence of multiple business units, but the presence of a continuous false ceiling provided faster fire travel. To simulate the horizontal spread, an FDS model is generated to represent the spread of the fire on each floor. The fires on the 10th, 11th and 14th floors were primarily located in the northwestern area of the building. Therefore, in FDS, the fire calibrated based on the 10th floor is used to represent the fires on both the 11th and 14th floors. Similarly, the observed flames on the 12th and 13th floors were similar, except for the more intense fire on the southwestern side of the 13th floor. However, for the studies in the chapter, the fire simulation is conducted until Event 8/9 (the first collapse and second collapse).

To simulate the vertically travelled fire, different fire initiation timings are applied by introducing time delays for each floor. Table 1 presents the time delays for the fire to reach the upper floors, derived from vertical fire spread modelling. These timings are incorporated into the fire simulation output. For instance, for the 11th-floor fire, which utilises thermal data from the 10th-floor fire simulation, the initial fire time is set at 360 seconds (Table 1) to account for vertical fire spread in the structural model.

Floor	10th floor	11th floor	12th floor	13th floor	14th floor	15th floor
Time delay (sec)	0	360	620	900	1100	1300

Table 14 Time delays are to be used to apply thermal load on each floor.

In later stages, the fire was observed spreading horizontally from a similar location (the northwestern corner of the building), as shown in Figure 6.5, agreeing with the visual evidence and testimonies. The vertical fire simulation provides two critical pieces of information, i.e., (1) the fire reached the upper floors during the early stages of the fire, even before any firefighting operation began, and (2) the fire initiation location was similar at each floor. Therefore, only a few floor models are calibrated to obtain realistic thermal data for all floors to reduce the

computational cost.

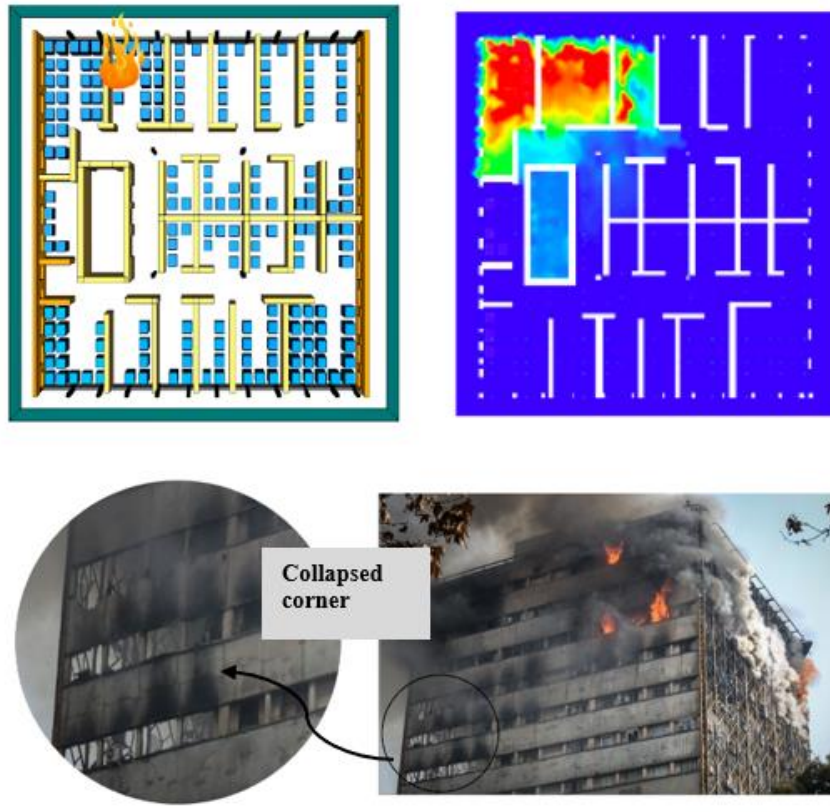


Figure 6.5 CFD model simulation showing the horizontal fire spread (Khan, Domada, et al., 2022)

The vertical fire spread simulated using the model from the 10th to 15th floor, closely matched with the available photographic evidence; see the Figure 6.4(c) This vertical fire spread, as confirmed by eyewitnesses, occurred in the early stages of the fire, i.e., during the first 1-2 hours of the fire incident. The easy availability of fuel, ventilation, and sufficient quantity of air can ascertain the reason for the rapid-fire spread.

Figure 6.4(b), obtained from the FDS simulation, shows that the fire reached the upper floors within 30 minutes of the ignition, similar to what was observed during the fire accident. In later stages, the fire was observed spreading horizontally from a similar location (the northwestern corner of the building), agreeing with the visual evidence and testimonies. Figure

6.4(d) shows the temperature contour plot showing the rise in temperature of the upper floors.

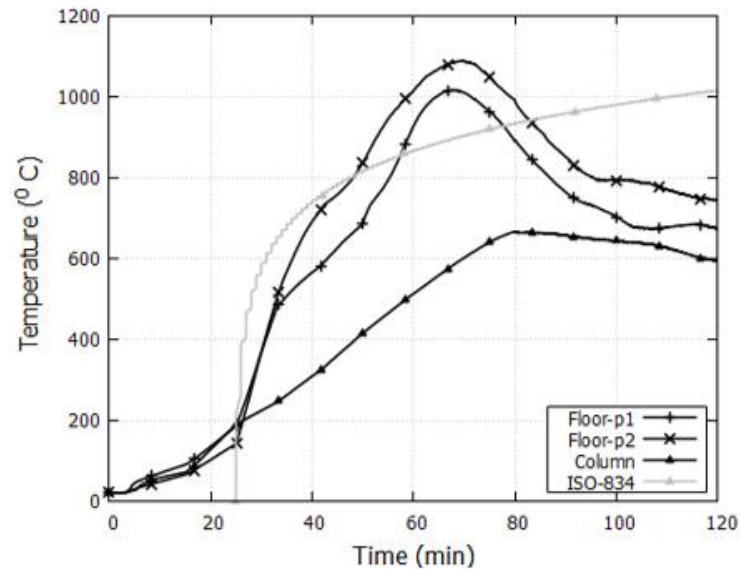


Figure 6.6 Gas temperatures at different locations; p1, p2 correspond to centre and edge locations on the corner area of the 11th floor.

Figure 6.6 shows the plot of the gas temperatures at locations on the 11th floor (ceiling of 10th floor) and the column. The magnitudes of temperatures are around 110 °C for the first 20 minutes of the fire, and after 25 minutes, the fuel burning rate increased enormously, resulting in a sudden increase in temperatures. The temperatures crossed 500 °C after 33 minutes and 1000 °C after 60 minutes of fire. For comparison, the standard ISO 834 curve is plotted (in grey colour) on the same plot with gas temperatures obtained from the CFD analysis. The standard ISO curve is shifted 25 minutes on the time axis for easy understanding. The temperature values on the ISO curve rise rapidly until 600 °C and then gradually until 800 °C, and then a much slower rise beyond that point. This difference in temperature rise shows how differently fires grow in real-life fires. According to the CFD model, peak temperatures are observed about an hour after fire initiation despite the slower rise in the beginning. For comparison, temperatures of 1000 °C or more are seen after 90 minutes in the ISO standard fire.

In general, a thermo-mechanical analysis in non-composite structures is not affected by the time factor, i.e., for non-travelling fire accidents, the response of a structure to temperature load remains the same whether temperature loads are applied in a 1-hour or 2-hour period. Time-dependent temperature loading plays a major role when different components of a structure attain peak temperatures at different times, in composite structures or when dynamic effects are considered, which is expected in the case of full floor fire spread.

In this chapter, two thermo-mechanical analyses were conducted. In the first analysis, the ISO 834 curve was employed to simulate the behaviour of the corner floors. The primary objective of this first study was to test and evaluate the coupling framework and compare the results obtained from the second study, where a Computational Fluid Dynamics (CFD) approach was employed to simulate the fire. In the second study, gas temperature output from a detailed multi-floor fire analysis of the Plasco building, carried out by Khan (2022a) & Khan, Khan, et al. (2022) is used.

6.4.3. Resolution of the thermal load applied

While the ISO 834 curve was used for the first study, CFD model output was used for generating thermal load in the second study. In the second study, a lower thermocouple resolution was used to study the structural response to recalibrate the fuel load and gas temperature under a situation where the structural response deviates significantly from the available visual evidence. It is essential to highlight that in the context of heat transfer and structural analyses, the fire on the 10th floor is effectively heating the 11th floor. Consequently, for heat transfer and structural analysis purposes, when referring to the 11th floor, we are essentially considering the fire on the 10th floor and so forth. In the Figure 6.7, an example of the data communication between the HT module of OpenSees and FDS for a particular thermocouple is shown. It can be seen from the FDS output of the marked thermocouple on the 12th floor (temperature vs time data) that the temperature was below 100 °C initially, and after 500 seconds, the temperature rose to 400 °C, indicating the arrival of fire in that area. The initiation and arrival of fire at different locations can be verified by comparing the temperature vs time data from thermocouples. The thermocouple data at the NW corner area of three different floors is shown in the Figure 6.8.

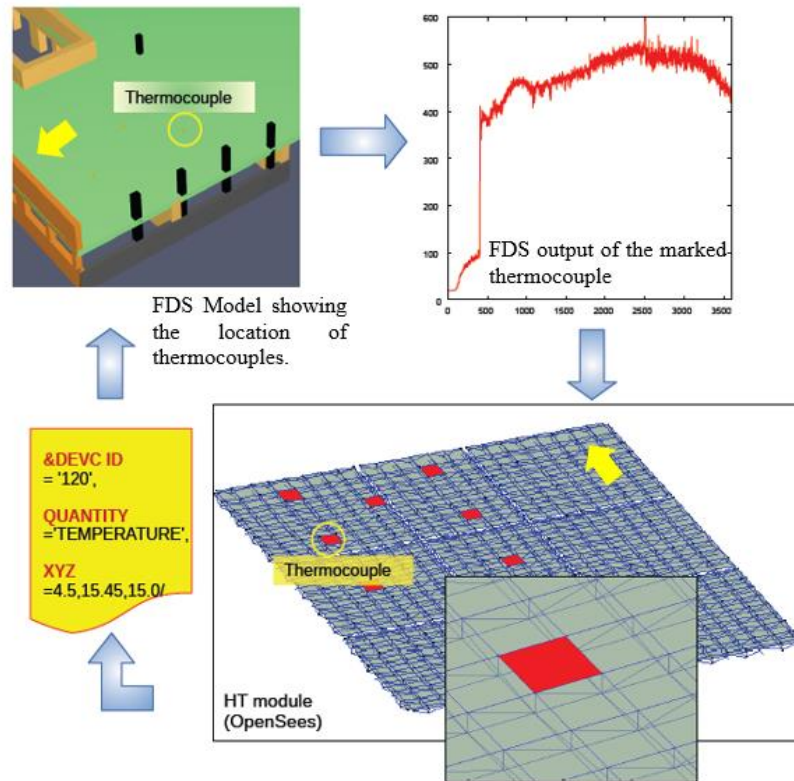


Figure 6.7 Thermocouple data exchange between the FDS and HT module of OpenSees.

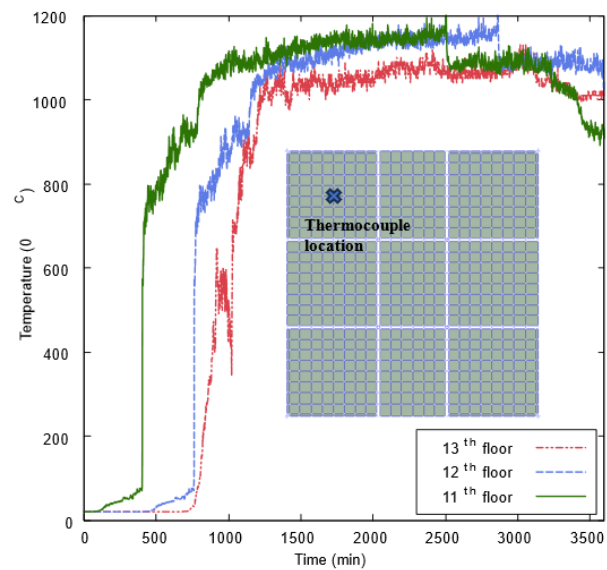


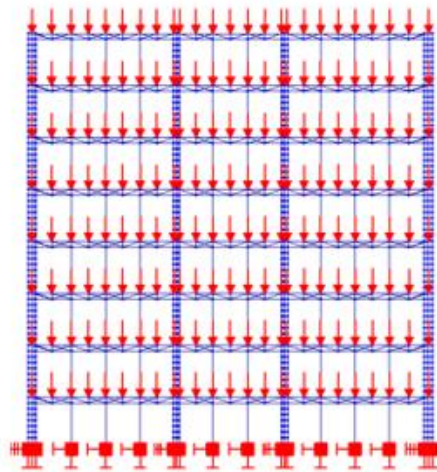
Figure 6.8 Comparison of temperature vs time data of thermocouples on the 11th, 12th and 13th floors.

6.5. OpenSees Modelling

GiD interface (developed by V Papanikolaou at Aristotle University of Thessaloniki, Greece) (Kaounis, 2017) which has pre- and post-processing capabilities, was used to build the model and generate *tcl* script for the OpenSees analysis. For modelling the truss/beam elements *dispBeamColumnThermal* and for the shells *ShellNLDKGQThermal*, element classes of ‘OpenSees for fire’ were used (L. Jiang et al., 2021b; A. Orabi et al., 2019).

In this study, only the top eight floors of the building are considered to reduce the computational load. The fiber section approach is followed while modelling the sections where each Fiber Section object comprises multiple fibres. The *fiberSecThermalobject* class, modified by Orabi et al. (2022), enables the user to apply thermal load at 25 points across the width and depth of the section, which linearly interpolates the temperature values across all the fibres of the section.

The connection between the slab and steel truss system was modelled by rigidly connecting the nodes on the beam and shell elements. The meshing size for all elements ranges from 0.3 to 0.5 m. Steel was modelled using *Steel01Thermal* material class, which uses temperature-dependent properties according to EN 1993-1-2 (Eurocode 3, 2006) carbon steel at elevated temperatures, whereas concrete was modelled using the Concrete Damage Plasticity material model. The fully meshed model consisted of 0.15 million elements of both shells and beams combined. The analysis consumed 30 Gigabytes of RAM while a 4.02GHz Intel Xenon CPU worked at 15% utilisation.



(a) OpenSees model



(b) Plasco tower photo (1960s)

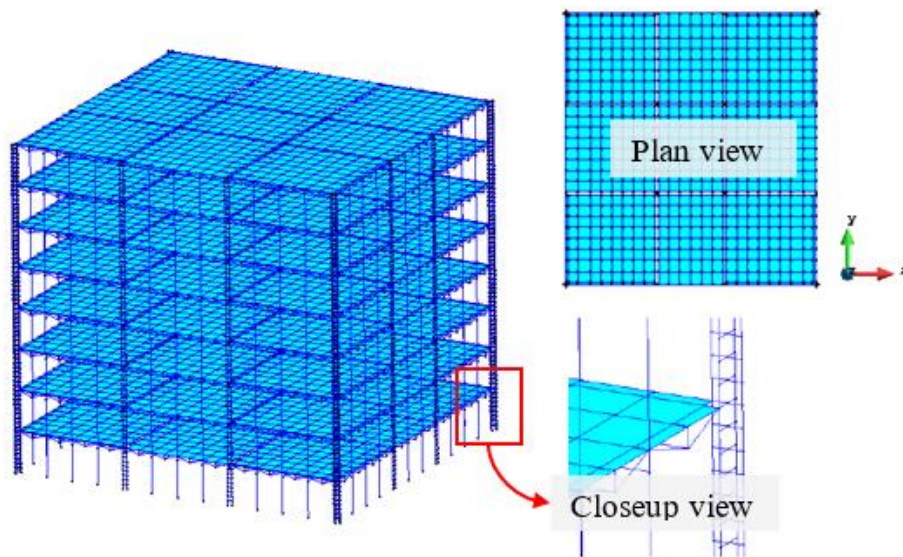


Figure 6.9 Plasco tower model as visualised in GiD+OpenSees interface

6.6. Heat Transfer Analysis

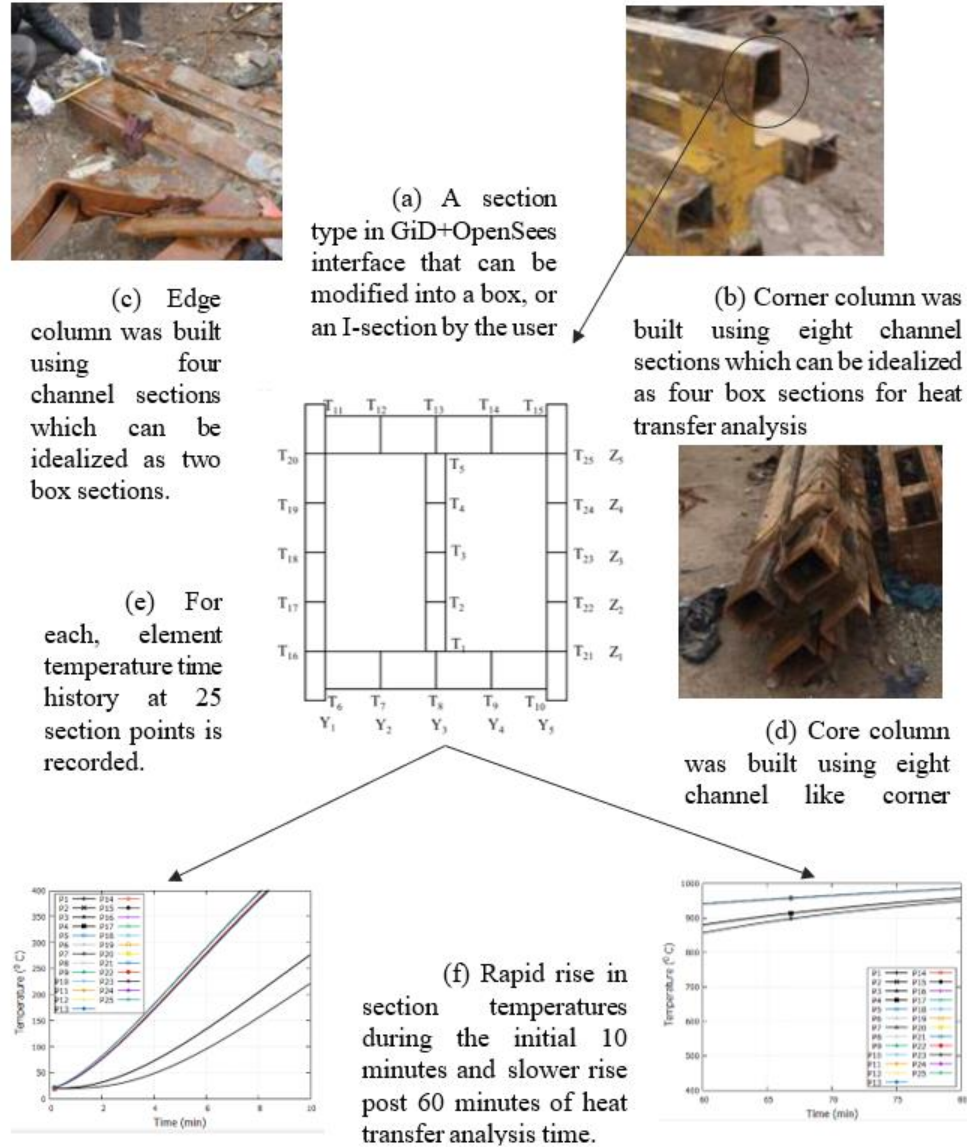


Figure 6.10 (a) Section type available in GiD+OpenSees interface and box sections (b), (c) and (d) of Plasco building.

In the GiD+OpenSees interface, augmented by M. A. Orabi, Khan, et al. (2022) the heat transfer analysis tasks are fully automated, where the HT module of OpenSees is called by the interface without much effort from the user. Firstly, the user needs to select the elements using the GUI of the GiD interface for which heat transfer analysis needs to be carried out. Then, the geometric section details of each element are generated and sent to the HT module in an

automated process. The details of automation work are explained in detail in the PhD dissertation of M. A. Orabi (2022). The section types available in the GiD+OpenSees Interface were modified to suit the heat transfer analysis of Plasco tower structural members. This process generates time-temperature histories for all the structural elements at 25 different locations as seen in Figure 6.10 (a) and written in a file format and input in the next step, thermomechanical analysis.

6.7. Structural response

6.7.1. Response against ISO 834 fire

The thermo-mechanical analysis of the model showed (Figure 6.12) large downward sagging deformations higher than 1000mm; see Figure 6.11(b). The floor deformations were only 50mm downwards when the compartment temperatures were around 600 °C. The deformations continued to increase to 400mm as compartment temperatures reached 780 °C. Beyond 800 °C, the floors experienced runaway failure, reaching more than 1000mm by 850 °C.

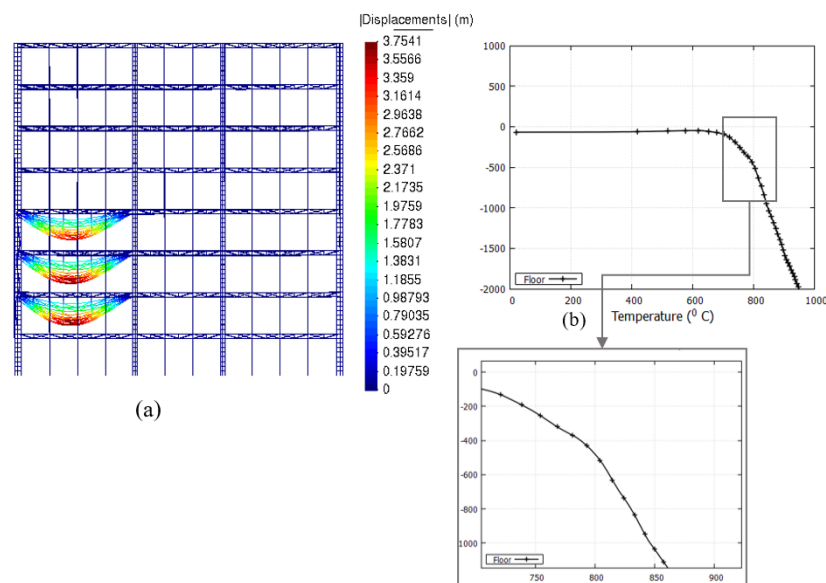


Figure 6.11 (a) Contour plot showing the maximum floor deformations in the corner; (b) plot showing maximum deformation against the compartment temperature.

Dead load analysis of the Plasco tower revealed that each core column transfers 11% of the total building weight to the ground, i.e., all the core columns transfer 44% of the total weight. The core and secondary main columns transfer nearly 65% of the weight. Each corner column transfers only 2% of the total load, as they are not designed for gravity load. They are designed to resist global lateral and twisting forces. The NW corner column, stiffer than the other peripheral columns, underwent a lesser lateral (outward) push in both X and Y directions. The NW corner column experienced a maximum lateral displacement of only 50mm at 600 °C, while secondary columns experienced a lateral displacement of around 120mm at temperatures

of 750 °C, see Figure 6.13(a).

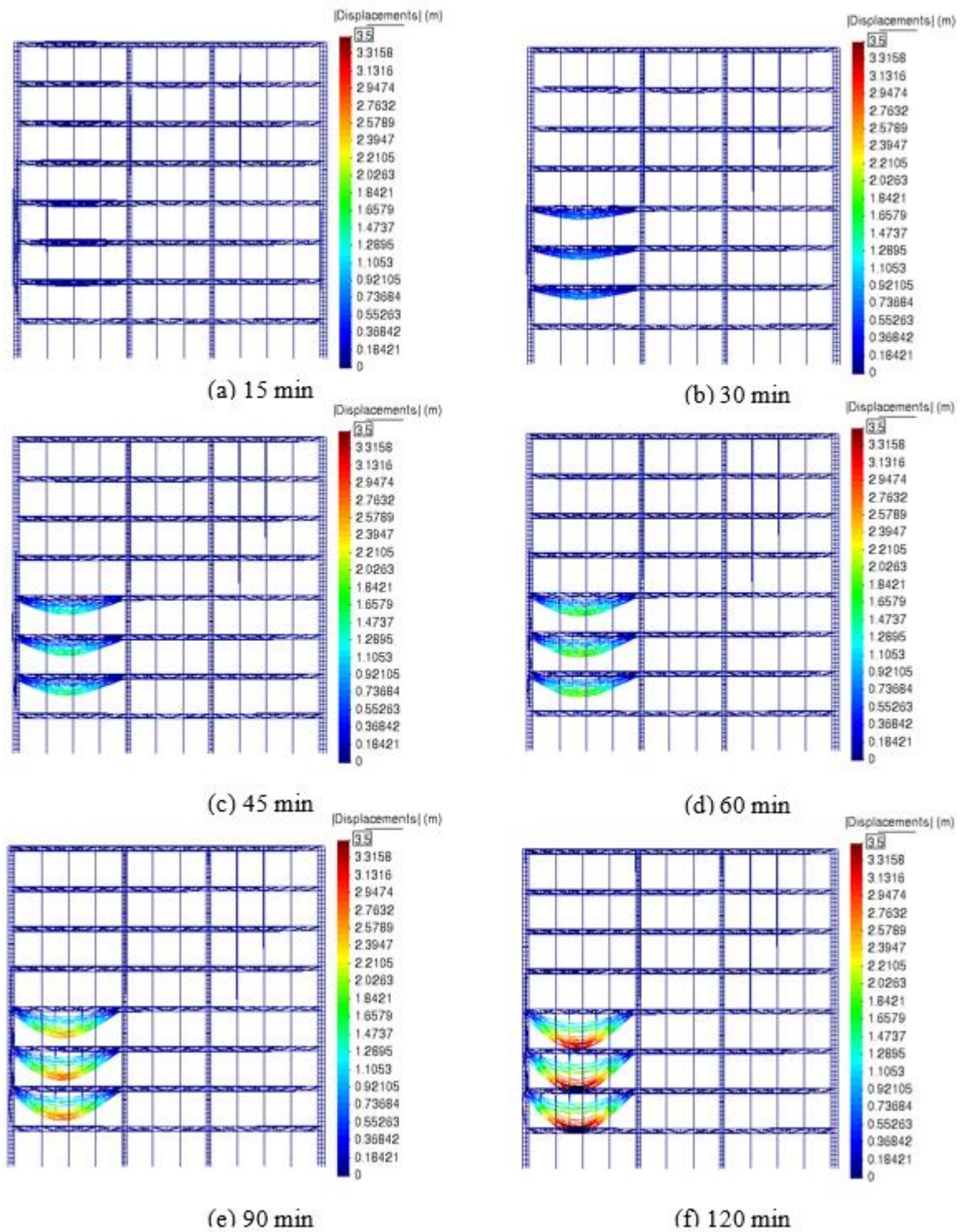


Figure 6.12 Floor deformations in NW corner at different stages of compartment fire; as seen from West to East direction of the building model.

As observed in the previous chapter, the lateral displacement of secondary columns is higher than that of the secondary main columns. This can be explained by the difference in stiffnesses and primary beams undergoing lesser axial expansion due to their relatively colder temperatures. The floor of the Plasco tower in a North-South direction with Vierendeel beams (Y direction in the model, see Figure 6.9) was longer compared to the East-West direction with truss beams. The thermal expansion of the floor is different in both directions. The outward push and then subsequent inward pull forces on the columns are higher in the Y-direction in comparison to the X-direction.

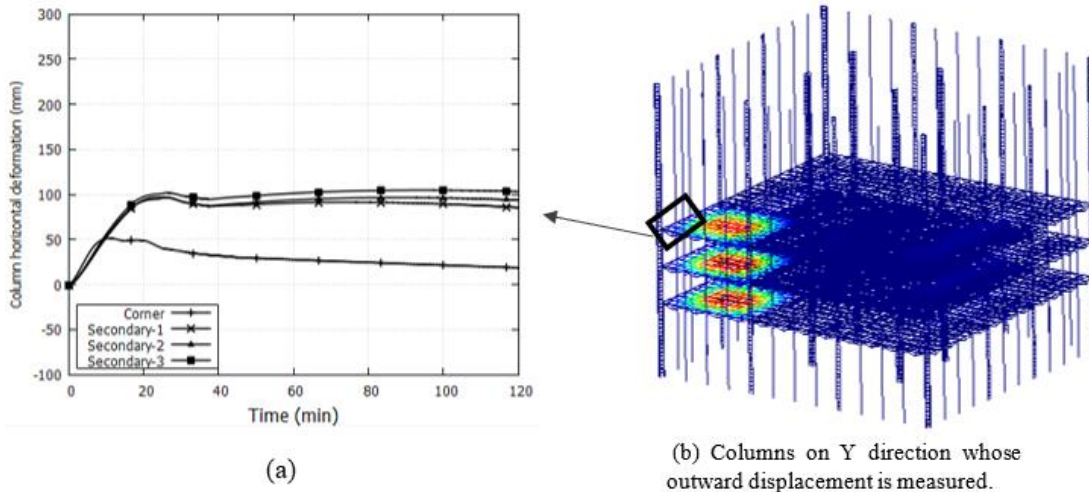


Figure 6.13 (a) Lateral column displacement of Corner column and Secondary columns on North face, as shown in (b) where non-fire floors are hidden for clarity.

The reversal of lateral column displacements occurred when compartment temperatures were between 670 °C and 750 °C, which is reflected in the changing axial forces of Vierendeel beams. It can be seen in the Figure 6.14(a) which shows that the bottom chord, which was initially under tension, started experiencing compression as the floor expanded. The expanding Vierendeel beams started losing strength around the temperature of 670 °C. As a result, large downward displacements occurred, which explains why the bottom chord reverted to tension.

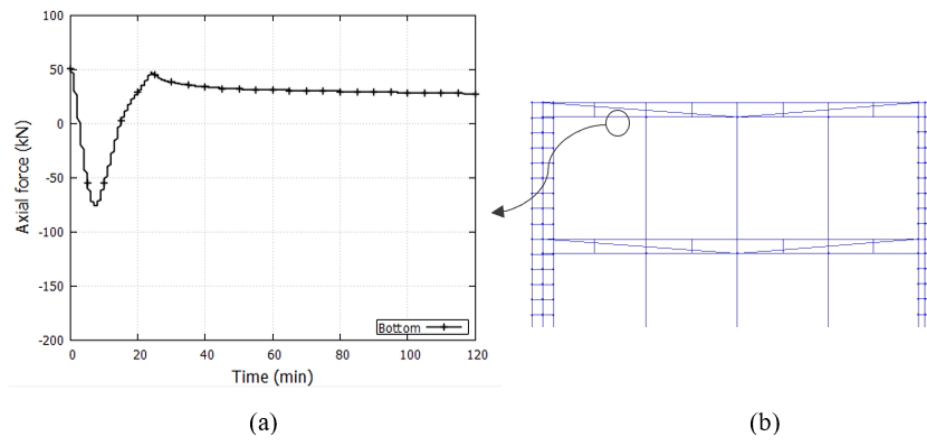


Figure 6.14 (a) Axial force reversal in the bottom chord of the Vierendeel beam; highlighted in (b) a single 10m span of the beam.

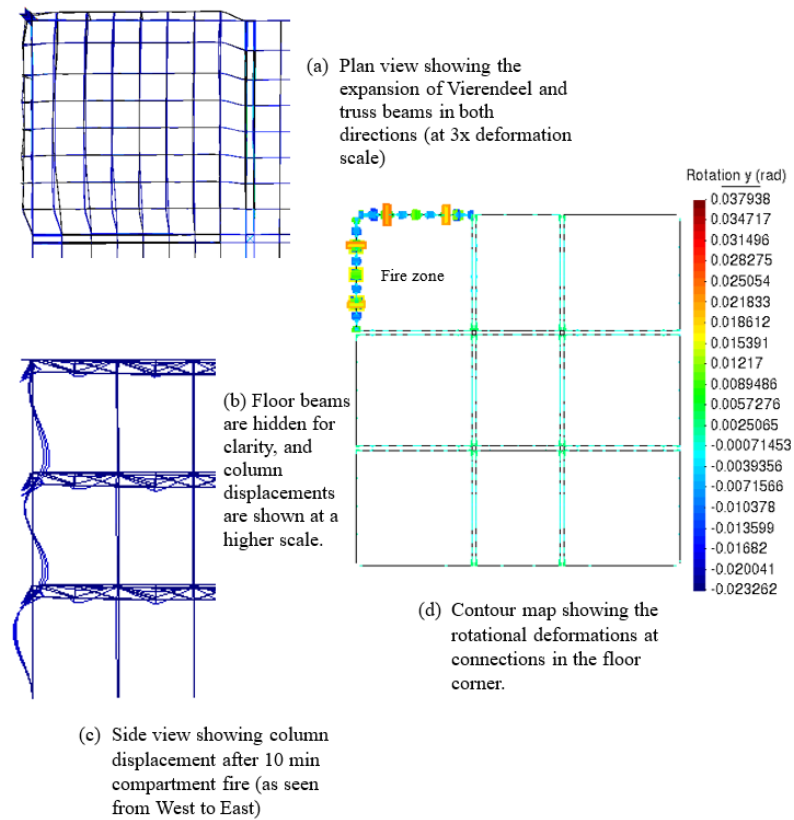


Figure 6.15 Visualisation of expansion of corner beams and rotational deformations at connections.

It is reasonable to believe that large displacement variations in columns, in horizontal and vertical directions, would have damaged the steel connection in the NW corner, thus causing a local structural failure.

In the partial collapse stage, the fire caused three floors of the tower's Northwest corner to collapse due to the failure of connections between the peripheral columns and secondary beams traversing in both directions. The tower remained stable after this corner failure for over an hour. The total collapse took place only after the fire reached critical core areas. Photographic evidence, seen in Figure 6.16, substantiating that the tower was stable with no corner floors present.



Figure 6.16 The photo shows the loss of fire-affected corner floors while the tower still stood.

To simulate this scenario, another OpenSees model is created, see Figure 6.17 in which the fire-affected floors of the corner zone are removed, with only the peripheral columns and edge beams present. The objective of analysing this model is to back-calculate the levels of safe (or unsafe) temperatures that could have been present during and after the partial collapse and to understand the role and behaviour of non-gravity columns under fire. As observed before, the failure of corner floors occurred between 600 °C and 750 °C, and the structural response of columns without floors was analysed after this period. As peak temperatures attained in column members are lower by 400 °C when compared with floor temperatures, their structural response is studied within the temperature range of 300 °C and 600 °C.

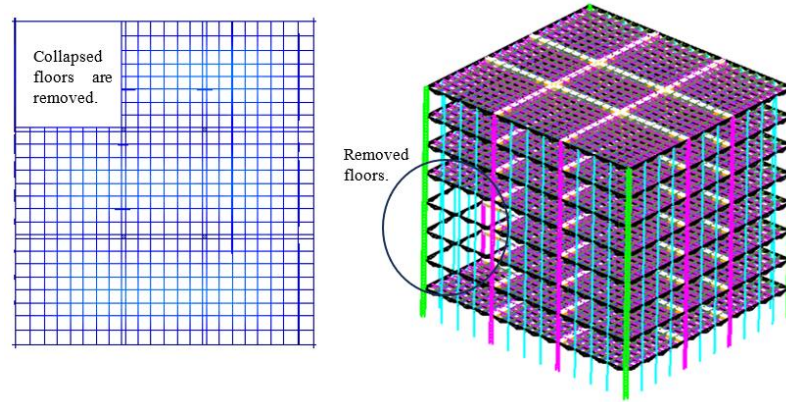


Figure 6.17 OpenSEES model with fire affected floors removed shown in (a) plan view and (b) 3D perspective view.

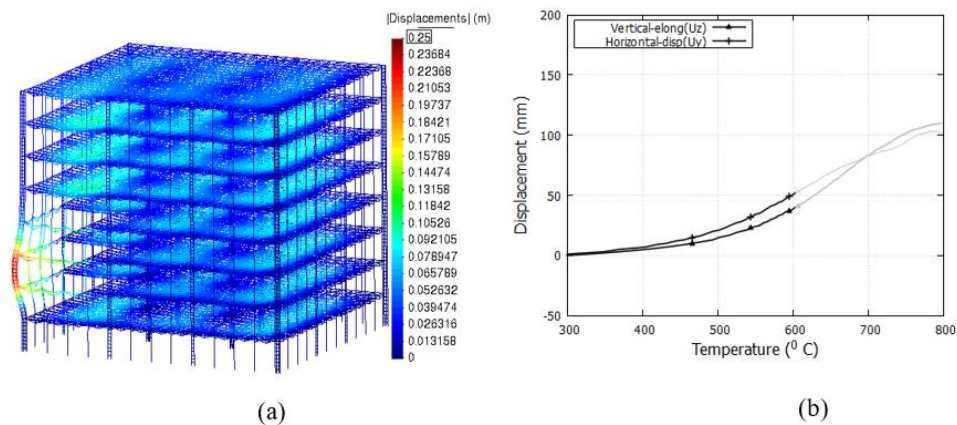


Figure 6.18 (a) Corner column response with collapsed floors; (b) displacement and elongation of the corner column.

The results from the study have shown that the magnitude of deformation experienced by the corner column is around 40-50mm, see Figure 6.18 in both vertical and horizontal directions. From a global stability point of view, these deformations are not critical since the corner columns were not designed to bear gravity loads. As previously discussed, the total gravity load transferred to each corner column is only around 2%. Even if corner columns are exposed to extreme temperatures in local fires, it is not likely that this would cause any instability in the building. Interestingly, the amount of base reaction in the corner column is higher than its service load case reaction. A contour plot showing base reactions of all columns,

see Figure 6.20(b) compares the base reaction of the fire-affected corner column and the other three corner columns.

The fire-affected span of the corner column experienced outwards displacements in both X and Y directions as the rest of the structure provided strong restraint.

After the partial collapse of the corner floors, the 10.2m long span of the corner column is relatively less restrained laterally. The same can be said about other peripheral secondary columns, but they did not attract larger redistributed loads because of their smaller cross-sectional areas. This increase in effective length should reduce the buckling load-carrying capacity of all the fire-affected columns. In the case of the Plasco building, all columns are designed as built-up box sections joined together with battens, as shown in Figure 6.19(b); the strength quality of welding of these battens (steel members used to hold together individual members) adds to the complexity of assessing their buckling strength, which is not the focus of this study.

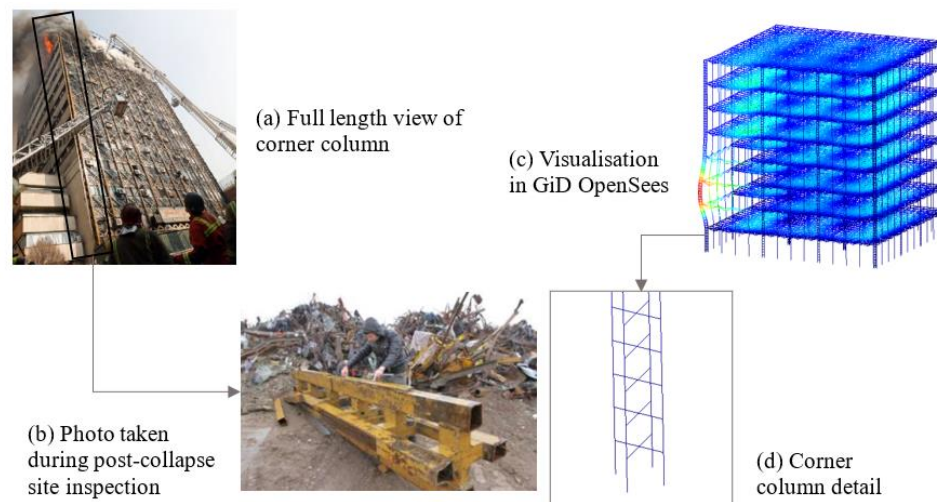


Figure 6.19 Post-collapse photo and computational model of the corner column

As the temperatures in the column increased to 600 °C, the outer box members are seen experiencing tension forces and the inner box members compression forces over the entire span of 10.2m, as seen in the Figure 6.20(a) and (b). Unlike rolled steel sections acting monolithically as a single member, built-up sections may not behave as a single unit at elevated temperatures.

The corner column did not affect global stability. Still, the same could not be said about central core columns, which are also built up similarly and heated to higher temperatures at the

later stages of the fire. At advanced stages of fire spread, floors surrounding the core column in the Southeast direction have collapsed. Under such conditions, the response of core columns and their expected resistance to fire-induced forces in a single monolithic fashion is worth exploring in much more detail.

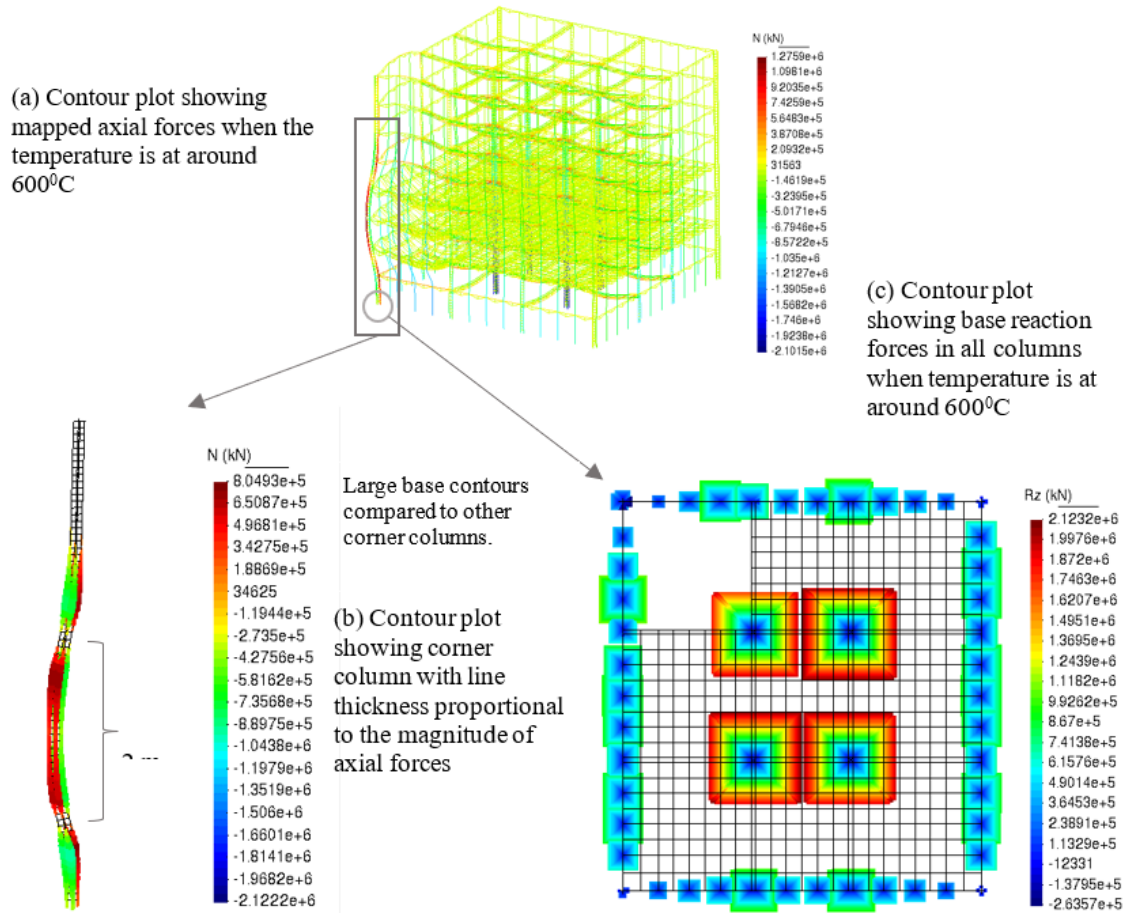


Figure 6.20 Visualisation of corner column response under fire

6.7.2. Effect of composite floor action

In the previous analysis, the composite action is assumed absent owing to the age of the concrete and the lack of information about the floor system. In an actual structure, a slab changes the simple expansion of steel beams to bowing deformation irrespective of the amount of composite action present. Therefore, an OpenSees model for analysing the composite floor response in the Plasco building has been created.

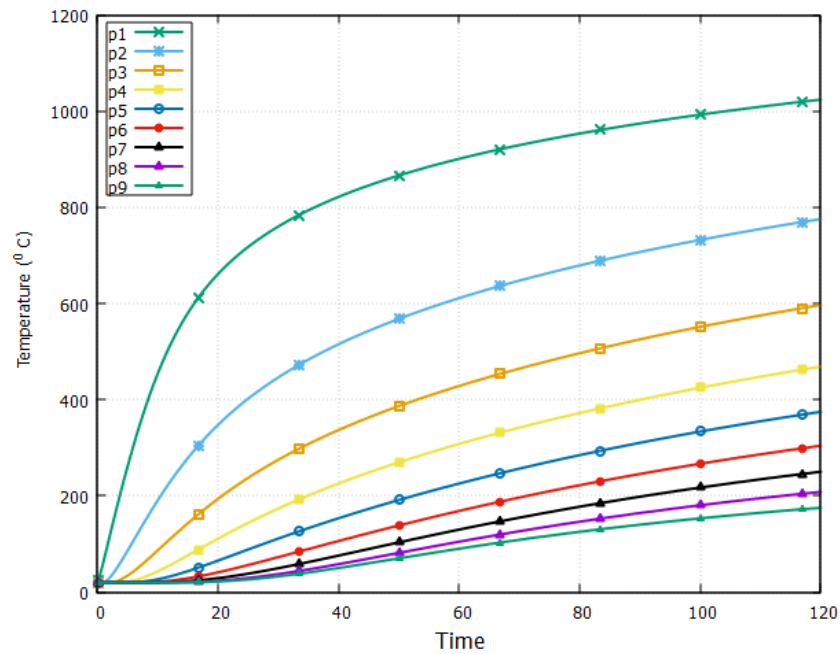


Figure 6.21 Temperature gradient across the slab section

In this study, slabs are modelled using the nonlinear shell element class *ShellNLDKGQThermal* (L. Jiang et al. (2021c)) and concrete material using the Concrete Damage Plasticity model (CDP) available in the OpenSees library, see

Table 15. A concrete slab of 120 mm thickness with reinforcement of 12mm diameter bars spaced at 100 mm in both directions is considered. In this study, the standard fire curve was used for HT analysis to estimate the thermal gradient across the slab section; the output of HT analysis can be seen in the Figure 6.21. A drawback of the model is that it assumes complete composite action of the floor, which may not be realistic in the case of a 55-year-old Plasco building. It is likely that the realistic response of the floor lies somewhere in between fully composite and non-composite floor response. Therefore, this study forms the case of one extreme response envelope.

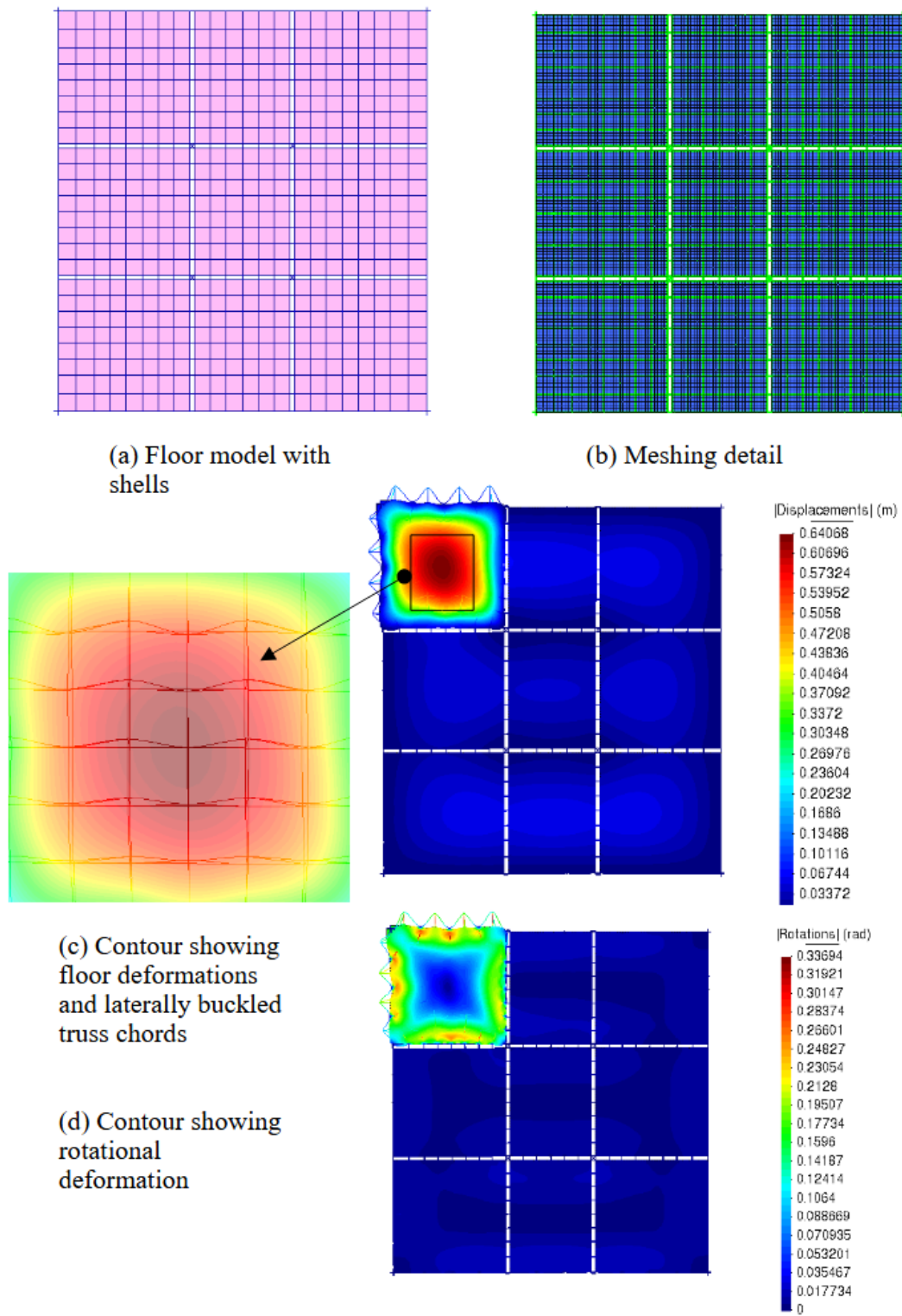


Figure 6.22 Slab detail and simulation response to the standard fire

Table 15 Concrete material properties

CDP Material properties	Value	Units
Modulus, E_c	1.5e+10	N/m ²
Poisson's ratio, ν	0.2	
Tensile strength, f_t	2.2e+06	N/m ²
Compressive strength, f_c	2e+07	N/m ²
Fracture energy (tension), g_t	1452	kg·m ² ·s ⁻²
Fracture energy (compression), g_c	120000	kg·m ² ·s ⁻²

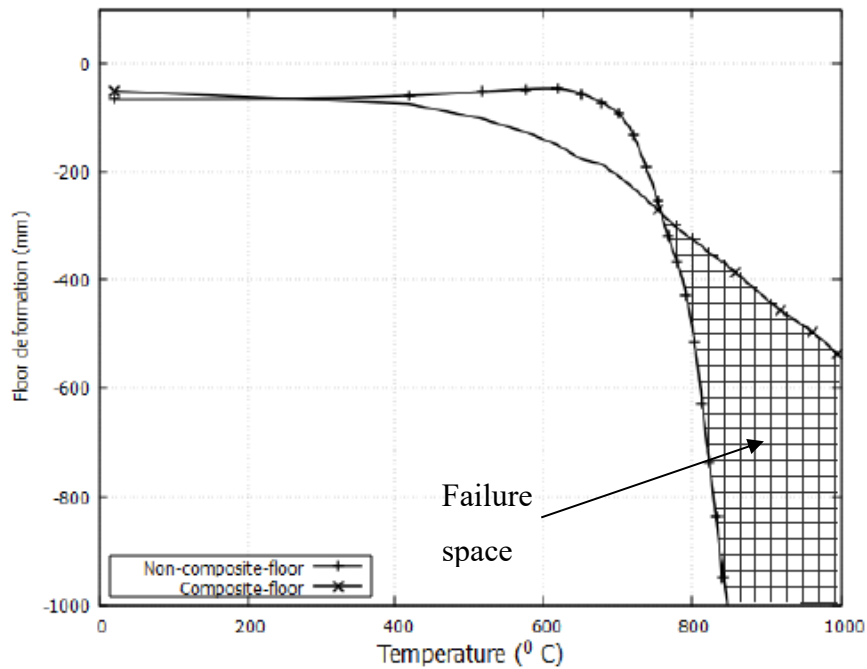


Figure 6.23 Plot showing maximum floor displacement (centre of the floor slab) with and without composite action.

As expected, the analysis showed that the composite action of the slab resulted in lower floor displacements than the non-composite floor model. For comparison, maximum floor displacements of composite and non-composite floors are plotted together, where non-composite floors experienced runaway failure at temperatures of 650 – 700 °C, while

displacements in the composite floor model increased gradually. At 600 °C, the maximum displacement in the non-composite floor is around 40mm, whereas the composite floor experienced nearly three times higher 135mm displacement due to thermal bowing. By the end of the analysis, the maximum displacement observed in the composite model is 640 mm (nearly 10% of the span length), see Figure 6.22 (c) and Figure 6.23. It can be reasoned that a realistic failure space would exist somewhere between the full composite and non-composite response. Based on the studies carried out so far, it is proposed that the local floor failure in the Plasco building started with thermal bowing, which initiated the buckling of truss members, see Figure 6.22(c). This, combined with a partial composite action, would have caused significant downward displacement, exerting critical rotational strains on the connections between trusses and Vierendeel beams with peripheral columns, leading to local failure.

In the next stage of this research work, thermal load will be modelled after HT analysis using CFD-based data. As accurate information on the reinforcement details is unavailable, a sensitivity study on floor response by varying the steel reinforcement parameters is required.

6.7.3. Response against CFD-based thermal load

Unlike the previous study, where only the corner floor segment was subjected to the thermal load, in this case, the fire load was modelled to cover adjacent areas, representing the actual case.

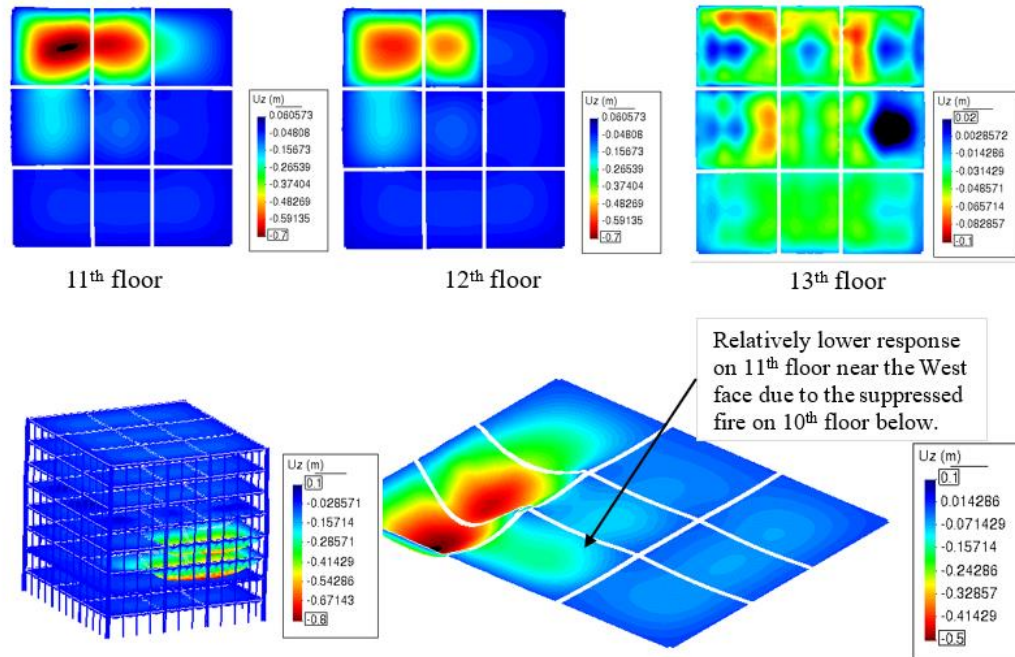


Figure 6.24 Deformation contour maps of the 11th, 12th and 13th floors.

The thermomechanical response predicted the failure of nearly 67% of the NW floor area on the 11th and 12th floors of the building, see Figure 6.24. The deformations observed in the region on the 11th and 12th floors of the structure are more than 600mm. Deformations of 205mm and 110mm are noticed on the West and interior regions of the 11th floor, respectively. This is because the fire that started on the 10th floor NW corner moved westwards and was quickly suppressed due to easy reachability (externally) for firefighting. The North face of the tower was not easily reachable; hence, the region saw quick fire growth and spread.

The failure of the 11th floor marks Event 8, as shown in the established fire timeline used for this study. Events 9 and 10 occur after the failure of the 11th floor (Event 8), and both involve significant damage on the 13th floor. In this exercise, the deformation contours showed only the arrival and fire spread on the 13th floor, but did not show deformations of comparable

scale. Therefore, an investigation is carried out into the FDS and HT analyses done on the 13th floor. It was realised that there is a need to recalibrate the temperature input on the 13th floor by managing the cooling part of the temperature vs time data of thermocouples. This study focuses on the first and second collapse (till Event 9), where a reduction in temperatures due to cooling was not an issue, as fire in this zone re-emerged even after initial suppression and persisted till the first collapse.

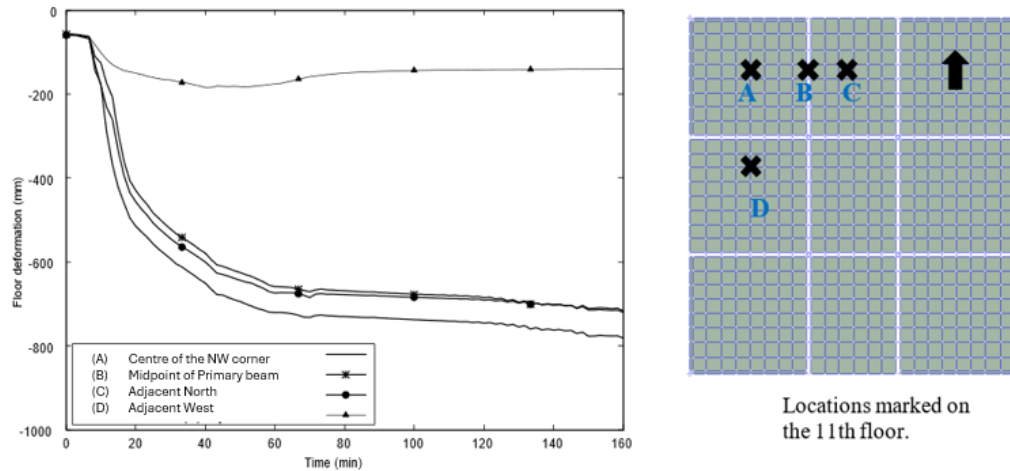


Figure 6.25 Plot showing deformations at different locations on the 11th floor.

The deformations on the 11th floor at different locations, see Figure 6.25, show the failure of the NW corner and the adjacent area on the North side. The adjacent side on the West shows relatively lower deformations (200mm). The thermomechanical response indicating the failure of 2/3rd of the North side of the 11th floor agrees well with the visual evidence, thus proving the accuracy of the fire modelling. The fire load on the 13th and remaining floors (14-16) should be calibrated before analysing Event 9 and Event 10.

In the second study, only a limited number of thermocouples are positioned at various locations to monitor thermal gradients on each floor. However, the structural model used in Chapter 7 will use detailed data from CFD, increasing the resolution of thermocouples on all floors to capture the structural response more accurately. Fire will be calibrated for the upper floors (13th floors and above) to simulate the structural response of Event 10. Using the data from all fire simulations, the progressive collapse of the building will be simulated with respect to the travelling fire phenomenon.

6.7.4. Comparison of the response against ISO 834

Based on the results observed, it can be noted that the maximum displacement of the corner floor calculated using the CFD-based fire simulation is not significantly different from the outcome estimated by the fire based on the standard ISO 834 curve. The first analysis carried out using ISO 834 predicted a maximum displacement of around 640mm (Figure 6.24) by the end of the analysis, while the CFD-based analysis showed a maximum displacement of 600mm in the centre of the NW corner floor (Figure 6.23). Visual evidence indicated that the upper floors in the northwest (NW) corner of the building were already engulfed in intense fires before the commencement of firefighting operations, see Figure 6.1. Both the ISO 834-based fire and CFD-based simulations showed maximum temperatures exceeding 800°C. The similarity in response can be attributed to the extensive spread of the fire in the northwest corner.

During the actual incident, the fire persisted for 2 hours and 50 minutes in the NW corner section of the Plasco tower before the partial collapse. CFD analyses indicate that peak temperatures were observed between 60 to 80 minutes after the fire started; see Figure 6.6, with temperatures gradually decreasing as the analysis continued. In contrast, the standard fire curve does not account for the cooling phase and is thus unable to simulate the effects of a cooling-stage fire on the structure. Hence, it can be concluded that the reason for the similarity in response is mainly due to two reasons...

- (a) The whole NW region was considered to be affected by the fire.
- (b) The region was severely affected by very high temperatures, where steel lost its strength significantly.

However, this scenario differs in other areas of the tower. The extent of fire spread in these regions, and the observed peak temperatures, vary significantly. For instance, on the west and southwest sides of the tower, the fire spread is less pronounced compared to the southeastern corner. Referring back to the OpenFIRE chapter (Chapter 5), see Figure 6.26, it becomes apparent that structural damage predominantly took place in the southeastern corner, where the final collapse was initiated.

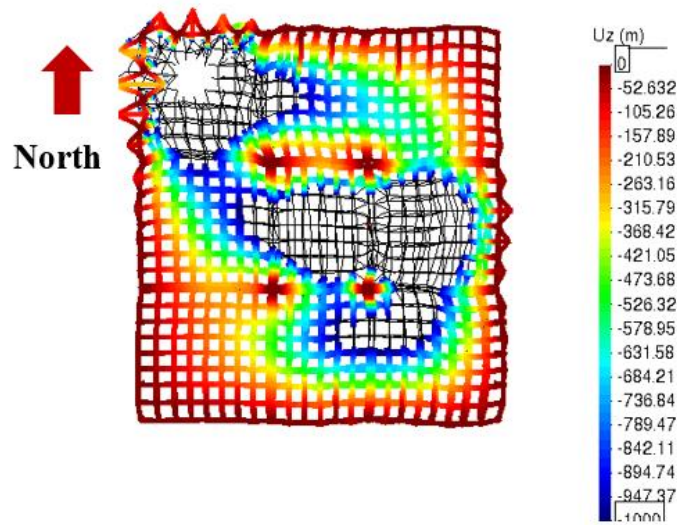


Figure 6.26 Structural damage on the 13th floor

As observed by Khan (2022a), the fire intensity on the 13th floor of the Plasco tower surpassed that of all other fires recorded in the building. Conversely, the fire on the western side was brief due to the effective firefighting carried out by the firefighters. Therefore, in the CFD simulations, the modelling of fire intensity and spread considered the limited duration of the fire in the western area. The fire spread varied across different floors of the building. The fire mainly affected the northwest corner and partially extended to the adjacent sections on the 11th and 12th floors. On the 14th floor, the fire spread resembled that of the 11th and 12th floors, but with elevated temperatures in the core region. Similarly, the extent of fire spread on the 13th, 15th, and 16th floors was comparable, with the 13th floor experiencing higher fire intensity.

Given the diverse extent of fire spread and varying fire intensities on different floors, relying on a thermal load based on ISO 834 for a comprehensive analysis is not a reasonable approach. Each fire incident in the tower exhibited a unique peak temperature occurrence. For example, the fire in the northwest corner has entered the cooling stage, while the fire in the southeastern corner on the 13th floor and above is in the growing stage. In the comprehensive multiple-floor analysis detailed in Chapter 7, CFD-based fire spanning the 3-hour and 20-minute duration of the fire event is employed.

6.8. Conclusions

The first analysis, which used ISO 834-based fire at three different floor levels, gave insights into how the location of fire load geometry affected structural response, leading to partial collapse. The second analysis used realistic thermal loads based on the CFD analyses. Based on these two analyses, the following conclusions can be drawn.

1. Both studies demonstrate that integrated simulation is necessary for the forensic simulation of structural collapses in fire, systematically considering the fire through FDS, followed by heat transfer and thermo-mechanical analysis through OpenSEES.
2. It was reasoned that floors expanded under elevated temperatures until 600°C, pushing the external columns outwards. After the runaway failure of Vierendeel and secondary beams is seen, connections of the beams experience large strains, potentially leading to the local partial collapse of one floor over the other, leaving three levels with no floor beams.
3. The study highlights the dangers of using built-up sections, as it is not easy for engineers to accurately calculate the thermal history and, therefore, the magnitude of forces (and force reversals) in structural members under fire loads. It was seen that battens nearly 400mm in length may compromise the expected monolithic behaviour of steel columns.
4. The study showed that despite the failure of the corner zone, elevated temperatures in all peripheral columns in the NW part of the frame are not detrimental to global stability. It is likely that the core columns were not severely affected by the fire for the first two hours of the incident.
5. The simulation using the composite model showed the possibility of lateral buckling of truss members, which can further weaken the flexural capacity of the floor.
6. The second study demonstrates the integration between FDS, the HT module, and the thermomechanical analysis module of OpenSees. Multiple floor fires involving the 11th, 12th, and 13th floors of the Plasco tower are simulated using the thermal data acquired from the FDS. This study used a low-resolution thermocouple distribution, and the model accurately predicts the response of the 11th floor to fire, i.e., the arrival of Event 8, numerically.
7. Vertical and horizontal fire spread is presented using FDS, where vertical fire spread

provides the arrival time of the fire on the upper floor, which eventually introduces a delay in the timescale of thermal-mechanical response. Thermal data is transferred from the FDS to OpenSees to conduct heat transfer and structural analyses.

8. The simulations show that the West side of the 11th floor did not see runaway failure like the North side, so the fire modelling and thermal load application were reasonable. In the next chapter, higher-resolution thermal data will be utilised for each floor, and additional events, such as the second collapse and progressive collapse, will be analysed using the methodology outlined in this paper.
9. However, using an ISO 834-based curve may suit an analysis where temperatures are relatively the same over a large area, like in the NW corner of the Plasco tower fire. The scale of the structure is such that the fire in the northwest corner had transitioned to the cooling phase, whereas the fire in the southeastern corner, specifically on the 13th floor and above, was still intensifying. Due to the diverse extent of fire spread and varying fire intensities on different floors, a full-scale thermo-mechanical analysis requires CFD-based fire.

Chapter 7: Collapse Simulation of the Plasco Tower

7.1. Introduction

This chapter examines the in-depth structural assessment carried out using the thermal load obtained from the extensive CFD analysis. This thermo-mechanical evaluation applies the entire 3 hours and 20 minutes of thermal load on the multi-storey finite element model. Throughout this evaluation, a significant volume of thermal data was generated and transformed into a compatible format to achieve the desired full-scale CFD-FE connection. Further elaboration on this linking approach is provided in the subsequent section, which details the volume of data and its flow. The conclusions drawn from the analysis and the knowledge acquired from the modelling procedures in chapters 4, 5, and 6 are utilised in this investigation.

In Chapter 5, an integration methodology utilising OpenFIRE software was implemented to conduct a comprehensive thermo-mechanical evaluation. Although the coupling process was successful, it posed challenges, requiring a substantial user effort for complex structures. The coupling methodology detailed in Chapter 6 addresses the challenges encountered in previous chapters. This research showcased a seamless integration of CFD and FE models, which is particularly beneficial for analysing tall building structures.

Drawing from the insights obtained from examining substructures that represent the Plasco tower—specifically, a single floor in Chapter 5 and multiple floors in the northwest corner in Chapter 6—Chapter 7 endeavours to conduct a comprehensive analysis of the entire multi-storey structure. This investigation centres on an 8-floor model featuring composite steel and concrete construction across all levels, incorporating intricate heat transfer and structural analyses.

7.2. Objectives of the chapter

The study aims to achieve the following objectives:

1. Showcase the effective use of open-source tools—FDS and OpenSEES—for forensic investigations into structural collapses caused by fire.
2. Tackle the challenges of scale differences when integrating CFD and FE models.
3. Conduct an elaborate structural analysis of the Plasco tower model and propose collapse hypotheses elucidating the factors contributing to the collapse.

7.3. CFD-FE coupling scheme

Achieving simpler and more efficient coupling between CFD and FE models in an ideal scenario necessitates identical attributes such as scale, geometry, and orientation. While maintaining such uniformity is feasible for smaller structures, it becomes computationally inefficient for larger structures like the Plasco tower, which spans 29x31m in plan view and 60m in elevation. Given that the fire affected the top six floors of the tower, the scale of the FE model was reduced by 50% by modelling the upper eight floors of the 16-storey building in OpenSEES. However, creating a CFD model encompassing all six fire-affected stories is impractical due to the extensive efforts and computational expenses involved. Hence, only a single floor of the CFD model is modelled.

7.3.1. FE model

The finite element (FE) model utilised in the study comprises 102,000 nodes and 147,000 finite elements, incorporating shell and beam elements. The dimensions of the model are 29.5 x 31.0 meters in area and 30.4 meters in height. The FE model has 17 different types of steel sections and a concrete slab.

7.3.2. CFD model

The investigation involved analysing six distinct fire scenarios using a single CFD model calibrated and detailed in Chapter 4. For additional insights into the calibration process, it is recommended to refer to the PhD thesis of Khan (2022b).

7.3.3. Coupling

Within the GiD+OpenSees interface, users are tasked with specifying the structural elements to which thermocouples should be linked. Each finite element that requires thermal load

is assigned a unique thermocouple with an individual identification tag. This identification tag serves as a crucial attribute for generating FDS-compatible thermocouples. For example, if a beam element in GiD is associated with a thermocouple bearing an identification tag (ID) of 36, the thermocouple location is then exported to the FDS model, leading to the retrieval of temperature time histories for the corresponding FE element stored in a file named FDS36.dat. This process is fundamental to the coupling framework, facilitating the extraction of detailed thermal loading data.

In the multistorey finite element model, the number of nodes and finite elements on each floor remained constant, leading to consistent node and element numbering sequences across all floors. For example, if each floor of an FE model consisted of n nodes. Consequently, node one on the first floor, node $n+1$ on the second floor, node $2n+1$ on the third floor, and so on share identical x and y coordinates, with only the z value varying between floors. This same numbering pattern applies to the finite elements as well. As a result of this repetitive floor layout, the numbering of thermocouples remains uniform throughout all floors. To simplify user efforts, thermocouples are assigned to one floor of the finite element model at a time. This approach enables the creation of a thermocouple list tailored for export to the relevant FDS analysis model. A visual representation of this approach is provided in Figure 7.1 for clarity.

Floor number	Thermocouple script for FDS
11	&DEVC ID = '1', QUANTITY='TEMPERATURE', XYZ=10.5,1.45,11.2/
12	&DEVC ID = '1', QUANTITY='TEMPERATURE', XYZ=10.5,1.45,15/
...	...
16	&DEVC ID = '1', QUANTITY='TEMPERATURE', XYZ=10.5,1.45,30.2/

Table 16 FDS-compatible script for thermocouple ID 1 across multiple floors

In this study, six identical multi-storey finite element (FE) models were created specifically for performing heat transfer analyses, as illustrated in Figure 7.1. Thermocouples within each FE model were assigned to the FE elements on a single floor, from the 11th to the 16th floor.

Consequently, six sets of thermocouple lists were generated in GiD software in a format compatible with FDS. As mentioned, six distinct fire scenarios were evaluated using a Computational Fluid Dynamics (CFD) floor model after placing the thermocouples imported from these lists. Each list contained 4307 thermocouples with identical ID, x, and y coordinates, while the z values varied among the six sets of thermocouple lists, as detailed in Table 16. The temperature-time profiles obtained from each CFD model were utilised for conducting heat transfer analyses within the corresponding heat transfer FE models, as shown in Figure 7.1. Subsequently, the results from the individual heat transfer FE models were applied as thermal loads in a consolidated multi-storey FE model to facilitate thermo-mechanical analyses.

The uniform geometry between the Finite Element (FE) and Computational Fluid Dynamics (CFD) models on a single floor was leveraged in the coupling strategy adopted for this research. This method notably reduced the computational costs linked to CFD analyses while upholding the required thermal load resolution across all floors. A smooth integration of CFD and FE models was efficiently achieved by utilising the identical FE model for both heat transfer and thermo-mechanical analyses. Consequently, in scenarios where the structure under examination is compartmentalised and exposed to a stationary fire, additional reductions in the size of the CFD model can be implemented to enhance computational efficiency.

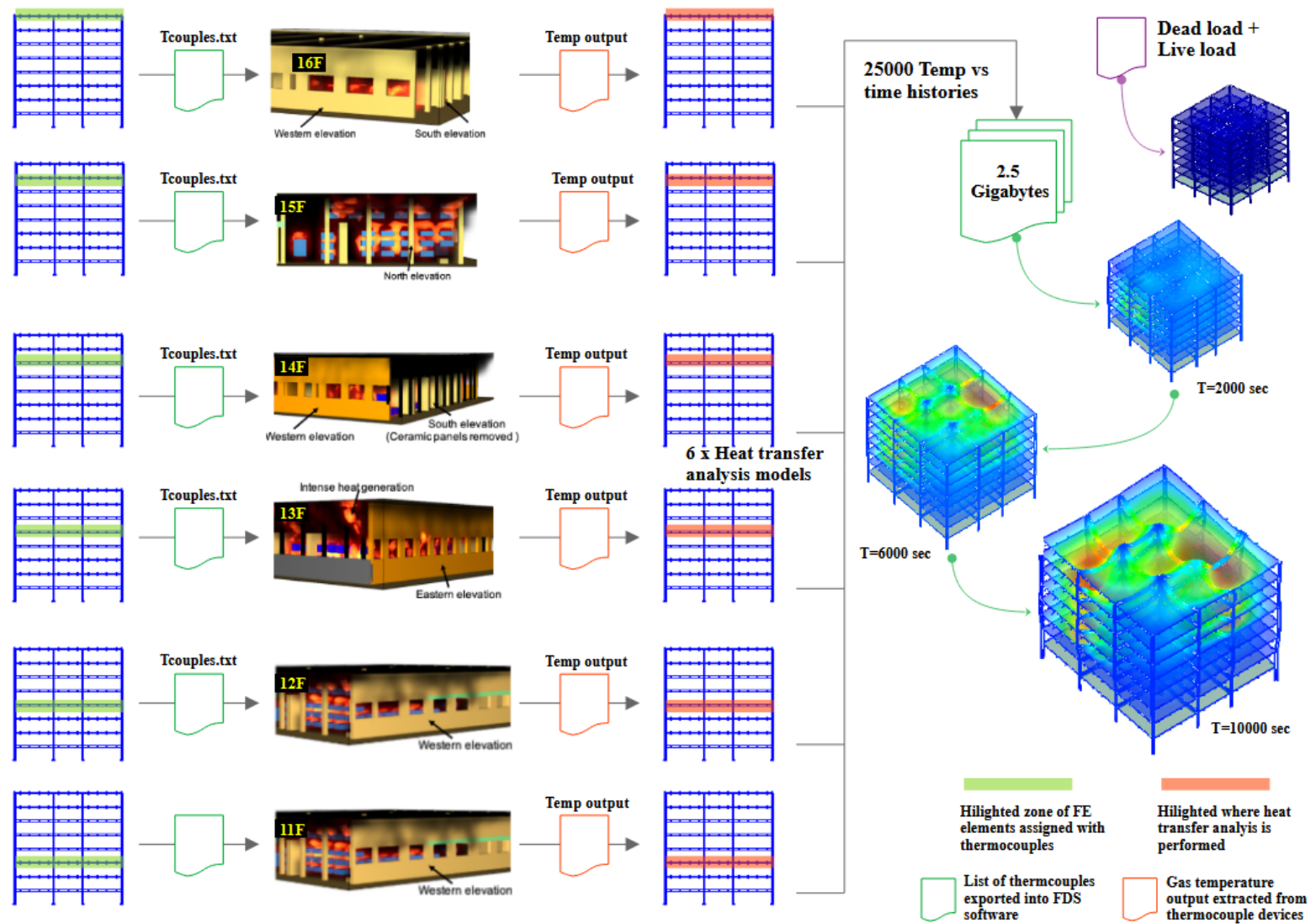


Figure 7.1 Coupling scheme employed in the study

7.4. Analysis parameters

In this study, six cases of CFD analyses, six sets of heat transfer analyses, and one case of thermo-mechanical analysis were performed. This section outlines the key analysis parameters used in these analyses.

7.4.1. Heat transfer analysis

The output from each CFD model generated temperature-time histories at 4307 locations. Temperature readings were recorded at intervals of every 10 seconds ranging from 0 to 126,000 seconds, equivalent to 3 hours and 20 minutes. In the heat transfer analysis, the temperatures in the steel cross-sections were computed at every 10-second interval. Initial attempts using intervals of 20, 50, and 100 had convergence issues, leading to the adoption of the 10-second interval for accurate calculations.

7.4.2. Thermo-mechanical analysis

Thermo-mechanical analysis was conducted in two stages—first with dead and live loads and then with thermal loads. The dead load was applied in 10 steps, each with a load factor of 0.1 per step. The *UmfPack* solver was utilised for both stages to construct a sparse system of equations in OpenSEES. For the dead + live load step, the *ModifiedNewton* algorithm was employed, while the *KrylovNewton* algorithm was used for the thermal load step.

The dead + live load analysis was performed as a simple static analysis. In contrast, the thermo-mechanical analysis was performed as a transient static analysis without dynamic effects across 200 steps. Each step had a time increment of 63 seconds, resulting in a total analysis duration of 12,600 seconds (equivalent to 3 hours and 20 minutes). A maximum of 100 iterations was allowed per step. The outcomes of this study will be discussed in detail in the subsequent sections.

7.5. Preliminary evaluation of thermal response

The simulation results demonstrated significant downward displacements on all six floors affected by the fire. The most substantial floor displacement observed in the simulation occurred on the roof or ceiling of the 15th floor (sometimes referred to as the 16th floor for convenience). This was attributed to the columns supporting the roof being less laterally restrained compared to columns on other floor levels, see Figure 7.2.

The displacement patterns on the 11th, 12th, and 15th floors were similar due to comparable fire spread conditions. In contrast, the displacement patterns on the 13th, 14th, and 16th floors were more severe, particularly near the northwest (NW) and southeast (SE) corners of the tower. These distinct displacement trends across the different floors were a result of varying levels of lateral restraint and fire impact, highlighting the complex interplay between structural elements and fire effects in the simulation. In this section, displacement contours are provided at regular intervals to illustrate the magnitude of downward displacements across different floors, denoted as U_z in meters.

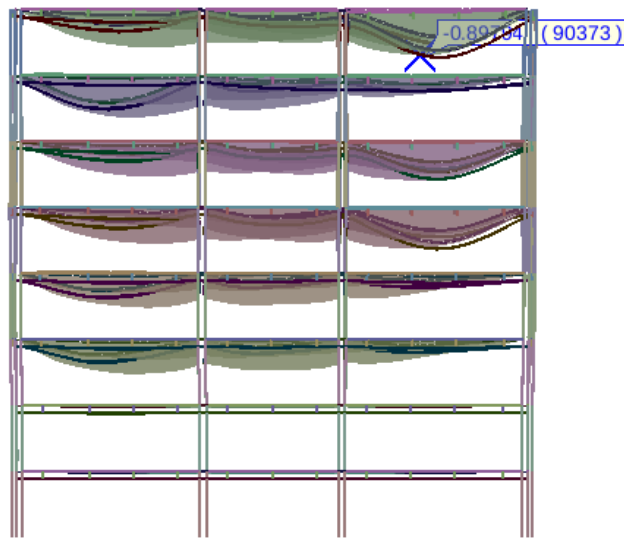


Figure 7.2 Deformation showing the location of maximum floor displacement (South elevation) by the end of the analysis

7.5.1. 16 minutes after fire initiation

At 1000 seconds into the fire, roughly 17 minutes after the fire initiation, the maximum displacement of nearly 420 mm was observed on the 11th floor (or the ceiling of the 10th floor), as shown in Figure 7.3. By this time, the fire had spread to the 11th floor, resulting in approximately 220 mm displacement on the 12th floor, as depicted in the contour of the 12th floor. The other four floors above remained unaffected at this point in time.

During this period, firefighters were not yet present at the scene, and a rapid progression of the fire was noted, exacerbating the structural displacements on the affected floors.

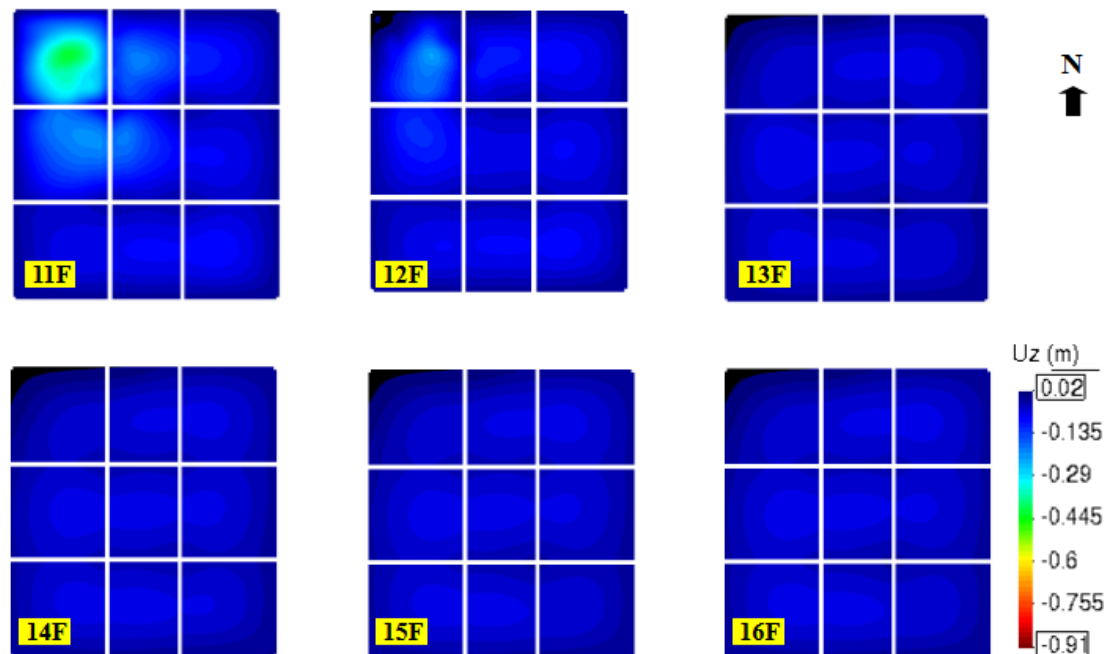


Figure 7.3 Vertical floor displacements at $t=1000$ sec (17 min)

7.5.2. 33 minutes after fire initiation

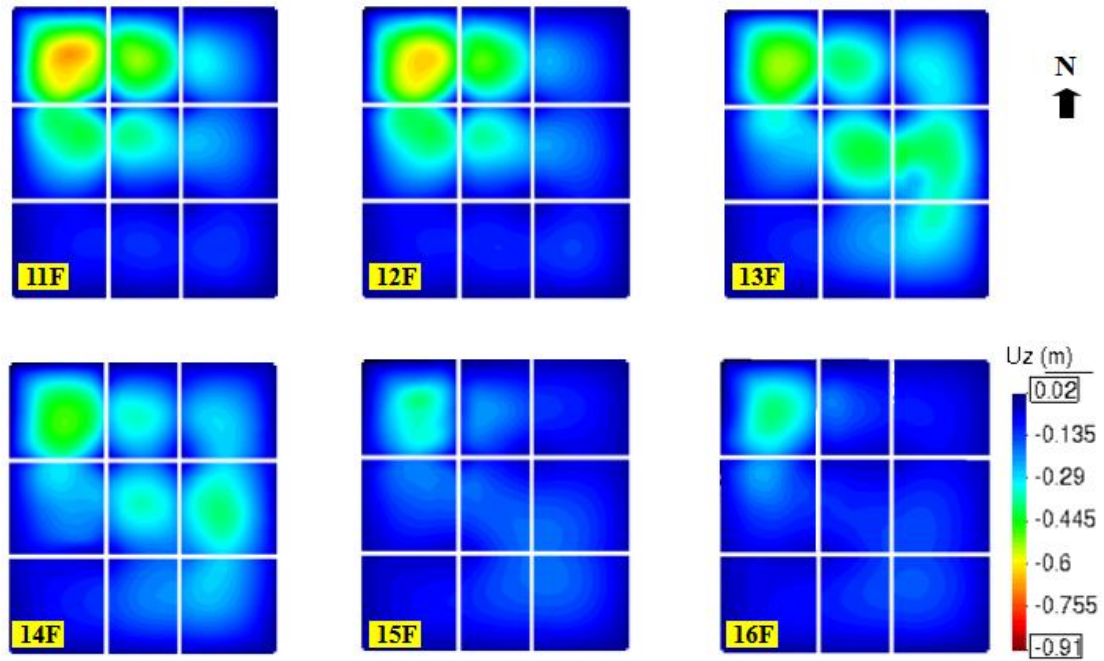


Figure 7.4 Vertical floor displacements at $t=2000$ sec (33 min)

Around this time, the fire had vertically travelled multiple floors in the northwest (NW) corner of the tower. Due to a substantial delay in commencing firefighting operations, the fire had already extended to the upper levels. Upon the arrival of the initial responders at the Plasco Building, preliminary tasks preceding firefighting, such as connecting several hoses and setting up ladders, needed over 20 minutes for the firefighters to access the 10th floor (Ahmadi et al. (2020) & Khan (2022b)).

The results depicted in Figure 7.4 showcase the floor displacements approximately 5 minutes after firefighting commenced. Notably, the maximum vertical displacement of 590 mm was observed in the northwest corner of the 11th floor, with similar locations on the 12th, 13th, and 14th floors exhibiting displacements of 520 mm, 280 mm, and 130 mm, respectively. These substantial displacements underscore the severity of the fire in the NW corner. The deformation on 15F is relatively less due to the lower intensity of the fire.

7.5.3. 50 minutes after fire initiation

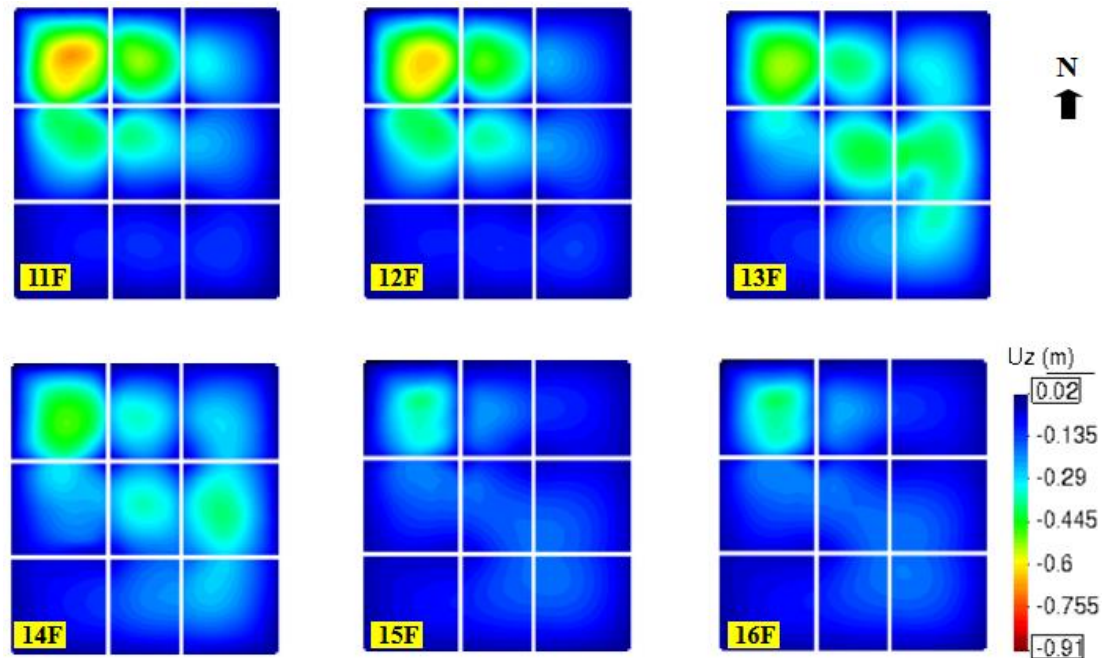


Figure 7.5 Vertical floor displacements at $t=3000$ sec (50 min)

Firefighting efforts were primarily focused on the northwest (NW) corner of the tower, only in the latter 30 minutes of the 50-minute duration of the fire. By this time, the fire had spread significantly across the 13th and 14th floors. The displacement contours depicted in Figure 7.5 show substantial vertical displacements of approximately 670 mm and 620 mm in the NW corner of the 11th and 12th floors. Visible damage can be observed on the adjacent and interior floor segments on these levels.

On the 13th, 14th, and 15th floors, displacements ranging from 200 mm to 500 mm are evident across extensive areas in the NW, SE, E (east), and core regions. Notably, on the 15th floor, displacements in the NW corner reach around 300 mm specifically. Consequently, the fire in the NW corner resulted in significant displacements across all six floors above the 10th floor, underscoring the extensive structural impacts caused by the fire in this region.

7.5.4. 1 hour and 40 minutes after fire initiation

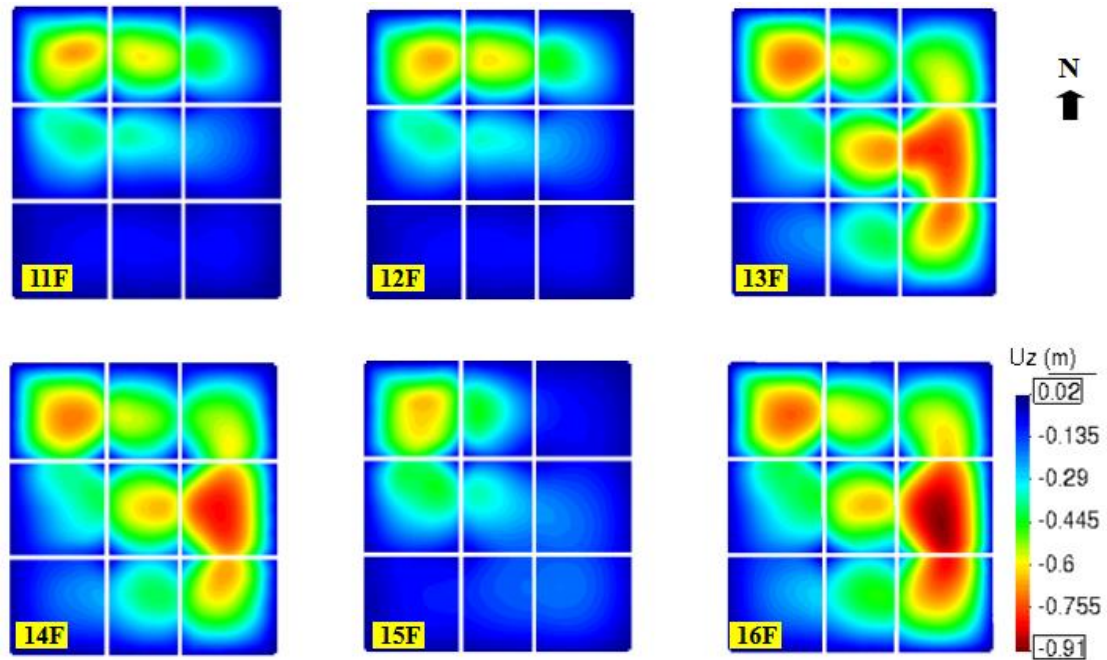


Figure 7.6 Vertical floor displacements at $t=6000$ sec (1 hour and 40 min)

Up to this point in time, firefighting efforts were going on the 10th and 11th floors. The contours in Figure 7.6 represents the moment that marks the beginning of Event 6 (temporary fire suppression in the NW area) based on the established fire timeline discussed in Chapter 4. It is crucial to note that the fire on the 10th and 11th floors led to displacements on the 11th and 12th floors. Temporary success was achieved in controlling the fire on these two floors, which prevented its spread towards the western direction.

As a result, the contours in Figure 7.6, illustrating the displacement of the 11th and 12th floors, show relatively lesser floor displacement in western areas. Conversely, displacements exceeding 800 mm are observed on the 13th, 14th, and 16th floors. Throughout this period, indications of the fire were noticeable near the edges of both the western and eastern sides of the building on the 12th floor and above.

7.5.5. 2 hour and 50 minutes after fire initiation

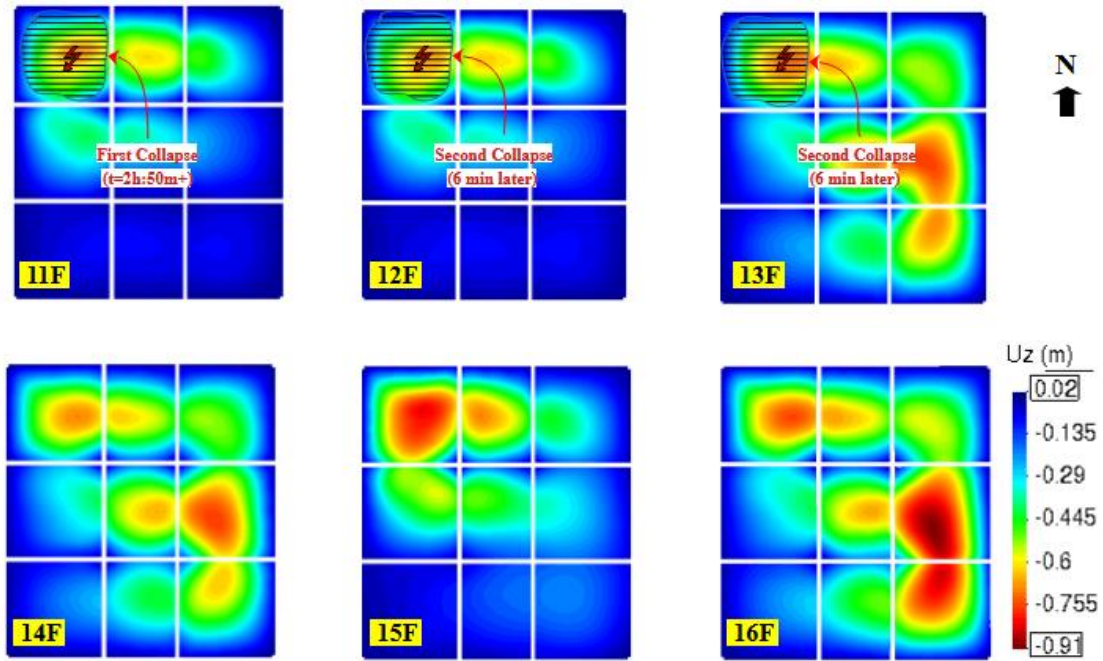


Figure 7.7 Vertical floor displacements at $t=102000$ sec (2 hours and 50 min)

The fire started at 7:56 AM in the morning, and after 2 hours and 50 minutes, approximately at 10:50 AM, the first partial collapse of the 11th floor over the 10th floor was observed. The displacement contours in the simulation predicted the large displacements on all floors at this specific moment. About 6 minutes later, the floors of the 12th and 13th floors also collapsed onto the 10th floor. The impact of these collapsed floors, marked in Figure 7.7, led to the subsequent failure of the 10th floor and multiple floors below it.

Despite the partial collapse of floor segments in the northwest (NW) corner of the tower, the overall stability of the tower remained intact. The global stability of the tower was not compromised because the fire did not critically affect the primary components of the load transfer system (refer to Chapter 3), such as core columns, secondary main columns, and primary beams (especially in core areas). This resilience in the primary load-bearing elements contributed to the ability of the tower to maintain its structural stability even in the face of localised floor failures.

7.5.6. Moments before global collapse (i.e., 3 hours and 20 min after fire initiation)

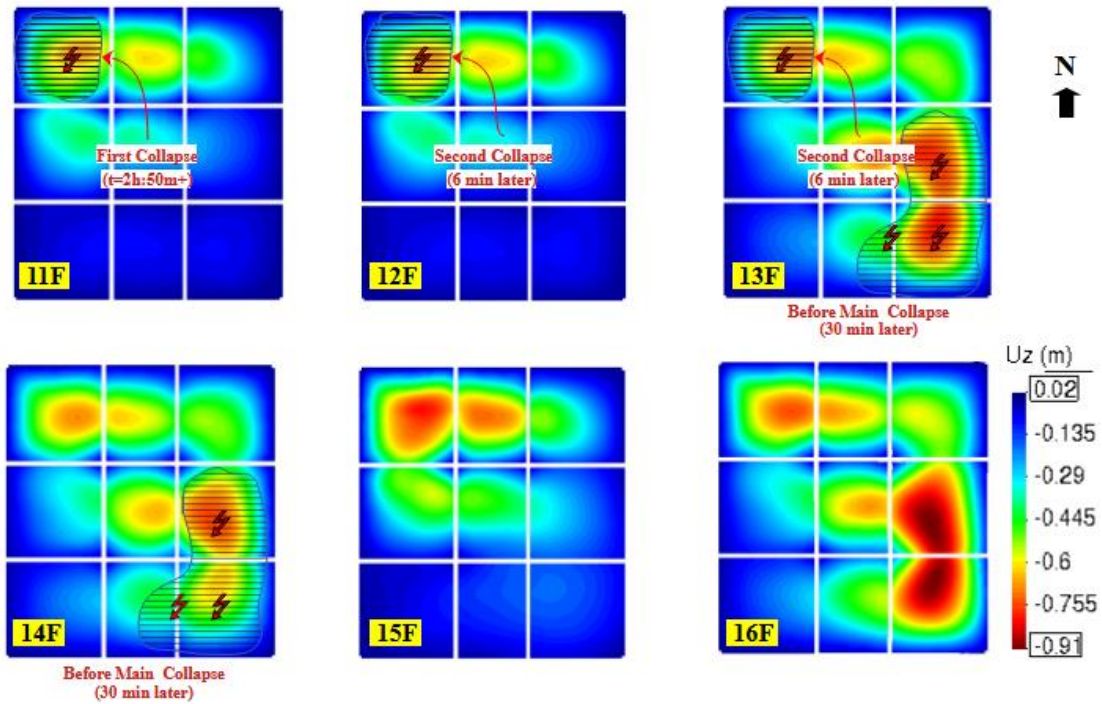


Figure 7.8 Vertical floor displacements moments before the global collapse, i.e., at $t=126000$ sec (3 hours and 20 min)

Around this time, the fire intensified, with heat rapidly emanating from the southeastern edge of the building. Video evidence indicated the collapse of floor segments in the southeast (SE) regions, as marked in Figure 7.8. It is reasonable to infer that the SE floor section of the 13th or 14th floor collapsed over the floor below. This collapse propagated to multiple floors below, resulting in the loss of lateral bracing support for the perimeter columns.

This initial assessment shows the displacement state of all six fire-affected floors. The progression of floor displacements provides insight into how the fire spread within the tower. The following section will provide a detailed analysis and interpretation of the thermal response output, shedding further light on the thermo-mechanical structural responses to the fire incident.

7.6. Comprehensive analysis of thermal response

This section will conduct a comprehensive analysis of the floor response, column response, and other critical components. The investigation will investigate the factors contributing to both the partial collapses observed within the tower and the subsequent global collapse.

7.6.1. Partial collapse of NW corner floors

The partial collapse of the 10th-floor ceiling (the 11th floor) is identified as Event 8 on the established event timeline from Chapter 4. Six minutes later, the 12th and 13th floors collapsed onto the 10th floor, resulting in a substantial impact load that led to the collapse of multiple floors below. This event is marked as Event 9 on the timeline.

This section will delve into the potential reasons behind the collapse of the corner floors, which occurred approximately 2 hours and 50 minutes after the initiation of the fire.



Figure 7.9 Photo showing the fully exposed steel members (Shakib et al. (2020))

Based on the observed floor response, the corner floor segments exhibited downward displacement within 7 minutes after the fire initiation. This rapid response of the floors can be attributed to the high-temperature gradients within the floor system. As discussed in Chapters 1 and 4, it was noted that the steel members in the tower are fully exposed to the fire, as shown in Figure 7.9.

Heat transfer analysis

All structural components (except columns) are in close proximity to the fire due to the storage of fabric material in the false ceiling. Consequently, peak temperatures recorded in the steel sections exceed 800°C in the northwest corner area. Simultaneously, due to its low thermal conductivity, concrete remained at relatively lower temperatures, except at the bottom faces where it was subjected to higher heat fluxes. This disparity in temperatures between the steel and concrete components played a significant role in the observed displacements and responses of the floor segments to the fire.

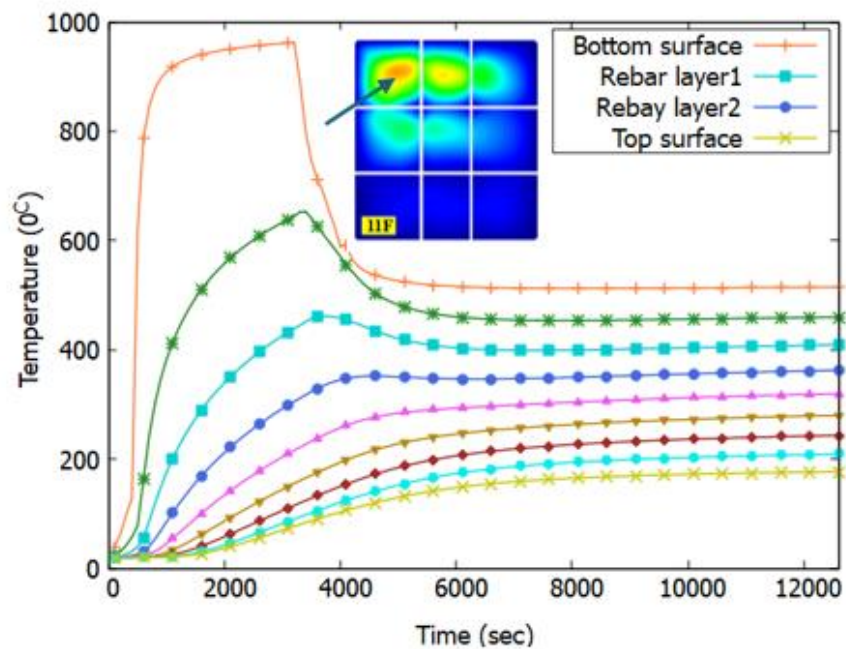


Figure 7.10 Temperature profile across the concrete slab section near the centre of the NW floor segment.

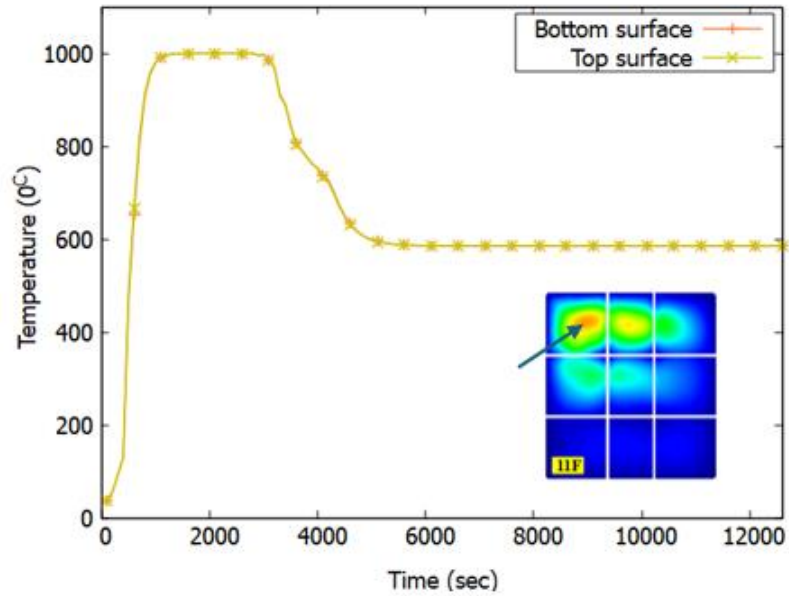


Figure 7.11 Temperatures in the steel section of the NW floor segment.

The heat transfer analysis of the shell element selected in the centre of the corner floor segment reveals that the temperatures at the top surface of the concrete stabilised around 523°C, while at the bottom surface, the temperature stabilised at 179°C, as depicted in Figure 7.10.

In the transverse and longitudinal reinforcement, temperatures are approximately 410°C and 360°C, respectively. It is crucial to note that the strength degradation of steel typically begins after 400°C, indicating that the rebars in the structure retain nearly full strength.

Figure 7.11 illustrates the temperatures in the bottom chord steel section at the bottom and top surfaces. The temperatures at both surfaces remain similar at all times, given that the section was fully exposed to the fires (refer to Figure 7.9). The bottom chord steel section is a UNP 100 channel section with a web thickness of 6mm. Due to the thinness in majority of trusses, significant temperature variation across the steel temperatures was not observed following the heat transfer calculations especially in areas where fire was intense.



Figure 7.12 The NW corner of the tower is engulfed in fire.

Thermo-mechanical response of floors

Figure 7.13 displays the floor displacements in the northwest (NW) corner at various time points, providing a visual representation of how the displacements progressed over time leading up to the collapse event.

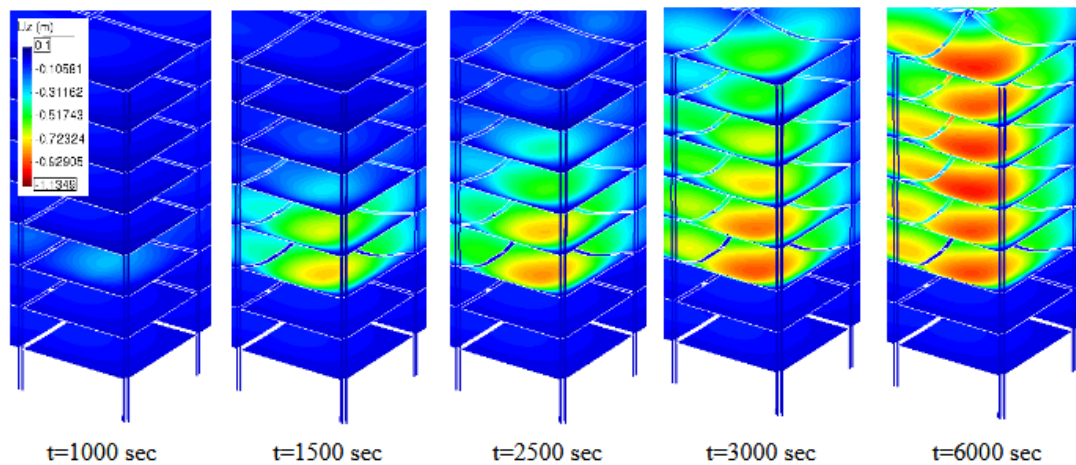


Figure 7.13 Displacement contours at different times in the NW corner zone

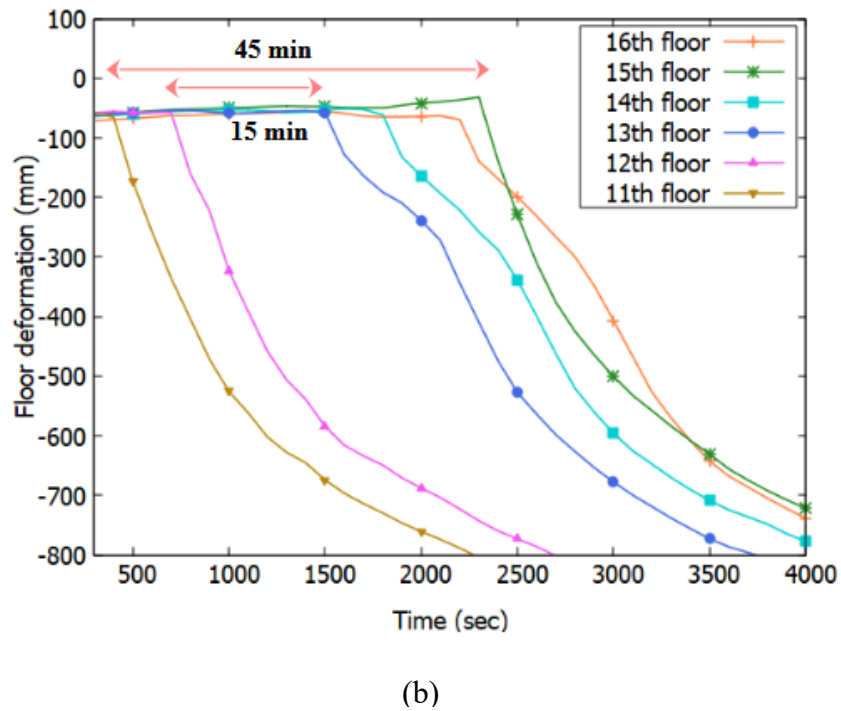
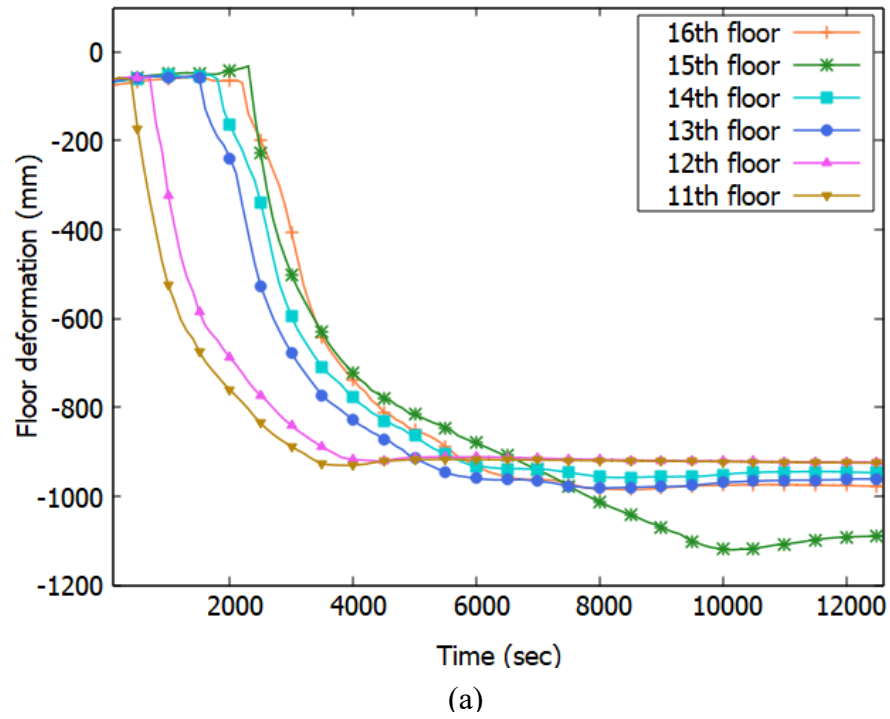


Figure 7.14 (a) Maximum floor displacements near the NW corner of all six floors; (b) closer view

Upon heating, the 11th floor (or the ceiling of the 10th floor) experienced thermal bowing displacement at approximately 6.67 minutes, as illustrated in Figure 7.14(b). Subsequently, 6 minutes later, the 12th floor exhibited thermal bowing behaviour. There was a gap of 15 minutes before the 13th floor responded similarly. The remaining three floors responded similarly following the thermal bowing observed on the 13th floor.

In all the floors, displacements up to 800mm were noticed due to rapidly increasing temperatures. However, beyond the 800mm mark, the displacements increased more gradually before eventually stabilising.

This observed behaviour is due to the reduction in thermal gradient (after 4000 sec) and the stabilisation of temperatures within the concrete slab, as depicted in Figure 7.14(a). The gradual increase in displacements in the later stage before reaching a stable state highlights the complex interplay between temperature changes, material properties, and structural responses in the context of fire-induced displacements in building floors.

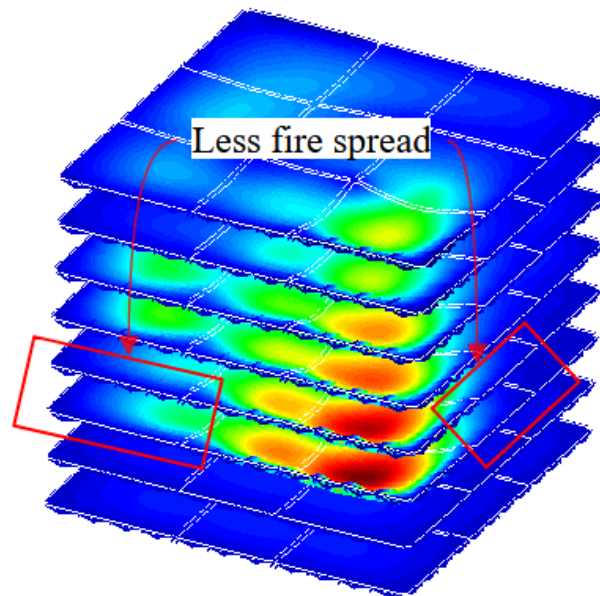


Figure 7.15 Marked areas on the 11th and 12th floors where the fire-induced displacements are lower ($t=3000$ sec).

The vertical displacements observed in the upper floors, specifically from the 13th to the 16th floors, are notably higher compared to what was observed on the 11th and 12th floors, see

Figure 7.6 and Figure 7.13. This difference in displacement can be attributed to the variation in the extent of fire spread between the upper and lower floors. In areas adjacent to the northwest corner on the 10th and 11th floors, where the fire spread was contained, the primary beams remained unaffected, resulting in lesser floor displacements in these regions (Figure 7.15). The maximum displacements on the 11th and 12th floors were approximately 70-80mm lower than those observed on the 13th and 15th floors and 180mm lower than on the 16th floor.

The higher displacements on the 16th floor can be attributed to the non-continuity of the columns beyond that level. This lack of column continuity led to roof-level columns leaning inwards, contributing to increased downward floor displacements. These variations in fire spread, firefighting effectiveness, and structural configurations resulted in differing levels of displacement across the various floors of the building.

Thermal response of columns

In the corner, the columns were constrained from freely displacing due to the presence of steel bracings and edge beams, especially in the early stages of the fire or as long as they were not directly exposed to the fire. The force contours (thickness contours) extracted from the simulation indicate that as the floor trusses expand outwards, tie beam action is activated in the bracing and edge beams, as the increased tension forces are observed, see Figure 7.16.

It's important to note that only the perimeter columns were heated based on the CFD output, see Figure 7.12. The core columns are not heated, assuming the presence of masonry, even though they were not fully covered at some locations.

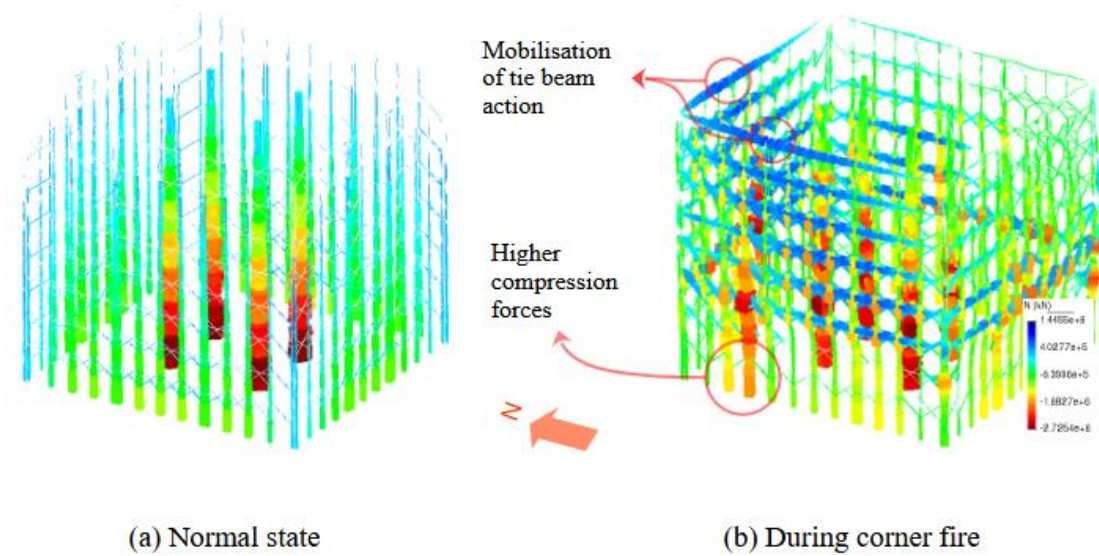
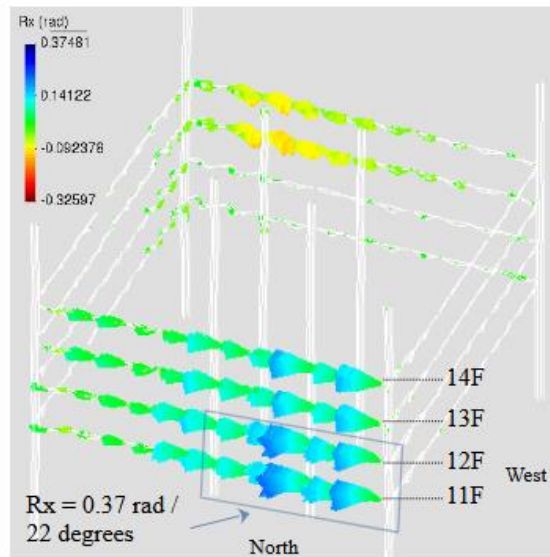


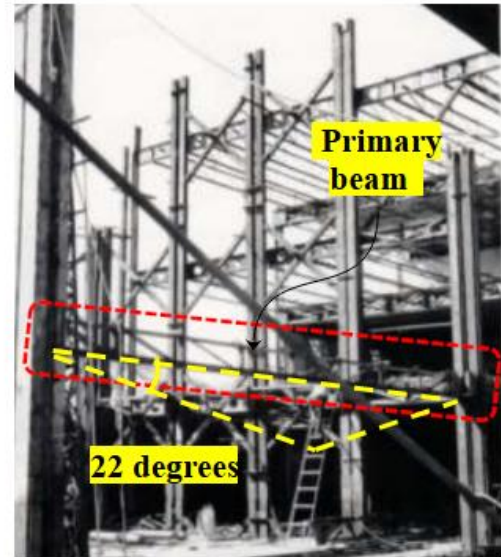
Figure 7.16 Line thickness contours showing the axial force evolution

In this study, connection behaviour is not explicitly modelled, leading to all connections in this FE model being assumed to be rigid. Therefore, only nodal rotations are extracted to analyse how they evolved.

Given that the first collapse took place approximately 2 hours and 50 minutes after the initiation of the fire, the conditions existing at the floor truss and column connections during the instance of failure can be examined. At the moment of the first collapse, the magnitude of rotations at the beam-column connections was extracted. The contours depicted in Figure 7.17(a) revealed a maximum connection rotation of 0.37 radians, equivalent to 22 degrees about the east-west direction, or X-axis in the model. A similar magnitude of rotation was observed near the west side of the corner, which is not displayed in the figure.



(a) $t=10200$ sec



(b) 22 degrees tangent at the ends

Figure 7.17 (a) Nodal rotations about the X axis (R_x) in the NW corner; (b) construction stage photo showing primary beam.

Given that all beams in the floor system are designed as trusses with a depth of 400, the bottom chord members are susceptible to buckling under significant vertical displacements induced by thermal bowing. Photographic evidence (Figure 7.18) collected from the debris substantiates the occurrence of buckling failures in the truss chords observed in thermal response.



Figure 7.18 Buckled truss beam found in debris

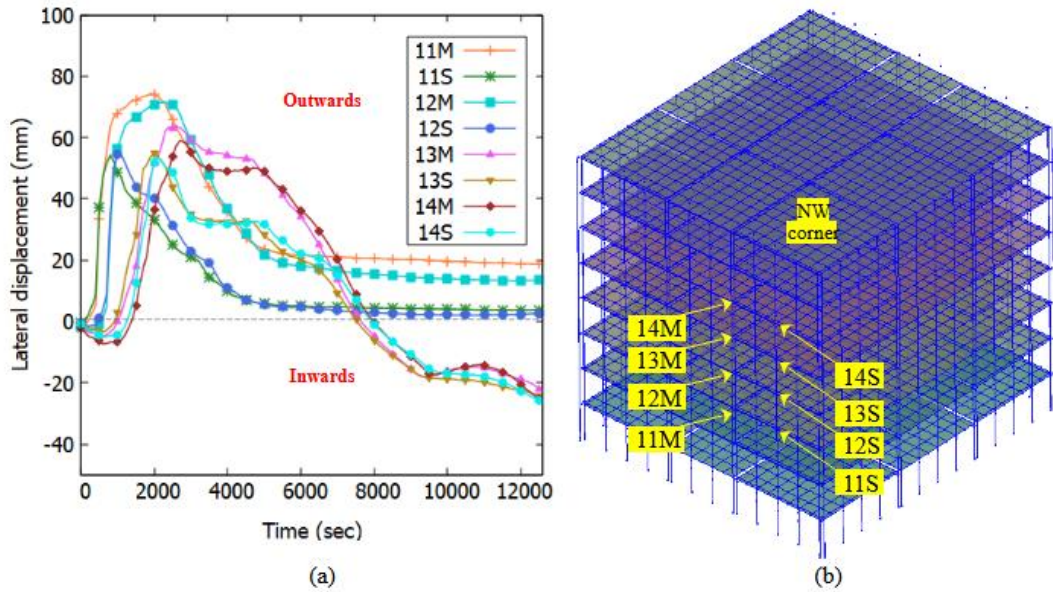


Figure 7.19 (a) Plot showing the lateral column displacement at (b) locations near the NW corner as indicated.

As a result of thermal bowing in the floor system and the expansion of truss beams, the columns near the perimeter underwent a maximum outward displacement of 75mm, as depicted in Figure 7.19(a). The outer columns, comprising secondary main columns and secondary columns (marked as 'M' and 'S' in Figure 19 (b)), experienced sideways displacement due to the thermal expansion of truss beams. Despite being stiffer, the lateral displacement of the secondary main columns exceeded that of the secondary columns, as shown in Figure 19(a). This could be attributed to the lesser thermal bowing effect near the primary beam when compared to the centre of the NW area.

In Figure 19(a), the column at position 11M shifted outward by 74mm and 11S by 53mm, while 13M and 13S moved 63mm and 54mm. The discrepancies in displacement are linked to the extensive fire spread on the 13th floor, unlike the 11th and 12th floors. The effect of fire on the northern side of the 13th floor created significant thermal gradients in the concrete floor segments on either side of the primary beam at 13M, explaining the varying displacements observed.

Columns on each floor exhibited varying times to reach their maximum lateral displacement. Additionally, out-of-phase lateral displacement is also observed among columns on the same floor due to differing lateral stiffness and the impact of fire, as previously discussed. This can lead to significant stresses on beam-column connections when a vertical fire spread occurs. In

Figure 7.19(a), the secondary main columns at 11M and 12M peak at 2000 seconds, while peaks at 13M and 14M occur at 2500 seconds. While a reversal in column lateral displacement is seen on the 13th and 14th floors, this is not observed on the 11th and 12th floors. This is attributed to the presence colder structure adjacent to the northwest corner on the lower floors, whereas fire spread on the upper floors results in higher inward pull forces. Figure 7.19(a) illustrates a maximum inward pull of 25mm observed by the end of the analysis.

Composite action

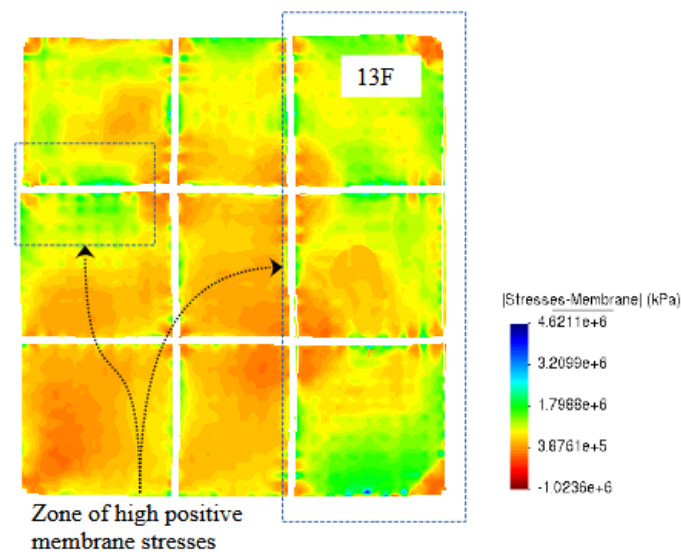


Figure 7.20 Contour map showing the membrane stresses on the 13th floor (t=10200 sec)

Figure 7.20 shows the zones of positive (tensile) membrane stress contours on the 13th floor at 10200 seconds, where NW floor segments experienced partial collapses. Moreover, since there was a notable absence of column inward pulling during different phases of the fire (except on NW and SE of the 13th floor), it is improbable that tensile membrane action across large floor areas was initiated. The floors in the core, west and southern regions primarily experienced membrane compression, mainly due to edge restraint. It should be noted that the study assumes a full composite interaction between the concrete slab and steel truss system, overlooking any potential slippage between these components. The method of connecting the shell and beam elements in the analysis assumes a rigid coupling of nodes. In reality, the connection between the concrete floor and truss beams is semi-composite and relies on insufficient shear keys, as noted by Shakib et al. (2020) and Behnam (2019). In Chapter 6, to assess the difference in behaviour between fully composite and non-composite, a study was conducted; refer to Figure 23 (in Chapter

6). Based on the comparison, it can be said the realistic floor displacements should fall somewhere in between what was predicted by both models.

In practice, the presence and effectiveness of decking, steel reinforcement, and shear keys play crucial roles in the structural behaviour of composite floors. Yet, specific details about these elements are lacking in the analysis. To comprehensively assess the realistic behaviour of the concrete slab, a thorough parametric study involving variations in concrete strength, degree of composite action, rebar spacing, etc., is essential. However, conducting such an in-depth investigation falls outside the scope of the current thesis.

Reasons for partial collapses

The 11th floor, which experienced lower floor displacements compared to the upper floors, was the first floor to collapse. The collapse of the 11th floor could potentially be attributed specifically to reasons (a) and (b), while all four reasons contributed to the partial collapse in the northwest (NW) area.

- a. **Duration of Fire Exposure:** The 11th and 12th floors endured the fire for the most extended duration compared to the other floors. Prolonged exposure to high temperatures can significantly weaken the connections, leading to a loss of load-bearing capacity and eventual collapse.
- b. **Thermal Restraint:** The adjacent floor segments of the 11th and 12th floors were relatively at colder temperatures; see Figure 7.15. This temperature differential can create higher thermal restraint, resulting in increased rotations at the connections (Figure 7.17(a)). The higher rotations at the connections can induce additional stresses in the structural elements, potentially leading to failure despite lower overall displacements.
- c. **Thermal Effects:** The rapid heat generation from the fuel heated the thin steel truss members to high temperatures, creating significant thermal gradients in the slab sections. This resulted in substantial thermal bowing displacement and large rotational displacements of around 22 degrees in the beam-column connections.
- d. **Column Movements:** The significant displacements induced by thermal bowing and variations in column stiffnesses in the northwest corner resulted in varying lateral displacements of the columns, posing risks to the integrity of beam-column connections. Out-of-phase lateral movements of the columns, caused by vertical fire spread, led to

columns undergoing S-shaped deformations, potentially causing welds in the beam-column joints to fail.

The main factors contributing to the partial collapse of the northwest corner floor segments were high thermal gradients, vertical fire spread, and out-of-phase lateral column displacements, all of which collectively compromised the structural integrity of the affected floors. It can be concluded that the complex interplay of the mentioned factors can influence the structural stability in fire-affected structures.

7.6.2. Interim developments

During the initial 15 minutes, the impact of the fire was localised to the northwest corner of the tower, affecting the 11th and 12th floors primarily, as depicted in Figure 7.3. However, by the 33-minute mark, significant displacements ranging from 100-400mm were observed in the floor sections adjacent to the northwest corner, as shown in Figure 7.4. Similar displacements were also noted on the eastern side of the tower, specifically on the 13th and 14th floors, posing a greater threat to overall stability compared to the corner fire. It was discussed in the robustness study in Chapter 3, which highlighted the critical nature of fires affecting the edge floor segments involving two primary beams.

A temporary stability in displacements was evident when comparing Figure 7.5 to Figure 7.4, except in the northwest region. This stability might have been influenced by firefighting efforts on the south and eastern sides. However, displacements predicted at the 50-minute mark, as shown in Figure 7.6, indicated fire severity near the eastern facade, with displacements surpassing 800mm due to both primary beams being compromised. Throughout this period, displacements in the central panel increased slower than in the outer panels, attributed to lower ventilation leading to reduced fire effects in the core region compared to the outer floor segments.

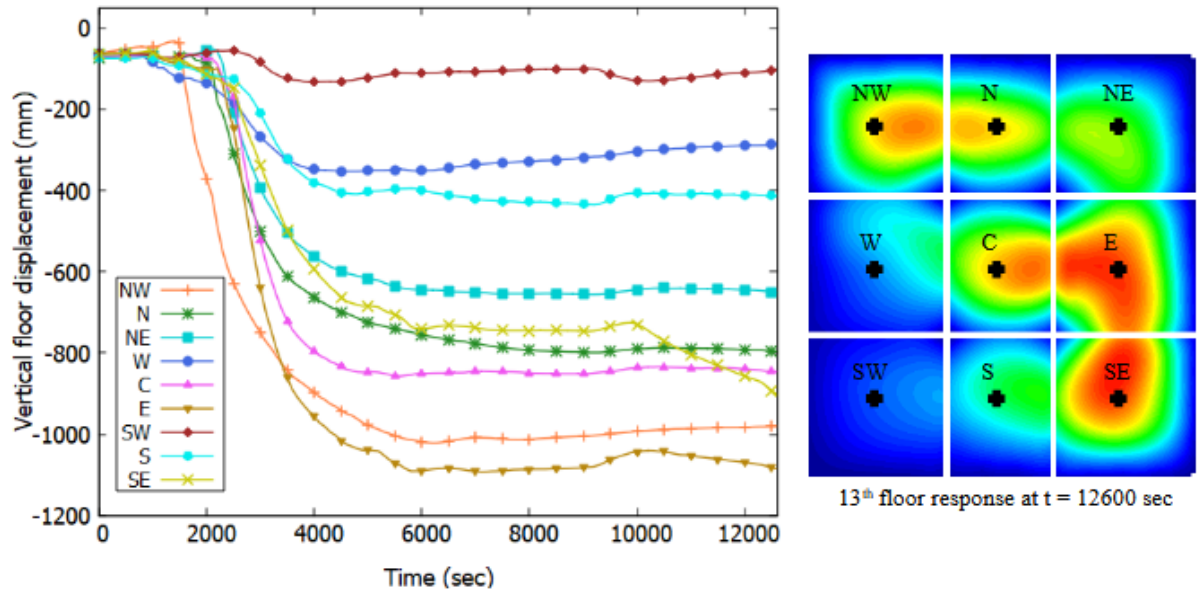


Figure 7.21 Response of the 13th-floor segments at different locations are marked.

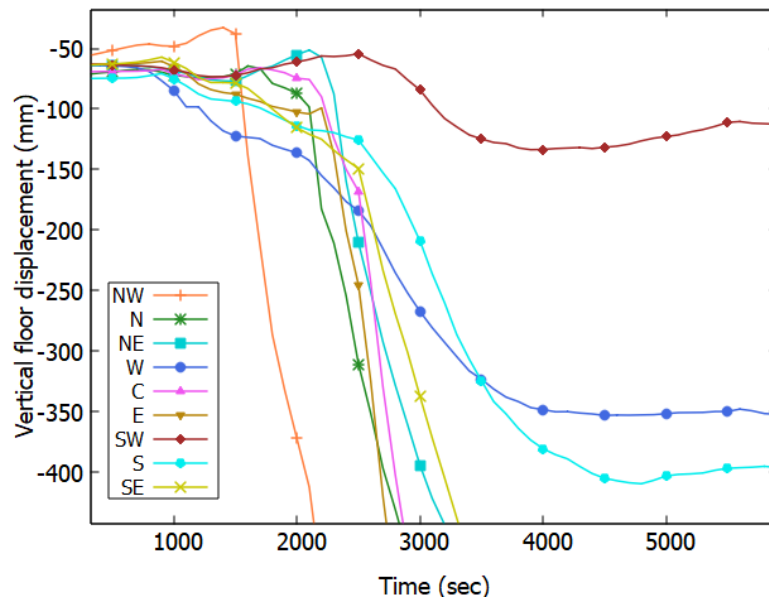


Figure 7.22 Response of the 13th floor in the first hour.

For instance, the scenario involving the fire on the 13th floor is illustrated through Figure 7.21 and Figure 22. These plots depict the vertical displacements at the centre of each floor segment plotted against time. Each data point is labelled according to its location on the floor plan. In Figure 7.21, the displacements at W, SW, and S remain under 400mm. The results predict the most significant downward displacements at the NW and E floor sections, surpassing 1000mm after 6000 seconds. After 10000 seconds, an increase in displacement is also observed at the SE

floor segment. According to the visual representations and established event timeline in Chapter 4, the collapse of the NW floor segment occurred at 102000 seconds, followed closely by the E and SE segments just before the overall structural failure. Figure 7.22 is plotted for a better illustration of the onset of vertical deflections of the floor segments.

Observations

The following observations are made during the 30-minute gap period between collapses.

- a. Due to minimal heating, the vertical displacement rates at W, SW, and S are comparatively low. The absence of fire spreading in these zones led to the roof showing a tilt towards the eastern side moments preceding the collapse.
- b. The patterns and extents of floor displacements on the 14th and 16th floors mirror each other, albeit with lesser displacements at SE and E.
- c. The displacements on the 12th and 15th floors exhibit similarities to those on the 11th floor.
- d. The progression of the fire onto the 13th and 14th floors, particularly towards the south and southeast regions, triggered floor failures that eventually culminated in widespread structural instability.

Reasons for stability during the interim period

The floor collapse in the NW area could not impact the global stability of the tower. The structure withstood the damage and survived nearly 30 minutes until the global collapse triggered by the floor collapse near the south and eastern areas. The reasons for the stability during this period can be ascertained to...

- a. Fire in the NW area did not affect external columns or interior columns. The building could maintain stability if the fire affected the secondary trusses.
- b. Adequate fire suppression near the western face

7.6.3. Moments before the final collapse

At this juncture, the tower had already suffered the collapse of several floors adjacent to the northwest corner, extending below the 13th floor. Meanwhile, a significant fire had intensified in the southeast corner of the tower, particularly affecting the 13th and 14th floors. As with the northwest corner, the abundance of air and ventilation in the area had facilitated high temperatures. The final moments were marked by numerous smoke eruptions, signalling the failure of floor segments in the southeast sector. This progression can be observed in Figure 7.23, where an increase in the number of floors emitting smoke is evident as one moves from left to right.

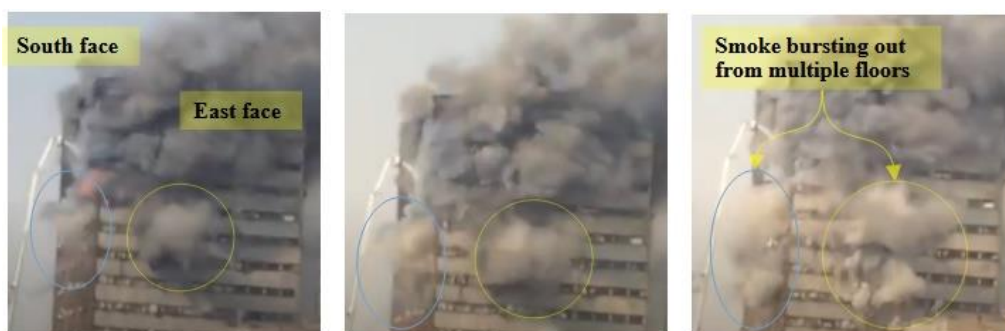


Figure 7.23 Photo of the east and south faces showing the bursting-out smoke

In the photo on the left, smoke emerged due to the collapse of either the 11th or 12th floors, whereas in the photo on the extreme right, it was evident that several floors, possibly those below the 12th floor, failed in succession. This stage of multiple local collapses lasted for 10 seconds.

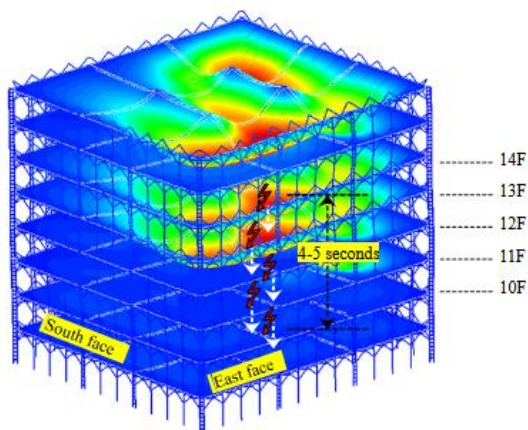


Figure 7.24 Displacement contours of all floors in 3D perspective, moments before the collapse

The response of the floors, primarily influenced by thermal bowing, resulted in significant displacements in the SE corner and the floor sections to the east, as depicted in Figure 7.24. In contrast to the fire incident in the NW corner, the fire on the eastern side impacted both primary beams, leading to large displacements evident throughout the eastern edge (as shown in Figure 7.24). This side of the building was challenging to reach with external firefighting equipment, increasing the fire duration in this area. The fire intensity was particularly heightened in the SE corner of the 13th floor due to the ample availability of unrestricted airflow.

The simulation results predicted the highest rotational displacement at the primary connection near the eastern side of the 13th floor, as illustrated in Figure 7.25. The left contour image denotes the nodal rotations in the north-south direction (R_y), while the right contour image (R_x) represents the nodal rotations in the east-west direction. The analysis reveals that the primary and adjacent secondary beams underwent rotations approaching 0.33 radians or approximately 19 degrees at the connections. But in reality, the edge beams on the eastern side exhibit greater resistance to twisting forces and increased connection stresses compared to the southern edge beams because of the presence of masonry walls, as depicted in Figure 7.23. The visual evidence of the vertical damage propagation in Figure 7.23 agrees well with the anticipated failure location as predicted by the thermo-mechanical model shown in Figure 25.

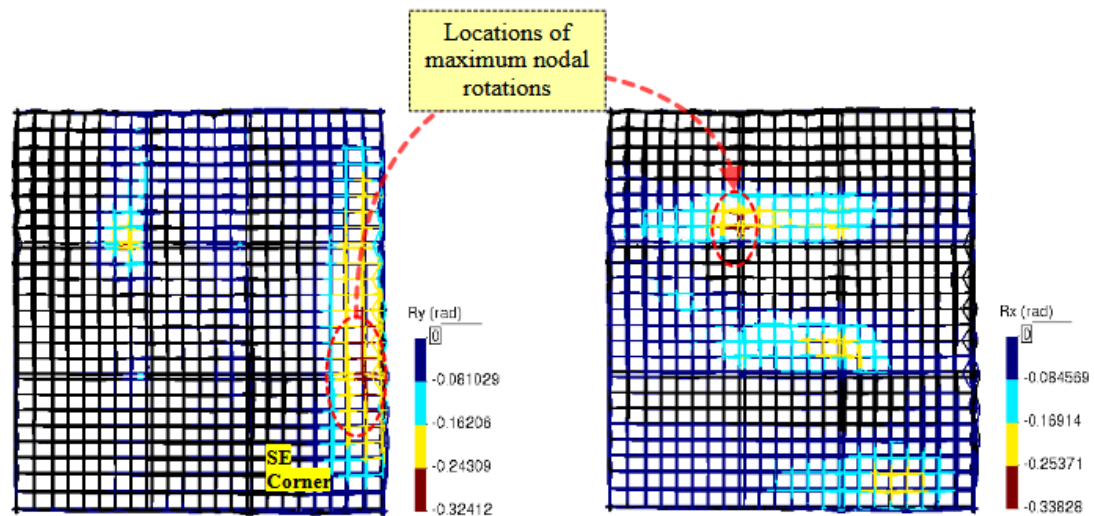


Figure 7.25 Contour map showing maximum nodal rotations- R_x and R_y , on the 13th floor.

WTC towers vs Plasco tower

The Plasco tower used welds and gusset plates to connect truss beams with columns, a method that limits the extent of free rotation compared to the connections in the World Trade Center (WTC) 1 and 2 towers. In the WTC towers, the primary girders connect to external columns through truss seats, where only the top chords come into contact with the supports, as depicted in Figure 7.26(a). External columns in the WTC were outfitted with a standoff plate to which seat angles were bolted, providing vertical support to the main girders.

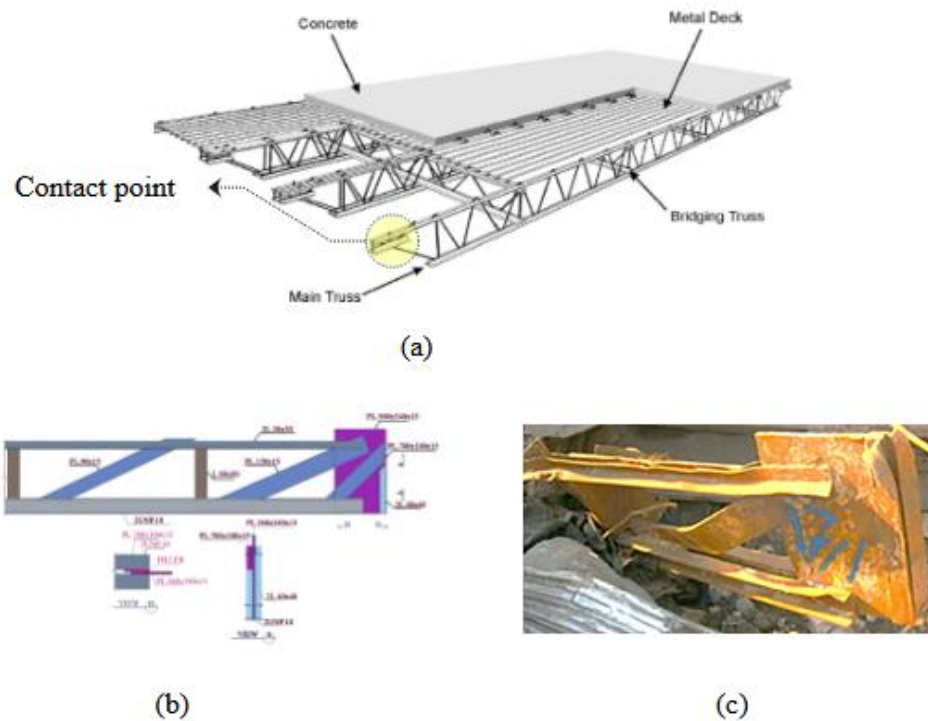


Figure 7.26 Connections of main trusses in (a) WTC (NIST (2005)) and (b) & (c) Plasco tower (Epackachi et al. (2022)).

On the other hand, in the Plasco tower, the bottom chords, top chords, and diagonal plates are welded to a 400mm deep gusset plate, as shown in Figure 7.26(b) and (c). This configuration establishes the connection between the column and main trusses through welds extending 400mm on each side of the gusset plate. Consequently, large displacements in the trusses can only be accommodated through the buckling of bottom chords or the rupture of top chords. In critical scenarios, connection failures occurred due to the rupture of welds between gusset plates and

columns. Photographic evidence documented all three types of failures - buckled and ruptured chords, as well as failed welds.

Load redistribution before the global collapse

Temperature loading was specifically applied on the column members from the 13th floor to the 15th floor on the eastern side and southeast (SE) corner of the structure. Figure 7.27 shows the intense fires engulfing the SE corner regions of the 13th and 14th floors. Hence, it is logical to infer that the box-shaped columns endure heating from all directions. The thermo-mechanical analysis highlighted a notable redistribution of loads from the heated zones to the neighbouring sections. Figure 7.28 illustrates the evolution of axial forces in the columns from their ambient state to the condition just before collapse. In this visualisation, varying line thicknesses are proportioned to compression forces experienced by the columns, with thinner lines representing lower compression and thicker lines indicating higher compression forces. The horizontal blue lines near the colder regions suggest the mobilisation of tie actions.



Figure 7.27 Intense fire near the SE corner on 13th and 14th floors

The findings and visual cues suggest that the adjacent columns successfully withstood the additional compressive loads resulting from the load transfer from the heated columns. Notably, the adjacent columns remained stable without buckling, likely due to the presence of cooler

structural elements in the western and southwestern (SW) regions of the building, as depicted in Figure 7.21. Load redistribution before the global collapse was successful because of the intact peripheral beam. Stability mechanism during this phase is akin to what was described in section 3.5.3, refer to Figure 3.19.

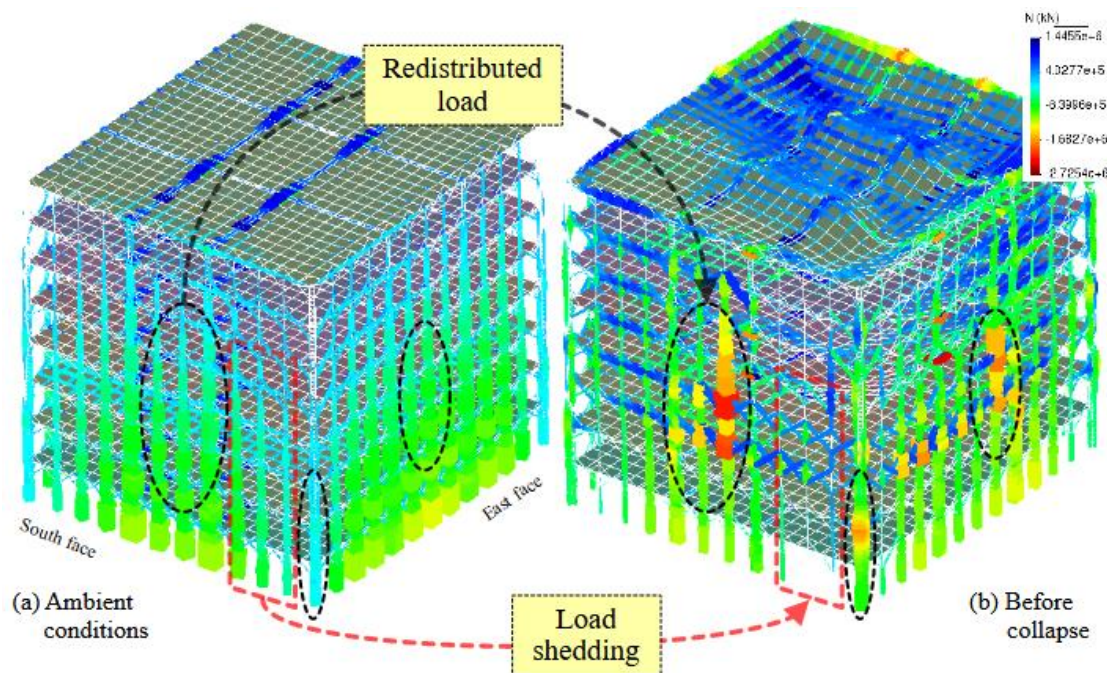


Figure 7.28 Line thickness contours showing the column axial forces at (a) ambient conditions and before collapse.

Column displacements before the global collapse

The simulation results reveal a distinct pattern of column displacements within the tower. Initially, columns on the eastern face exhibit outward displacement during the initial hour of the fire. Subsequently, columns on the 13th and 14th floors shift inward, while columns on the remaining floors maintain their previous trend, as illustrated in Figure 7.29. The maximum outward displacement of a column on the eastern face observed between the 15th floor and the roof amounts to 240mm, as depicted in the plot in Figure 7.29. Simultaneously, an inward displacement of approximately 13mm (negative) is noted on the 14th floor, resulting in a net column eccentricity of 253mm.

Furthermore, the highest inward displacement of a column on the eastern face, around 40mm (negative), is observed on the 14th floor, with a corresponding outward displacement of roughly 160mm, resulting in a column eccentricity value of 200mm. Throughout most of the fire duration, the columns on the east side experienced eccentricities ranging from 200mm to 250mm, primarily due to the fire affecting the eastern face of the 13th and 14th floors.

The displacement of the east side frame, as observed by Ahmadi et al. (2020) in his visual evidence-based collapse study aligns with the simulated response in this study.

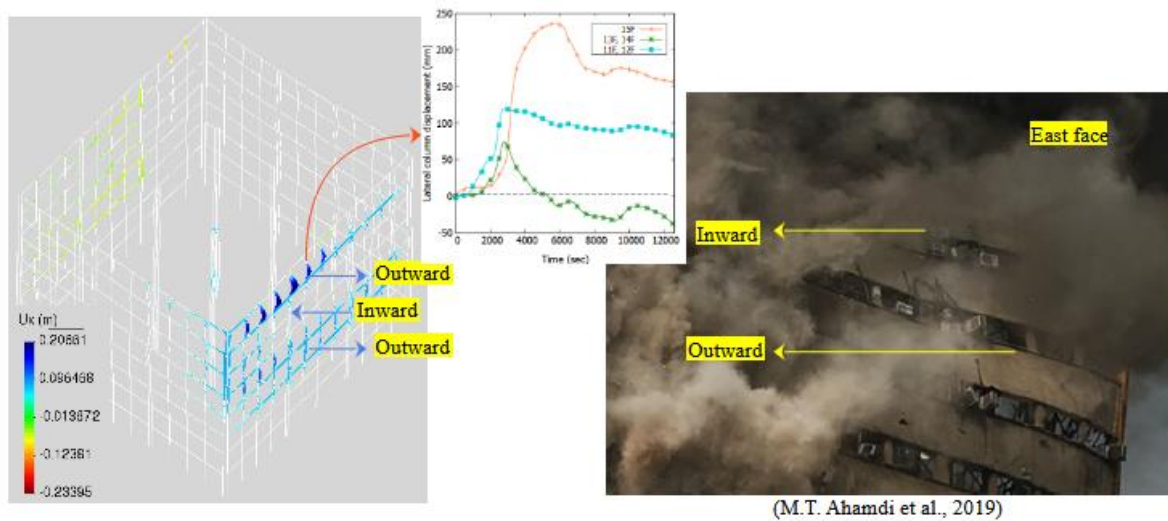


Figure 7.29 Outward displacement of columns on the east face

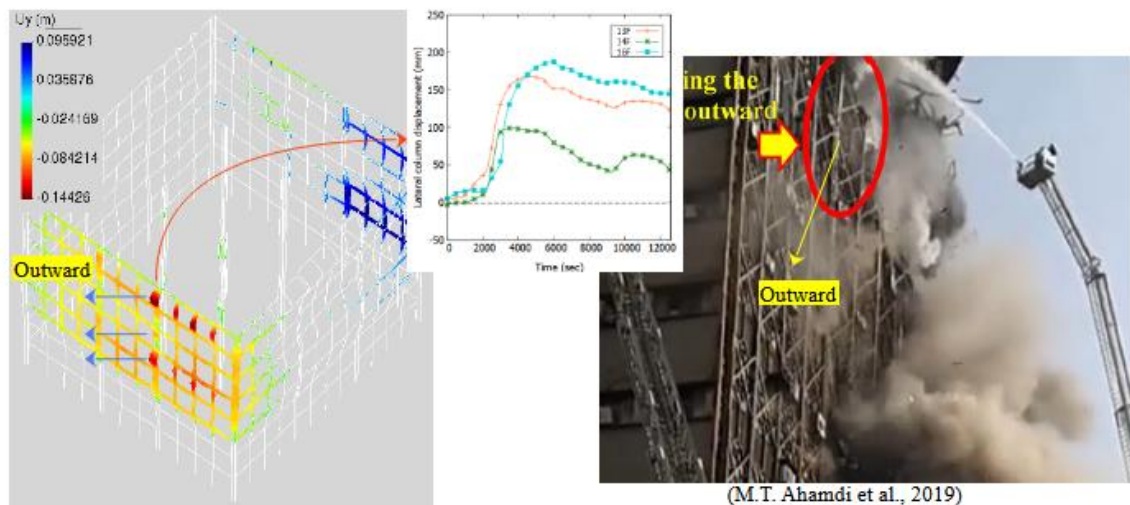


Figure 7.30 Outward displacement of columns on the south face

On the southern face, the lateral displacements of the columns peaked at 163mm and 188mm on the 13th and 16th floors, respectively, while reaching 96mm on the 14th floor. The maximum net eccentricity observed was 100mm throughout the analysis. Due to the extensive spread of the fire, the column eccentricities on the eastern face exceeded those on the southern face, with values reaching 253mm. Both external columns on the eastern and southern sides exhibited a reversal in lateral displacement after 4000 seconds (1 hour and 6 minutes) of the fire duration. This suggests that even if connections manage to withstand the damage, there are hypothetical fire conditions that could potentially trigger global collapses. In the context of the Plasco tower, it is plausible to suggest that connection failures led to premature and abrupt collapse, thereby limiting the opportunity to witness the collapse induced through altering structural geometry.

Local collapses before the global collapse

Before the overall collapse of the tower, it is probable that the primary beams close to the southeast (SE) corner of the 14th floor experienced failure at the location highlighted in Figure 7.25. Consequently, a significant portion of the 13th floor collapsed, impacting two primary beams that supported the floor segment of the SE corner.

The collapse sequence, lasting 4-5 seconds, is illustrated in Figure 7.31. Owing to dynamic forces at play, the damage propagated vertically downward, reaching as far as the 8th floor. This progression is supported by observable evidence, such as smoke (dust) bursts on both the south and east faces of the tower, as depicted in Figure 7.23.

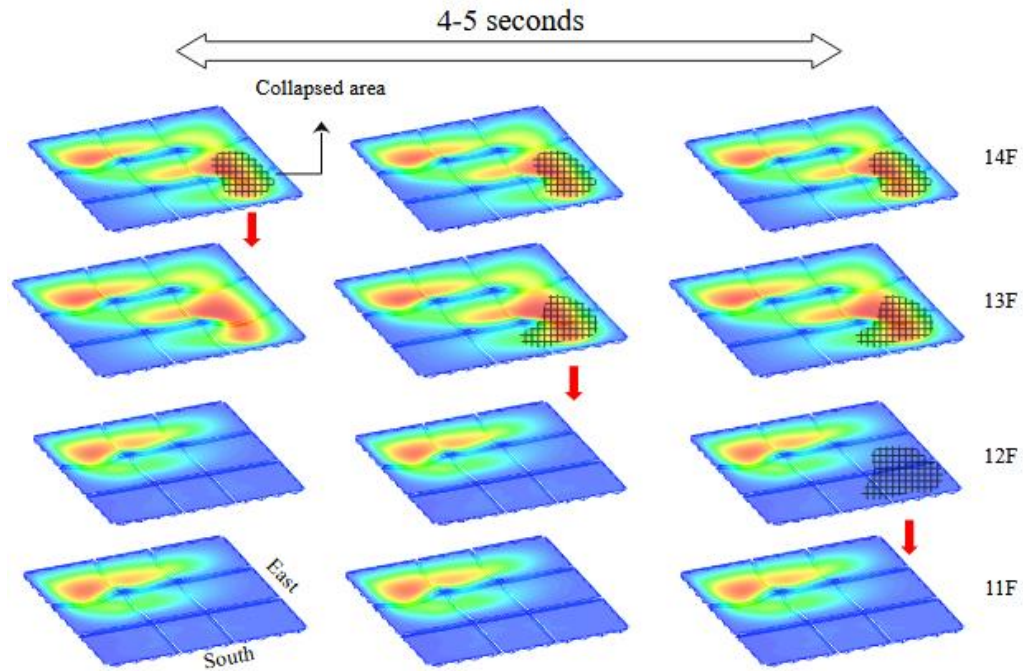


Figure 7.31 Sequence floor collapse near the SE corner of the tower

7.6.4. Global collapse

Video recordings demonstrate that the complete collapse occurred as the external columns near the southern facade started to displace inwards during the final stages. Figure 7.32 illustrates that the roof encountered its most significant displacement precisely over the external primary column, visibly buckling inwards. This column, which was built using two box sections (each box section again was built up using 2 UNP channels), was seen undergoing a splitting failure.



Figure 7.32 A significant moment during the global collapse

Thermo-mechanical response

The structure that experienced the complete collapse differed significantly from its original state which it was in moments prior. The partial collapses in the southeast (SE) corner area notably extended the unsupported buckling lengths of the columns. In the most conservative case, columns near the SE region lost lateral support from at least two floors, leading to an increase in the unsupported lengths to approximately 7-8 meters (after accounting for the end support conditions). The simulation outcomes, conducted using the revised model incorporating the missing local floors, are outlined below.

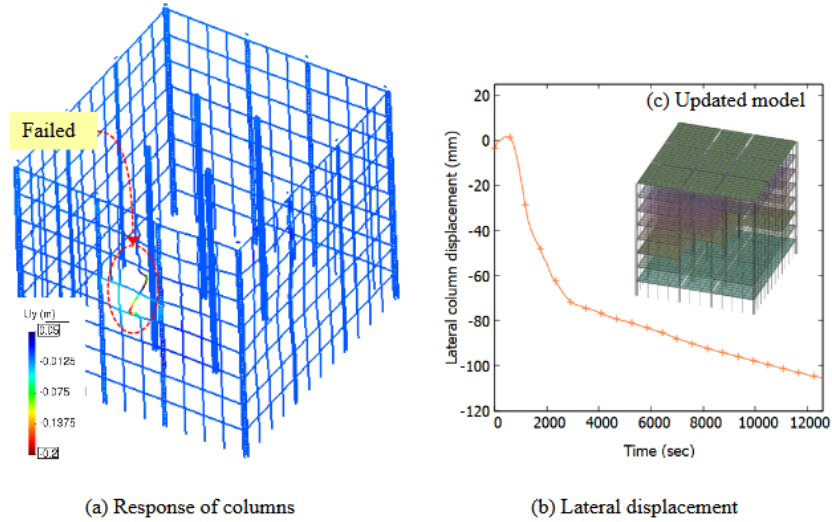


Figure 7.33 Response of columns based on the revised model

Multiple floors near the southeast (SE) corner were removed, and thermal loading was exclusively applied to the external columns. The simulation predicted the failure of the column adjacent to the secondary primary column, as depicted in Figure 7.33(a). This column deforms in an 'S' shape, exhibiting a maximum lateral displacement of around 100mm inward and 100mm outward. Figure 7.33(b) illustrates the lateral displacement of the column. Since this analysis is based on static loading, the reliability of the response is limited to the point of failure initiation. Therefore, once the collapse commences, the displacements escalate swiftly within a short timeframe. In the present model, only the outcomes corresponding to 4-5 seconds before the collapse are considered worthy of discussion.

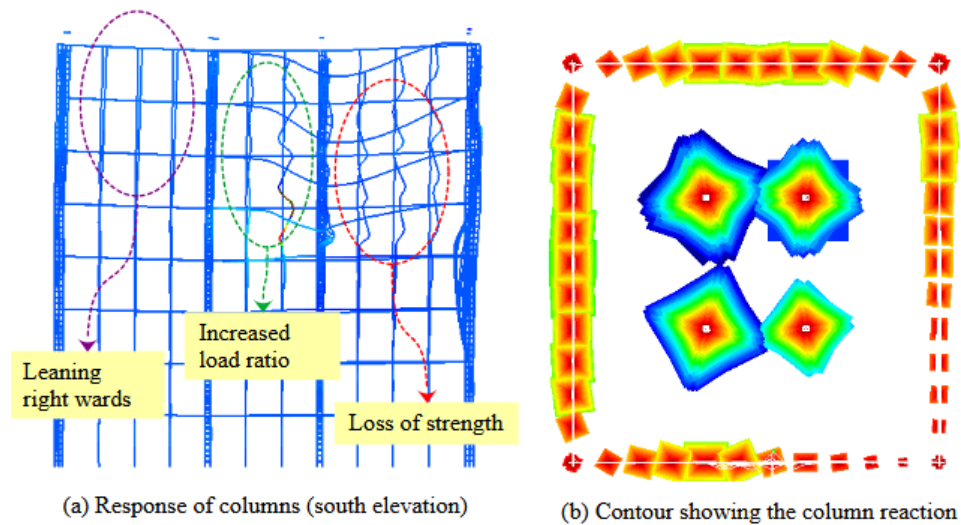


Figure 7.34 South elevation view of the model showing vertical displacements and column base reactions

The depiction in Figure 7.34(a) illustrates the response of columns on the southern facade of the model. The columns near the southeast (SE) corner failed because of fire, leading to load shedding and subsequently transferring the load to adjacent columns. Figure 7.34(b) demonstrates the increased base reaction of the columns situated in the middle of the edge frame. Due to the removal of floor segments near the corner region, the corner column did not exhibit increased base reactions. Columns positioned in the centre of the frame display 'S' shaped displacements, signalling the failure initiation. Consequently, the columns on the far left are observed leaning inwards. In the upcoming sections, the global response simulated using the updated model will be compared with available video evidence.

To date, there are only three collapse videos available, offering limited but valuable insights into the rapid final collapse lasting 2-3 seconds.

Video evidence 1



Figure 7.35 Collapse sequence observed in video evidence 1

Figure 7.35 presents the progression of the global collapse from start to finish in four frames (a), (b), (c), and (d) spaced at intervals of 4.2, 1.5, and 5 seconds. Owing to the angle and distance of the video capture, limited information can be inferred regarding lateral column instability.

- a. The transition from frame (a) to frame (c) reveals an increased roof displacement, suggesting the loss of vertical support.
- b. Frame (d) exhibits the complete collapse of the external frame on the southern side, while the frame on the western side remains intact. From this perspective, the corner column near the southeast (SE) corner is still visible, indicating a failure in the connection between the edge beams and the column.

Video evidence 2

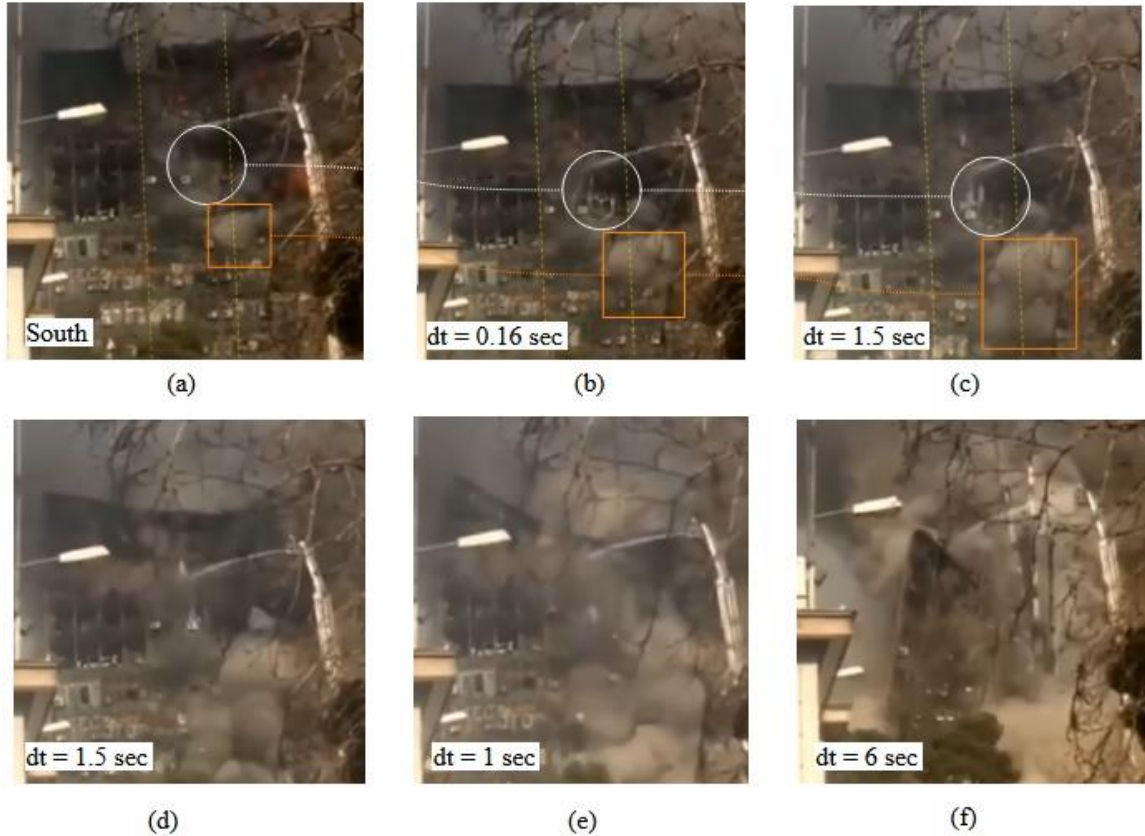


Figure 7.36 Collapse sequence observed in video evidence 2

Drawing insights from the video footage, several facets of the collapse can be discerned across frames (a) to (f): roof displacement, the progression of dust and smoke, and the inward displacement of external columns. In frames (a), (b), and (c), the external main columns (constructed from two built-up box sections) are not visible, prompting the addition of guiding dotted yellow lines for investigative purposes.

- c. Frame (a) to (b): Minor vertical roof displacement is centred around the southeast (SE) corner. Secondary columns adjacent to the main columns (highlighted with white circles) are observed bending inwards at an angle. Connected by bracing members, two columns move in unison. Vertical dust spread signifies localised floor collapses (outlined by an orange rectangle).

- d. Frame (b) to (c): Columns neighbouring the main columns undergo further inward displacement, with the roof displacing downwards at the centre. Dust and smoke extend downward.
- e. Frame (c) to (e): Secondary columns adjacent to the main column on both sides are seen failing. Extensive roof displacement towards the SE area indicates connection failures with the corner column.
- f. Frame (f): The western and southwestern sections of the tower visibly rotate in a rigid manner.

In light of the second video evidence, the initial failure likely occurred in the secondary main column. Subsequent to this, the adjacent secondary columns succumbed to the increased load ratio, ultimately resulting in the failure of 6-7 columns on the southern facade. Consequently, the roof and the 15th floor collapsed, severing connections with the corner column in the SE corner.

Video evidence 3

Video evidence 3 offers a perspective of the tower facade similar to video evidence 2, with clear visibility of the secondary main columns, as depicted in Figure 7.37(a). Both videos 1 and 2 corroborate the main column failure along with the adjacent columns. Furthermore, in the present video, a vertical progression of damage is evident (in frame (c)), leading to substantial vertical roof displacement. Subsequently, the failure spreads horizontally to the floors above the 14th floor, as observed in frame (d). At this juncture, dynamic forces come into play, triggering the collapse of upper floors and resulting in multiple connection failures, causing the entire south facade to collapse except for the bottom left portion. The collapse of the western and eastern facades followed approximately 3-5 seconds later.



Figure 7.37 Collapse sequence observed in video evidence 3

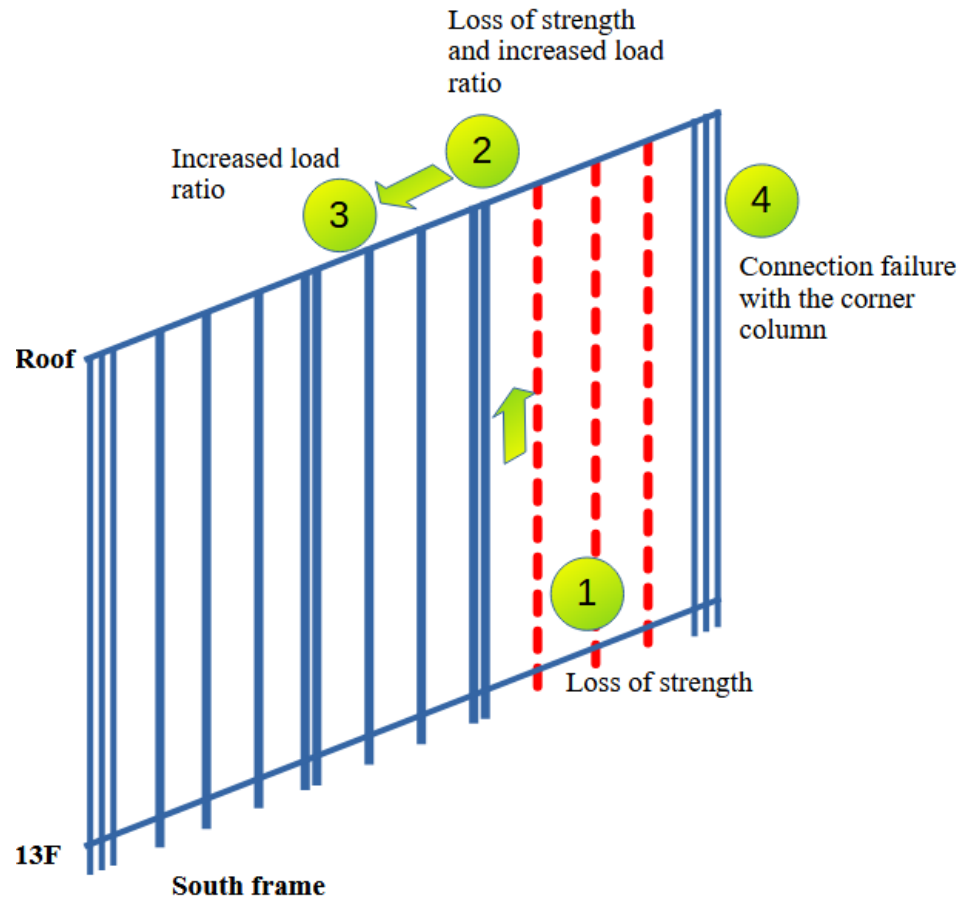


Figure 7.38 Summary of the video evidence & simulation: In-plane propagation of external column failures

The final collapse was primarily triggered by the in-plane propagation of external column failures. The simulation agreed with the video evidence by accurately depicting how these failures spread horizontally, leading to a cascading effect that ultimately resulted in the complete collapse of the structure.

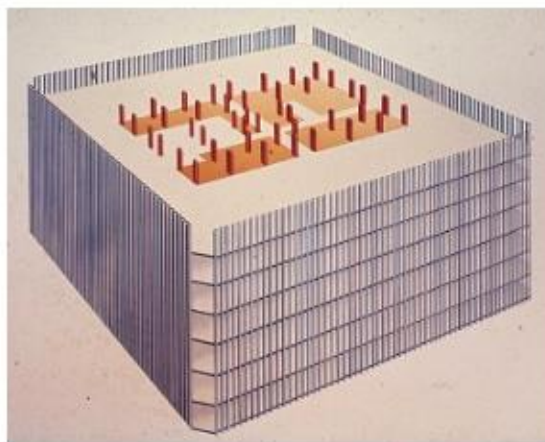
7.7. Discussion

7.7.1. Framing

The structural design of the Plasco Tower, with 38 perimeter columns and four core columns, differs significantly from that of the World Trade Center (WTC) towers, which featured 236 perimeter columns, and a core constructed using 46 box columns (NIST (2005)).

In the WTC towers, the core columns were interconnected by massive beams, creating a structural system where the columns collectively acted as a bundle of sticks. This design facilitated the redistribution of loads during extreme events. Conversely, in the Plasco Tower, the limited number of core columns deviates from the typical tubular structure design. In the event of a severe incident impacting a core column, the load redistribution mechanism differs. A considerable magnitude of load is transferred to external columns that may not be designed to handle such increased load ratios or bending moments.

In the WTC towers, lateral forces were primarily resisted by thin external columns distributed along the perimeter, as depicted in Figure 7.39(a) (Archives of Michigan (n.d.)). However, in the Plasco Tower, the corner columns are designed to resist lateral loads, reducing the demand on the perimeter columns. This design approach can be risky in situations where external columns are subjected to overloading. The structural design of the Plasco Tower appears to be vulnerable to challenges related to load redistribution efficiency during extreme events, highlighting potential flaws in the design to withstand and respond to significant structural stresses and disturbances.



(a) Framed tube of WTC 1 and 2



(b) External columns in Plasco tower

Figure 7.39 External framing in the WTC towers and Plasco tower

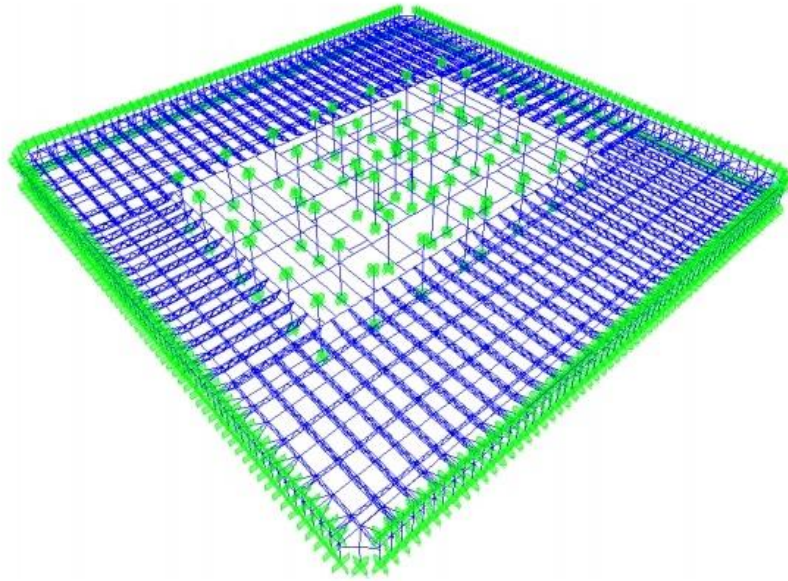


Figure 7.40 Truss arrangement in WTC towers (NIST (2005)).

The structural plan employed for the Plasco Tower can offer advantages in specific situations, such as edge bay or edge floor segment fires. For instance, as outlined in Chapter 3, even if an edge bay fire were to impact secondary main columns, the tower managed to endure. During such occurrences, the transfer of loads to corner columns occurs through a temporary stable mechanism, as depicted in Figure 19 within Chapter 3.

7.7.2. Structural segmentation

The design of Plasco Tower was based on three key elements - core columns, primary beams, and secondary main columns - with the remainder of the structure being supported by these components. Despite partial floor collapses in the northwest corner, the tower remained stable due to its effective structural segmentation against disproportionate failures. The inability of failures on the 11th to 13th floors in the northwest corner to spread horizontally was attributed to the containment of the fire within the area defined by the primary beams, see Figure 7.12. The stability of the tower was only compromised when the fire extended to floor segments adjacent to and including the primary beams, as depicted in Figure 7.23 and Figure 7.25.

7.7.3. Structural continuity

On the other hand, the presence of corner columns provided structural continuity against local collapses while ensuring global safety, provided secondary columns are well connected with the corner columns. In instances of out-of-plane displacement of exterior columns, the corner column is strategically positioned to counter outward movements. For instance, in the case of the World Trade Center (WTC) towers, where external column strength is uniform, the structural behaviour is two-dimensional due to lower resistance in the third dimension. On the other hand, towers like the Plasco Tower defy 2D modelling due to the added resistance to lateral displacement introduced by corner columns. This study demonstrates such resistance, leading to the generation of tensile forces in bracings and edge beams. At the same time, the inclusion of corner columns enabled a weaker design of perimeter columns. Therefore, discussions surrounding the development of more effective fire-resistant tall building designs become intricate due to these intertwined considerations.

7.7.4. Segmentation vs continuity

Structures can be engineered to allow localised collapses while averting a disproportionate collapse. Nevertheless, in the context of the Plasco Tower, the extensive local collapses in the southeast corner resulted in significant damage to critical load-bearing components such as primary beams and secondary perimeters. Visible evidence suggests that the collapse was instigated by the inward-pulling action of a primary beam on the external column adjacent to the southern facade. Consequently, the magnitude of the local collapses in the southeast corner is not conducive to the type of failures that designers should allow within a structure. The subject of design philosophies for ensuring the global stability of tall structures under fire conditions is an area that has not received extensive attention within the scientific community. As a result, there is a significant need for further research and exploration in this field in the future.

7.7.5. Firefighting

The primary firefighting operations focused initially near the northwest corner, effectively containing the spread of the fire towards the west. However, as the fire advanced to the eastern section during later stages, firefighting efforts were hindered by limited accessibility on the eastern side, as depicted in Figure 7.41. Furthermore, the presence of masonry walls on the western facade,

as shown in Figure 7.42, presented challenges in extinguishing the fire. Consequently, extensive areas in the east experienced intense fire due to these factors.



Figure 7.41 Satellite view of the tower showing directions



Figure 7.42 Western face of the tower in different instances

Weight factors can be assigned based on the load ratios, redundancy, etc. In the event of fires, firefighters can be guided to suppress fires affecting high-risk areas so that global failures can be mitigated or delayed. For example, in the case of the Plasco tower, when an entire floor was on fire, it would have been effective, and collapse would have been delayed if efforts had been concentrated near the secondary main columns on the eastern and western sides.

Focusing firefighting efforts on the primary load transfer system components of the southern facade of the tower could have improved firefighting effectiveness. Viewing firefighting from a structural engineering point of view offers practical insights and optimises emergency responses. Understanding how fires impact structures can guide targeted firefighting strategies, enhancing structural stability and safety rather than focusing on suppressing the fire alone. Integrating structural engineering principles into firefighting tactics not only improves response efficiency but also enables responders to create tailored interventions for better outcomes. A deep exploration of this topic is needed and is not within the scope of the thesis.

7.8. Conclusions

- a. This chapter demonstrated the successful integration of open-source tools—FDS and OpenSEES—in conducting forensic investigations of structural collapses induced by fire. The scale-related hurdles encountered when using differently sized CFD and FE models were addressed. A comprehensive structural analysis of the Plasco tower model was executed, with collapse hypotheses presented that elucidated the collapse-contributing factors effectively. The collapse of the Plasco tower is likely even if core column is subjected to elevated temperatures. This scenario was explored in Chapter 5, in which a single floor model was analysed against the CFD-based fire. However, analysis in this chapter explores other possibilities, such as the SE core column not being exposed to fire and only the external columns and floors being exposed to fire. The following conclusions can be drawn based on the forensic structural analysis.
- b. The collapse of the less-displaced 11th floor at the Plasco Tower can be attributed to prolonged fire exposure, which weakened connections, and high thermal gradients, which induced higher restraints and increased stresses.

- c. Simulation results from the northwest corner of the Plasco Tower model shed light on the partial collapse of floors 11 to 13. High thermal gradients caused significant thermal bowing and rotations in beam-column connections. Out-of-phase lateral column displacements due to fire spread compromised structural integrity. This intricate interaction of factors underscores how thermal effects can critically impact structural stability, highlighting the complexity of structural behaviour under fire conditions.
- d. Due to minimal heating, vertical displacements near the west and southwest regions were lesser, with the roof tilting eastward before the collapse. Floor displacement patterns on the 14th and 16th floors mirrored each other. Similarities in displacements between floors 12, 15, and 11 were observed. Fire progression onto the 13th and 14th floors, especially towards the south and southeast regions, triggered floor failures, leading to widespread structural instability.
- e. The simulation results predicted the highest rotational displacement at the primary connection near the eastern side of the 13th floor, with primary and adjacent secondary beams experiencing rotations of around 20 degrees. The welding and gusset plate connections impacted the extent of free rotation. Weld rupture between gusset plates and columns contributed to connection failures, evident in buckled and ruptured chords and failed welds found in the debris.
- f. Structural design of the Plasco tower, with fewer core columns compared to the WTC towers, differs significantly. In the WTC towers, interconnected core columns formed a load-bearing bundle facilitating load redistribution during extreme events. In contrast, Plasco tower may face challenges in load redistribution efficiency during severe incidents due to limited core columns, potentially impacting external columns not designed for additional redistributed loads.
- g. The design of the Plasco tower is centred around core columns, primary beams, and secondary main columns, forming the structural backbone. Despite localised floor collapses in the NW corner, the stability of the tower was maintained through effective segmentation. However, stability was compromised only when two primary beams on the eastern side were exposed to the severe fire.

- h. The presence of corner columns in structural design ensured local and global stability, particularly when they were well-connected to secondary columns, but resulted in weaker perimeter columns.
- i. Design philosophies (structural segmentation or structural continuity) ensuring global tall structure stability under fire conditions lack thorough scientific exploration, highlighting the necessity for future research in this critical area.
- j. Initial firefighting operations at the Plasco Tower contained the fire near the northwest (NW) corner but faced challenges in the east due to limited access and masonry walls. Focusing on the primary load transfer system on the southern facade could have enhanced firefighting efficacy. Integrating structural engineering into firefighting strategies offers insights for targeted responses, improving overall safety and response effectiveness.

Chapter 8: Conclusions and future work

8.1. Evolution of the research

The research aimed to conduct a detailed forensic study of the collapse of the Plasco tower in a fire using open-source tools. The research work started with thermo-mechanical analysis with simplistic thermal loading in Chapter 3. At the time, applying a realistic thermal load was impossible with native OpenSees commands. Due to the 17 different types of steel and the scale, detailed thermo-mechanical analysis was not within reach. Chapter 4 detailed the reconstructed fire incident of the Plasco tower.

In Chapter 4, the progression of the fire in the Plasco tower is carried out using CFD analysis to recreate a probable timeline of the fire progression. Within the research (Khan (2022b)), two separate CFD models were created and assessed. The first model represented a multistorey configuration, concentrating specifically on the fire in the NW corner of the Plasco tower, where a partial collapse occurred around 3 hours into the fire incident. The second CFD model was designed to simulate a typical floor of the Plasco tower and was examined under six different fire scenarios. As the fire affected the top six floors of the building, six distinct fire scenarios were reconstructed and simulated during the CFD investigation.

In the initial stages of finite element (FE) modelling, basic thermal loading was employed to assess the structural response of the tower. The fire module within OpenSEES provides options such as uniform thermal loading, linearly changing thermal loading, and the ability to input temperatures at nine specific points along the depth of the section. The study utilising the initial thermal loading can be found in Yarlagadda et al. (2018). R. Domada et al. (2020) carried out structural analysis using thermal loading that varies linearly across the steel sections. Later, with the development of the GiD+OpenSees interface, several ISO 834 fire-based structural robustness studies were carried out in Chapter 3. Subsequently, the availability of CFD data and the CFD-FE coupling methodology (via OpenFIRE) enabled a more sophisticated approach to thermal loading in later phases.

In Chapter 5, an integration methodology utilising OpenFIRE software was implemented to conduct a comprehensive thermo-mechanical evaluation. Although the coupling process was

successful, it posed challenges, particularly requiring substantial user effort, especially for complex structures. The coupling method showed limitations, particularly in cases where meshing was not uniformly applied. Challenges related to non-convergence in the analysis were more pronounced when utilising shell elements in meshing. Each meshing iteration necessitated updated input in the OpenFIRE system. Nevertheless, the primary objective of integrating CFD and FE analyses was achieved.

The coupling methodology detailed in Chapter 6 addressed the challenges encountered in previous chapters. In this research, the heat transfer analysis was fully automated, and the meshing constraints were resolved using a third-party interface developed by GiD. M. A. Orabi, Khan, et al. (2022) refined the GiD+OpenSees interface to automatically generate an OpenSEES-compatible heat transfer script and conduct heat transfer analyses on each steel section individually. Throughout this investigation, modifications were made to the GiD interface to facilitate heat transfer analyses on steel and concrete sections representing the structure of the Plasco tower. This process showcased a seamless integration of CFD and FE models, which was particularly beneficial for analysing tall building structures.

Building on the knowledge acquired from studying substructures and applying limited thermal loading—specifically, a single floor in Chapter 5 and multiple floors in the northwest corner in Chapter 6—Chapter 7 detailed a comprehensive analysis of the entire multi-storey structure. This study integrated detailed heat transfer and thermal-mechanical analysis. The thesis completed this examination, thoroughly simulating the Plasco tower response to the realistic reconstructed fire scenario.

8.2. Insights from the research

8.2.1. Plasco tower collapse pattern

Four instability collapses were identified: pancake, domino, section, and instability collapses. The global collapse started with a pancake collapse in the NW corner, leading to failures on lower floors. Damage near the SW corner involved sectional failure, instability, and possible domino collapses.

8.2.2. Weaknesses of the Plasco tower against fires

Design elements like structural continuity were not given due consideration. Tensile membrane action was doubtful. Uncertainties existed regarding shear studs and composite floor slab behaviour under fire conditions. The lack of intermediate columns impacted load paths, with primary reliance on the core, secondary main columns, and primary beams for stability. Load redistribution from failed core columns was non-uniform, leading to higher load ratios in adjacent columns. Failure of primary beams could affect significant floor areas but might not cause global failure. Secondary main columns, the most critical primary load transfer components after core columns and primary beams, faced potential buckling under multi-floor fire loads. The secondary main columns can experience splitting failure due to weld failures.

8.2.3. Predicted reasons for the collapse

The collapse of the 11th floor was primarily due to prolonged fire exposure, weakening connections, and high thermal gradients, inducing significant restraints and stresses. Simulation results from the northwest corner revealed how high thermal gradients led to thermal bowing and rotations in beam-column connections, causing the partial collapse of floors 11 to 13. Out-of-phase lateral column displacements due to fire spread compromised structural integrity, emphasising the critical impact of thermal effects on stability. Simulation predictions indicated the highest rotational displacement at the primary connection on the eastern side of the 13th floor, with primary and adjacent secondary beams experiencing significant rotations. Welding and gusset plate connections ruptured due to substantial rotations.

8.2.4. What if connections did not fail?

Due to the wide fire spread, the column eccentricities were greater on the eastern facade than on the southern side, reaching 253mm. After 1 hour and 6 minutes into the fire, external columns on the eastern and south aspects experienced a reversal in lateral displacement. This implies that under certain hypothetical fire scenarios, conditions exist that could potentially initiate global collapses even if connections can endure the damage. In the context of the Plasco tower, it is conceivable to propose that failures in connections precipitated the sudden collapse, thereby preventing the observation of a collapse induced by changes in structural configuration.

8.3. Future work

8.3.1. Fire-induced structural collapses

In the Plasco Tower, local collapses in the southeast corner led to notable damage to crucial load-bearing elements like primary beams and secondary perimeters. Observable evidence indicates that the collapse was initiated by the inward force exerted by a primary beam on the external column adjacent to the southern facade. As a result, the scale of the localised collapses in the southeast corner does not align with the failures that designers might allow (through the approach of structurally segmented design). The discussion around design principles to ensure the overall stability of tall buildings in fire scenarios remains an area that has not received thorough examination in the scientific community. Therefore, there is a pressing need for further research and investigation in this domain in the future.

8.3.2. Optimising firefighting efforts

Directing firefighting attention towards the primary load transfer elements of the southern facade of the Plasco tower may delay the collapse. Comprehending the structural effects of fires informs specific firefighting strategies, improving structural stability and safety beyond mere fire suppression. Incorporating structural engineering principles into firefighting methods boosts response efficiency and empowers responders to tailor interventions for delaying/preventing collapses.

8.3.3. Resolution of CFD-FD data mapping

The study used more than 25000 thermocouple sensors distributed across the six levels of the finite element model. It was seen in Chapter 6 that employing a basic fire curve produced satisfactory outcomes when simulating structural responses to the fire, such as a northwest corner fire. This suggests that such fires may not require high thermal load resolution, unlike those occurring on the eastern and western sides of the tower. This underscores a crucial inquiry into determining the optimal level of thermal load resolution. Optimising the number of thermocouples according to the fire characteristics and structural setup can significantly reduce computational expenses.

References

- Aghakouchak, A. A., Garivani, S., Shahmari, A., & Heshmati, M. (2021). Structural investigation of the collapse of the 16-story Plasco building due to fire. *Structural Design of Tall and Special Buildings*, 30(1). <https://doi.org/10.1002/tal.1815>
- Ahmadi, M. T., Aghakouchak, A. A., Mirghaderi, R., Tahouni, S., Garivani, S., Shahmari, A., & Epackachi, S. (2020). Collapse of the 16-Story Plasco Building in Tehran due to Fire. *Fire Technology*, 56(2), 769–799. <https://doi.org/10.1007/s10694-019-00903-y>
- Alos-Moya, J., Paya-Zaforteza, I., Garlock, M. E. M., Loma-Ossorio, E., Schiffner, D., & Hospitaler, A. (2014). Analysis of a bridge failure due to fire using computational fluid dynamics and finite element models. *Engineering Structures*, 68, 96–110. <https://doi.org/10.1016/J.ENGSTRUCT.2014.02.022>
- Architizer. (n.d.). *Idea 2805766: New Plasco Building by Mohamad rasoul moosapour in Iran*. Retrieved August 25, 2024, from <https://architizer.com/idea/2805766/>
- Archives of Michigan. (n.d.). *PHOTOS: The World Trade Center designs are owned by the state of Michigan*. Retrieved August 21, 2024, from <https://www.michiganpublic.org/arts-culture/2017-09-11/photos-the-world-trade-center-designs-are-owned-by-the-state-of-michigan>
- BBC (Middle East). (2017, January 17). Tehran fire: Twenty firemen killed as high-rise collapses. *BBC News*.
- Behnam, B. (2019). Fire Structural Response of the Plasco Building: A Preliminary Investigation Report. *International Journal of Civil Engineering*, 17(5), 563–580. <https://doi.org/10.1007/s40999-018-0332-x>
- Cao, Y., Jiang, J., Lu, Y., Chen, W., & Ye, J. (2023). Progressive collapse of steel structures exposed to fire: A critical review. *Journal of Constructional Steel Research*, 207, 107985.
- Command Manual - OpenSeesWiki*. (n.d.). Retrieved June 8, 2024, from https://opensees.berkeley.edu/wiki/index.php?title=Command_Manual

- Dai, W., Usmani, S. &, Dai, X., Jiang, L., Maclean, J., Welch, S., & Usmani, A. (2016). *A Conceptual Framework for a Design Travelling Fire for Large Compartments with Fire Resistant Islands* (Vol. 2, p. 1039). Interscience Communications Ltd. <https://www.research.ed.ac.uk/en/publications/a-conceptual-framework-for-a-design-travelling-fire-for-large-com>
- Davis, T. A. (2004). Algorithm 832: UMFPACK V4. 3---an unsymmetric-pattern multifrontal method. *ACM Transactions on Mathematical Software (TOMS)*, 30(2), 196–199.
- DeHaan, J. D., FABC, Fssd., & Icove, D. J. (2011). *Kirk's fire investigation*. Pearson Higher Ed.
- Department of Defense. (2016). *UNIFIED FACILITIES CRITERIA (UFC) DESIGN OF BUILDINGS TO RESIST PROGRESSIVE COLLAPSE APPROVED FOR PUBLIC RELEASE; DISTRIBUTION UNLIMITED*. <http://dod.wbdg.org/>.
- Domada, R. V. V., Khan, A. A., Khan, M. A., & Usmani, A. (2020). *OpenSees simulation of the collapse of Plasco tower in fire*.
- Domada, R., Yarlagadda, T., Jiang, L., & Usmani, A. (2020). Preliminary Stage OpenSEES Simulation of the Collapse of Plasco Tower in Fire. *Indian Structural Steel Conference*, 143–155.
- Epackachi, S., Mirghaderi, S. R., & Aghelizadeh, P. (2022). Failure analysis of the 16-story Plasco building under re condition. *Scientia Iranica*, 29(3A), 1107–1124. <https://doi.org/10.24200/SCI.2022.57903.5495>
- Eurocode, 1. (2002). Actions on structures–part 1–2: general actions–actions on structures exposed to fire. In *EN 1991-1-2: 2002*. European Committee for Standardization Brussels.
- Eurocode 1. (2006). Eurocode 1: Actions on structures—. *British Standard, United Kingdom*.
- Eurocode 3. (2006). *Design of Steel Structures, " Part 1-2: General Rules, Structural Fire Design*, .
- FDS-SMV*. (n.d.). Retrieved July 17, 2024, from <https://pages.nist.gov/fds-smv/>
- Flint, G., Usmani, A., Lamont, S., Lane, B., & Torero, J. (2007). Structural response of tall buildings to multiple floor fires. *Journal of Structural Engineering*, 133(12), 1719–1732.

- Flint, G., Usmani, A., Lamont, S., Torero, J., & Lane, B. (2006). Effect of fire on composite long span truss floor systems. *Journal of Constructional Steel Research*, 62(4), 303–315.
- Gillie, M., Usmani, A. S., & Rotter, J. M. (2002). A structural analysis of the Cardington British steel corner test. *Journal of Constructional Steel Research*, 58(4), 427–442.
- Github (Aatif). (n.d.). *aatif85*. Retrieved August 1, 2024, from <https://github.com/aatif85/>
- Govt. of Iran. (2017). *National Report of Plasco Building Investigation*
- Gross, J. L., & Mcallister, T. P. (n.d.). *NIST NCSTAR 1-6 Federal Building and Fire Safety Investigation of the World Trade Center Disaster Structural Fire Response and Probable Collapse Sequence of the World Trade Center Towers*.
- Jian, J., Jiang, J., Jiang, L., Jiang, L., Jiang, L., Jiang, L., Kotsovinos, P., Kotsovinos, P., Zhang, J., Zhang, J., Usmani, A., Usmani, A., McKenna, F., McKenna, F., Li, G., & Li, G.-Q. (2015). OpenSees Software Architecture for the Analysis of Structures in Fire. *Journal of Computing in Civil Engineering*. [https://doi.org/10.1061/\(asce\)cp.1943-5487.0000305](https://doi.org/10.1061/(asce)cp.1943-5487.0000305)
- Jiang, J., Chen, L., Jiang, S., Li, G.-Q., & Usmani, A. (2015). Fire safety assessment of super tall buildings: A case study on Shanghai Tower. *Case Studies in Fire Safety*, 4, 28–38. <https://doi.org/https://doi.org/10.1016/j.csfs.2015.06.001>
- Jiang, J., & Li, G.-Q. (2017). Progressive collapse analysis of 3D steel frames with concrete slabs exposed to localized fire. *Engineering Structures*, 149, 21–34. <https://doi.org/https://doi.org/10.1016/j.engstruct.2016.07.041>
- Jiang, J., Li, G.-Q., & Usmani, A. (2014a). Progressive collapse mechanisms of steel frames exposed to fire. *Advances in Structural Engineering*, 17(3), 381–398.
- Jiang, J., Li, G.-Q., & Usmani, A. (2014b). Progressive collapse mechanisms of steel frames exposed to fire. *Advances in Structural Engineering*, 17(3), 381–398.
- Jiang, J., Qi, H., Lu, Y., Li, G.-Q., Chen, W., & Ye, J. (2022). A state-of-the-art review on tensile membrane action in reinforced concrete floors exposed to fire. *Journal of Building Engineering*, 45, 103502. <https://doi.org/https://doi.org/10.1016/j.jobbe.2021.103502>

- Jiang, L., Orabi, M. A., Jiang, J., & Usmani, A. (2021a). Modelling concrete slabs subjected to fires using nonlinear layered shell elements and concrete damage-plasticity material. *Engineering Structures*, 234, 111977.
- Jiang, L., Orabi, M. A., Jiang, J., & Usmani, A. (2021b). Modelling concrete slabs subjected to fires using nonlinear layered shell elements and concrete damage-plasticity material. *Engineering Structures*, 234, 111977. <https://doi.org/10.1016/J.ENGSTRUCT.2021.111977>
- Jiang, L., Orabi, M. A., Jiang, J., & Usmani, A. (2021c). Modelling concrete slabs subjected to fires using nonlinear layered shell elements and concrete damage-plasticity material. *Engineering Structures*, 234, 111977.
- Jiang, L., & Usmani, A. (2018). Towards scenario fires—modelling structural response to fire using an integrated computational tool. *Advances in Structural Engineering*, 21(13), 2056–2067.
- Jiang, Y., Jiang, Y., Kotsovinos, P., Kotsovinos, P., Usmani, A., Usmani, A., Rein, G., Rein, G., Stern-Gottfried, J., & Stern-Gottfried, J. (2013). Numerical investigation of thermal responses of a composite structure in horizontally travelling fires using OpenSees. *Procedia Engineering*. <https://doi.org/10.1016/j.proeng.2013.08.120>
- Kaounis, T. K. (2017). *GiD+ opensees interface: a major extension to nonlinear finite element analysis*.
- Khan. (2022a). Modeling the collapse of the Plasco Building. Part I: Reconstruction of fire. *Building Simulation*, 15(4), 583–596. <https://doi.org/10.1007/s12273-021-0825-4>
- Khan, A. A. (2022b). *Reconstruction of tall buildings fires for thermal response analysis*.
- Khan, A. A., Domada, R. V. V., Huang, X., Khan, M. A., & Usmani, A. (2022). Modeling the collapse of the Plasco Building. Part I: Reconstruction of fire. *Building Simulation*, 15(4), 583–596. <https://doi.org/10.1007/s12273-021-0825-4>
- Khan, Khan, A. A., Usmani, A. S., & Huang, X. (2022). Can fire cause the collapse of Plasco Building: A numerical investigation. *Fire and Materials*, 46(3), 560–575. <https://doi.org/10.1002/fam.3003>

- Khan, Khan, M. A., Cashell, K. A., & Usmani, A. (2023). An open-source software framework for the integrated simulation of structures in fire. *Fire Safety Journal*, 140, 103896.
- Khan, Khan, M. A., Zhang, C., Jiang, L., & Usmani, A. (2021). OpenFIRE: an open computational framework for structural response to real fires. *Fire Technology*, 1–28.
- Khan, Usmani, A., & Torero, J. L. (2021). Evolution of fire models for estimating structural fire-resistance. *Fire Safety Journal*, 124, 103367.
- Kiakojour, F., Sheidaii, M. R., De Biagi, V., & Chiaia, B. (2021). Progressive collapse of structures: A discussion on annotated nomenclature. *Structures*, 29, 1417–1423. <https://doi.org/https://doi.org/10.1016/j.istruc.2020.12.006>
- Kirby, B. R. (2000). British Steel data on the Cardington fire tests. *British Steel*.
- Lamont, S., Lane, B., Flint, G., & Usmani, A. (2006). Behavior of structures in fire and real design—a case study. *Journal of Fire Protection Engineering*, 16(1), 5–35.
- Lamont, S., Lane, B., Jowsey, A., Torero, J., Usmani, A., & Flint, G. (2006). Innovative structural engineering for tall buildings in fire. *Structural Engineering International*, 16(2), 142–147.
- Lange, D., Röben, C., & Usmani, A. (2012a). Tall building collapse mechanisms initiated by fire: Mechanisms and design methodology. *Engineering Structures*, 36, 90–103.
- Lange, D., Röben, C., & Usmani, A. (2012b). Tall building collapse mechanisms initiated by fire: Mechanisms and design methodology. *Engineering Structures*, 36, 90–103.
- Li, Q., Zhang, C., & Li, G.-Q. (2021). Symmetric modeling of the thermal actions in a structural fire experiment on a long-span composite floor beam in a compartment. *Fire Safety Journal*, 120, 103079.
- Lu, X., Li, Y., Guan, H., & Ying, M. (2017). Progressive collapse analysis of a typical super-tall reinforced concrete frame-core tube building exposed to extreme fires. *Fire Technology*, 53, 107–133.
- Majid Haghdoust. (2017). *Mehr News Agency - Plasco rescue operations, debris removal continues*. <https://en.mehrnews.com/photo/123007/Plasco-rescue-operations-debris-removal-continues>

- McGrattan, K., Hostikka, S., McDermott, R., Floyd, J., Weinschenk, C., & Overholt, K. (n.d.). Fire dynamics simulator technical reference guide volume 2: verification. *Fse-Italia.EuK McGrattan, S Hostikka, R McDermott, J Floyd, C Weinschenk, K OverholtNIST Special Publication, 2013•fse-Italia.Eu*. <https://doi.org/10.6028/NIST.SP.1018-2>
- McKenna, F. (1997). *Object-oriented finite element programming: frameworks for analysis, algorithms and parallel computing*. <https://search.proquest.com/openview/1af20965123abeb431f131a388a8e0c3/1?pq-origsite=gscholar&cbl=18750&diss=y>
- McKenna, F. T. (1997). *Object-oriented finite element programming: frameworks for analysis, algorithms and parallel computing*. University of California, Berkeley.
- Melendo, A., Coll, A., Pasenau, M., Escolano, E., & Monros, A. (2018). www.gidhome.com. www.gidsimulation.com
- Moss, P. J., Dhakal, R. P., Wang, G., & Buchanan, A. H. (2008). The fire behaviour of multi-bay, two-way reinforced concrete slabs. *Engineering Structures*, 30(12), 3566–3573. <https://doi.org/https://doi.org/10.1016/j.engstruct.2008.05.028>
- Newman, G. M. (1991). Structural fire engineering investigation of Broadgate phase 8 fire. *Steel Construction Institute, Ascot*.
- Newmark, N. M. (1959). A method of computation for structural dynamics. *Journal of the Engineering Mechanics Division*, 85(3), 67–94.
- NFPA 101. (2012). *NFPA 101 Life Safety Code*. Quincy: National Fire Protection Association.
- NIST. (2005). Final report on the collapse of the World Trade Center Towers. *National Construction Safety Team for the Federal Building and Fire Safety Investigation of the World Trade Center Disaster, National Institute of Standards and Technology, Gaithersburg, MD*.
- Orabi, A., Khan, A., & Usmani, AS. (2019). An Overview of Opensees for Fire,. *OpenSEES Days Eurasia, The Hong Kong Polytechnic University*.
- Orabi, M. A. (2022). *State of the art large scale simulation of buildings in fire: the case of WTC7*.

- Orabi, M. A., Jiang, L., Usmani, A., & Torero, J. (2022). The collapse of world trade center 7: revisited. *Fire Technology*, 1–28.
- Orabi, M. A., Khan, A. A., Jiang, L., Yarlagadda, T., Torero, J., & Usmani, A. (2022). Integrated nonlinear structural simulation of composite buildings in fire. *Engineering Structures*, 252, 113593.
- Papanikolaou, V. K., Kartalis-Kaounis, T., Protopapadakis, E., & Papadopoulos, T. (2017). A new graphical user interface for OpenSees. *1st European Conference on OpenSees*, 73–76.
- Porcari, G.-L. F., Zalok, E., & Mekky, W. (2015). Fire induced progressive collapse of steel building structures: A review of the mechanisms. *Engineering Structures*, 82, 261–267.
- Prasad, K., & Baum, H. R. (2005a). Coupled fire dynamics and thermal response of complex building structures. *Proceedings of the Combustion Institute*, 30(2), 2255–2262.
- Prasad, K., & Baum, H. R. (2005b). Coupled fire dynamics and thermal response of complex building structures. *Proceedings of the Combustion Institute*, 30(2), 2255–2262. <https://doi.org/10.1016/J.PROCI.2004.08.118>
- Ramesh, S., Ramesh, S., Choe, L., Seif, M., Hoehler, M., Grosshandler, W. L., Sauca, A., Bundy, M., Luecke, W. E., & Bao, Y. (2019). *Compartment fire experiments on long-span composite beams with simple shear connections part 1: Experimental design and beam behavior at ambient temperature*. US Department of Commerce, National Institute of Standards and Technology.
- Rose, P., Bailey, C., Burgess, I., Constructional, R. P.-J. of, & 1998, undefined. (n.d.). The influence of floor slabs on the structural performance of the Cardington frame in fire. *Infona.PIPS Rose, CG Bailey, IW Burgess, RJ PlankJournal of Constructional Steel Research*, 1998•infona.Pl. Retrieved July 17, 2024, from <https://www.infona.pl/resource/bwmetal.element.elsevier-1b012710-14d9-3830-bb05-4722198cbfdf>
- Scott, M. H., & Fenves, G. L. (2010). Krylov subspace accelerated Newton algorithm: application to dynamic progressive collapse simulation of frames. *Journal of Structural Engineering*, 136(5), 473–480.

- SFPE. (2016). *SFPE Handbook of Fire Protection Engineering: Vol. 5th Editio.*
[https://doi.org/10.1016/s0379-7112\(97\)00022-2](https://doi.org/10.1016/s0379-7112(97)00022-2)
- Shakib H et al. (2017). Final Report on the Technical, Management, and Legal Aspects of the Plasco Fire. 2017.
- Shakib, H., Pirizadeh, M., Dardaei, S., & Zakersalehi, M. (2018). Technical and Administrative Assessment of Plasco Building Incident. *International Journal of Civil Engineering*, 16(9), 1227–1239. <https://doi.org/10.1007/s40999-018-0283-2>
- Shakib, H., Zakersalehi, M., Jahangiri, V., & Zamanian, R. (2020). Evaluation of Plasco Building fire-induced progressive collapse. *Structures*, 28, 205–224. <https://doi.org/10.1016/j.istruc.2020.08.058>
- Shepherd, P. G., & Burgess, I. W. (2011). On the buckling of axially restrained steel columns in fire. *Engineering Structures*, 33(10), 2832–2838.
- Silva, J. C. G., Landesmann, A., & Ribeiro, F. L. B. (2016a). Fire-thermomechanical interface model for performance-based analysis of structures exposed to fire. *Fire Safety Journal*, 83, 66–78.
- Silva, J. C. G., Landesmann, A., & Ribeiro, F. L. B. (2016b). Fire-thermomechanical interface model for performance-based analysis of structures exposed to fire. *Fire Safety Journal*, 83, 66–78. <https://doi.org/10.1016/J.FIRESAF.2016.04.007>
- Starossek, U. (2007). Typology of progressive collapse. *Engineering Structures*, 29(9), 2302–2307.
- Stern-Gottfried, J., & Rein, G. (2012). Travelling fires for structural design-Part II: Design methodology. *Fire Safety Journal*, 54, 96–112. <https://doi.org/10.1016/J.FIRESAF.2012.06.011>
- Sun, R., Huang, Z., & Burgess, I. W. (2012). Progressive collapse analysis of steel structures under fire conditions. *Engineering Structures*, 34, 400–413.

- Suwondo, R., Cunningham, L., Gillie, M., & Bailey, C. (2021). Analysis of the robustness of a steel frame structure with composite floors subject to multiple fire scenarios. *Advances in Structural Engineering*, 24(10), 2076–2089.
- Torero, J. L. (2011). Fire-induced structural failure: The World Trade Center, New York. *Proceedings of the Institution of Civil Engineers: Forensic Engineering*, 164(2), 69–77. <https://doi.org/10.1680/FENG.2011.164.2.69/ASSET/IMAGES/SMALL/FENG164-069-F7.GIF>
- Usmani, A., Drysdale, D., Rotter, J., Sanad, A., Gillie, M., Lamont, S., O'Connor, M., O'Callaghan, D., Elghazouli, A., & Izzuddin, B. (2000). Behaviour of steel framed structures under fire conditions. *DETRPIT Project Final Report*.
- Usmani, A. S. (2005). Stability of the World Trade Center Twin Towers Structural Frame in Multiple Floor Fires. *Journal of Engineering Mechanics*, 131(6), 654–657. [https://doi.org/10.1061/\(ASCE\)0733-9399\(2005\)131:6\(654\)](https://doi.org/10.1061/(ASCE)0733-9399(2005)131:6(654))
- Usmani, A. S., Chung, Y. C., & Torero, J. L. (2003). How did the WTC towers collapse: A new theory. *Fire Safety Journal*, 38(6), 501–533. [https://doi.org/10.1016/S0379-7112\(03\)00069-9](https://doi.org/10.1016/S0379-7112(03)00069-9)
- Usmani, A., Zhang, J., Jiang, J., Jiang, Y., & May, I. (2012a). Using opensees for structures in fire. *Journal of Structural Fire Engineering*, 3(1), 57–70.
- Usmani, A., Zhang, J., Jiang, J., Jiang, Y., & May, I. (2012b). *Using Opensees for Structures in Fire* (Vol. 57, Issue 1).
- Wickstrom Ulf, S. N., Duthinh, D., & Mcgrattan, K. (2007a). *Adiabatic surface temperature for calculating heat transfer to fire introduction*. Most.
- Wickstrom Ulf, S. N., Duthinh, D., & Mcgrattan, K. (2007b). *Adiabatic Surface Temperature for Calculating Heat Transfer To Fire Introduction*. Most, 2.
- Wikimedia Commons. (1961). *File:Plasco tower, old 01.jpg - Wikimedia Commons*. <Http://Fararu.Com/>. https://commons.wikimedia.org/wiki/File:Plasco_tower,_old_01.jpg

- Yang, K. C., & Yang, F. C. (2015). Fire performance of restrained welded steel box columns. *Journal of Constructional Steel Research*, 107, 173–181.
- Yarlagadda, T., Hajiloo, H., Jiang, L., Green, M., & Usmani, A. (2018). Preliminary modelling of Plasco Tower collapse. *International Journal of High-Rise Buildings*, 7(4), 397–408. <https://doi.org/10.21022/IJHRB.2018.7.4.397>
- Zarghamee, M. S., Kitane, Y., Erbay, Ö. O., Mcallister, T. P., & Gross, J. L. (n.d.). *Federal Building and Fire Safety Investigation of the World Trade Center Disaster Global Structural Analysis of the Response of the World Trade Center Towers to Impact Damage and Fire*.
- Zhang, C., Silva, J. G., Weinschenk, C., Kamikawa, D., & Hasemi, Y. (2016). Simulation methodology for coupled fire-structure analysis: modeling localized fire tests on a steel column. *Fire Technology*, 52, 239–262.